Modelling the phenological effects of environmental drivers on mosquito abundance: implications for West Nile virus transmission potential in the UK

David EWING

Submitted in fulfillment of the requirements for the Degree of Doctor of Philosophy

School of Mathematics and Statistics

College of Science and Engineering

University of Glasgow

August 29, 2017

Abstract

Modelling the phenological effects of environmental drivers on mosquito abundance: implications for West Nile virus transmission potential in the UK

by David EWING

Mosquito-borne diseases cause substantial mortality and morbidity worldwide. These impacts are widely predicted to increase as temperatures warm, since mosquito biology and disease ecology are strongly linked to environmental conditions. However, direct evidence linking these changes to mosquito-borne disease is rare, and the ecological mechanisms that may underpin such changes are poorly understood. I focus on West Nile virus (WNV), a mosquito-borne arbovirus infecting avian hosts, that can spill over into humans. Outbreaks of WNV are common in Africa, and Southern and Eastern Europe, with recent outbreaks reported in France and Spain. There has yet to be an outbreak in the UK, but there is current concern that passerine migratory bird species could introduce the disease northward. However, the question remains, if WNV is introduced in the UK, can the disease establish? I present a mechanistic environmentally-driven stage-structured host-vector mathematical model for predicting the seasonal dynamics of WNV in current and future climates in the UK. The model predicts that WNV is unlikely to establish in the foreseeable future, although climate change is likely to increase the risk, with only extreme climate predictions leading to possible WNV outbreaks.

Chapter 2 develops an environmentally driven, variable-delay delay differential equation model to estimate seasonal abundance of each life stage of the WNV vector mosquito species, *Cx. pipiens*. The model shows that timing and intensity of warm periods can be more influential in shaping abundance patterns than average temperatures.

Chapter 3 presents an extensive body of fieldwork, which led to a high temporal resolution seasonal abundance dataset of each life stage of *Cx. pipiens*.

Chapter 4 challenges assumptions of the DDE model from Chapter 2 in light of the seasonal abundance data collected in Chapter 3. The importance of using appropriate, high temporal resolution input temperature datasets is displayed.

Chapter 5 extends the DDE model from Chapter 4 to explicitly model WNV transmission cycles between vectors and avian hosts. Temperatures are predicted to be too low for WNV transmission in the UK before the 2080s, when only the most extreme climate projections suggest the possibility of a disease outbreak.

Contents

List of Tables

List of Figures

Acknowledgements

Firstly, I would like to thank my supervisors Dr. Steven White, Dr. Christina Cobbold, Dr. Beth Purse and Dr. Miles Nunn for their support, encouragement and advice in completing my thesis. I would also like to thank Steffi Schaeffer for her knowledge and assistance in planning and implementing the fieldwork. Thanks also go to the other students at CEH Wallingford who helped with the fieldwork and to Jim Jones who helped me with the dry ice deliveries and battery charging.

I am grateful for the funding that I have received from the National Environment Research Council, without which I would have been unable to undertake this work. Further, I would like to thank the Centre for Ecology & Hydrology for their support during my studies.

I would also like to thank my parents for their financial and emotional support through all my endeavours, both academic and sporting. I would never have started this PhD, never mind finished it, without their support, encouragement and guidance.

Finally, I would like to thank my wife Ailith for her endless love and support: from driving back and forth between Cambridge and Didcot most weekends for two years, to maintaining my sanity whilst I counted over half a million mosquito larvae, to spending countless hours sitting in sports halls watching me play korfball. Her support in all areas of my life the past nine years has been incredible.

Declaration of Authorship

I, David EWING, declare that this thesis titled, "Modelling the phenological effects of environmental drivers on mosquito abundance: implications for West Nile virus transmission potential in the UK" and the work presented in it are my own. I confirm that:

- This work was done wholly or mainly while in candidature for a research degree at the University of Glasgow.
- Where any part of this thesis has previously been submitted for a degree or any other qualification at this University or any other institution, this has been clearly stated.
- Where I have consulted the published work of others, this is always clearly attributed.
- Where I have quoted from the work of others, the source is always given. With the exception of such quotations, this thesis is entirely my own work.
- I have acknowledged all main sources of help.
- Where the thesis is based on work done by myself jointly with others, I have made clear exactly what was done by others and what I have contributed myself.

Signed:

_____

Date:

_____

"*Every man, at some point in his life, is going to lose a battle. He is going to fight and he is going to lose. But what makes him a man, is that in the midst of that battle, he does not lose himself.*"

Coach Eric Taylor

List of Abbreviations

CEH	Centre for Ecology & Hydrology	
DDE	Delay differential equation	Delay differential equations are a type of differential equation in which the derivative of the unknown function at a certain time is given in terms of the values of the function at previous times.
DDT	Dichloro-diphenyl-tichloroethane	A chemical pesticide
DTR	Diurnal temperature range	The range of the temperatures experienced across a day.
EIP	Extrinsic incubation period	The time required for the development of a disease agent in a vector, from the time of uptake of the agent to the time when the vector is infective.
GLM	Generalised linear model	The generalized linear model is a flexible generalization of ordinary linear regression that allows for response variables that have error distribution models other than a normal distribution.
MFIR	Minimum filial infection rate	The minimum number of offspring infected with an infectious agent per 1,000 offspring from an infected parent.
MIR	Minimum infection rate	The number of infectious vectors per 1000 adult females
ODE	Ordinary differential equation	An ordinary differential equation is a differential equation containing one or more functions of one independent variable and its derivatives

PDE	Partial differential equation	A partial differential equation is a differential equation that contains unknown multivariable functions and their partial derivatives
SEIR	Susceptible-Exposed-Infectious-Recovered	
UKCIP	UK Climate Impacts Programme	
WNV	West Nile virus	A flavivirus transmitted by mosquitoes, usually between birds, but sometimes causing epidemics of disease (typically fever or encephalitis) in humans and horses.
WNF	West Nile fever	The illness caused by West Nile virus.

Chapter 1

Introduction

1.1 Aims of the thesis

The main aims of the thesis are:

- To develop and validate an environmentally driven seasonal abundance model for *Cx. pipiens*, a temperate mosquito vector, which accounts for changing environmental conditions by explicitly incorporating variation in developmental delays of each life stage.
- To use this model to predict the possible risks of West Nile virus (WNV) introduction and subsequent transmission within the UK.

1.2 Virus and vector background

1.2.1 Overview of vector-borne diseases

Organisms which transmit parasites and pathogens from infected to uninfected individuals are called vectors. There are a huge range of species which act as vectors, though the most common group are arthropods (Kalluri et al. 2007). Vectors can be split into two groups, defined as mechanical vectors and biological vectors. Mechanical vectors transmit the infectious agent without that agent being able to replicate or develop within their body. For example, synanthropic flies have been linked to outbreaks in diarrheal diseases in urban and rural areas of developing countries (Graczyk et al. 2001). Biological vectors take the infectious agent into their system, where it replicates and develops before being passed on to another host. Biological vectors are typically obligate blood feeders which have adapted to

use semi-aquatic or aquatic breeding sites either in domestic settings or in peridomestic settings near livestock. Examples of well known and particularly problematic biological vector species include tsetse flies, which spread human sleeping sickness and animal trypanosomiasis (Brun et al. 2010) and ticks, which spread Lyme disease (Burgdorfer 1984). Perhaps the most well known vector species are mosquitoes, which transmit a range of human and animal diseases, including malaria (Ross 1898) and dengue fever (Bancroft 1906). These diseases cause serious morbidity and mortality in the affected species and often come with large associated medical, ecological and financial costs (Brownlie et al. 2006).

Mosquitoes were first implicated as a disease vector in the late 19th century when they were found to act as vectors of the avian malaria parasite *Plasmodium relictum* by Ross (1898), who allowed mosquitoes to feed first on infected birds and then uninfected birds and showed that transmission had occurred. Shortly after this mosquitoes were also found to vector human malaria (Grassi et al. 1899), yellow fever (Reed et al. 1900) and dengue fever (Bancroft 1906). Since then mosquitoes have been found to act as vectors for hundreds of pathogen species, 38 of which affect humans (Smith et al. 2014). To satisfactorily incriminate a mosquito species as a vector of a pathogen one must assert a temporal and spatial relationship between the mosquito species and disease cases, provide evidence of direct contact between the mosquito species and the host, and provide evidence that the mosquito species harbours the pathogen in its salivary glands (Beier 2002). Efforts to eradicate mosquito-borne pathogens were undertaken at a large scale in the 1950s and 1960s through the Global Malaria Eradication Programme (GMEP). The GMEP placed a strong focus on the implementation of mosquito eradication measures, primarily through the use of the insecticide DDT (dichloro-diphenyl-tichloroethane) (Smith et al. 2012). However, the programme's rigid approach to eradication through DDT spraying meant little focus was given to continuing research into malaria control (Najera et al. 2011). Mosquitoes were observed to develop resistance to DDT (Gjullin and Peters 1952), which combined with numerous other factors brought about the end of the GMEP in 1969. In the subsequent years many of the diseases previously thought to be under control have expanded their range and increased their prevalence (Gubler 1998; Zell 2004; Reiner et al. 2013). Mosquito-borne diseases are now thought to be a major global public health concern, with the burden of these diseases increasing substantially in many regions in recent decades (Reiner et al. 2013; Gubler 2002).

This increase stems not only from the re-emergence of diseases previously thought to be under control, such as Dengue (Decker 2012) but also from the geographical expansion of diseases to new areas, as with West Nile fever (WNF) (Reisen 2013). Calculation of an R_0

value is a standard, useful technique by which the level of risk a population faces due to a vector-borne disease can be quantified. This is the number of secondary infections caused by introducing one infectious individual into a population which is entirely susceptible. R_0 values are a standard way to assess the outbreak potential of a pathogen, with values greater than one implying that an epidemic will take place and values below one meaning the disease will die out. A range of factors including societal, land use and habitat changes, have been linked to changes in exposure to mosquitoes, which will influence the ratio of vectors to humans, (Gubler 2002), the frequency with which vectors may bite humans rather than other hosts, and consequently R_0 values. In particular, unprecedented human population growth and reduction in mosquito control have increased exposure to mosquitoes in existing endemic areas, whilst increased global travel has expanded the range of vector-borne diseases (Gubler 2002). These factors combine with widespread predictions that rising temperatures may increase mosquito development (Rueda et al. 1990; Loetti et al. 2011) and biting rates (Wimberly et al. 2014), resulting in increases in mosquito population size (Paz and Albersheim 2008; Mirski et al. 2012; Beck-Johnson et al. 2013) and increased exposure. Warming is also expected to increase the hazard posed by mosquito populations, with higher temperatures leading to reduction in the length of the extrinsic incubation period and increasing the R_0 value, as mosquitoes become infectious sooner after taking a blood meal (Reisen et al. 2006a).

Further, it is thought that changing rainfall patterns will influence the availability of larval habitat, though the predicted effects of this are less clear and may show greater regional variability (Githeko et al. 2000). In the UK we expect to see increased mean precipitation and increased extreme rainfall events through the winter months, though summer precipitation is expected to decrease (Osborn and Hulme 2002; Beniston et al. 2007; Murphy et al. 2010). This reduction in habitat during the biting season may lead to a decrease in available larval habitat, which could reduce exposure. However, it has been shown that, in times of low rainfall, people will often store water in their gardens, creating mosquito habitats in urban areas, which may increase exposure (Townroe and Callaghan 2014). This idea has been mirrored in the variable effects precipitation has been seen to have on disease outbreaks (Morin and Comrie 2013; Wimberly et al. 2014).

The non-linear and opposing impacts of temperature and rainfall on vector demographic rates cause problems with attribution of climate change as a causal agent of changes in vector-borne disease (Rogers and Randolph 2006). Consequently, detailed mathematical models which explicitly account for environmental impacts on different vector life cycle processes are required to attempt to tease out the effects of climate change on vector populations, and

consequently disease dynamics.

1.2.2 West Nile virus

West Nile fever (WNF) is a mosquito-borne disease caused by West Nile virus (WNV), which has expanded its range and public health burden over recent years and is now endemic in areas of Europe, with reported cases in Northern Italy in a number of recent years (61 cases in 2015, 23 cases in 2014, 69 cases in 2013) (ECDC 2016b). WNV is a flavivirus which was originally discovered in Uganda in 1937 (Smithburn et al. 1940). WNF is symptomless in $70 - 80\%$ of cases and presents with cold and flu-like symptoms in most symptomatic individuals, though in extreme cases ($< 1\%$) it can result in encephalitis and death (Hart et al. 2014). Since its initial discovery, epidemics of WNF were initially very sporadic, with outbreaks in Israel (1951-54 and 1957) and South Africa (1974) being the most notable. In the mid-1990s, however, the epidemiology of the virus appeared to change, causing epidemics and epizootics in humans and horses (outbreaks were reported in Romania 1996; Morocco 1996; Tunisia 1997; Italy 1998; Russia and Israel 1999; and Israel, France 2000) (Petersen and Roehrig 2001). Moreover, these outbreaks showed a substantial increase in human disease cases (confirmed human infections in recent outbreaks: Romania, 393 cases; Russia [Volgograd], 942 cases; Israel, 2 cases in 1999 and 417 in 2000) (Petersen and Roehrig 2001). Further, until 1999 WNV was restricted to Old World countries, however since then WNV has spread across North America resulting in $43,937$ reported cases and $1,911$ reported deaths in humans from 1999-2015 (Figure 1.1) (CDC 2016b). This expansion across North America, alongside the outbreaks in Israel, was accompanied by a high mortality in the avian population, which was previously unobserved, suggesting that a new strain of the virus had emerged, which may be been transported from Israel to New York by air travel (Petersen and Roehrig 2001). In Europe, cases have regularly been reported across the Mediterranean basin and into central and eastern parts of the continent, with human cases as close to the UK as southern France and northern Italy in 2015 and 2016 (Figure 1.2). The unexpected but highly successful introduction and rapid spread of WNV in North America highlights the ability of the virus to establish itself in previously uninfected areas (Reisen 2013). The relative proximity of cases in Southern France and Northern Italy to the UK has raised some concerns about the possible likelihood of WNV introduction and subsequent transmission, perhaps through the arrival of infected migratory birds (Higgs et al. 2004; Bessell et al. 2014). This possibility is particularly concerning because the UK is already host to a high abundance of the mosquito *Culex pipiens*, which is known to be an effective vector of WNV

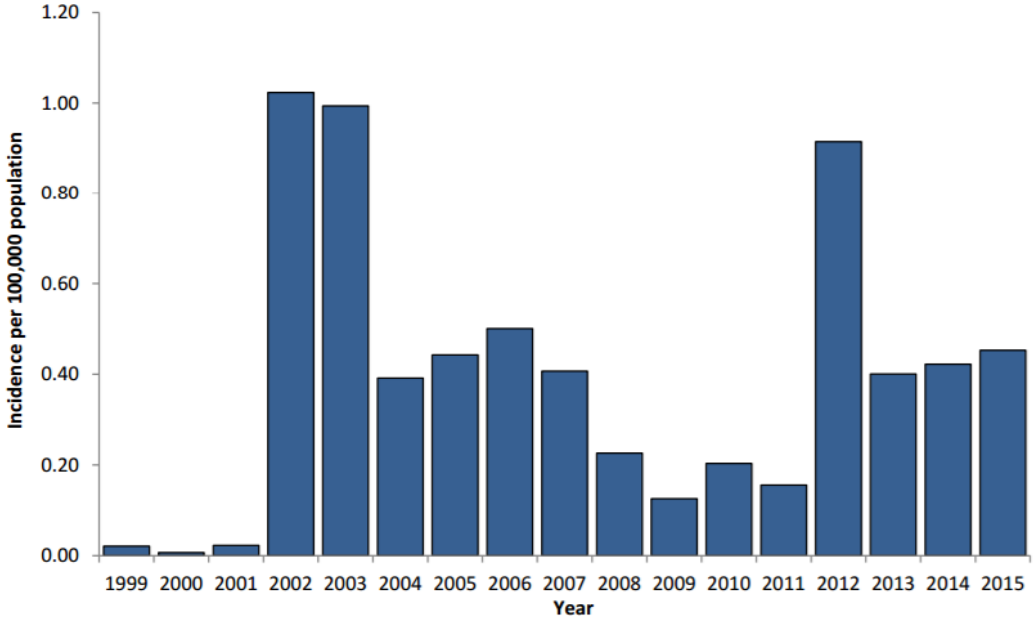

Figure 1.1: USA WNV cases: West Nile virus neuroinvasive disease incidence reported to CDC by year, 1999-2015 (CDC 2016b).

(Golding 2013). Further, it is predicted climate change will cause increases in UK temperatures in the coming years (MetOffice 2009), which may increase the ability of these vectors to effectively transmit WNV if it were to be introduced.

The WNV transmission cycle

WNV is primarily transmitted in a cycle between a vector mosquito species and a wide variety of host bird species (Komar et al. 2003), especially those in the order Passeriformes (Reisen 2013), with the possibility that the virus can then spill over into equine and human populations. Infected humans and equines act as dead-end hosts meaning that mosquitoes cannot contract the virus from them, however infection can result in serious health implications for these populations (Figure 1.3). Given this, the epidemiology of WNV is primarily driven by avian host and vector dynamics and not human dynamics, as is the case for dengue and malaria. The virus is spread by adult female mosquitoes who first take a blood meal from an infected bird, contracting the virus themselves. The virus then infects and replicates in the cells of the mosquito midgut as the blood meal is being processed, after which it travels to the salivary glands (Turell et al. 2002). Eventually, sufficient levels of the virus accumulate in the salivary glands to allow it to be transmitted to new avian or mammalian hosts during feeding (Turell et al. 2002). Once infected, an adult mosquito can pass the infection on to its offspring, though rates of such vertical transmission are very low (Anderson and Main 2006).

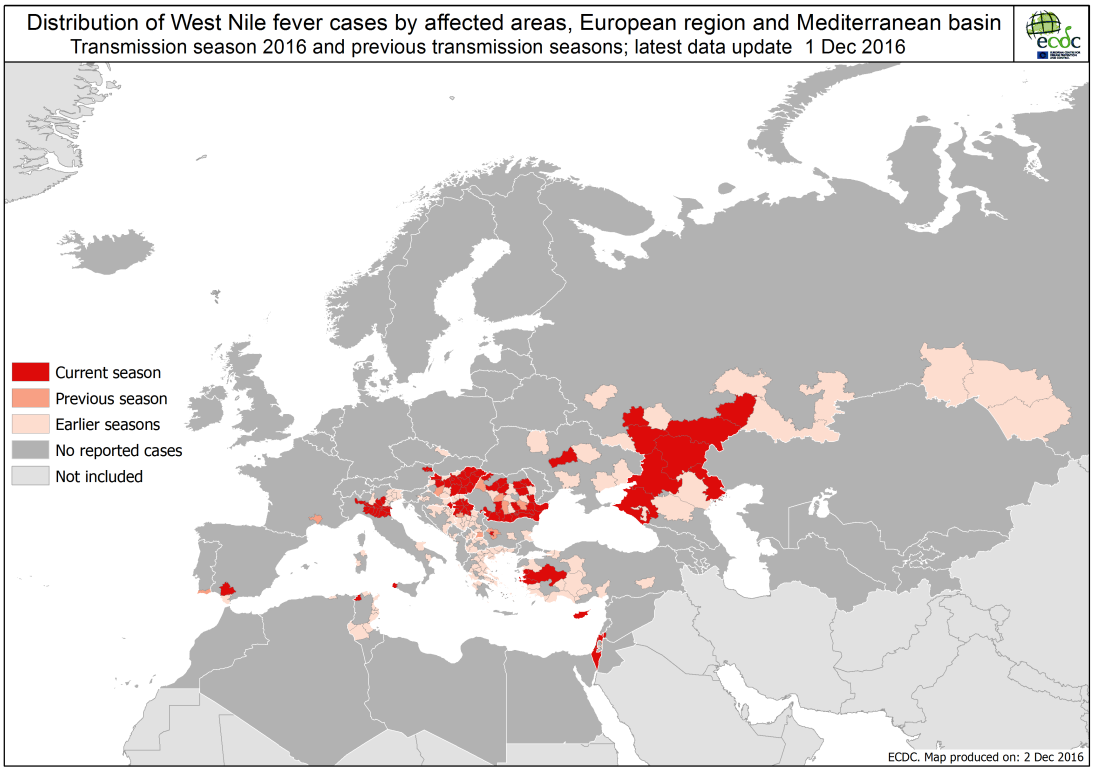

Figure 1.2: European WNV cases: A map showing WNV cases in Europe in recent years (ECDC 2016a).

In common with other arthropod-borne infections, males do not contribute to transmission of the virus as they do not blood feed, instead feeding on nectar.

There are two routes by which WNV persistence between seasons via overwintering females is believed to be achieved. The first route is through overwinter survival of infected, parous (blood-fed) females (Andreadis et al. 2010). Whilst the majority of diapausing females are nulliparous (not blood-fed) (Mitchell and Briegel 1989), Andreadis et al. (2010) found over three years that the percentage of parous females in collections in April ranged from 0.9% to 10%. This fact, combined with the fact that gonotrophic dissociation (the process of diapause-ready females taking a blood meal) has been shown to occur in WNV vectors (Eldridge 1966) implies that WNV persistence between seasons may occur, to varying degrees, through both of these processes. The second route is by vertical transmission at the end of one season, followed by horizontal transmission at the beginning of the next (Anderson and Main 2006). Vertical transmission of WNV has been shown to occur both in the laboratory (Dohm et al. 2002a) and naturally (Nelms et al. 2013), with estimates of the minimum filial infection rate (MFIR) (the minimum number of mosquitoes infected with WNV per 1,000 offspring) ranging from 0.04 to 8.1 in laboratory studies (Nelms et al. 2013). This provides

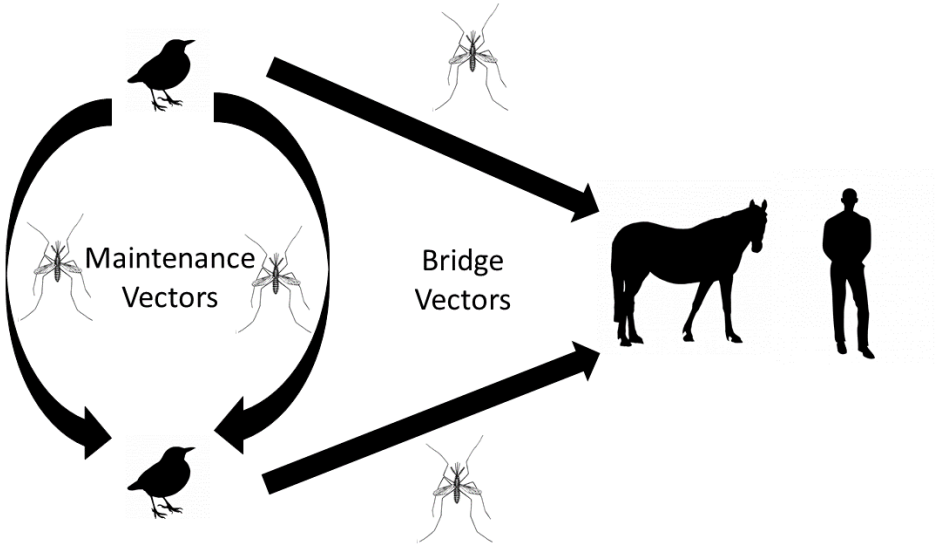

Figure 1.3: WNV transmission cycle: The diagram shows the WNV transmission cycle.

evidence for the possibility of WNV overwintering in vertically infected *Cx. pipiens* leading to further spread of the virus through horizontal transmission the following spring.

For, WNV it is mosquitoes of the genus *Culex* which are the primary vectors in nature (Colpitts et al. 2012). Consequently, in order for successful introduction and transmission of WNV into a new habitat, such as the UK, to take place a key requirement is that the habitat either already supports, or is suitable for, the vector population.

Candidate UK vectors for WNV

Thorough reviews of potential WNV vectors in the UK are given by Higgs et al. (2004) and Chapman et al. (2016). These studies identify thirteen mosquito species resident in the UK which have been shown to act as vectors of WNV (Figure 1.4 highlighted in red). Whilst all thirteen of these species have been shown to act as vectors of WNV virus, only those which are widespread in the UK and are ornithophilic, meaning they feed on birds, are likely to act as vectors on a national level. Six of the thirteen species meet these criteria: *Anopheles maculipennis, Culex pipiens, Coquillettidia richiardii, Ochlerotatus cantans, Ochlerotatus punctor* and *Culiseta annulata*. Of these species, *Ochlerotatus punctor* and *Culiseta annulata* have only been shown to be laboratory-competent vectors and have not been implicated in disease transmission worldwide (Chapman et al. 2016). The remaining four vectors all

are likely to contribute to WNV transmission, however *Cx. pipiens* is widely regarded to be main driver of WNV transmission in Europe and North America, due to its strong preference for feeding on birds (Gubler 2002; Zeller and Schuffenecker 2004; Higgs et al. 2004; Calistri et al. 2010; Reisen 2013). Further, it has been shown that *Cx. pipiens* is very common within the UK (Golding 2013). As such, I assume that *Cx. pipiens* would act as the key maintenance vector of WNV within the UK.

Whilst *Cx. pipiens* is likely to act as the WNV maintenance vector in an UK transmission scenario, other vectors are likely to act as bridge vectors by which human or equine cases may arise. In particular *Anopheles maculipennis, Coquillettidia richiardii* and *Ochlerotatus cantans* are all known to bite mammals and therefore may contribute to transmission and act as bridge vectors. Further, *Culex modestus*, which has been found in the North Kent marshes in south-east England, is known to vector WNV and to aggressively bite humans (Golding et al. 2012). Consequently, *Cx. modestus* habitats may be areas of particularly high infection risk to humans if WNV transmission were possible within the resident bird population. Potential changes in the climate may also expand the range of *Cx. modestus* within the UK, potentially increasing the areas home to both maintenance and bridge vectors. Therefore, general studies of vector abundance focussing on key maintenance vectors are important, though it is also important that consideration is given to local variability in mosquito population distributions to identify key risk areas.

Culex pipiens life cycle and ecology

In the case of WNV, the effective vector *Culex pipiens* is already widely distributed across the UK and the entire Northern Hemisphere and has been shown to be a competent vector of the virus in a range of temperate climates including North America (Colpitts et al. 2012), Europe (Fros et al. 2015) and South America (Micieli et al. 2013). As with all mosquito species, the *Cx. pipiens* life cycle consists of four main stages: egg, larval, pupal and adult. After taking a blood meal, adult females *Cx. pipiens* lay rafts of eggs on the surface of stagnant pools of water. Larvae hatch from these eggs within a couple of days and feed on organic matter in the water as they develop through four larval instars. At the end of the fourth instar, the larvae develop into pupae and emerge as new adults a few days later (Figure 1.5). This cycle is repeated throughout the spring and summer months through approximately 3-4 generations, dependent on environmental conditions (Madder et al. 1983b), until inseminated adult female mosquitoes enter a diapausing state to enable survival throughout the winter months when temperatures are too cold for immature development (Wilton and Smith 1985).

Aedes	***Coquillettidia***	***Ochlerotatus***
aegypti	*metallica*	*atlanticus*
africanus	*microannulata*	*atropalpus*
albocephalus	*perturbans*	*canadensis*
albopictus	*richiardii*	*cantans*
albothorax	***Culiseta***	*cantator*
cinereus	*annulata*	*caspius*
circumluteolus	*inornata*	*detritus*
juppi + caballus	*melanura*	*excrusians*
madagascarensis	***Culex***	*japonicas*
vexans	*antennatus*	*punctor*
Aedomyia	*decens* group	*sollicitans*
africana	*erraticus*	*taeniorhynchus*
Anopheles	*ethiopicus*	*triseriatus*
atropos	*guiarti*	*trivittatus*
barberi	*modestus*	*tormentor*
brunnipes	*neavei*	*signifera*
coustani	*nigripalpus*	***Mimomyia***
crucians/bradleyi	*nigripes*	*hispida*
maculipalpis	*perexiguus*	*lacustris*
maculipennis	*perfuscus* group	*splendens*
plumbeus	*pipiens*	***Psorophora***
punctipennis	*poicillipes*	*ciliate*
quadrimaculatus	*pruina*	*columbiae*
subpictus	*quinquefasciatus*	*ferox*
walkeri	*restuans*	***Uranotaenia***
	salinarus	*sapphirina*
	scottii	
	tarsalis	
	territans	
	theileri	
	tritaeniohynchus	
	univittatus	
	vishnul group	
	weschei	
	Deionocerites	
	cancer	

Figure 1.4: WNV vectors: All known vectors of WNV are shown, with those present in the UK highlighted in red (Higgs et al. 2004).

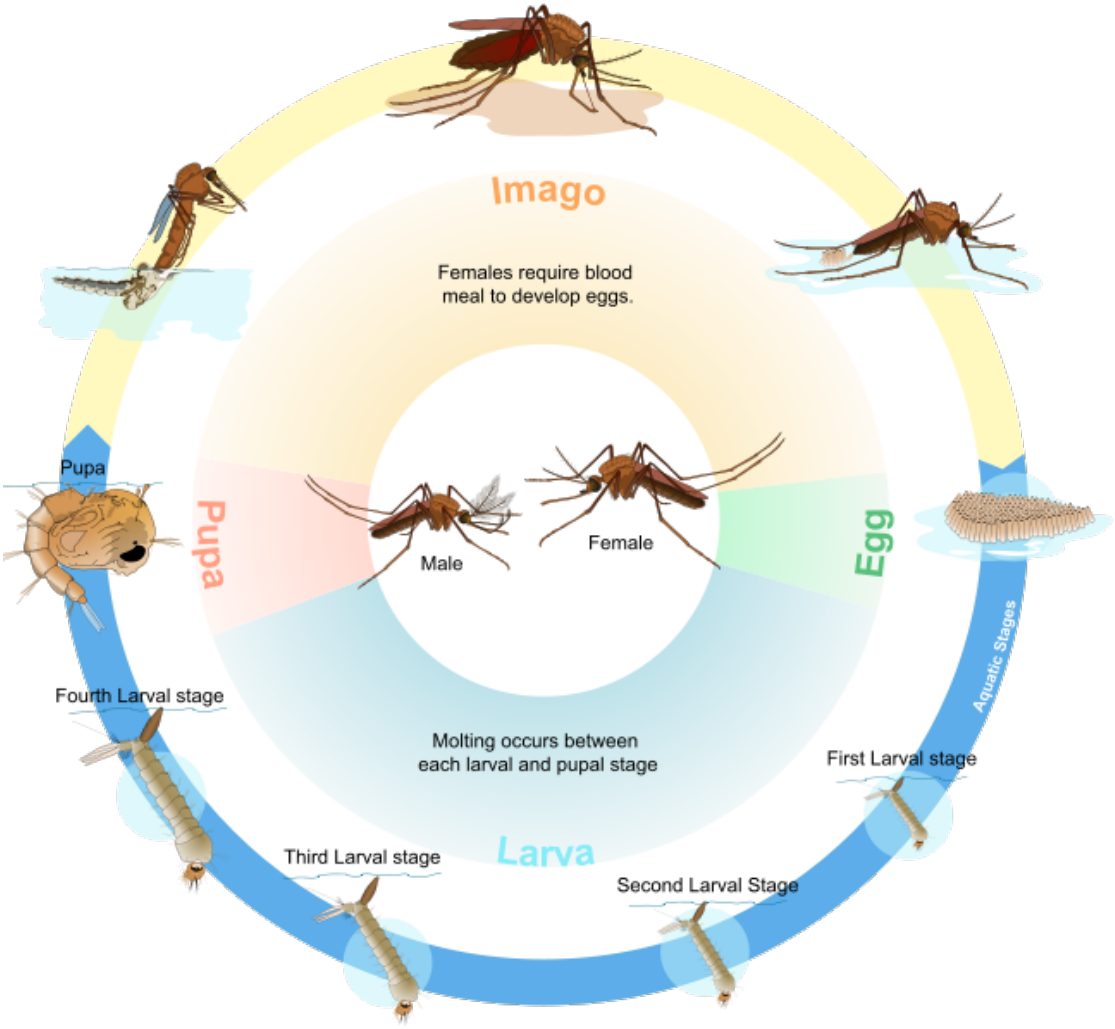

Figure 1.5: *Culex pipiens* life cycle: A diagram showing the *Cx. pipiens* life cycle. The imago is the final and fully developed adult stage (Landscapes 2016).

Cx. pipiens is primarily ornithophilic (bird-biting). This makes *Cx. pipiens* a very effective maintenance vector, as birds are the most competent host for the virus, meaning that the mosquitoes can continue to circulate the virus within the host population (Figure 1.3) (Petersen and Roehrig 2001). However, *Cx. pipiens* has also been shown to feed on mammals, including humans, meaning it can act as a bridge vector between the avian and humans populations (Hamer et al. 2009). WNV has been shown to overwinter in temperate regions in both Europe (Sabatino et al. 2014) and North America (Reisen 2013) following some large epidemics, such as in Italy in 2008-2009 (Monaco et al. 2011) and in the USA in 1999-2000 (Reisen 2013). However, the relative contributions of *Cx. pipiens* and host bird populations to this overwinter pathogen persistence are not clear (Calistri et al. 2010; Monaco et al. 2011), with both birds (Hinton et al. 2015) and adult female *Cx. pipiens* (Nasci et al. 2001) having been shown to act as overwintering virus reservoirs. Consequently, it is unclear whether or how pathogen persistence may occur in the UK.

Avian hosts

An important determinant of the extent of WNV transmission following introduction to a new area is the structure of the bird population in that area. It is known that different bird species vary in disease-induced death rates, recovery rates and viremia levels such that the overall bird population will be composed of species with a range of different host competencies (Komar et al. 2003; Pérez-Ramírez et al. 2014). These factors will have a profound effect on disease transmission. The level of viremia reached by a given host will determine the transmission probability from host to vector with higher levels of viremia increasing transmission rates and R_0 values. Further, recovery rate of the hosts is an important parameter, with slower avian recovery rates leading to increased potential for transmission. Finally, the avian ecology will affect the overlap between bird, mosquito and human populations, which will influence the vector-to-host ratio. The range and relative frequency of bird species with different competencies means that the composition of the host population may have a profound impact on disease transmission, with high abundances of highly competent hosts leading to virus amplification and the opposite leading to dilution of the virus. These factors mean that not only vector population dynamics, but also host dynamics, are expected to influence disease transmission.

Komar et al. (2003) calculated reservoir competence indices for a range of North American bird species by combining susceptibility to infection, mean viremia levels and infection duration (Table 1.1). This work highlighted that Passeriformes were particularly competent hosts for WNV, with the four most competent hosts in their study all being Passeriformes. A recent review by Pérez-Ramírez et al. (2014), drawing together a range of studies into avian WNV infections supports this view, showing that Passeriformes are by far the most well studied species but also appear to show the highest viremias, in general. However, it is important to note that they also emphasise that there are exceptions to this observation, with some Passeriformes presenting with low viremias and species from other orders showing high viremias. Further, they show that the strain of the virus affects the viremia of the host, with hosts from the same species showing different viremias when infected with different strains. This was observed upon introduction of WNV into North America, as the virus caused substantial mortality amongst the local bird populations, with mortality rates amongst the American crow being particularly high (Reisen 2013). This high avian mortality in the New World had not previously been observed in the Old World, where the virus had been circulating for longer (McLean et al. 2001). This suggests that different species will react very differently to WNV reaction, not only due to differences at a species level but also due to differences in the strain of the virus and their previous exposure (Ciota and Kramer 2013).

Common name	Susceptibility	Mean infectiousness	Mean duration (days)	Reservoir competence index
Blue Jay	1.0	0.68	3.75	2.55
Common Grackle	1.0	0.68	3	2.04
House Finch	1.0	0.32	5.5	1.76
American Crow	1.0	0.50	3.25	1.62
House Sparrow	1.0	0.53	3	1.59
Ring-billed Gull	1.0	0.28	4.5	1.26
Black-billed Magpie	1.0	0.36	3	1.08
American Robin	1.0	0.36	3	1.08
Red-winged Blackbird	1.0	0.33	3	0.99
American Kestrel	1.0	0.31	3	0.93
Great Horned Owl	1.0	0.22	4	0.88
Killdeer	1.0	0.29	3	0.87
Fish Crow	1.0	0.26	2.8	0.73
Mallard	1.0	0.16	3	0.48
European Starling	1.0	0.12	1.8	0.22
Morning Dove	1.0	0.11	1.7	0.19
Northern Flicker	1.0	0.06	1	0.06
Canada Goose	1.0	0.10	0.3	0.03
Rock Dove	1.0	0	0	0
American Coot	1.0	0	0	0
Japanese Quail	1.0	0	0	0
Northern Bobwhite	1.0	0	0	0
Ring-necked Pheasant	1.0	0	0	0
Monk Parakeet	1.0	0	0	0
Budgerigar	0.7	0	0	0

Table 1.1: Host competencies of some bird species: A table taken from Komar et al. (2003) showing reservoir competence indices for a range of North American birds.

One of the most likely pathways by which WNV may be introduced into the UK would be through the arrival of infected migratory birds (Higgs et al. 2004; Bessell et al. 2014), potentially leading to a disease outbreak. Firstly, for introduction to be possible the virus would need to have a sufficiently mild impact on the bird's fitness that it was able to successfully complete the migration whilst infected. If the bird's immune system were so effective at fighting off the virus that it were no longer infectious upon arrival then clearly no transmission could take place. Further, the ecology of the resident bird population would be very important if the virus were to be successfully introduced, as the mixture of different host competency levels would help determine the likelihood of virus amplification or dilution in the population. For example, Ezenwa et al. (2006) found that increasing non-passerine species richness decreased WNV prevalence in Louisiana, USA, and Allan et al. (2009) found that decreasing species richness across all bird species increased WNV prevalence at both regional and national levels in the USA. However, Loss et al. (2009) found no evidence of an effect of avian species richness on WNV transmission in Chicago, Illinois. This variability suggests that understanding the likely impact of the ecology of avian populations at the introduction site will be a key factor in our ability to predict WNV transmission risks. Beyond this, the resident bird population may also be very important as a possible overwinter reservoir for the virus. It has been seen that WNV can overwinter in roosts of North American crows (Hinton et al. 2015). WNV is believed to have overwintered in the Mediterranean basin in recent years, though it is currently unclear whether this overwintering was facilitated by the mosquito or avian population (Calistri et al. 2010; Sabatino et al. 2014), leaving this as an area requiring further investigation. The avian population is modelled explicitly in Chapter 5. First, in Chapters 2 - 4 I focus on the vector dynamics.

1.2.3 Environmental drivers of vector-borne disease

The mosquito life cycle (Figure 1.5), and thus the disease transmission cycle (Figure 1.3), of all mosquito species are affected by environmental conditions in a range of ways (Table 1.2). Mosquitoes are ectothermic, meaning that their physiology is governed by temperature (Ciota et al. 2014). The initiation and termination of the *Cx. pipiens* diapause process has been shown to respond to temperature and photoperiod cues (Sanburg and Larsen 1973; Madder et al. 1983b) and the immature stages of the life cycle are dependent on hydrological processes to create suitable habitats. It is also believed that other processes such as humidity may affect adult behaviour in a range of mosquito species (Lebl et al. 2013; Carrieri et al. 2014) and we know that temperature affects disease transmission processes (Hartley et al.

Process	Increasing temperature	Increasing larval habitat
Immature development rate	+	+
Immature survival	+/-	+
Adult lifespan	-	0
Gonotrophic cycle length	-	0
EIP duration	-	0
Biting rate	+	0

Table 1.2: Environmental driver effects on life cycle and transmission process: The table shows the direct effects of environmental drivers on life cycle and disease transmission processes: + signals an increase, - signals a decrease and 0 signals no change. Secondary effects, such as the potential for increased larval habitat to affect body size and therefore survival of emergent adults, are not considered.

2012). All of these environmental drivers can affect the mosquito life cycle in complex, non-linear ways, which makes understanding the impacts of environmental changes very challenging. I develop a mathematical model which explicitly incorporates the effects of some of these key environmental drivers on the mosquito life cycle to predict the impact of these drivers on seasonal abundance. Below, I present an overview of the wide range of environmental variables which impact *Cx. pipiens* life cycle and disease transmission processes.

Temperature

The development rate of the immature mosquito life stages is substantially influenced by temperature, with development from egg hatch until adult emergence of *Cx. pipiens* having been shown to take between 39 days at $10\,^{\circ}\mathrm{C}$ and 8 days at $30\,^{\circ}\mathrm{C}$ (Loetti et al. 2011). In the same study, Loetti et al. (2011) also found that immature survival ranged from 0% at $7\,^{\circ}\mathrm{C}$ to 76.4% at $25\,^{\circ}\mathrm{C}$, but dropped to 1.6% at $33\,^{\circ}\mathrm{C}$. Similarly, it has been shown that *Cx. pipiens* adult survival is strongly temperature-dependent, with expected adult longevity ranging from approximately 10 days at $32\,^{\circ}\mathrm{C}$ to just over 75 days at $16\,^{\circ}\mathrm{C}$ (Ciota et al. 2014). Further, adult biting behaviour is affected through the temperature-dependent progression of the gonotrophic cycle, which is the time required for an adult to digest a blood meal and use it for ovarian development. Madder et al. (1983b) found gonotrophic cycle lengths in *Cx. pipiens* varied from 15 days at $17\,^{\circ}\mathrm{C}$ to 5 days at $25\,^{\circ}\mathrm{C}$. This variability in adult longevity and gonotrophic cycle length will influence both the frequency of egg-laying events and the number of eggs laid in an individual's lifespan. These findings also show that the effects of temperature on population processes can also often be opposing, with increased temperatures leading to shorter adult life spans but also causing increased egg-laying rates. Temperature effects on the vector life cycle such as these will affect the exposure of at-risk populations

to vectors, thus influencing the R_0 value, through changes to the vector-host ratio, the biting rate and the mortality rate of vectors.

Temperature not only affects the population dynamics of mosquito species but also influences disease transmission processes and thus the hazard posed by vectors. The time taken for the virus to replicate in the cells of the mosquito midgut and travel to the salivary glands at high enough levels for the mosquito to become infectious is called the extrinsic incubation period (EIP) and is strongly temperature-dependent. Reisen et al. (2006a) found that the EIP for *Cx. tarsalis* infected with WNV ranged from approximately 30 days at $18\,^{\circ}\mathrm{C}$ to 6 days at $30\,^{\circ}\mathrm{C}$. This adds to the aforementioned complexity of the effects of temperature, as there is a trade off between increasing temperatures decreasing the length of the EIP but also decreasing the mosquito lifespan. Understanding variable effects of temperature on population and disease processes require models which explicitly incorporate the wide range of processes at play. By utilising functional relationships between temperature, life cycle and disease processes it is possible to make predictions about whether or not predicted climate change will increase WNV transmission risks in previously unaffected areas like the UK.

Photoperiod

It has been shown that temperature can also interact with photoperiod to trigger initiation and termination of diapause in *Cx. pipiens* (Spielman and Wong 1973; Sanburg and Larsen 1973; Madder et al. 1983b). This process will define the length of the mosquito biting season, thus influencing the exposure parameters to mosquitoes. Various laboratory studies have shown either one or both of temperature and photoperiod to be determinants of diapause behaviour. A general trend can be established that increasing photoperiod and temperature can be expected to decrease incidences of diapause in a given population (Spielman and Wong 1973; Sanburg and Larsen 1973; Madder et al. 1983b). However, diapause behaviour appears to be very variable across locations, dependent on both the lineage of the *Cx. pipiens* population in question and the rearing conditions of that population. For example, Spielman and Wong (1973) found that $< 5\%$ of adult females were diapausing at $18\,^{\circ}\mathrm{C}$ and 14 hours 45 minutes of sunlight for a population from Boston, Massachusetts. Madder et al. (1983b) found that 35% of individuals entered diapause in warmer conditions of $25\,^{\circ}\mathrm{C}$ with equal sunlight levels, for a population in Guelph, Ontario. However, the findings of each individual study show that, for a fixed photoperiod, increasing temperature should lead to a decreased incidence of diapause. The fact that comparing between studies shows the opposite effect implies that there must be some underlying difference between the two *Cx. pipiens* populations studied. This

geographic variation in diapause behaviour can make parametrising functions difficult without existing studies on the diapause behaviour of the geographic strain in question. There are currently no studies which draw together data from a range of locations to investigate geographic relationships between environmental drivers and diapause behaviour.

Hydrology

The first three life stages of *Cx. pipiens* (egg, larval and pupal) are aqueous stages with *Cx. pipiens* primarily choosing to lay their eggs in stagnant pools of water with a high organic content, which act as a food source (Vinogradova 2000). Given this, rainfall patterns combined with terrestrial hydrology will have a large impact on habitat availability and consequently on abundance patterns (Wang et al. 2011). Decreased rainfall will lead to an decrease in the number and size of available oviposition (egg-laying) sites, increasing the larval density across those sites. This causes an increase in both intra- and inter-specific competition for resources, leading to increased density-dependent mortality (Madder et al. 1983b) and an increase in development times (Alto et al. 2012). Further, droughts may lead to a decrease in the number of predator-free oviposition sites, as *Cx. pipiens* are known to be opportunistic in their egg-laying behaviour and will utilise small temporary pools such as cow hoof prints and pools of water in discarded tyres. Predation has been shown not only to increase larval mortality but also to increase development times as larvae use energy to avoid predators (Beketov and Liess 2007; Fischer et al. 2012).

However, it is also important to consider that dry periods will not necessarily lead to a decrease in mosquito abundance because of artificial wetting events. During dry periods people are known to increase their use of hose pipes and store water outside for their garden. This behaviour can create perfect mosquito breeding habitat even when environmental conditions are not good (Tran et al. 2013; Townroe and Callaghan 2014). In such cases, incidences of WNF may actually increase as mosquito populations may become concentrated in urban areas where human activities create breeding sites (Githeko et al. 2000). This would increase the rate at which vectors feed on humans, increasing the human biting rate, alongside increasing the vector-host ratio within urban areas. Further, it has been shown that droughts in semi-permanent wetlands, which only dry during drought years, may cause explosions in the mosquito population the year following a drought due to the removal of predators during the drought year (Chase and Knight 2003). In these ways it can clearly be seen that both biotic and a range of abiotic factors will interact to influence mosquito development, vector population size and exposure to vectors.

Other factors affecting population and disease processes

Some statistical studies using mosquito field capture data have shown that there is a positive relationship between relative humidity and *Cx. pipiens* abundance (Lebl et al. 2013; Carrieri et al. 2014). Wind speed has been seen to influence egg-laying behaviour, with strong winds interfering with mosquito flight and delaying oviposition (Lebl et al. 2013). However, these relationships have not been tested or quantified in laboratory or field studies, so further research would be required in order to include it in mathematical models. The source of the blood meal taken by the adult female mosquito is also known to affect the egg raft size, with individuals which have fed on birds generally developing larger egg rafts than those that have fed on mammals (Vinogradova 2000). The blood meal taken may have other effects but there is insufficient data to draw general conclusions or patterns.

1.2.4 Empirical field data collection

Mosquito trapping and surveillance programmes are key parts of disease monitoring networks and are also invaluable for the purpose of validating mathematical models of mosquito abundance. At present, such programmes tend to involve running networks of adult mosquito traps, which measure the number of host-seeking adults. Collections of the immature life stages, which give further information about the overall pattern of seasonal abundance across the life cycle, remain relatively rare. These programmes are well established in a number of different countries across continental Europe (Bogojević et al. 2009; Rosà et al. 2014; Ibanez-Justicia et al. 2015) and North America (CDC 2016a), where incidences of vector-borne disease occur regularly. However, given that mosquitoes do not presently transmit disease in the UK, surveillance remains minimal, though efforts have increased slightly in recent years (Townroe and Callaghan 2014; Medlock and Vaux 2015; Townroe and Callaghan 2015). Public Health England operates a network of twenty adult traps for two weeks of each month from mid-April to mid-October (PHE 2016), however these traps use a mammal lure and so are generally not attractive to *Cx. pipiens*, which are ornithophilic.

As previously alluded to, both different rearing conditions and differences in the strain of *Cx. pipiens* studied mean that there can be variability in life cycle response to environmental conditions (Tauber et al. 1986; Olejnícek and Gelbic 2000; Ruybal et al. 2016). Firstly, this means that using data collected from populations outwith the UK to parametrise my models may lead to slightly different predictions than those obtained if we were to calculate vital rates for UK populations directly. Secondly, it is likely that diapause behaviour in particular, of UK mosquitoes will differ from behaviour observed in other parts of *Cx. pipiens* range.

These facts highlight the importance of being able to compare model predictions from the UK with UK seasonal abundance data. This will allow necessary adjustments to be made to account for differences between the strains studied in the literature and those present in the UK and will allow us to understand whether extrapolating between the two can be considered valid. By comparing UK data with seasonal abundance data from across the *Cx. pipiens* range it will also be possible to correlate geographic trends in key behaviours and events, like diapause, with factors like photoperiodic and temperature regimes and determine whether the inferred relationships are consistent with mathematical population models.

1.3 Mosquito and disease modelling

1.3.1 Review of existing modelling approaches

Mosquito population models and disease models have typically been developed independently of one another, rarely being combined to understand patterns of transmission. The earliest models in the field tended to focus on disease transmission, without considering the life cycle of the vector or host populations. After the failure of DDT to eradicate mosquito populations due to the development of resistant genotypes, alongside the realisation of the environmental damage caused by DDT (Najera et al. 2011), models slowly began to look more closely at mosquito population dynamics (Reiner et al. 2013). Finally, researchers have begun to combine vector population models with disease transmission dynamics to make predictions about mosquito-borne disease, though these studies remain relatively rare (Smith et al. 2014).

Disease models that neglect vector dynamics

The theory supporting mathematical models of mosquito-borne pathogen transmission is commonly considered to have its origins in the works of Ronald Ross and George MacDonald (Ross 1898, 1910; MacDonald et al. 1968), though several mathematicians contributed to what is now considered the "Ross-MacDonald" model, which in actuality is a modelling framework based on a set of assumptions, rather than a single defined model (Smith et al. 2012). The "Ross-MacDonald model" has been written mathematically in a wide range of forms and is based on a simple description of the pathogen life cycle: pathogens are passed from the mosquito to the vertebrate host through blood-feeding, they multiply within the

vertebrate host until they reach sufficiently high densities in the hosts blood to infect a secondary mosquito, the secondary mosquito replicates the virus to transmissible levels and infects a second host through blood feeding. This work was developed with a focus on modelling malaria infections, however the same principles can be applied across the wide range of mosquito-borne diseases.

Perhaps the most common mathematical formulation of a "Ross-MacDonald" model centres around the use of ordinary differential equations (ODEs), though examples of Ross-MacDonald models based on delay-differential or difference equations can also be found. A good overview of the history and development of many of these models is given by Smith et al. (2012). The simplest Ross-MacDonald models focus on infectious mosquitoes, the pathogen itself and the vertebrate host population. One example of such a model developed to study malaria transmission is given in Smith and McKenzie (2004),

$$\begin{aligned} \frac{dX}{dt} &= \overbrace{\iota\mathcal{B}\mathcal{T}_{AX}A(1-X)}^{\text{rate of infection}} - \overbrace{\mathcal{R}X}^{\text{death}}, \\ \frac{dA}{dt} &= \underbrace{\mathcal{B}\mathcal{T}_{XA}X(\underbrace{e^{-\delta\tau_{EIP}}}_{\text{EIP delay}} - A)}_{\text{rate of infection}} - \underbrace{\delta A}_{\text{death}}, \end{aligned} \tag{1.1}$$

where X denotes the proportion of infected humans, A gives the proportion of infected adult mosquitoes, ι represents the vector to host ratio, $\mathcal{B}$ is the mosquito biting rate, $\mathcal{T}_{AX}$ and $\mathcal{T}_{XA}$ are the mosquito-to-human and human-to-mosquito transmission rates, respectively, τ_{EIP} is the length of the EIP, $\mathcal{R}$ is the recovery rate of humans and δ is the death rate of mosquitoes.

By utilising a relatively straightforward modelling framework like this it is possible to calculate a range of useful metrics to help understand the epidemiology of the disease. One such metric is the entomological innoculation rate, EIR, which gives the number of infectious bites received per day by a human and is considered as a good, relative measure of transmission intensity in a region (Kelly-Hope and McKenzie 2009)

$$EIR = \frac{\iota\mathcal{B}^2\mathcal{T}_{XA}Xe^{-\delta\tau_{EIP}}}{\delta + \mathcal{B}\mathcal{T}_{XA}X}. \tag{1.2}$$

Another useful quantity which can be defined for this model is the vectorial capacity, C_v. The vectorial capacity is defined as the total number of potentially infectious bites that would

eventually arise from all mosquitoes biting a single perfectly infectious host (a host from which all bites resulted in infection of the vector) on a single day (Brady et al. 2016)

$$C_v = \frac{\iota \mathcal{B}^2 e^{-\delta \tau_{EIP}}}{\delta}. \tag{1.3}$$

The vectorial capacity is widely used in considering mosquito control measures, as reducing the number of potential infectious bites arising from a single infectious host would clearly reduce the potential for disease transmission. Another closely related metric is the R_0 value, which is also used to asses control scenarios, with R_0 values greater than one signifying that a disease outbreak can be expected,

$$R_0 = \frac{\iota \delta C_v}{\mathcal{R}}. \tag{1.4}$$

These metrics and relationships can be very useful in considering a range of different epidemiological scenarios. For example, one could predict the extent of an outbreak if a pathogen was introduced to a new area, or one could investigate the effects of different control scenarios on R_0 values, and thus on the possibility of an epidemic. In the example highlighted from Smith et al. (2004), the authors examine the relationships between EIR and R_0 values and the equilibrium infection in the human population. This information is used to explore the effectiveness of malaria control measures.

Whilst it is a valuable tool, this classical Ross-MacDonald-style model makes a number of simplifying assumptions about the transmission dynamics and how they are affected by the mosquito life cycle. Some examples of this include that this model ignores seasonality in the vector population, assuming that mosquito and human population sizes remain fixed, which will affect the vector to host transmission rate and thus predictions of the EIR, C_v, and R_0. Further, there is no consideration of immunity or asymptomatic individuals, which will affect transmission dynamics, meaning that humans can no longer be categorised as simply infected or uninfected, again affecting the metrics calculated. Further, the mortality during the EIP of the virus is included but the time delay is not. If this were to be modelled accurately then it may affect the entire dynamics of the system. Work in the field of mosquito-borne diseases over the last half century has centred around understanding the effects of the simplifying assumptions of the Ross-MacDonald framework (Reiner et al. 2013). I continue this trend by explicitly modelling the life cycle of the vector population, and in Chapter 5 the host

population and the temperature dependence on the EIP in the vector, thus removing a great many assumptions from the original Ross-MacDonald model.

A number of papers utilised and extended the Ross-MacDonald framework to look specifically at the dynamics of WNV (Bowman et al. 2005; Liu et al. 2006; Maidana and Yang 2009; Hartley et al. 2012; Bergsman et al. 2015; Robertson and Caillouet 2016). Cruz-Pacheco et al. (2005) develop a model where the vector and avian populations are split into compartments according to whether they are susceptible (S), infectious (I) or recovered (R) and vertical transmission of the virus within the vector population is allowed to occur. This SIR-type model is consistent with the classical Ross-MacDonald framework but allows hosts to potentially develop immunity after recovery. By using a relatively simple modelling structure it is straightforward to perform mathematical analyses on the model, allowing calculation of the R_0 value,

$$R_0 = \frac{\overbrace{\iota \mathcal{T}_{AX} \mathcal{T}_{XA} \mathcal{B}^2}^{\text{vector \& host}}}{\underbrace{(1 - p_{vt})\delta_A}_{\text{vector}} \underbrace{(\mathcal{R}\delta_A \delta_{WNV})}_{\text{host}}}, \tag{1.5}$$

where p_{vt} is the probability of vertical transmission, δ_A and δ_B are the adult mosquito and bird death rates, $\mathcal{R}$ is the recovery rate of birds, δ_{WNV} is the WNV-induced death rate of birds and all other parameters are as previously defined. Cruz-Pacheco et al. (2005) calculated R_0 values for eight well-studied bird species and found values ranging from 3.60 to 6.97. The authors also carry out model simulations, showing that the system exhibits damped oscillations towards an endemic equilibrium of WNV infection in the bird population. They show that WNV prevalence is expected to become very high immediately after introduction, with approximately 30% infection after 10 days, dependent on the bird species. Infection then settles to an equilibrium prevalence of approximately 0.05%, again dependent on the bird species.

The high initial levels of infection in the bird population are to be expected given the relatively high R_0 values reported. However, the EIP, which is a key feature of the disease transmission cycle has been omitted in this model. Inclusion of this process would be expected to delay the peak prevalence seen in the avian population, as mosquitoes will take longer to become infectious. Further, it could be expected to substantially reduce the R_0 and

vectorial capacity values, as was previously seen to occur in Equations 1.3 and 1.4. The classification of adults as only either infected or uninfected also ignores the physiological factors which influence the adult behaviour, such as the completion of successive gonotrophic cycles. Only adult females which have taken a blood meal and completed a gonotrophic cycle may then be infectious when taking subsequent blood meals, which will affect the proportion of infectious adults. Another key feature of this study is that it typically takes well in excess of one year to reach the endemic equilibrium infection in the avian population, which is clearly much longer than the scale of seasonality in environmental variables. This highlights that, whilst the initial dynamics upon introduction are very important, the long term dynamics must be interpreted with caution, as seasonality in the vector and host populations will substantially affect disease transmission. Further, the R_0 values calculated do not account for temporal variation in parameters due to seasonality in drivers like temperature and photoperiod. Many of the parameters involved in calculation of R_0, such as the biting rate and the vector-to-host ratio will be seasonal and temperature-dependent. In this case, approaches such as that presented by Charron et al. (2011), who calculate a seasonally varying $R_0(t)$ to quantify the risks of bluetongue transmission amongst cattle by biting midges, can be used. This allows the number of secondary infections from a single infection at time t, given by $A(t)$, to be calculated, giving a series of estimated R_0 values if the virus were to be introduced at each point in time throughout the season. The average seasonal risk is then given by R_s, which is the average of $A(t)$ over the season. The authors are able to use this approach to examine the efficacy of different vaccination strategies.

Mosquito population models

The dependence of disease transmission processes on the mosquito life cycle means that mosquito population models can be used to add information to disease models. Explicit modelling of the mosquito life cycle can give more information about important features, such as patterns of seasonal abundance or mosquito dispersal, which will influence exposure to mosquitoes. As with disease models, ODEs are a commonly used tool for modelling the vector life cycle because they are easily analysed and simulated (Cailly et al. 2012; Lunde et al. 2013; Lutambi et al. 2013; Tran et al. 2013; Wang et al. 2016). One example of this can be found in the work of Erickson et al. (2010b), who develop a stage-structured,

temperature-forced *Aedes albopictus* population model using ODEs:

$$\begin{aligned}
\frac{dE}{dt} &= A_r e_p - E(g_e + \delta_e), \\
\frac{dL}{dt} &= ET_e - L(g_l + \delta_l) - K_0 L^2, \\
\frac{dP}{dt} &= LT_1 - P(g_p + \delta_p), \\
\frac{dA_i}{dt} &= PT_p - A_i(g_i + \delta_a), \\
\frac{dA_G}{dt} &= A_i\delta_i + A_r g_r - A_G(g_G + \delta_a), \\
\frac{dA_r}{dt} &= A_G\delta_G - A_r(g_r + \delta_a),
\end{aligned} \tag{1.6}$$

where E, L and P denote the immature life stages of eggs, larvae and pupae respectively, A_i, A_G and A_r denote immature, gestating and reproducing adults, e_p is the number of eggs per oviposition, δ_x and g_x gives the mortality and development rates of a given stage, x, respectively, and K_0 is the larval death rate. By explicitly capturing the immature stage dynamics this model can make more informed predictions about adult mosquito abundance. This model also captures the dynamics within the adult stage by defining adults as immature, gestating, or ovipositing, thus giving a more realistic estimate of what proportion of adults have the potential to be infectious. The authors calculate steady states and carry out stability and sensitivity analyses to understand which model parameters are particularly influential determinants of mosquito abundance. The authors found that the inclusion of seasonality, through temperature-dependence, led to substantial seasonality in the sensitivity of the model to different parameters. They also extend their series of ODEs to a series of stochastic differential equations (SDEs) to take into account stochasticity in the population and to compare simulations with a 7-year empirical field dataset on *Ae. albopictus* in Texas. The model performs well, capturing between 62.1% and 77.5% of observed non-zero data points within its 95% confidence limit. However, the authors report that one of the main shortcomings of their model was that the timing of seasonal peaks predicted by the model often differed from those observed in the field. One possible reason for this phase difference between field observations and predictions is that the hatching time of the overwintering egg population may have been poorly estimated or the development rate of one or more of the life stages may not have represented field conditions. It is also possible that this discrepancy between timings may stem from the fact that the model structure used does not allow the explicit inclusion of developmental lags. This means that time spent in each class is exponentially distributed with a constantly varying mean dependent on the temperatures experienced. When using ODEs, developmental lags can be approximated by using the linear-chain trick, by splitting a

given stage into multiple sub-stages so that the total stage length becomes gamma-distributed (Wearing et al. 2004). This approach was applied in a dengue model by McLennan-Smith and Mercer (2014), though here the authors do not account for the temperature-dependence of the vital rates.

To explicitly incorporate stage duration when modelling vector populations, one can include stage-structure directly within the model framework (Liu et al. 2002). This involves splitting the population into stages corresponding to the life stages of the modelled species, under the assumption that all individuals within a stage are functionally identical. Matrix population modelling is a common tool by which stage-structured populations can be modelled (Caswell 2001). The general formulation is such that a population, n, of k stages, at time t, can be defined by the stage-distribution vector, $\mathbf{n}(t)$, such that

$$\mathbf{n}(t) = \begin{bmatrix} n_1(t) \\ n_2(t) \\ \vdots \\ n_k(t) \end{bmatrix}. \tag{1.7}$$

Changes in this population through each time step are then applied using the population-projection matrix, $\mathbf{A}$, with

$$\mathbf{A} = \begin{bmatrix} F_1 + P_1 & F_2 & \cdots & F_k \\ G_1 & P_2 & \cdots & 0 \\ \vdots & \vdots & \ddots & \vdots \\ 0 & \cdots & G_{k-1} & P_k \end{bmatrix}, \tag{1.8}$$

where F_i gives the fecundity of stage i, G_i gives the probability of surviving stage i and growing to stage $i+1$ and P_i gives the probability of surviving stage i. The projection matrix can be modified depending on the dynamics of the population being modelled.

In mosquito modelling, these models inherently allow for the population to be broken down into life stages by assigning rows in a matrix to each life stage, where individuals transition between stages with a given probability, generally dependent on current climatic conditions (Ahumada et al. 2004; Schaeffer et al. 2008; Yusoff et al. 2012; Lončarić and Hackenberger 2013). This modelling framework was utilised by Schaeffer et al. (2008) who modelled

seasonal dynamics of different mosquito species of the *Aedes* genus, accounting for rainfall effects on habitat size and availability. They simulated mosquito abundances over a year and saw slight overestimation of the population size, though the agreement between the model and data with regards to the model's ability to capture the trend was good. Like the SDE approach (Erickson et al. 2010a), this approach accounts for stochasticity in population processes well and it is relatively straightforward to simulate. However, this model was designed to estimate mosquito abundances in the Ivory Coast, which experiences a tropical climate and so temperature-dependencies were excluded from the model in favour of dependencies on rainfall patterns.

Lončarić and Hackenberger (2013) develop climate-dependent matrix population models for *Aedes vexans* and *Cx. pipiens* with one-day projection intervals and extend this framework by splitting each life stage into numerous sub-stages, thus creating developmental lags. For example, the authors split the larval stage into 26 sub-stages and on any given day allow members of each sub-stage to either transition to the next full stage with some probability or to transition within the existing stage to the next sub-stage. This novel approach addresses many of the shortcomings of previous matrix population models by ensuring that the probability an individual progresses to the next life stage is dependent not only on the current life stage and environmental conditions but also on the length of time spent in that stage. The authors simulated this model over a three year period, comparing the simulated results to field data, and found good agreement for *Aedes vexans* but not for *Cx. pipiens*, where the model was prone to overestimation of annual abundance. The authors hypothesise that this may be due to ongoing control efforts and the relative rarity of *Cx. pipiens* in the study area. However, I would also suggest that the overestimation of abundance may stem from their estimate of zero adult mortality in winter, which is inaccurate (Sulaiman and Service 1983). One shortcoming of this method is that it requires that each life stage is split into a suitable number of sub-stages and that one must find an appropriate method by which transition probabilities for each sub-stage can be accurately defined. Defining these transition probabilities for each stage is difficult in absence of clear biological endpoints at which to measure. This is a very involved and cumbersome approach, particularly when the number of life stages and sub-stages is large.

Mosquito population models are very valuable as they give important information about the seasonality of the vector population, which will affect disease transmission through terms like the vector-to-host ratio and the mosquito biting rate. However, without explicitly incorporating disease transmission processes one cannot test the likelihood that epidemic or endemic scenarios may occur upon pathogen introduction. Given this, combined approaches

which incorporate the mosquito life cycle, the disease transmission cycle and environmental effects on both processes will be required.

Combined vector and disease models

Models which combine the vector life cycle with disease transmission processes are rare and can vary massively in complexity, with the simplest extensions only taking very small steps beyond standard disease models. At present, a common technique is to utilise ODE models, adopting an SEIR compartmental framework. Wonham et al. (2004) extend an ODE-based SEIR model for WNV by including a compartment for the larval mosquito population (Figure 1.6). This relatively simple extension increases the biological realism of the model, by accounting for the development time required for offspring to join the adult class. This allows more informed predictions about the adult population size to be made, giving more information about the vector-to-host ratio. By keeping the complexity of the model structure to a minimum and ignoring the relationship between environmental variables and life cycle parameters, the model remains analytically tractable and the authors can calculate R_0 values and equilibrium abundances by standard techniques. However, the relative simplicity of the model means that many of the problems faced by standard disease models are still present. In particular, the lack of climate dependencies mean that development rates and mortalities of the mosquito life stages, along with key disease transmission cycle parameters, such as the biting rate and the EIP, will be inaccurate. This will be particularly true in climates where temperature variations will be large. The authors incorporate some seasonality in the model, though they do so by using a step function which forces the mosquito population to take one size in summer and another in winter. This approach was taken to maintain a model which was analytically tractable, though it is not very biologically realistic. Some information can be gleaned about the sensitivity of disease transmission to variability in population size, however it does not consider the causes of these population fluctuations and the joint impacts these may have on disease transmission.

More complex ODE models which account for a wider range of mosquito life cycle and disease transmission processes have also been developed. Erickson et al. (2010a) present a dengue model for a dynamic *Aedes albopictus* population, including compartments for eggs, larvae, pupae, immature adults, gestating adults and reproducing adults, alongside compartments for susceptible, exposed, infectious and recovered humans (Figure 1.7). By incorporating this range of mosquito adult sub-stages, alongside progression between susceptible, exposed and infectious classes, the complex vector biology is captured in much more detail than in previous models. The authors examine the behaviour of the model over a period of

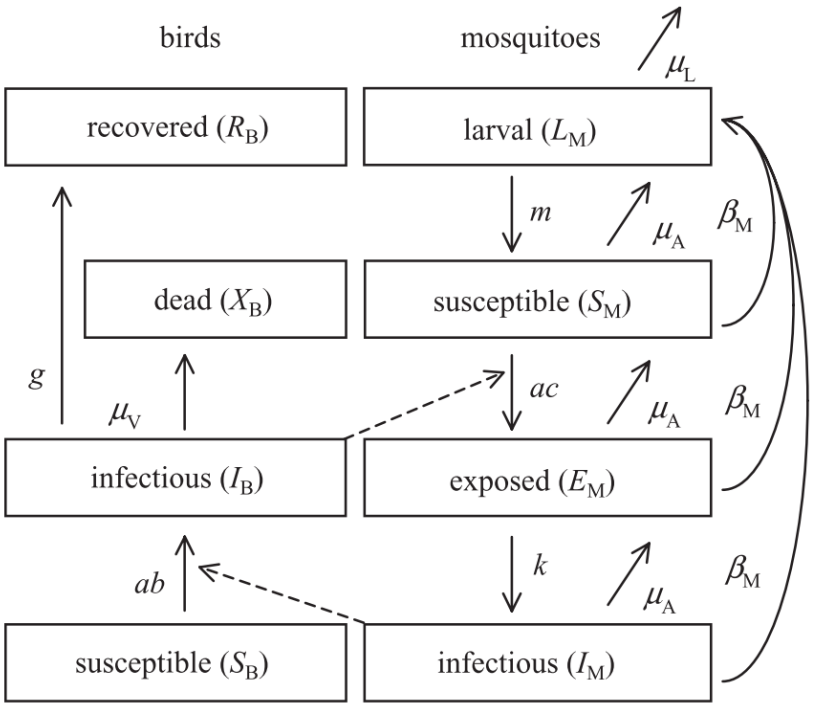

Figure 1.6: Wonham et al. (2004) model flow chart. The notation is as given in the Wonham et al. (2004) paper.

a year, both under constant temperature conditions and under temperatures observed in Lubbock, Texas. Without comparing the model to empirical field data it is not possible to draw conclusions about whether or not the added complexity of this model leads to a more accurate representation of mosquito and disease seasonality. However, the use of ODEs again means that the stage durations for each life stage and for the EIP will be exponentially distributed, which is unlikely to be a true representation of the duration (Wearing et al. 2004). Given this, an approach which allows a temperature-dependent delay, where all individuals which enter the stage at time $t - \tau(T)$ will leave at time t, where T denotes the temperature and $\tau(T)$ denotes the stage length, would be desirable.

1.3.2 The delay-differential equation method

Delay-differential equations (DDEs) were championed as a tool for modelling the life cycle of insect populations by Gurney et al. (1983). The authors sought to develop a framework to encourage an increased focus on age structure effects when studying natural populations: an area which had previously been widely neglected due to technical difficulties in formulating age-structured models. At the time some study had been devoted to the area, however the existing continuous-time approach developed by Sharpe and Lotka (1911) and Foerster (1959) was sufficiently mathematically complex to discourage the majority of modellers. A discrete

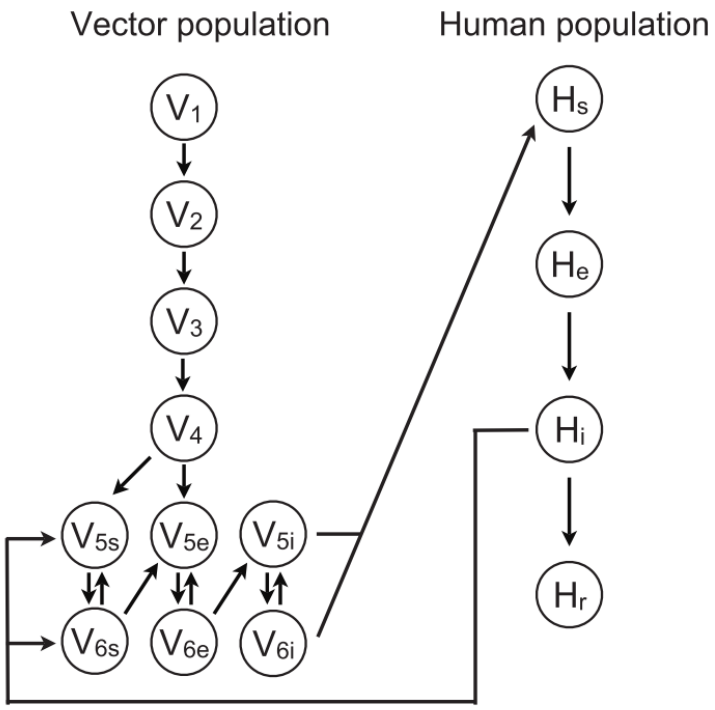

Figure 1.7: Erickson et al. (2010a) model flow chart: The notation is as given in the Erickson et al. (2010a) paper. The model depicted contains susceptible H_s, exposed H_e, infectious H_i, and recovered H_r human populations and a mosquito population with 6 life stages (eggs, V_1; larvae, V_2; pupae, V_3; immature adults, V_4; gestating adults, V_5; reproducing adults, V_6). The last two adult mosquito stages are further broken down into susceptible (V_{5s} and V_{6s}), exposed (V_{5e} and V_{6e}), and infectious stages (V_{5i} and V_{6i}). All of the human populations contribute to new humans, who are born susceptible (H_i). Only the reproducing adult mosquitoes (V_6) lay eggs (V_1). The lines depicting population growth were omitted to simplify the figure

time approach was also available, in the Leslie matrix approach, however this relied on the partition of the population into a series of equal duration age classes, which excluded the possibility of splitting the population according to life stages, which may have variable development (Leslie 1945, 1948). Gurney et al. (1983) develop a framework utilising key principles from the continuous age-structured partial differential equation (PDE) framework put forth by Sharpe and Lotka (1911) and Foerster (1959). By assuming all individuals in a particular age class are functionally identical the authors retain the mathematical rigour of the original von Foerster description whilst substantially reducing the complexity of the mathematical analysis. The assumption that all individuals in a particular developmental stage are functionally identical means the integro-differential equations used to describe age-structured populations can be replaced by a set of coupled DDEs, which are much more straightforward to solve numerically. This framework is particularly appropriate for insect populations since individuals often must develop through multiple stages, moulting many times, before reaching maturity and the behaviours and vital rates of individuals within a stage are generally very similar. Modelling in this way results in some loss of age-distribution realism, however it grants greater analytical and computational tractability.

Lumped age class formalism

Here I present a detailed derivation of the Gurney et al. (1983) framework by which the population can be modelled through a series of lumped age classes, as this forms the basis of my work. First, consider the situation where individuals are treated as having a continuous age distribution and all individuals of age a at time t have the same per capita death and reproduction rates given by $\delta(a,t)$ and $b(a,t)$, respectively. The age-distribution can be defined as

$$f(a,t) \equiv \lim_{da \to 0} \left[\frac{\text{no. of individuals aged between } a \text{ and } a + da \text{ at } t}{da} \right]. \tag{1.9}$$

Changes in the age distribution as a result of deaths and ageing can then be described by the von Foerster equation, as

$$\frac{\partial f(a,t)}{\partial t} = \underbrace{-\frac{\partial f(a,t)}{\partial a}}_{\text{ageing}} \underbrace{-\delta(a,t) f(a,t)}_{\text{death}}. \tag{1.10}$$

Considering that all newborn individuals must enter the system at age zero this must be solved subject to the renewal condition

$$f(0,t) = B(t) = \int_0^\infty f(a,t)b(a,t)da, \tag{1.11}$$

where $B(t)$ gives the number of newborns at time t, assuming that the population is closed.

Equation 1.10 can be solved using the method of characteristics. Parameterising the characteristic curve by ξ and applying the chain rule to reduce the PDE to a series of ODEs gives,

$$\frac{\partial f}{\partial \xi} = \frac{\partial f}{\partial a}\frac{\partial a}{\partial \xi} + \frac{\partial f}{\partial t}\frac{\partial t}{\partial \xi} = -\delta(t)f, \tag{1.12}$$

with,

$$\frac{\partial a}{\partial \xi} = 1, \tag{1.13}$$

$$\frac{\partial t}{\partial \xi} = 1, \tag{1.14}$$

$$\frac{\partial f}{\partial \xi} = \delta(t)f. \tag{1.15}$$

$$\tag{1.16}$$

Solving Equations 1.13 and 1.14 for a and t gives

$$a = \xi + c_1 \text{ and } t \quad = \xi + c_2, \qquad c_1, c_2 \in \mathbb{R}. \tag{1.17}$$

Now determine the boundary conditions,

$$\xi = 0 \Rightarrow a(0) = 0, \tag{1.18}$$

$$t(0) = c_2 \tag{1.19}$$

since the starting age is zero. Hence, $a(0) = \xi$ and $t(0) = \xi + c_2$. Therefore,

$$\begin{aligned} \frac{df}{d\xi} &= -\delta(\xi) f, \\ f(\xi) &= f(0) \exp\left(- \int_{\xi'=0}^{\xi} \delta(\xi') d\xi' \right), \end{aligned} \tag{1.20}$$

where ξ' is a dummy variable. Shifting back to a and t gives

$$f(a,t) = f(a(0), t(0)) \exp\left(- \int_{t'=0}^{t} \delta(t') dt' \right). \tag{1.21}$$

Using the fact that $a(0) = 0$ and $t(0) = c_2$ in combination with $t(\xi) = \xi + c_2$ and $a(\xi) = \xi$ it follows that $\xi = a$ and $t(\xi) = a(\xi) + t(0)$. Hence, $t(0) = t - a$ and the solution to Equation 1.10 can be written as

$$\begin{aligned} f(a,t) &= f(0, t-a) \exp\left(- \int_{t-a}^{t} \delta(t') dt' \right), \\ &= B(t-a) S(t-a, a), \end{aligned} \tag{1.22}$$

where the cumulative survival probability for the population is defined as

$$\begin{aligned} S(t,a) &\equiv \text{Probability an individual born at time t survives to at least age a,} \\ &= \exp\left(- \int_{t}^{t+a} \delta(x-t, x) dx \right). \end{aligned} \tag{1.23}$$

Now, consider that the population is split into n age classes, such that $i = 1, 2, ..., Q$ denotes the ordered age class. It is assumed that all individuals within an age class are functionally identical, such that

$$\begin{aligned} \delta(a,t) &= \delta_i(t) \qquad \forall a_i \le a \le a_{i+1}, \\ b(a,t) &= b_i(t) \qquad \forall a_i \le a \le a_{i+1}, \end{aligned} \tag{1.24}$$

and that transitions between classes take place at fixed ages. Consider the age of entry into functional class i to be a_i and the age of maturation into class $i+1$ to occur at age a_{i+1}. The sub-population of class i at time t, $N_i(t)$, is then the number of individuals in the age range $a_i \le a \le a_{i+1}$,

$$N_i(t) = \int_{a_i}^{a_{i+1}} f(a,t)da. \tag{1.25}$$

Equations for N_i can be expressed in the form of the balance equation

$$\frac{dN_i(t)}{dt} = R_i(t) - M_i(t) - \delta_i(t)N_i(t) \qquad \text{[recruitment - maturation - deaths]}, \tag{1.26}$$

where $R_i(t)$ is the rate of recruitment from class $i-1$ into class i at time t and $M_i(t)$ is the rate of maturation from class i into class $i+1$ at time t. By integrating Equation 1.10 over the interval $a_i \le a \le a_{i+1}$ one can arrive at expressions for $R_i(t)$ and $M_i(t)$ as follows

$$\begin{aligned} \int_{a_i}^{a_{i+1}} \frac{\partial f(a,t)da}{\partial t} &= -\int_{a_i}^{a_{i+1}} \frac{\partial f(a,t)da}{\partial a} - \int_{a_i}^{a_{i+1}} \delta(a,t)f(a,t)da, \\ \frac{dN_i(t)}{dt} &= -f(a_{i+1},t) + f(a_i,t) - \delta_i(t)N_i(t), \\ \text{Hence,} \qquad R_i(t) &= f(a_i,t) \quad \text{and} \quad M_i(t) = f(a_{i+1},t). \end{aligned} \tag{1.27}$$

Defining that newborns go into age class $i = 1$ ($a_i = 0$), and using the assumption that birth rates are constant within an age class (Equation 1.24), it can be seen from Equation 1.11 that

$$R_1(t) = f(0,t) = B(t) = \sum_{j=1}^{Q} b_j \int_{a_i}^{a_{i+1}} f(a,t)da, \tag{1.28}$$

$$= \sum_{j=1}^{Q} b_j(t)N_j(t). \tag{1.29}$$

By substituting the solution (Equation 1.22) into the continuity equations (Equation 1.27) it can be seen that

$$\begin{aligned} R_i(t) &= B(t-a_i)S(t-a_i,a_i) \qquad i = 2,...,Q \\ M_i(t) &= B(t-a_{i+1})S(t-a_{i+1},a_{i+1}) \qquad i = 1,...,Q-1. \end{aligned} \tag{1.30}$$

Now, define the duration of age class i to be $\tau_i \equiv a_{i+1} - a_i$. The survival, $S_i(t)$ of an individual through age class i is

$$S_i(t) = \frac{\overbrace{S(t-a_{i+1}, a_{i+1})}^{\text{Survival of individuals born at } t-a_{i+1} \text{ to age } a_{i+1}}}{\underbrace{S(t-a_{i+1}, a_i)}_{\text{Survival of individuals born at } t-a_{i+1} \text{ to age } a_i}} \tag{1.31}$$

to be the proportion of individuals at $t - \tau_i$ who survive to $i + 1$ at t. Using Equations 1.30 with these definitions for τ_i and $S_i(t)$ one can relate maturation to recruitment as follows

$$\begin{aligned}
\frac{M_t(t)}{R_i(t-\tau_i)} &= \frac{B(t-a_{i+1})S(t-a_{i+1}, a_{i+1})}{B(t-a_i-\tau_i)S(t-a_i-\tau_i, a_i)} \\
\frac{M_t(t)}{R_i(t-\tau_i)} &= \frac{B(t-a_{i+1})S(t-a_{i+1}, a_{i+1})}{B(t-(a_i+\tau_i))S(t-(a_i+\tau_i), a_i)} \\
\frac{M_t(t)}{R_i(t-\tau_i)} &= \frac{B(t-a_{i+1})S(t-a_{i+1}, a_{i+1})}{B(t-a_{i+1})S(t-a_{i+1}, a_i)} = S_i(t).
\end{aligned} \tag{1.32}$$

The rate of maturation out of class i at time t is simply the rate of recruitment into class i at $t-\tau_i$ multiplied by the probability of survival. This allows us to rewrite the balance equation (Equation 1.26) as

$$\frac{dN_i(t)}{dt} = R_i(t) - R_i(t-\tau_i)S_i(t) - \delta_i(t)N_i(t), \tag{1.33}$$

so instead of the PDE one can now describe population densities using a system of coupled delay-differential equations. By setting the τ_i terms to correspond to the durations of mosquito life stages, or disease transmission processes like the EIP, one can capture the developmental delays in the mosquito life cycle. The recruitment equations can be written explicitly as

$$R_i(t) = \begin{cases} \sum_{j=1}^{Q} b_j(t)N_j(t) & \text{if } i = 1, \\ R_{i-1}(t-\tau_{i-1})S_{i-1}(t) & \text{if } i = 2, ..., Q. \end{cases} \tag{1.34}$$

To solve the Equation 1.33 initial conditions for $t = 0$ and historical values for $t < 0$ are required. The standard approach is to consider a system where

$$N_i(t) = 0 \qquad \forall i \text{ and for } t \leq 0. \tag{1.35}$$

Inoculation of the system occurs for a small time period $0 \leq t \leq T_1$ over which individuals are added to the system. This is done by modifying the recruitment equations, such that

$$R_i(t) = \begin{cases} B(t) + I_i(t), & \text{if } i = 1 \\ M_{i-1}(t) + I_i(t), & \text{if } i = 2, ..., Q \end{cases} \tag{1.36}$$

where $I_i(t)$ is the rate at which individuals aged exactly a_i are added to the age class at time t and $B(t)$ is the birth rate of individuals into the first age class. $I_i(t)$ can be specified such that

$$I_i(t) = \begin{cases} J_i, & 0 \leq t \leq t_1 \\ 0, & \text{otherwise} \end{cases} \tag{1.37}$$

where J_i denotes the rate at which individuals are added to the system. The inoculation equations can then be added into the recruitment equations to describe the system for all t,

$$R_i(t) = \begin{cases} \sum_{j=1}^{Q} b_j(t) N_j(t) + I_i(t), & \text{if } i = 1 \\ R_{i-1}(t - \tau_{i-1}) S_{i-1}(t) + I_i(t). & \text{if } i = 2, ..., Q \end{cases} \tag{1.38}$$

In summary, we arrive at the set of delay-differential equations

$$\frac{dN_i(t)}{dt} = R_i(t) - R_i(t - \tau_i) S_i(t) - \delta_i(t) N_i(t), \tag{1.39}$$

subject to the initial conditions

$$\begin{aligned} &N_i(t) = R_i(t) = I_i(t) = 0 \qquad -\max_i(\tau_i) \leq t \leq 0, \text{ all } i, \\ &S_i(0) = \exp\left(- \int_{-\tau_i}^{0} \delta_i(x) \right) dx. \end{aligned} \tag{1.40}$$

The first of these simply states that the system is empty in the time leading up to $t = 0$. The second defines the probability of survival for class i in the period, of length its lag, leading up to $t = 0$.

As discussed by Gurney et al. (1983), the use of time delays, τ_i, which make the model so well suited to modelling age structured populations, make models of this form very difficult to analyse. Whilst exceptions exist, analysis of models within this framework is often restricted to the determination of steady states and their corresponding stability.

1.3.3 Extension to include variable delays

The work presented by Gurney et al. (1983) allows for the explicit inclusion of developmental delays in the mosquito life cycle. However, to allow these delays to be variable, dependent on the environmental conditions experienced, one must look to the work of Nisbet and Gurney (1983). This work extends the framework to allow dynamically varying stage durations. In doing so the authors allow progression between the stages to occur as a result of a developmental process, rather than by chronological age. In the model developed by Nisbet and Gurney (1983) this variation in stage duration is dependent on the rate of weight gain, which is determined by the availability of food. Their approach can be extended to allow variation as a result of a range of biotic or abiotic factors, including temperature.

Formalism for dynamically varying stage duration

I present the theory behind the Nisbet and Gurney (1983) framework and describe how the underlying continuous age structure PDE model can be reduced to a set of DDEs. Consider the density function $f(a, m, t)$ defined such that $f(a, m, t)dadm$ is the number of individuals at time t with age in the infinitesimally range a to $a + da$ and at a point on some arbitrary development (or maturation) scale in the similarly small range m to $m + dm$. The use of this development scale differentiates this method from the previous age-dependent formalism, as individuals now move between stages based on the rate of development, which may vary, rather than purely through ageing. This gives the following balance equation to describe the processes of ageing, development and death of individuals present in the population at time t

$$\frac{\partial f}{\partial t} = -\frac{\partial f}{\partial a} - \frac{\partial}{\partial m}[gf] - \delta f, \qquad (a > 0) \tag{1.41}$$

in which g and δ (both functions of development, m, and age, a, at time t) represent the development (or growth) and instantaneous per capita death rate of individuals respectively. Equation 1.41 is solved subject to a renewal condition

$$f(0,m,t) = \int_{a=0}^{\infty}\int_{m=0}^{\infty} b(a,m',m,t)f(a,m',t)\,da\,dm', \tag{1.42}$$

in which $b(a,m',m,t)$ is the per capita rate of production of offspring of development level m at time t by individuals of development level m' and age a. Equation 1.41 and 1.42 can be simplified by assuming that g, b and δ are independent of age, allowing Equation 1.41 to be recast by defining

$$\rho(m,t) \equiv \int_{0}^{\infty} f(a,m,t)da. \tag{1.43}$$

Integrating Equation 1.41 over all ages then gives

$$\frac{\partial\rho}{\partial t} = f(0,m,t) - \frac{\partial}{\partial m}[g\rho] - \delta\rho. \tag{1.44}$$

Now by assuming that all individuals are equally developed at birth, $m = m_1$, then $f(0,m,t) = 0$ unless $m = m_1$, and so Equation 1.41 can be rewritten as

$$\frac{\partial\rho}{\partial t} = -\frac{\partial}{\partial m}[g\rho] - \delta\rho, \qquad (m > m_1) \tag{1.45}$$

where $\rho(m,t)dm$ represents the number of individuals in the development range m to $m+dm$ regardless of age. To obtain a boundary condition for Equation 1.45, simplify Equation 1.42 by assuming age-independent rates

$$R_1(t) = \int_{m_1}^{\infty} b(m,t)\rho(m,t)dm. \tag{1.46}$$

To derive a boundary condition note that the total recruitment during the infinitesimal time interval t to $t+dt$ is given by $R_1(t)dt$ and that these recruits will, at time $t+dt$ be developed

in the range m_1 to $m_1 + dm_1$ where $dm_1 = g(m_1, t)dt$. Since the total number of individuals with masses in that range is $\rho(m_1, t)dm_1$ it follows that

$$R_1(t)dt = \rho(m_1, t)dm_1 = \rho(m_1, t)g(m_1, t)dt, \tag{1.47}$$

meaning

$$g(m_1, t)\rho(m_1, t) = \int_{m_1}^{\infty} b(m, t)\rho(m, t)dm \tag{1.48}$$

is the renewal condition. Therefore, an insect population with fecundity, growth, and death rates which are mass dependent but age independent and where all recruits start with the same mass, has dynamics completely specified by the balance equation 1.45 and the renewal condition 1.48.

By making simplifying assumptions the PDE formulation can be reduced to a system of structured DDEs:

- We assume that growth of the insects involves n developmental stages

$m_1 \to m_2$	$m_2 \to m_3$	$\cdots$	$m_n \to m_{n+1}$
stage 1	stage 2	$\cdots$	stage n
eggs	1st instar larvae	$\cdots$	adults

  such that transitions from stage $i - 1$ to i occur on achieving development level m_i.

- All individuals within a stage have the same instantaneous growth rates and per capita death rates independent of mass

$$\left.\begin{aligned} g(m, t) &= g_i(t) \\ \delta(m, t) &= \delta_i(t) \\ b(m, t) &= b_i(t) \end{aligned}\right\} \quad \text{if} \quad m_i \le m \le m_{i+1}$$

- The adult population has a constant sex ratio and all females have the same fecundity.

Define the subpopulations by

$$N_i(t) \equiv \int_{m_i}^{m_{i+1}} \rho(m,t)dm, \tag{1.49}$$

which by integrating Equation 1.44 between m_i and m_{i+1} gives $N_i(t)$ satisfying

$$\frac{dN_i(t)}{dt} = R_i(t) - M_i(t) - D_i(t). \qquad \text{[recruitment - maturation - deaths]} \tag{1.50}$$

Hence, the rate of change in a particular stage is given by the rate of recruitment, minus the maturations and deaths from that stage, where

$$\begin{aligned} R_i(t) &= g_i(t)\rho(m_i^+,t), \\ M_i(t) &= g_i(t)\rho(m_i^-,t), \\ D_i(t) &= \delta_i(t)N_i(t), \end{aligned} \tag{1.51}$$

with

$$\begin{aligned} \rho(m_i^+,t) &= \lim_{\epsilon\to 0^+} \rho(m_i+\epsilon,t), \\ \rho(m_i^-,t) &= \lim_{\epsilon\to 0^+} \rho(m_i-\epsilon,t), \end{aligned} \tag{1.52}$$

with the detailed definitions of ρ required because ρ is not normally continuous across stage boundaries. Recruitment into stages other than the first occurs solely through maturation and so $R_i(t) = M_{i-1}(t)$ if $i \neq 1$ and $R_i(t) = \sum_{j=1}^{n} b_j(t)N_j(t)$ otherwise. Obtaining an explicit expression for the maturation rate, $M_i(t)$, requires that the balance Equation 1.45 is solved within the ith age class only, subject to the boundary condition in Equation 1.47 (slightly modified to apply to the ith age class)

$$\rho(m_i^+,t) = \frac{R_i(t)}{g_i(t)}. \tag{1.53}$$

To find $\rho(m_i^+,t)$, a solution of Equation 1.45 is required within developmental class i, for which $m_i \leq m \leq m_{i+1}$. We find such a solution by introducing the new variable

$$\mu = m_i + g_i(t)t, \tag{1.54}$$

and defining $\rho'(m,\mu) = \rho(m,t)$, $\delta_i'(\mu) = \delta_i(t)$ and $g_i'(\mu) = g_i(t)$. Equation 1.45 can be rewritten in terms of μ by using the chain rule to say that

$$\frac{\partial \rho}{\partial t} = \frac{\partial \rho'}{\partial \mu}\frac{\partial \mu}{\partial t}. \tag{1.55}$$

Further, it can be see that

$$\frac{\partial}{\partial m}(g_i(t)\rho) = \frac{\partial}{\partial m}(g_i'(\mu)\rho'(m,\mu)) = g_i'(\mu)\frac{\partial \rho'}{\partial m}, \tag{1.56}$$

Hence, Equation 1.45 becomes

$$\frac{\partial \rho'}{\partial \mu}\frac{\partial \mu}{\partial t} = -g_i'(\mu)\frac{\partial \rho'}{\partial m} - \delta_i'(\mu)\rho'. \tag{1.57}$$

Now, $\mu = m_i + g_i'(\mu)t$, so $\frac{\partial \mu}{\partial t} = 0 + g_i'(\mu)$. Hence, Equation 1.58 becomes

$$\frac{\partial \rho'}{\partial \mu} = -\frac{\partial \rho'}{\partial m} - \frac{\delta_i'(\mu)}{g_i'(\mu)}\rho' \qquad a_i \le a \le a_{i+1} \tag{1.58}$$

This equation is the standard von Foerster equation and can be solved by the method of characteristics. Parameterise the characteristic curve by ξ so $(a(\xi), \mu(\xi))$ is the characteristic curve. So

$$\begin{aligned} \frac{\partial \rho'}{\partial \xi} &= \frac{\partial \rho'}{\partial \mu}\frac{\partial \mu}{\partial \xi} + \frac{\partial \rho'}{\partial m}\frac{\partial m}{\partial \xi}, \\ &= -\frac{\delta_i'(\mu)}{g_i'(\mu)}\rho, \\ \text{with} \qquad \frac{\partial \mu}{\partial \xi} &= 1, \quad \frac{\partial m}{\partial \xi} = 1, \quad \frac{\partial \rho'}{\partial \xi} = -\frac{\delta_i'(\mu(\xi))}{g_i'(\mu(\xi))}\rho'. \end{aligned} \tag{1.59}$$

Solving the equations for μ and m it follows that

$$\mu(\xi) = \xi + c_1, \qquad m(\xi) = \xi + c_2, \quad c_1, c_2 \in \mathbb{R}. \tag{1.60}$$

Now determine the boundary conditions, for $\mu > m$ since $\mu \geq m_i$,

$$\xi = 0 \Rightarrow m(0) = m_i, \tag{1.61}$$

and $\mu(0)$ gives the times of entries into class i. So $c_1 = m_i$, hence $m(\xi) = \xi + m_i$ and $\mu(\xi) = \xi + c_2$. Therefore,

$$\begin{aligned} \frac{\partial \rho'}{\partial \xi} &= -\frac{\delta_i'(\mu(\xi))}{g_i'(\mu(\xi))}\rho', \\ \rho'(\xi) &= \rho'(0)\exp\left(-\int_{\xi'=0}^{\xi} \frac{\delta_i'(\mu(\xi'))}{g_i'(\mu(\xi'))}d\xi'\right), \end{aligned} \tag{1.62}$$

where ξ' is a dummy variable. Now, changing back to the original variables and using the fact that $\frac{d\mu}{d\xi} = 1 \Rightarrow d\mu = d\xi$, gives

$$\rho'(m,\mu) = \rho'(m(0),\mu(0))\exp\left(-\int_{\mu(0)}^{\mu(\xi)} \frac{\delta_i'(\mu')}{g_i'(\mu')}d\mu'\right), \tag{1.63}$$

where μ' is a dummy variable. Now, note that $m(0) = c_1$ and $\mu(0) = c_2$, but $\mu(\xi) = \xi + c_2$ and $m(\xi) = \xi + m_i$, so $\xi = m(\xi) - m_i$. Hence, $\mu(0) = \mu - m + m_i$ and

$$\rho'(m,\mu) = \rho'(m_i,\mu - m + m_i)\exp\left(-\int_{\mu-m+m_i}^{\mu} \frac{\delta_i'(\mu')}{g_i'(\mu')}d\mu'\right) \qquad m \in (m_i, m_{i+1}). \tag{1.64}$$

Now change the independent variable from μ back to t. Consider the integral,

$$\int_{\mu-m+m_i}^{\mu} \frac{\delta_i'(x)}{g_i'(x)}dx. \tag{1.65}$$

Setting $x = m_i + g_i'(x)t'$, gives $dt' = \frac{dx}{g_i'(x)}$. Using the fact that $x = t'$ and $\mu = t$ it can be shown that

$$\begin{aligned} & \mu = m_i + g_i'(\mu)t = m_i + g_i(t)t, \\ & t' = \frac{x - m_i}{g_i'(x)}, \\ \text{So, at } x = \mu \qquad & t' = \frac{m + g_i(t) - m_i}{g_i(t)} = t. \end{aligned} \tag{1.66}$$

Now, define the term $\tau_i(m,t)$ to be the time taken to develop from m_i to m by an individual who is at development level m at time t. Consequently,

$$\int_{\mu-m+m_i}^{\mu} \frac{\delta_i'(x)}{g_i'(x)} dx = \int_{t-\tau_i(m,t)}^{t} \delta_i(t')dt'. \tag{1.67}$$

Hence,

$$\begin{aligned} \rho(m,t) &= \rho(m_i, t - \tau_i(m,t)) \exp\left(-\int_{t-\tau_i(m,t))}^{t} \delta_i(t')dt'\right), \\ &= \frac{R_i(t - \tau_i(m,t))}{g_i(t - \tau_i(m,t))} \exp\left(-\int_{t-\tau_i(m,t)}^{t} \delta_i(t')dt'\right), \end{aligned} \tag{1.68}$$

is the solution to the balance equation (Equation 1.45) for developmental class i. The through-developmental class survival can be defined by

$$S_i(t) \equiv \exp\left(-\int_{t-\tau_i(m,t)}^{t} \delta_i(t')dt'\right), \tag{1.69}$$

and so the rate of maturation out of stage i can be expressed succinctly by

$$M_i(t) = \frac{g_i(t)}{g_i(t - \tau_i(t))} R_i(t - \tau_i(t)) S_i(t). \tag{1.70}$$

Finally we require an expression for the stage durations, which are defined as the time required for development from development point m_i to m_{i+1} and so can be deduced from the integral constraint

$$m_{i+1} - m_i = \int_{t-\tau_i(t)}^{t} g_i(t')dt'. \tag{1.71}$$

This development equation, which determines the stage duration, was not required in the previous age-dependent formalism as progression between the stages happened at fixed time points as the population aged, where here it requires that sufficient development has occurred. It is also necessary to consider the history of the population for all times prior to $t = 0$. As in the fixed delay case, it is assumed that the system is empty ($N_i = 0$) for all i and all $t \leq 0$ and then inoculated with some individuals after $t = 0$, assuming that any inoculants are at the minimum development level for this instar. This brings about modified recruitment equations

$$R_i(t) = \begin{cases} \sum_{j=1}^{Q} b_j(t)N_j(t) + I_i(t) & \text{if } i = 1, \\ M_{i-1}(t) + I_i(t) & \text{if } i = 2, ..., Q, \end{cases} \tag{1.72}$$

where $I_i(t)$ represents the rate at which individuals are added in stage i at time t

$$I_i(t) = \begin{cases} J_i & 0 \leq t \leq t_1, \\ 0 & \text{otherwise.} \end{cases} \tag{1.73}$$

At present the model formalism contains a series of integro-differential equations coupled with an integral constraint. These can be very difficult to analyse, however they can be rewritten as DDEs in the following way. First consider differentiation of the integral equation defining the developmental lags with respect to time, t,

$$\begin{aligned} m_{i+1} - m_i &= \int_{t-\tau_i(t)}^{t} g_i(t')dt', \\ \frac{d}{dt}(m_{i+1} - m_i) &= \left[g_i(t')\right]_{t-\tau_i(t)}^{t}, \\ 0 &= g_i(t) - g_i(t - \tau_i(t))\left(1 - \frac{d\tau_i(t)}{dt}\right), \\ 1 - \frac{d\tau_i(t)}{dt} &= \frac{g_i(t)}{g_i(t - \tau_i(t))}, \\ \frac{d\tau_i(t)}{dt} &= 1 - \frac{g_i(t)}{g_i(t - \tau_i(t))}. \end{aligned} \tag{1.74}$$

It can be seen from this result that if the environment is held constant then the rate of change of the stage duration will become zero and the system will reduce down to the constant case previously discussed. Using this, one can compute $\tau_i(t)$ at all $t > 0$ given the value τ_{i0} of

the lag at $t = 0$ and the history ($t < 0$). The historical values of $g_i(t)$ can be interpreted as the development rate of an individual introduced and allowed to feed in a non-varying environment. In the case where conditions are constant before $t = 0$ the unimpeded growth rate will be constant, g_{i0}, and the initial lag τ_{i0} is thus obtained from

$$m_{i+1} - m_i = \int_{t-\tau_i(t)}^{t} g_i(t')dt' = g_{i0}\tau_{i0}. \tag{1.75}$$

There is also an integral in the definition of $S_i(t)$. This can also be transformed into a DDE by taking the derivative

$$\begin{aligned} S_i(t) &= \exp\left(-\int_{t-\tau_i(m,t)}^{t} \delta_i(t')dt'\right), \\ \frac{dS_i(t)}{dt}\frac{1}{S_i(t)} &= -\left[\delta_i(t) - \delta_i(t-\tau_i(t))\left(1 - \frac{d\tau_i(t)}{dt}\right)\right], \\ \frac{dS_i(t)}{dt} &= S_i(t)\left[\delta_i(t-\tau_i(t))\left(1 - \frac{d\tau_i(t)}{dt}\right) - \delta_i(t)\right], \\ \frac{dS_i(t)}{dt} &= S_i(t)\left[\frac{g_i(t)\delta_i(t-\tau_i(t))}{g_i(t-\tau_i(t))} - \delta_i(t)\right], \end{aligned} \tag{1.76}$$

which can be solved subject to the initial condition

$$S_i(t) = \exp\left(-\int_{t-\tau_{i0}}^{t} \delta_i(t')dt'\right) = \exp(\delta_{i0}\tau_{i0}), \tag{1.77}$$

where constant conditions are assumed for $t < 0$ and δ_{i0} is the per capita death rate for a single individual prior to $t = 0$.

The use of a development scale to signal progression between different stages of the life cycle means that this approach differs from the purely age-structured model described previously. In the case of mosquitoes, this means that development through the life stages can occur at a rate dependent on biotic and abiotic factors such as temperature, competition and food availability, as is the case in the field, rather than progression being determined by chronological age.

1.3.4 Applications of the variable-delay-differential equation framework

In their original paper, Nisbet and Gurney (1983) model a hypothetical insect population, where development and survival through the immature stages is dependent on food availability. In the first example the authors present, where adults have a long expected lifetime and a low fecundity, a rapid approach without oscillations to a steady state (Figure 1.8), which can also be found analytically, is observed. However, altering the parameters of the system such that adults have a shorter expected lifetime and a higher fecundity, the population exhibits oscillatory behaviour (Figure 1.9). Oscillatory behaviour, such as this, is commonly observed in insect populations and is a common property of DDEs. Such oscillatory dynamics have been well studied in a number of organisms including the Australian sheep blowfly *Lucilia cuprina* (Nicholson 1954) and the Indian meal-moth *Plodia interpunctella* (Gurney et al. 1983). The period of oscillations typically relates to the generation time of the organism (Jansen et al. 1990). These oscillations can make performing stability analyses on DDEs difficult because the characteristic equations describing the eigenvalues are often transcendental. Further, the dependence of the various vital rate functions, such as development and mortality rates, on environmental variables further precludes DDEs from direct mathematical analysis. Equilibrium solution values can only be found for constant temperature scenarios, which have little biological meaning for temperate mosquito species which exhibit substantial diurnality and seasonality. Given this the computation of numerical solutions of the DDEs is necessary. A discussion of how these solutions was obtained is given in Box 1.3.4.

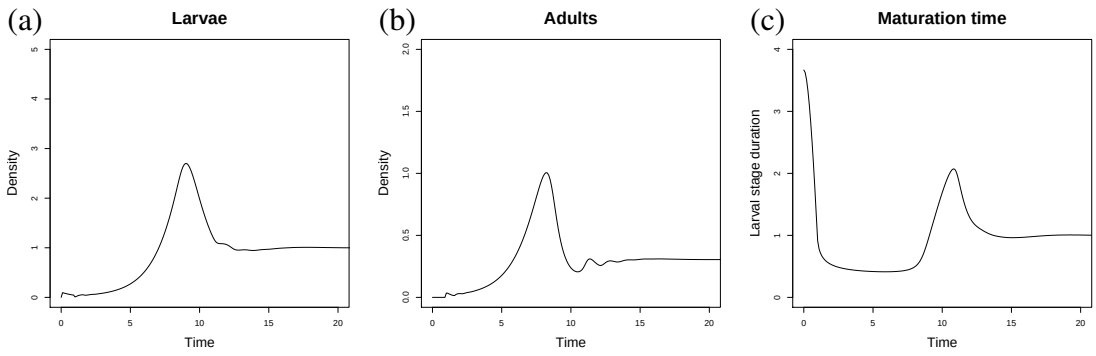

Figure 1.8: Stable damselfly Example: Output from simulations of the Nisbet and Gurney (1983) example using DDE_SOLVER. Parameters A'_{max} = 3, K'_F = 1, q' = 5 and δ'_A = 2, as defined in the original paper.

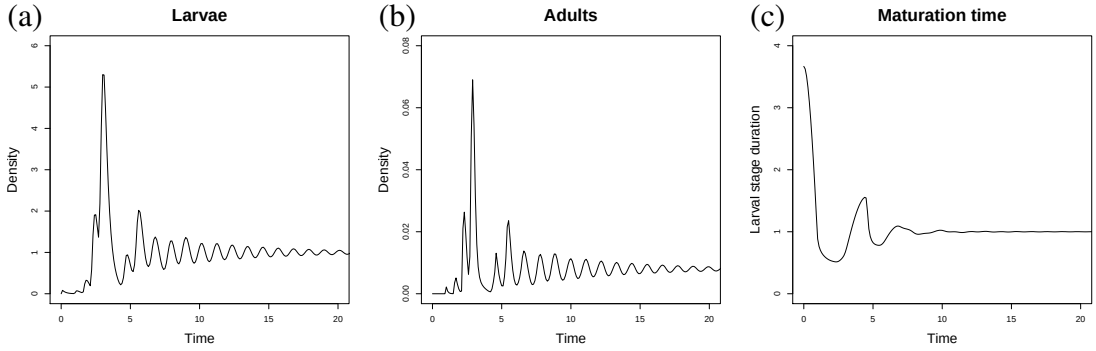

Figure 1.9: Oscillatory damselfly Example: Output from simulations of the Nisbet and Gurney (1983) example using DDE_SOLVER. Parameters $A'_{max} = 3$, $K'_F = 1$, $q' = 500$ and $\delta'_A = 10$, as defined in the original paper.

Box 1.3.1: Obtaining numerical solutions

The mosquito population model I develop in this thesis was run using the FORTRAN 90 (F90) DDE solver DDE_SOLVER published by Thompson and Shampine (2004). The program DDE_SOLVER is based on another FORTRAN DDE solver, DKLAG6 (Corwin et al. 1997), which uses continuously imbedded sixth-order Runge-Kutta methods to solve state-dependent functional differential equations containing delays. The purpose of DDE_SOLVER was to develop a FORTRAN DDE solver with an easily accessible and understandable user interface, as FORTRAN DDE solvers are often considered daunting to users. In developing DDE_SOLVER the authors also made improvements to the existing DKLAG6 program, which was originally written in FORTRAN 77 (F77), by utilising features made available by the release of F90.

The solutions to the damselfly example (shown in Figures 1.8 and 1.9) were found using DDE_SOLVER. These solutions were compared to those published in the original paper by Nisbet and Gurney (1983) to ensure that the solver code was performing as expected and both solutions displayed the same qualitative behaviour. Exact agreement of the numerics could not be determined because the original published work did not contain sufficient information regarding how the system was innoculated to allow for a direct comparison and system dynamics are sensitive to this process. However, the equilibrium solutions obtained using DDE_SOLVER were the same as those seen in the original paper. Further, the solutions were compared to those presented by Kettle and Nutter (2015), who use the damselfly system as a worked example in presenting “StagePop", a function for modelling stage-structured populations in R, and agreement between the numerics was found by plotting the solution values against

each other. Throughout the thesis I extended and built upon this base code, performing regular feasibility checks of the solutions when investigating the behaviour of my model. The code for each Chapter of this thesis is available at Ewing et al. (2016b).

This Nisbet and Gurney (1983) framework can be used to model a wide range of populations, provided the species in question is one which develops through multiple different life stages during its lifespan. Further, environmental factors can be allowed to influence behaviour in the same way as food availability did in the original example, by simply changing the function $g_i(t)$ to reflect the species and relationship of interest. However, despite the appropriateness of this method, DDEs with variable delays have until recently remained underutilised in the modelling of insect population dynamics. One recent example of variable delay DDEs can be seen in the work of Amarasekare and Coutinho (2013), who investigated the effects of climate warming on the viability of generic ectothermic populations. The authors used functions rooted in biomechanics to define the birth, development and death rates of ectotherms at different temperatures. By adopting a simple, two-stage model for juveniles and adults using the Nisbet and Gurney (1983) framework they were able to predict population growth and decline rates in seasonally varying environments using projected climate warming scenarios. This work showcases the generality of the DDE approach, as the authors elected to model the broad group of all ectotherms rather than focussing specifically on one species.

Recent work by Beck-Johnson et al. (2013) shows how the framework can be used to make specific predictions about a particular species, as the authors investigated the effect of temperature on *Anopheles* population dynamics and discussed the implications for disease transmission. Beck-Johnson et al. (2013) was the first variable-DDE model developed for a mosquito population. The authors split the population according to the four main mosquito life stages (eggs, larvae, pupae and adults), though they assumed the same temperature-dependent development and death rates for each of the immature stages. In doing this, the authors were able to simplify the model by transforming it onto the physiological time scale. In this way, the total immature development time fluctuated with temperature and the individual stages accounted for a fixed proportion of this time. In doing this, the system of four DDEs could be collapsed to a pair of DDEs corresponding to juvenile and adult development. This study makes use of the Nisbet and Gurney (1983) framework to answer questions about a tropical mosquito species, its equilibrium abundance, and what this may mean for disease transmission. However, in applying the framework to a temperate species such as *Cx. pipiens*, further complications arise. In temperate climates there will be increased seasonal variability in environmental variables with potentially greater impacts on variability

in mosquito populations and life cycle parameters. Beck-Johnson et al. (2013) give some consideration to seasonality in their analysis, however the largest seasonal temperature range they consider is $10\,^{\circ}\mathrm{C}$. This is smaller than the range experienced in temperate climates like the UK, where a temperature dataset (obtained using FetchClimate (Microsoft 2014) and aggregating values from the UEA Climatic Research Unit (UEA 2015) and Hijmans et al. (2005)) from the North Kent marshes from 1951-2010 found annual fluctuation in mean daily temperatures ranged from 10 – $16\,^{\circ}\mathrm{C}$, with daily temperature fluctuations increasing this range.

For a species like *Cx. pipiens* one must first consider how the seasonal variation in temperatures will affect development and death rates and what effect this will have on population and disease dynamics. For example, how might early or late temperature increases in spring affect seasonal dynamics throughout the rest of the year? Most crucially, however, when considering temperate species we are confronted with the question of how best to model adult mosquito diapause, which is not experienced by tropical mosquito species such as *Anopheles*, modelled by Beck-Johnson et al. (2013). The decreased photoperiod and temperature throughout the winter months induce a drastic change in adult behaviour patterns, with activity ceasing for many months. This problem has not previously been addressed using a DDE-based model and is an interesting topic of exploration within this thesis.

Another previously unexplored question is how disease transmission dynamics can be explicitly included into a DDE-based population abundance model to capture environmental effects on vector populations and disease simultaneously. Beck-Johnson et al. (2013) make inferences about disease transmission parameters given abundances, biting rates and expected longevities of adult mosquitoes but do not explicitly model disease transmission. I aim to combine both a DDE-based mosquito population model with an SEIR compartmental disease model to understand exactly how vectors and hosts may interact under variable environmental conditions (Figure 1.10). In doing this, I hope to understand how both environmental conditions and ecological factors, such as the response of the host population to virus infection or density-dependent regulation of mosquito populations, will influence disease transmission. This will help assess the risks of epidemic or endemic scenarios taking place.

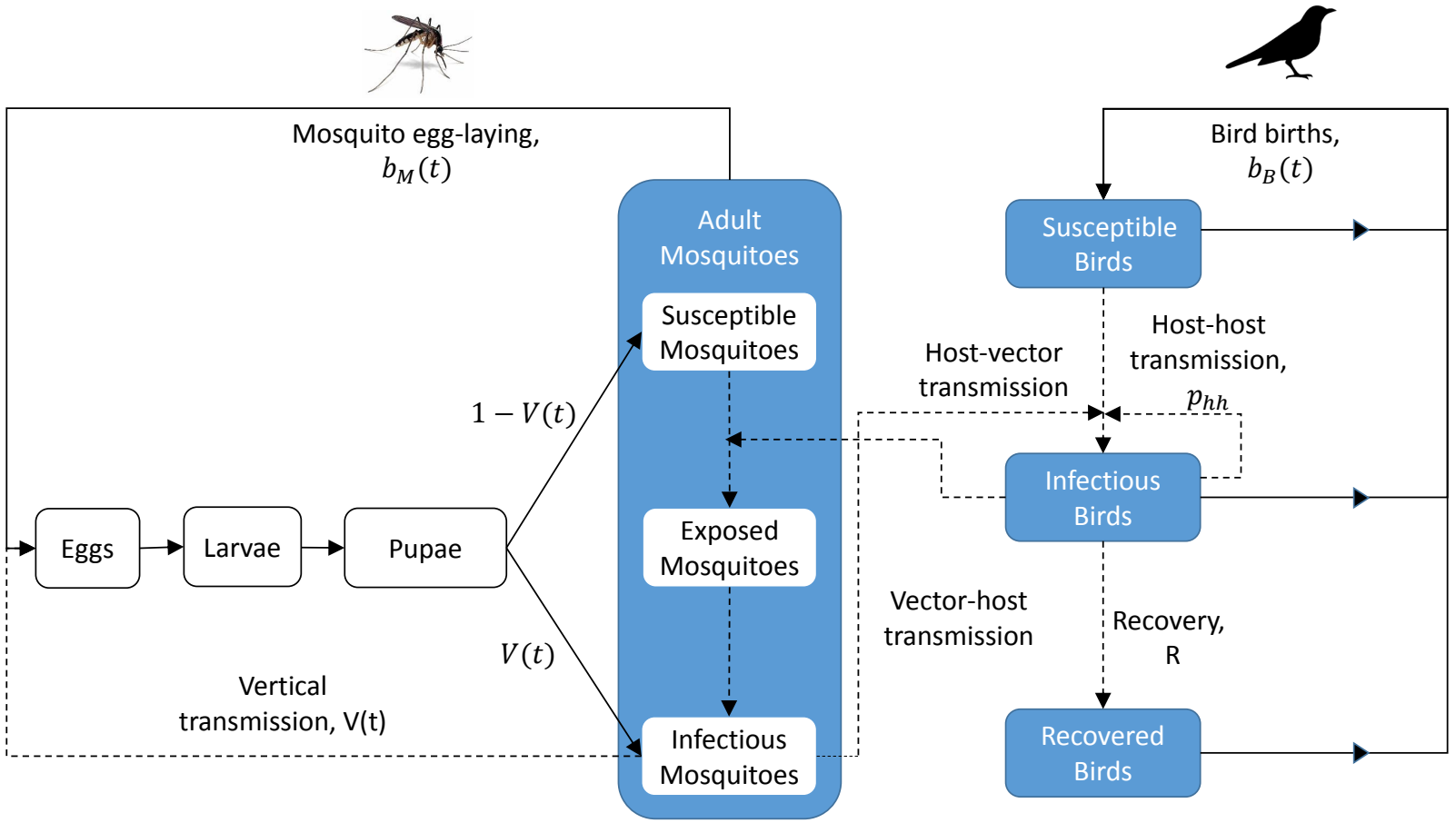

Figure 1.10: Disease model structure: Flowchart showing the model structure used in Chapter 5 and highlighting the disease-related parameters. All stages have an associated death rate, which is not displayed here for clarity. All disease transmission processes are shown by dashed lines, whilst life cycle processes are shown by solid lines.

1.4 Aims and structure of the thesis

The aim of the thesis was firstly, to develop an environmentally driven seasonal abundance model for a temperate mosquito vector, which accounts for changing environmental conditions by explicitly incorporating variation in developmental delays of each stage. Secondly, I used this model to predict the possible risks of WNV introduction and subsequent transmission potential within the UK. An extensive dataset concerning *Cx. pipiens* seasonal abundance was collected and used to validate the model, which was then extended to explicitly model WNV transmission.

1.4.1 Structure

Chapter 2 describes the development of a stage-structured variable-delay-differential equation model which captures the effects of temperature on key life cycle parameters of *Cx. pipiens* and produces seasonal abundance predictions given observed or simulated temperature variables. This model is then used to predict the effects of different annual temperature patterns on seasonal abundance of the mosquito, *Cx. pipiens*. Potential changes to the mosquito population under predicted UK climate warming scenarios are then presented. Finally, the impact of using simplified annual temperature patterns, based upon fitted sinusoidal curves is investigated.

In Chapter 3, I present a dataset gathered from an extensive period of fieldwork monitoring each life stage of *Cx. pipiens* populations which I carried out at the Centre for Ecology & Hydrology in Wallingford from April to October in 2015. I discuss the insights into UK *Cx. pipiens* seasonality gained from this dataset and use the data both to assess the representation of the mosquito ecology in the existing mosquito population model and to inform on areas in which the model could be improved. I place this information in the wider context of what is know about seasonality of the species across Europe and North America and search for geographical patterns in key seasonal life cycle processes that impact the timing and persistence of disease transmission, such as adult diapause. Finally, I discuss how data collection and publishing across the field could be improved to answer key ecological questions about the abiotic and biotic factors that govern seasonal mosquito populations.

Improvements to the model in light of the empirical UK data collection, along with a full discussion of the model performance, are presented in Chapter 4. The impacts of using air

temperature to approximate water temperature when modelling the immature stages of temperate mosquito species are also presented. Finally, I show an analysis of the importance of the temporal resolution of temperature datasets when predicting mosquito seasonal abundance.

Chapter 5 then extends the existing mathematical model, using an SEIR framework, to predict seasonal pathogen dynamics (Figure 1.10). I present a model for WNV transmission in the UK, including both the vector and the avian host populations to investigate the effects of different ecological and temperature scenarios on disease transmission. I highlight key transmission parameters and scenarios which may lead to increased risks of disease epidemics if WNV introduction were to occur.

Finally, in chapter 6, I present a general discussion of the thesis and its implications for the mathematical modelling of temperate mosquito species and management of the risk of transmission of WNV within the UK.

Chapter 2

Modelling temperature effects on temperate mosquito seasonal abundance

The work presented in this chapter forms the basis of a published paper (Ewing et al. 2016a).

2.1 Introduction

Climate change is expected to affect the distribution and seasonal dynamics of mosquito populations, with substantial implications for disease seasonality and persistence (Githeko et al. 2000). Globally, mosquito-borne diseases are a major public health concern (Gubler 2002), and increasingly so in temperate climates, with disease caused by mosquito-borne pathogens including West Nile (Sambri et al. 2013), Chikungunya (Grandadam et al. 2011), Usutu (Weissenböck et al. 2002) and Toscana (Charrel et al. 2005) viruses being reported in Europe in recent years. A range of factors including societal, land use and habitat changes, have been linked to changes in exposure to mosquitoes, which vector these diseases (Gubler 2002). These factors combine with widespread predictions that rising temperatures may increase mosquito population size, development rates and per host biting rate, producing increases in the incidence of mosquito-borne diseases (Mirski et al. 2012). The non-linear and opposing impacts of temperature on vector demographic rates require detailed modelling, incorporating the various biological processes at play, if we are to understand the likely impacts of climate change on vector abundance and understand the likelihood that predictions of increased exposure to vectors will be borne out (Rogers and Randolph 2006).

To model disease seasonality and persistence it is essential that epidemiological models are coupled with accurate seasonal predictions of vector density (Lord 2004). This is likely to become increasingly important in coming years, as the climate is expected to become more variable (Jones et al. 2009). Without accurate predictions of vector density, calculations of the basic reproduction number of the disease (R_0), which describes ability of a disease to persist in a susceptible population, will be subject to considerable error. However, many recent epidemiological studies of vector-borne disease do not account for seasonality in vector populations (Cruz-Pacheco et al. 2005; Bowman et al. 2005; Wonham et al. 2004). In this Chapter, I utilise a delay-differential equation (DDE) framework to explicitly model the effects of temperature on each of the life stages of the vector population. This gives valuable insight into how inter-annual variability in temperature may affect mosquito populations, which will have a direct effect on disease transmission.

There is considerable evidence showing that environmental drivers have a large impact on both the mosquito life and disease transmission cycles (Jian et al. 2014b; Lebl et al. 2013; Almeida Costa et al. 2006). Hence, understanding these mechanisms and resulting effects will aid predictions for vector-borne diseases. Increasing temperature is known to decrease the length of time spent in each of the immature stages and to decrease the lifespan of adults (Madder et al. 1983b; Loetti et al. 2011). Furthermore, the death rate of the immature stages is strongly linked to temperature (Ciota et al. 2014; Madder et al. 1983b; Loetti et al. 2011) and increasing temperature leads to decreases in the lengths of both the gonotrophic cycle (the time required for location of a blood meal, embryonic development and egg-laying) (Madder et al. 1983b; Vinogradova 2000) and the extrinsic incubation period (time between an adult vector contracting a pathogen and becoming infectious, referred to as EIP) (Hartley et al. 2012). With photoperiod, temperature is also believed to control the induction and termination of diapause (Spielman and Wong 1973; Madder et al. 1983a). Overwintering behaviour is a vital aspect of disease transmission because diapausing mosquitoes may act as a pathogen reservoir between seasons when hosts are no longer infectious (Nasci et al. 2001). The winter survival of mosquitoes may therefore influence disease persistence and seasonal population dynamics. Diapause, which I consider in my model, has been ignored in previous DDE models as the focus has generally been tropical mosquito populations which do not exhibit this behaviour (White et al. 2010; Beck-Johnson et al. 2013). Clearly temperature exhibits complex and opposing effects on different parts of the mosquito life and transmission cycles. As such, mathematical models are needed which explicitly incorporate the impact of temperature on each life stage if we wish to understand its effect on seasonal abundance.

Stage-structured matrix population models allow populations to be broken down according to their life stages, with climate dependencies on each stage included, making them a popular tool for modelling mosquito populations (Lončarić and Hackenberger 2013; Schaeffer et al. 2008). However, in many cases, these models make the assumption that development time for each stage is fixed (Schaeffer et al. 2008), when temperate species' generation times at high temperatures, can in fact exceed those observed at lower temperatures by a factor of more than four (Loetti et al. 2011). Combined with the effects of temperature on larval survival (Loetti et al. 2011), these models may substantially under- or over-estimate population size. One solution is to split each stage into multiple sub-stages and allow temperature to influence transition probabilities (Lončarić and Hackenberger 2013), substantially improving upon the assumption of a fixed development time. However, this approach requires that each life stage be split into an appropriate number of sub-stages ahead of time, whilst the required number of sub-stages will be dependent on temperature. Further, each sub-stage must be assigned its own transition probability, which accounts for both the current temperature and the length of time already spent in the stage, which can be cumbersome. Models based on ordinary differential equations (ODEs) also fail to account for temperature-induced variation in stage duration, as only the current conditions influence stage duration (Erickson et al. 2010b; Alonso et al. 2010).

Perhaps the most detailed mosquito population models previously developed are the Container-Inhabiting Mosquito Simulation Model (CIMSiM) (Focks et al. 1993a, 1993b) and Skeeter Buster (Magori et al. 2009), which builds on the capabilities of CIMSiM to account for spatial heterogeneity, stochasticity and population genetics in the mosquito population. CIMSiM is a weather-driven dynamic life table simulation model for *Aedes aegypti* and can be coupled with DENSiM, which models dengue transmission dynamics in human populations based on the mosquito population dynamics output from CIMSiM. CIMSiM incorporates temperature-dependence in the duration and survival of all life stages. Further, fecundity is modelled as a function of pupal size, which in turn is a function of the recent history of larval abundance, larval food, and temperature. Larval survival is not only dependent on temperature but is also a function of food availability and fat body reserves, whilst adult and egg survivals are determined by both temperature and humidity (Focks et al. 1993a). These models have been shown to adequately capture *Aedes aegypti* and dengue dynamics in a number of areas (Focks et al. 1993b), however the wide range of processes incorporated means that adaptation of this model to another mosquito species is not straightforward and that the model requires very detailed input data. In particular, CIMSiM simulates all cohorts of a single species of *Aedes* mosquito over a one hectare area but requires information on every potential breeding site in that area alongside daily inputs of maximum and minimum

air temperature, precipitation, relative humidity and saturation deficit. Consequently, whilst CIMSiM, DENSiM and Skeeter Buster estimate a very wide range of processes, they cannot be readily adapted from one species to another and model results will be highly localised to one studied location.

In contrast to life table or matrix-based approaches, one can look to work carried out by Gurney et al. (1983), who advocated using a system of DDEs to model stage-structured populations. These DDEs are derived from continuous age-structured partial differential equations (PDEs) by assuming lumped age classes, which are appropriate for many insect species with distinct life stages (see Section 1.3.2). This formulation can then be extended as shown in Nisbet and Gurney (1983) to allow variation in stage duration dependent on biotic or abiotic factors (see Section 1.3.3).

The stage-structured DDE framework has recently been utilised to investigate ectotherm population viability under a climate warming scenario (Amarasekare and Coutinho 2013) and to model the life cycle of *Anopheles*, a genus of tropical mosquito species that vector malaria (Beck-Johnson et al. 2013). To my knowledge, the work of Beck-Johnson et al. (2013) is the first DDE model, applied to mosquitoes, where the total length of the immature life stages was assumed to be temperature-dependent. Beck-Johnson et al. (2013) used this model to make inferences about the ability of *Anopheles* to transmit malaria, under various constant temperature regimes. As previously alluded to, further complications arise for temperate mosquito species due to greater fluctuation in seasonal temperatures and overwintering behaviour. To simplify their model, Beck-Johnson et al. (2013) also assume that all immature life stages are affected by temperature in the same way, which allows the delay equations to be transformed onto the physiological timescale and reduced from three separate equations into one. My review of the literature suggests that many temperate mosquito species have differential, temperature-driven rates of development between life stages, so I allow each stage to have a unique relationship between temperature and vital rates.

The DDE modelling framework can be applied to any temperate mosquito species by choosing parameters and vital rate curves to fit the data available for that species. I focus on modelling *Culex pipiens*, the most abundant potential vector of West Nile Virus (WNV) in the UK. WNV was chosen because it is the most significant cause of mosquito-borne disease in temperate regions including Europe and North America (Pervanidou et al. 2014; Barzon et al. 2013; Petersen et al. 2013).

Temperature is often considered to be the primary driver of mosquito development (Knies and Kingsolver 2010). By developing a stage-structured model which explicitly captures its effects on each life stage I aim to understand how predicted seasonal temperature changes may affect mosquito seasonality. Whilst mosquito surveillance in the UK has increased in recent years (Townroe and Callaghan 2014; Medlock and Vaux 2015; Townroe and Callaghan 2015) there remains a lack of publicly available empirical field data for UK *Cx. pipiens* populations, so accurate predictive modelling is needed to understand seasonal population dynamics and how vectors may be impacted by changing climate. I address this issue by providing testable theory which may guide future laboratory or field studies and which highlight in precisely which areas field and laboratory work is required. By carrying out a simulation study over a range of different temperature regimes predicted for the UK, I examine the effects of both intra- and inter-annual temperature variability on mosquito seasonal abundance to ascertain the climatic conditions that are most likely to lead to high vector abundance and hence to potential disease outbreaks. In particular, I explore the effects of varying mean temperature, amplitude of seasonal fluctuations, the timing of the summer and winter periods, and the sharpness of the summer season. Where possible, these changes were placed in the context of predicted changes for the UK climate. In addition, I used a 30-year UK temperature dataset from the North Kent marshes, a known habitat of *Cx. pipiens* and *Cx. modestus*, to investigate sensitivity of vector populations to subtle changes in seasonal temperature regimes as well as changes in mean temperature levels. The analysis highlights the importance of the explicit incorporation of temperature and its effects on mosquito seasonality, which will have a knock-on effect on disease transmission. Finally, by including over winter dynamics in the model, I tested the value of the DDE approach in stage structured modelling for understanding dynamics of temperate arthropod vectors.

2.2 Methods

2.2.1 Mathematical framework

The mosquito life cycle is composed of four main life stages: egg, larval, pupal and adult. Adult females lay rafts of eggs on the surface of pools of water. Eggs hatch into larvae which continue their development to become pupae. Pupae metamorphose into adults which mate and, if female, locate a host to obtain a blood meal and eventually lay more egg rafts. Many temperate mosquito species, including those of the genus *Culex*, overwinter through inseminated adult females entering diapause. The four stages of the mosquito life cycle can

be incorporated into a sequence of DDEs, which are solved to give the abundance of individuals in each life stage through time (Gurney et al. 1983). The general formalism of the model is analogous to that described by Nisbet and Gurney (1983) and a full derivation was presented in Sections 1.3.2-1.3.3. Here, I present an overview of the model framework used. Building on the Nisbet and Gurney (1983) framework, where changes in stage duration occurred due to food availability, I made the extension that variation in stage duration may occur as a result of changes in a range abiotic environmental drivers.

The four state equations which correspond to eggs, $E(t)$, larvae, $L(t)$, pupae, $P(t)$ and adults $A(t)$ at time t, are

$$\begin{aligned}
\frac{dE}{dt} &= R_E(t) - M_E(t) - \delta_E(T(t))E(t), \\
\frac{dL}{dt} &= R_L(t) - M_L(t) - (\delta_L(T(t)) + \delta_\pi(L(t)))L(t), \\
\frac{dP}{dt} &= R_P(t) - M_P(t) - \delta_P(T(t))P(t), \\
\frac{dA}{dt} &= R_A(t) - \delta_A(T(t))A(t),
\end{aligned} \tag{2.1}$$

where $T(t)$ gives the temperature, $\delta_i(T(t))$ ($i = E, L, P, A$) represents the stage-specific, density-independent, temperature-driven, mortality rate, $\delta_\pi(L(t))$ represents the larval mortality rate due to external predation and $R_i(t)$ and $M_i(t)$ represent the rate of recruitment to and maturation from stage i respectively. It was assumed that predation is the main source of density-dependent population regulation. The maturation equations are defined as

$$\begin{aligned}
R_E(t) &= b(t)A(t), \\
M_E(t) = R_L(t) &= R_E(t - \tau_E(t))S_E(t)\frac{g_E(T(t))}{g_E(T(t - \tau_E(t)))}, \\
M_L(t) = R_P(t) &= R_L(t - \tau_L(t))S_L(t)\frac{g_L(T(t))}{g_L(T(t - \tau_L(t)))}, \\
M_P(t) = R_A(t) &= R_P(t - \tau_P(t))S_P(t)\frac{g_P(T(t))}{g_P(T(t - \tau_P(t)))},
\end{aligned} \tag{2.2}$$

with $g_i(T(t))$ as the development rate at temperature $T(t)$, $b(t)$ as the egg-laying rate $\tau_i(t)$ and $S_i(t)$ as the survival of individuals in stage i ($i = E, L, P$) at time t respectively. Recruitment into the egg stage occurs solely as a result of egg laying by adults and recruitment into all other stages is a result of maturation of individuals from the stage before. The growth rate, $g_i(T(t))$, defines the speed at which individuals progress through the stage, allowing the duration of the immature stages to vary continuously. The term $\frac{g_i(T(t))}{g_i(T(t-\tau_i(t))}$ tells us how

variation in the growth rate through time alters the stage length. If stage duration is fixed then $g_i(T) = g_i(t - \tau_i(t))$. In my model, the temperature, T, varies as a function of time, such that $T = T(t)$. The proportion of individuals which survive from recruitment into one class, to maturation to the next, is defined by the following sequence of DDEs,

$$\begin{aligned}
\frac{dS_E}{dt} &= S_E(t)\left(\frac{g_E(T(t))\delta_E(T(t-\tau_E(t)))}{g_E(T(t-\tau_E(t)))} - \delta_E(T(t))\right),\\
\frac{dS_L}{dt} &= S_L(t)\left[\left(\delta_\pi(t-\tau_L(t)) + \delta_L(T(t-\tau_L(t)))\right)\left(\frac{g_L(T(t))}{g_L(T(t-\tau_L(t)))}\right) - \delta_\pi(L(t)) - \delta_L(T(t))\right],\\
\frac{dS_P}{dt} &= S_P(t)\left(\frac{g_P(T(t))\delta_P(T(t-\tau_P(t)))}{g_P(T(t-\tau_P(t)))} - \delta_P(T(t))\right).
\end{aligned} \tag{2.3}$$

Lastly, the rate of change of the duration of each life stage is given by

$$\frac{d\tau_i(t)}{dt} = 1 - \frac{g_i(T(t))}{g_i(T(t-\tau_i(t)))}. \tag{2.4}$$

Here the development rate, $g_i(T(t))$, is dependent on temperature, although the model formulation is sufficiently flexible to allow a range of environmental drivers to be incorporated simultaneously. We can then extend this idea, introduced by Nisbet and Gurney (1983), to define an analogous delay equation for the duration of the adult gonotrophic cycle. The gonotrophic cycle in the model is defined as the time required for an adult to locate and take a blood meal, digest this blood meal and produce eggs, and then locate an oviposition site and lay an egg raft. The duration of the gonotrophic cycle will directly affect the egg-laying rate, as we divide the number of eggs in a given raft by the length of the cycle to estimate a continuous egg-laying rate. In the field, the gonotrophic cycle length will also affect the rate at which individuals may enter traps because it is host-seeking females which are attracted to light traps, following emergence from the pupal stage or egg-laying (Hutchinson et al. 2007). As with immature development, I make the extension from the original Nisbet and Gurney (1983) framework that, rather than considering the growth from some mass, m_i, to some other mass, m_{i+1}, we can consider the growth from some "development point", at the start of a gonotrophic cycle to some later point, at the end of a cycle. By defining these development points we can then follow through the same arguments as for the durations of the immature

life stages to give

$$\frac{d\tau_G(t)}{dt} = 1 - \frac{g_G(T(t))}{g_G(T(t-\tau_G(t)))}. \tag{2.5}$$

where, G, denotes that we are concerned with the gonotrophic cycle.

In their paper, Nisbet and Gurney (1983) show the delay equation for each life stage at time, t. However, when coding this model it becomes necessary to reference stage durations at previous points in time by looking back through intermediate stage durations, which are themselves variable. This is required when there are multiple stages of variable length. The derivation of the delay which references back through two intermediate life stages is given below i.e. this will give the duration of the egg stage the length of the pupal stage and larval stage ago. This is the procedure required to obtain $\tau_E(t - \tau_P(t) - \tau_L(t - \tau_P(t)))$ where $i = E, i + 1 = L$ and $i + 2 = P$. The derivations of $\tau_E(t - \tau_L(t))$ and $\tau_L(t - \tau_P(t))$ are not presented as they reference through only one delay and so are simplified versions of this derivation.

$$\begin{aligned}
m_{i+1} - m_i &= \int_{t-\tau_{i+2}(t)-\tau_{i+1}(t-\tau_{i+2}(t))-\tau_i(t-\tau_{i+2}(t)-\tau_{i+1}(t-\tau_{i+2}(t)))}^{t-\tau_{i+2}(t)-\tau_{i+1}(t-\tau_{i+2}(t))} g_i(\psi)d\psi \\
\frac{d(m_{i+1} - m_i)}{dt} &= g_i(t - \tau_{i+2}(t) - \tau_{i+1}(t - \tau_{i+2}(t)))\left(1 - \frac{d\tau_{i+2}(t)}{dt} - \frac{d\tau_{i+1}(t - \tau_{i+1}(t))}{dt}\right) \\
&\quad - g_i(t - \tau_{i+2}(t) - \tau_{i+1}(t - \tau_{i+2}(t)) - \tau_i(t - \tau_{i+2}(t) - \tau_{i+1}(t - \tau_{i+2}(t)))) \\
&\quad \left(1 - \frac{d\tau_{i+2}(t)}{dt} - \frac{d\tau_{i+1}(t - \tau_{i+1}(t))}{dt} - \frac{d\tau_i(t - \tau_{i+2}(t) - \tau_{i+1}(t - \tau_{i+2}(t)))}{dt}\right)
\end{aligned} \tag{2.6}$$

Since the start and end points of each life stage are fixed it follows that $\frac{d(m_{i+1}-m_i)}{dt} = 0$ so

$$\begin{aligned}
&1 - \frac{d\tau_{i+2}(t)}{dt} - \frac{d\tau_{i+1}(t-\tau_{i+1}(t))}{dt} - \frac{d\tau_i(t-\tau_{i+2}(t)-\tau_{i+1}(t-\tau_{i+2}(t)))}{dt} \\
&= \frac{g_i(T(t-\tau_{i+2}(t)-\tau_{i+1}(t-\tau_{i+2}(t))))}{g_i(T(t-\tau_{i+2}(t)-\tau_{i+1}(t-\tau_{i+2}(t))-\tau_i(t-\tau_{i+2}(t)-\tau_{i+1}(t-\tau_{i+2}(t)))))} \\
&\left(1 - \frac{d\tau_{i+2}(t)}{dt} - \frac{d\tau_{i+1}(t-\tau_{i+1}(t))}{dt}\right)
\end{aligned} \tag{2.7}$$

$$\begin{aligned}
&\frac{d\tau_i(t-\tau_{i+2}-\tau_{i+1}(t-\tau_{i+2}(t)))}{dt} \\
&= \left(1 - \frac{d\tau_{i+2}(t)}{dt} - \frac{d\tau_{i+1}(t-\tau_{i+1}(t))}{dt}\right) \\
&\left(1 - \frac{g_i(T(t-\tau_{i+2}(t)-\tau_{i+1}(t-\tau_{i+2}(t))))}{g_i(T(t-\tau_{i+2}(t)-\tau_{i+1}(t-\tau_{i+2}(t))-\tau_i(t-\tau_{i+2}(t)-\tau_{i+1}(t-\tau_{i+2}(t)))))}\right)
\end{aligned}$$

Initial history and inoculation

To solve the equations from $t = 0$ onwards one must provide solution values for all points where $-\max_i(\tau_i) \le t \le 0$. For the system of balance equations (Equation 2.1) one can state that the system is empty, such that

$$\begin{aligned}
E(t) = L(t) = P(t) = A(t) &= 0 \\
R_i(t) = M_i(t) &= 0 \qquad -\max_i(\tau_i) \le t \le 0, \text{ all } i,
\end{aligned} \tag{2.8}$$

where i represents the stage, $i = E, L, P, A$. To determine initial conditions for the delay equations (Equation 2.4) is straightforward in the case where conditions are assumed to be constant for $-\max_i(\tau_i) \le t \le 0$. In all simulations it was assumed that conditions were constant before inoculation of the system. A discussion of the implications of allowing variable temperature conditions before $t = 0$ is given in Appendix A. In the constant case, the value for the initial duration of stage i, τ_{i0}, is given as

$$\tau_{i0} = \frac{1}{g_{i0}}, \tag{2.9}$$

where τ_{i0} and g_{i0} are the stage duration and development rate of stage i for $-\max_i(\tau_i) \leq t \leq 0$. Similarly, the initial value for the survival equation, S_{i0}, (Equations 2.3) can be calculated such that

$$S_{i0} = \exp(-\delta_{i0}\tau_{i0}), \tag{2.10}$$

where δ_{i0} is the death rate of individuals in stage i for $-\max_i(\tau_i) \leq t \leq 0$. Since it was stated that there were no larvae present before $t = 0$ there is no predation before this point.

To initiate the system, assume that some innoculation takes place at $t = 0$. This consists of adding individuals at a rate I_0 into the adult class over some small time interval (Murdoch et al. 2003) such that

$$I_A(t) = \begin{cases} I_0, & 0 \leq t \leq t_1 \\ 0, & \text{otherwise} \end{cases} \tag{2.11}$$

where $I_A(t)$ represents the rate at which adults are added to the system at time t. The number of individuals added has not been seen to affect the behaviour of the system past the first full year. As such, simulations were begun on the $1st$ of July and run for 18 months before taking results to ensure that the predicted seasonal abundance patterns had settled to stable annual cycles. These results where checked against results obtained with 30 months “burn-in" period and there was no change. When using the North Kent dataset the results of the first year were discarded to allow for this “burn-in" period, ensuring that the choice of initial conditions did not affect results.

2.2.2 Functional forms of demographic parameters with temperature

A literature review was carried out to identify and parametrise appropriate functional forms for the relationship of development and death rates of *Cx. pipiens* with temperature. The fitted parameter values for all functions are given in Table 2.1. The parameter values were fitted using the nonlinear least squares fitting procedure in the statistical software package R (R Core Team 2013). I took all data from *Cx. pipiens pipiens*, ignoring the other subspecies *Cx. pipiens restuans*, *Cx. pipiens torrentium* and *Cx. pipiens molestus*, as *Cx. pipiens*

pipiens is very common in the UK and laboratory data is readily available on this subspecies (Golding 2013).

Development rates

Growth rates for the immature stages were modelled using a power function, which mirrors the form used by Beck-Johnson et al. (2013) for *Anopheles* and gives development rates which increase with temperature (Figure 2.1)

$$g_i(T(t)) = \begin{cases} \alpha_i T(t)^{\beta_i}, & T(t) > \left(\frac{b_m}{\alpha_i}\right)^{\frac{1}{\beta_i}}, \\ b_m, & \text{otherwise} \end{cases}. \tag{2.12}$$

Here $i = E, L, P$ correspond to the egg, larval and pupal stages respectively. This is a biologically reasonable form to use as *Cx. pipiens* development rates are low at cool temperatures and increase within the thermal development range of $10-34\,^{\circ}\mathrm{C}$. Development may decrease beyond the $34\,^{\circ}\mathrm{C}$ upper limit, however the death rate is so high at these temperatures that the development rates become irrelevant in my model, as all immatures die before completing development. Using an equivalent R-squared value for a non-linear regression, equal to the regression sum of squares over the total sum of squares there is a good fit from the power function for all life stages: egg ($R^2 = 0.87$), larvae ($R^2 = 0.69$) and pupae ($R^2 = 0.56$).

At this stage, daily average water temperature was assumed to be equal to air temperature due to the lack of available information on water temperatures. The functional forms were chosen to be the same for each life stage as there was good agreement with the data, however different forms could be chosen in other models if deemed appropriate. It was assumed that the lower threshold of the development rate, b_m, should be set to stop development time dropping below 60 days ($b_m = \frac{1}{60} days^{-1}$) (Almirón and Brewer 1996)). The exact value chosen for b_m is unlikely to influence model output because only development rates outwith predicted thermal development thresholds (approximately $10 - 34\,^{\circ}\mathrm{C}$ Almirón and Brewer (1996) and Loetti et al. (2011)) are notably affected by this restriction. Beyond these thresholds, mortality is expected to occur before development completes.

Death rates

Death rates for the immature stages were modelled using a modified Gaussian functional form

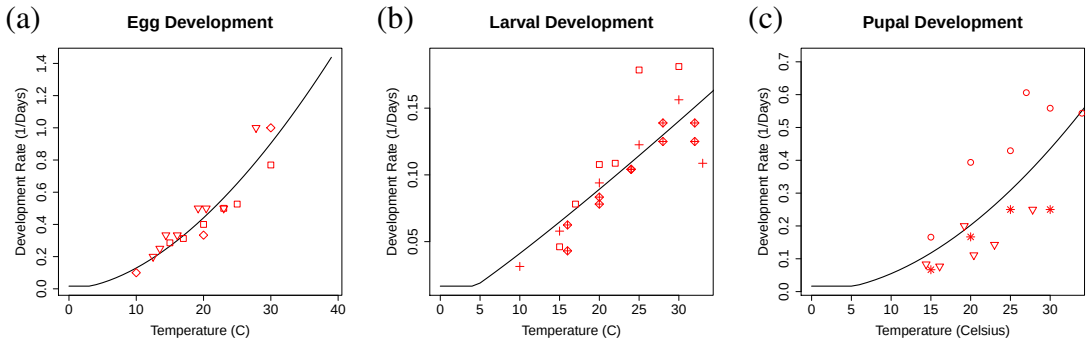

Figure 2.1: Immature development: The plots show curves fitted to data from the literature about the relationship between temperature and development rate of eggs (a) Madder et al. (1983b), Becker et al. (2010), and Jobling (1938), larvae (b) Madder et al. (1983b), Loetti et al. (2011), and Ciota et al. (2014) and pupae (c) Rueda et al. (1990), Jobling (1938), and Vinogradova (2000). Symbols represent the data source as follows: Madder et al. (1983b) - □, Becker et al. (2010) - ⋄, Jobling (1938) - ▽, Rueda et al. (1990) - ◯, Loetti et al. (2011) - +, Vinogradova (2000) - ⁎, Ciota et al. (2014) - ⊕.

$$\delta_i(T(t)) = \begin{cases} \nu_{0i} \exp\left(\left(\frac{T(t)-\nu_{1i}}{\nu_{2i}}\right)^2\right), & \nu_{1i} + \frac{\nu_{2i}}{2}\ln\left(\frac{b_{di}}{\nu_{0i}}\right) < T(t) < \nu_{1i} - \frac{\nu_{2i}}{2}\ln\left(\frac{b_{di}}{\nu_{0i}}\right), \\ b_{di}, & \text{otherwise}, \end{cases} \tag{2.13}$$

for $i = E, L, P$, which leads to expected survival times following a bell-shaped curve centred at ν_{1i} and bounded to be greater than or equal to $\frac{1}{b_{di}}$ (Figure 2.2). The choice of a modified Gaussian form again mimics that chosen by Beck-Johnson et al. (2013) for *Anopheles*. Biologically, this is an appropriate functional form as it leads to high death rates beyond the developmental thresholds of $10\,^{\circ}\mathrm{C}$ and $34\,^{\circ}\mathrm{C}$ and decreasing death rates between these thresholds towards some central minimum value. All immature stages were assumed to have the same temperature-dependent death rate because the vast majority of the literature presented survival percentages from egg hatch until adult emergence. There is a lot of variability in the mortality data obtained from the literature, which is not accounted for when fitting a function with temperature as the only explanatory variable (Figure 2.2, $R^2 = 0.28$). Couret et al. (2014) showed that temperature, larval diet, and density, and their interaction all affected development rates of the immature stages of *Aedes aegypti*. It was shown by Lyimo et al. (1992) that rearing temperature and larval density had a complex series of effects on larval survival, age at pupation, and adult size of *Anopheles gambiae*. Colless and Chellapah (1960) showed that increased body size led to increased egg raft size in two colonies of *Ae. aegypti* and it was shown by Ishii (1963) that increased larval density slowed the development of *Cx. pipiens* larvae. As such, it is not possible to capture all variability in mortality rates using temperature as the only explanatory variable. However, the shape of this functional form is supported by the physiological processes which govern mosquito development.

This modified Gaussian function is used as an approximation for this model and the need for inclusion of a wider range of environmental variables is considered in the discussion. With an unbounded death rate I encountered difficulties with the DDE solver code because the survival values became infinitesimally small. As such, an upper limit of b_{di} was imposed on the death rate (Figure 2.2). This limit was chosen such that the minimum expected lifespan was one day because all functions in the model are parametrised on a daily time scale. Upon varying this threshold within a range of values for which the DDE solver code worked there was no change in results, because development times are all greater than one day.

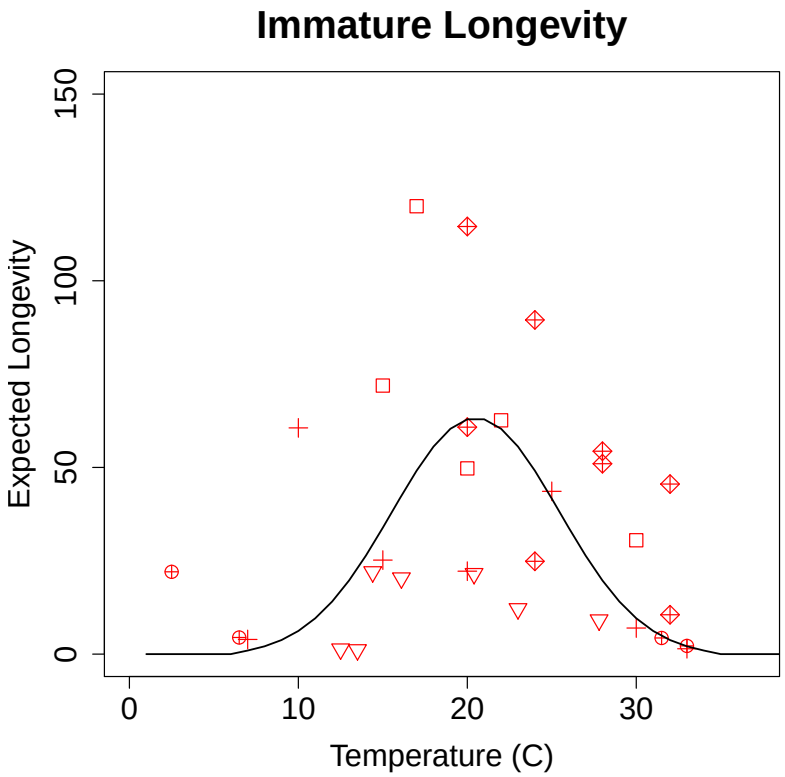

Figure 2.2: Immature longevity: Relationship temperature and expected longevity (reciprocal of the death rate) of immatures Madder et al. (1983b), Loetti et al. (2011), Ciota et al. (2014), Jobling (1938), and Farid (1948). Symbols represent the data source as follows: Madder et al. (1983b) - □, Jobling (1938) - ▽, Loetti et al. (2011) - +, Farid (1948) - ⊕, Ciota et al. (2014) - ⊕.

Adult death rates were modelled using a power function which was constrained below some threshold value (Figure 2.3 (a))

$$\delta_A(T(t)) = \begin{cases} \alpha_A T(t)^{\beta_A}, & T(t) > \left(\frac{b_{da}}{\alpha_A}\right)^{\frac{1}{\beta_A}} \\ b_{da}, & \text{otherwise} \end{cases} . \tag{2.14}$$

This captures the fact that mosquitoes can survive for long periods of time i.e. throughout the winter, at low temperatures and so should have a correspondingly low death rate. The death rate then increases with increasing temperature as reported by Ciota et al. (2014). This functional form shows a good fit to the data (R^2 = 0.65). The death rate was constrained not to drop below a base death rate of b_{da}, otherwise diapausing adults experience essentially zero mortality, which is unrealistic even when diapausing (Sulaiman and Service 1983; Onyeka and Boreham 1987). This overwinter survival rate was chosen to give percentage survival of roughly 10% depending on the length of the winter period, which falls within the range observed by Sulaiman and Service (1983). The value chosen was also consistent with some of the observations by Bailey et al. (1982), though they saw substantial variation between death rates of different groups and increasing death rates as diapause progressed, which is not incorporated here. At this stage, any relationship between humidity and adult mortality has also not been considered.

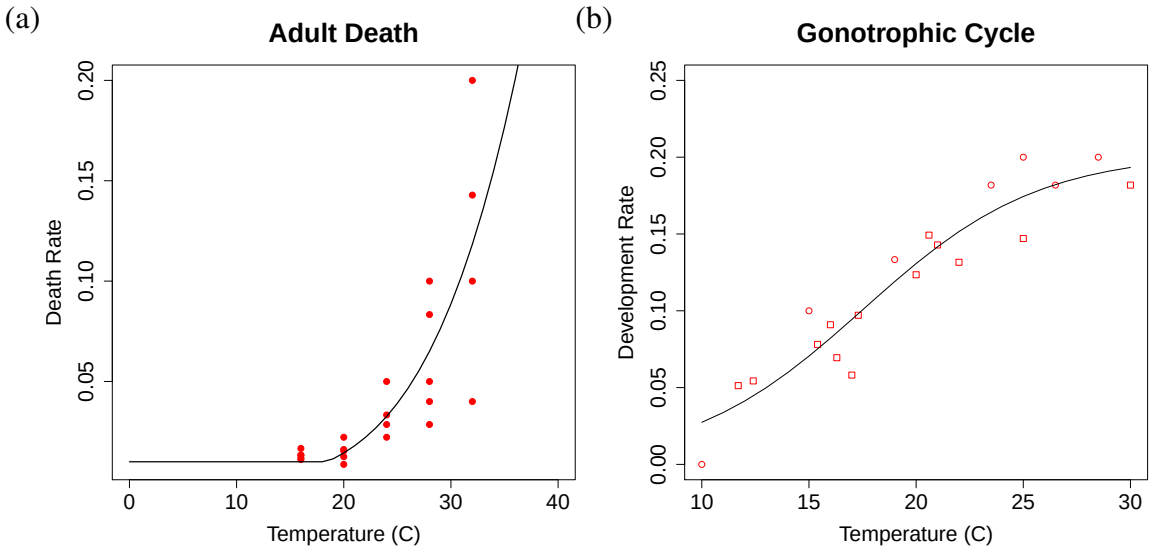

Figure 2.3: Adult vital rates: Temperature-dependent death rate of adults (a) Ciota et al. (2014) and gonotrophic cycle (b) Madder et al. (1983b) and Vinogradova (2000) (Symbols □ and ◯ respectively) fitted to data from the literature. Values for the gonotrophic cycle rate were calculated using the ovarian maturation times as stated in the literature but with 2 days added for locating a blood meal and ovipositing Hartley et al. (2012). All data is from *Cx. pipiens*.

Predation rate

Based on information from the literature I chose to represent the larval death rate due to predation by the Holling type II function (Marti et al. 2006; Fischer et al. 2013)

$$\delta_\pi(L(t)) = \frac{a\mathcal{P}(t)}{V + ahL(t)}. \tag{2.15}$$

where a is the attack rate, h is the handling time, V is the volume of habitat and $\mathcal{P}(t)$ is the number of predators at time t. I make the assumption that predator abundance is directly proportional to larval abundance such that $\mathcal{P}(t) = rL(t)$ where r is the number of predators per larva. This can be simplified and rewritten as

$$\delta_\pi(L(t)) = \frac{p_0 L(t)}{p_1 + L(t)}. \tag{2.16}$$

This gives a low death rate when larval density is low because the time the predator spends searching for prey is high. As larval density increases, the search time tends to zero and the death rate is governed by the handling time a predator needs to process each kill. This leads to an upper bound on the number of prey which can be consumed and thus on the death rate, δ_π.

In Equation 2.16, p_0 gives the upper limit to which the death rate due to predation tends, as larval density increases. The constant, p_1, gives the number of larvae required for the death rate to reach half of p_0. I was unable to find parameter estimates for p_0 and p_1 due to their sensitivity to predator behaviour (Onyeka 1983), habitat size, habitat type (Fischer et al. 2013) and oviposition behaviour (Angelon and Petranka 2002; Reiskind and Wilson 2004). I therefore performed a sensitivity analysis to understand the impact of variation in these values. This showed that seasonal abundance patterns could be quite sensitive to changes in p_0 below a certain threshold but that p_1 only affected population size.

Simulations showed that variation of p_1, the larval density at which the death rate due to predation reaches half its maximum, only resulted in changes to the absolute abundance without any effect on qualitative behaviour. The upper limit of larval death due to predation, p_0, can have a substantial effect on model behaviour. At low values of p_0 predation alone is insufficient to regulate the population, which exhibits growing oscillations year-on-year. I assume that either such situations do not occur in wild populations or that the population would also be regulated by larval competition at very high densities. Once p_0 becomes large enough to regulate the population a point is quickly reached where further increases only serve to repress population size with little difference in the pattern of seasonal abundance. I

chose to study the population for a value of $p_0 = 0.5$ as this was large enough for regulation but not large enough to result in unexpected extinctions.

Diapause

The proportion of active adults at any point in time, $\zeta(t)$, regulates the number of eggs laid per female, $b(t)$, and is dependent on both photoperiod, $\psi(t)$, such that

$$\zeta(t) = \begin{cases} \frac{1}{1+\exp(\omega_S(\xi_S - \psi(t)))} & : \psi(t) \text{ increasing}, \\ \frac{1}{1+\exp(\omega_A(\xi_A - \psi(t)))} & : \psi(t) \text{ decreasing}, \end{cases} \tag{2.17}$$

where $i = S, A$ and ξ_S is the spring photoperiod threshold for which greater than 50% of the population have left diapause (used when $\psi(t)$ is increasing) and ξ_A is the opposite threshold for the population entering diapause (used when $\psi(t)$ is decreasing). This means that individuals will enter and remain in diapause provided the photoperiod is below a given threshold, the values for which were chosen to coincide with presence of *Cx. pipiens* in overwintering shelters (Sulaiman and Service 1983). The effect of photoperiod on diapause behaviour is strongly dependent on rearing conditions (Vinogradova 2000). I chose to base my estimates on Sulaiman and Service (1983) because they carried out a UK-based study and I was interested in predicting for the UK. Photoperiod is calculated using the CBM model described in Forsythe et al. (1995), which is a function of latitude. For my simulations I chose the latitude of the North Kent marshes ($51\,^{\circ}$N) because it is a habitat for both *Cx. pipiens* and *Cx. modestus* (Golding et al. 2012). This area may also run a higher risk of introduction than other parts of the UK, due to possible introduction of mosquito-borne viruses through nearby ports (Golding et al. 2012). However, the model could readily be run for another latitude in the UK, as the data used to parametrise the functional forms is not specific to the North Kent marshes.

Egg-laying rate

Various factors including type of blood meal (Richards et al. 2012), number of gonotrophic cycles (Richards et al. 2012) and size of the female (Colless and Chellapah 1960; Cochrane 1972) have been shown to affect the number of eggs in a raft. For this model a constant egg raft size of R ($R = 200$) was selected to coincide with the average egg raft sizes found in the literature (Jobling 1938; Vinogradova 2000). To quantify the frequency with which egg rafts are laid the egg raft size is divided by the length of the gonotrophic cycle, which

is temperature-dependent. The functional form of the gonotrophic cycle development was chosen to reflect the data such that the gonotrophic cycle length increases as temperatures increase within the thermal development thresholds (Madder et al. 1983b; Vinogradova 2000; Hartley et al. 2012),

$$g_G(T(t)) = q_1/(1 + q_2 \exp(-q_3 T(t))), \tag{2.18}$$

where $g_G(T(t))$ is the rate of progression of the gonotrophic cycle at temperature $T(t)$, with q_1, q_2 and q_3 as fitted constants. The functional form was shown to give a good fit to the data, (adjusted $R^2 = 0.90$) (Figure 2.3). The egg-laying rate per adult female per day, $b(t)$, was then calculated according to

$$b(t) = \frac{1}{2\tau_G(t)} \times \zeta(t) \times R. \tag{2.19}$$

where the fraction of one half accounts for the fact that only females lay eggs and a 1:1 sex ratio is assumed (Vinogradova 2000).

2.2.3 Annual temperature variation

To determine the effect of changing seasonal temperature on mosquito populations a modified cosine wave was used to approximate the annual temperature curve for the UK (Figure 2.5 (a)),

$$T(t) = (\mu - \lambda) + 2\lambda \left(\frac{1}{2} + \frac{1}{2} \cos \left(\frac{2\pi(t - \phi)}{365} \right) \right)^{\gamma}, \tag{2.20}$$

where μ represents the annual midrange temperature, λ the amplitude of annual fluctuations, ϕ the timing of the temperature peak and γ the sharpness of the summer season, which acts as a measure of the duration of the warm period. This very flexible function allows the effects of a wide range of different seasonal temperature profiles on mosquito seasonal abundance to be studied. It is important to note that due to the power transformation, μ is only the mean temperature when $\gamma = 1$. A temperature dataset (obtained using FetchClimate (Microsoft 2014) and aggregating values from the UEA Climatic Research Unit (UEA 2015) and Hijmans et al. (2005)) from the North Kent marshes from 1951-2010 was examined to

Parameter	Definition	Value	Eqn	Reference
α_E	Fit parameter in egg maturation	2.20×10^{-3} $(days^{-1} \, ^\circ\mathrm{C}^{-\beta_i})$	2.12	Figure 2.1 (a)
β_E	Fit parameter in egg maturation	1.77	2.12	Figure 2.1 (a)
α_L	Fit parameter in larval maturation	3.15×10^{-3} $(days^{-1} \, ^\circ\mathrm{C}^{-\beta_i})$	2.12	Figure 2.1 (b)
β_L	Fit parameter in larval maturation	1.12	2.12	Figure 2.1 (b)
α_P	Fit parameter in pupal maturation	7.11×10^{-4} $(days^{-1} \, ^\circ\mathrm{C}^{-\beta_i})$	2.12	Figure 2.1 (c)
β_P	Fit parameter in pupal maturation	1.89	2.12	Figure 2.1 (c)
ν_{0L},ν_{0P}	Baseline immature death rate	0.0157 $(days^{-1})$	2.13	Figure 2.2 (b)
ν_{1E},ν_{1P}	Optimum temperature for immature survival	$20.5 \, ^\circ\mathrm{C}$	2.13	Figure 2.2 (b)
ν_{2E},ν_{2P}	Width parameter for immature death rate	$7 \, ^\circ\mathrm{C}$	2.13	Estimated from data
α_A	Fit parameter in adult death	2.17×10^{-8} $(days^{-1} \, ^\circ\mathrm{C}^{-\beta_i})$	2.14	Ciota et al. (2014)
β_A	Fit parameter in adult death	4.48	2.14	Ciota et al. (2014)
b_m	Baseline maturation rate	$\frac{1}{60}$ $(days^{-1})$	2.12	Almirón and Brewer (1996) Loetti et al. (2011)
b_{di}	Threshold immature death rate	1 $(days^{-1})$	2.13	Time-scale of model
b_{da}	Baseline adult death rate	0.01 $(days^{-1})$	2.14	Sulaiman and Service (1983)
a	Attack rate of predators	1	2.15	From simulation
h	Handling time of predators	0.002	2.15	From simulation
r	Max no. of predators per larva	0.001	2.15	From simulation
V	Volume of larval habitat	$200litres$	2.15	By calculation
R	Egg raft size	200 (eggs)	2.19	Vinogradova (2000)
q_1	Gonotrophic cycle fit parameter	0.202	2.18	Figure 2.3 (b)
q_2	Gonotrophic cycle fit parameter	74.5	2.18	Figure 2.3 (b)
q_3	Gonotrophic cycle fit parameter	0.246	2.18	Figure 2.3 (b)
ξ_S	Spring diapause threshold	14 (hours)	2.17	Sulaiman and Service (1983)
ξ_A	Autumn diapause threshold	13 (hours)	2.17	Sulaiman and Service (1983)
ω_S	Spring diapause transition	5	2.17	From fieldwork
ω_A	Autumn diapause transition	5	2.17	From fieldwork
φ	Latitude	51		Latitude of North Kent marshes

Table 2.1: Parameter values used for running the model

determine what range of parameter values could be expected at a UK site where *Cx. pipiens* is prevalent. This was particularly important in determining a range of timings for the annual peak in temperature, ϕ, and summer sharpness values, γ, (Figure 2.4 (c) and (d)) appropriate for the UK climate. The distribution of peak temperature dates was centred around the $1st$ of August, so all ϕ values are reported as +/- days from this central point. The summer sharpness parameter, γ, takes values in the range from $0.5 - 2.1$ with small values leading to a longer warm period and large values leading to a longer cold period (Figure 2.6 (a)). Upon examining the correlation coefficients between these parameters there was a moderate negative correlation between midrange and amplitude ($r_{\mu\lambda} = -0.55$) i.e. years with lower midrange temperatures tend to have a larger amplitude of temperature fluctuations. This is observable from the opposing skews of Figure 2.4 (a) and (b) and suggests that some of the most extreme high temperatures encountered by the model may not occur in reality, as high midrange temperatures and large seasonal fluctuations are unlikely to occur simultaneously. There was also a strong positive correlation between midrange temperature and sharpness of peak ($r_{\mu\gamma} = 0.80$) suggesting that more peaked summer periods are more likely to coincide with higher temperatures across the year.

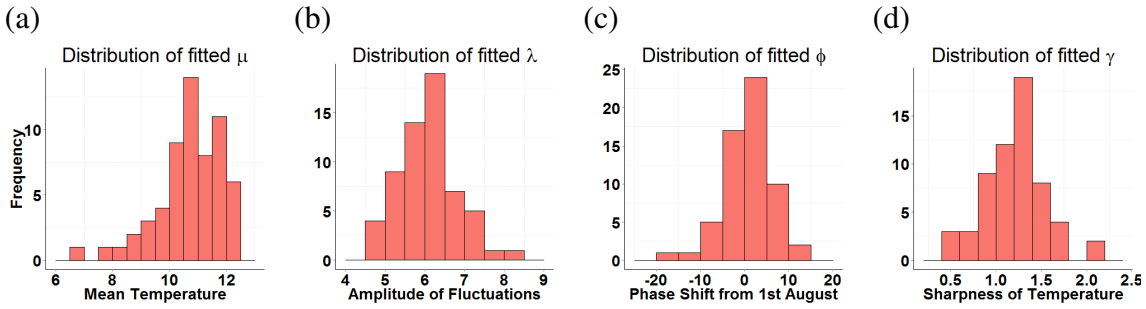

Figure 2.4: Temperature data from the North Kent marshes 1951-2010 was used to investigate typical values for the environmental variation parameters. Histograms of annual fitted values of the parameters are presented (a) midrange temperature, μ, (b) amplitude of fluctuations, λ, (c) phase shift presented as +/- days from the 1st of August (the mean date at which the peak occurred), ϕ, (d) sharpness of peak, γ (higher values indicate sharper peaks).

Air temperature was used in all parts of the model because information on water temperatures experienced by the aquatic stages was not available. Investigations of the relationship, and discrepancy, between air and water temperature have been carried out, primarily for tropical habitats. However, no appropriate functional form by which to link air and water temperatures was available. Furthermore, due to the large range of meteorological factors at play, relations between air and water temperature often cannot be extrapolated from one climatic region to another. The characteristics of each individual breeding site, with regards to a range of factors including sun exposure, water volume and container insulation, will

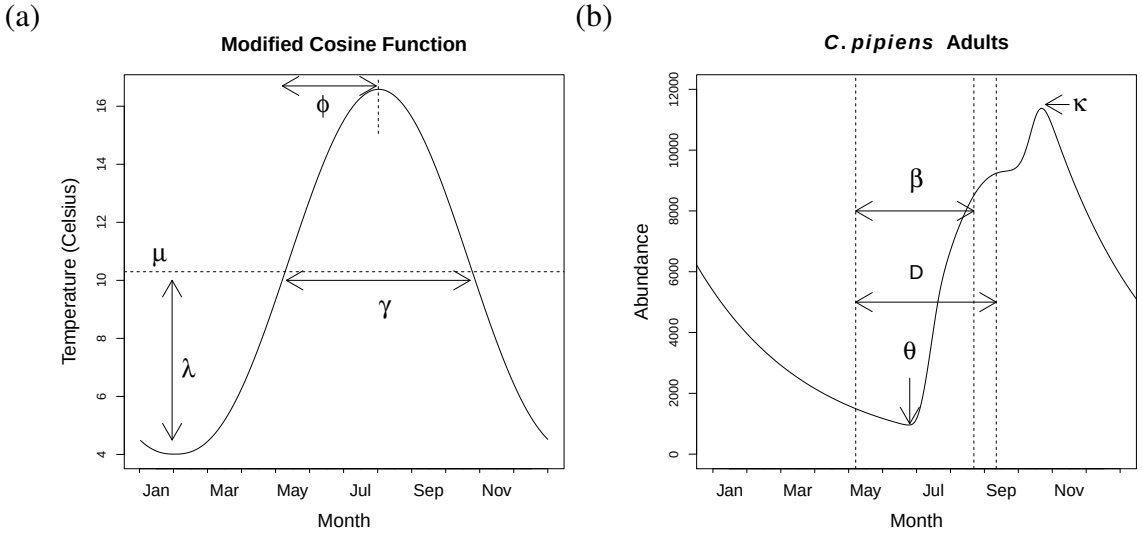

Figure 2.5: (a) The modified cosine curve showing the effect of each parameter on the shape of the curve: μ denotes the midrange temperature, λ is the amplitude of seasonal fluctuations, ϕ is the phase shift and γ a measure of the sharpness of the peak. (b) The abundance of adult mosquitoes through the year to illustrate summary statistics: κ is the peak in abundance, θ is the lowest abundance value, β is the length of the biting season and D shows the period between the two 50% thresholds for diapause.

also affect the relationship between air and water temperatures. Studies examining temperate habitats are rare, though a recent study on British container-breeding mosquitoes by Townroe and Callaghan (2014) found that water temperatures tended to slightly exceed air temperatures, particularly in urban settings, though the difference was generally negligible and never exceeded approximately $2\,^{\circ}\mathrm{C}$ at any point in the year. Due to the lack of a defined functional relationship between the two temperatures and the infrequent periods in which there was a substantial difference approximating all temperatures by the air temperature was considered reasonable at this stage.

The effect of covariation of these parameters on seasonal abundance of mosquito populations was described using three mosquito summary statistics (Figure 2.5 (b)). This discussion is focussed around effects on adult mosquitoes, as it is adults which transmit disease. However, example outputs for all life stages are shown in Figure 2.6. The peak adult abundance, κ, describes the largest mosquito population on a given day in a given year, with a high κ value signalling favourable conditions for mosquito development. Minimum abundance, θ, gives a measure of overwinter survival with small values clearly indicating a small population surviving through winter. Length of the biting season, β, defines the maximum length of time over which the mosquitoes are potentially active in transmission, in the event of a pathogen introduction. Initiation of the biting season occurs when more than 50% of the adult population have left diapause and the mean daily temperature exceeds $10\,^{\circ}\mathrm{C}$. The $10\,^{\circ}\mathrm{C}$ temperature

threshold was chosen because predicted thermal development thresholds are approximately $10 - 34\,^{\circ}\mathrm{C}$ (Almirón and Brewer 1996; Loetti et al. 2011). The end of the biting season is defined as occurring one full life cycle (time required for completion of the gonotrophic cycle and egg, larval and pupal development) before adult emergence of the autumn progeny, which are assumed not to bite before going into diapause i.e. it ends with the biting of the late-summer adults that give rise to this autumn generation. This approximation is made because most *Cx. pipiens* which overwinter, do so having developed in preparation for diapause through the immature stages and do not take a blood-meal on emergence but instead feed on nectar to increase lipid reserves (Mitchell and Briegel 1989). It is therefore assumed that the main biting season stops the length of one cycle before these diapausing individuals emerge. Within the biting season, the intensity of transmission will depend upon the ratio of adult vectors to hosts which fluctuates through the season.

2.2.4 UKCIP Climate Change Projections

Temperature profiles used for the simulations were chosen to coincide with the nature of climate warming predicted by the UK Climate Impacts Programme (UKCIP) (UKCIP 2010). The report details three warming scenarios corresponding to low, medium and high CO_2 emissions, with temperature changes by the 2020s, 2050s and 2080s reported relative to a baseline from 1961-1990 (MetOffice 2010). I present the expected value under the medium emissions scenario for each date range for South East England, the area with the highest estimated risk of WNV introduction from migratory birds (Bessell et al. 2014). Predictions under other climate warming scenarios can easily be obtained by examining the UKCIP projections but are not presented here as I only wish to give an overview, rather than a full region-by-region analysis accounting for a range of emissions scenarios.

2.2.5 Exploring sinusoidal temperature approximation

Many studies incorporate seasonal forcing of either parasite transmission (Altizer et al. 2006) or vector abundance (Smith et al. 2004; McLennan-Smith and Mercer 2014) through the use of a sinusoidal wave. Indeed, this analysis of how changing temperature affects seasonal abundance of temperate mosquitoes relies on the approximation of the annual temperature profile by a modified cosine wave. I wished to explore how this approximation may affect predictions of vector abundance and to understand the effects on population parameters of incorporating inter-annual variation in seasonal forcing. I compared results obtained when interpolating between mean daily temperature data points to those found using the modified cosine approximation, both incorporating and excluding variability between years. The

model was run for the full 1961-1990 baseline period (with the results from 1961 discarded to allow the equations to stabilise) interpolating between the mean daily temperature values in the North Kent marshes (Microsoft 2014). The model was then run 29 further times with each year replaced by the best fitting modified cosine wave for that year. Finally, 29 more runs were carried out with each year's daily temperature series replaced by a modified cosine wave which had been fitted to the full baseline time series simultaneously.

2.3 Results

An analysis of the effects of changing the temperature parameters on the mosquito summary statistics - maximum abundance, minimum abundance and length of biting season - was carried out to understand how different temperature regimes affected seasonal abundance. These results were also placed into the context of potential changes to the UK climate using the UKCIP predictions. A sensitivity analysis was then carried out to clarify which of the temperature parameters were expected to be the most influential drivers of mosquito abundance. Finally, the impacts of including intra- and inter-annual variability in temperature on mosquito seasonal abundance were examined, to help understand its potential influence on epidemiological models.

2.3.1 Maximum abundance (κ)

The effects of changing the temperature profile on maximum abundance, κ, are shown in Figure 2.7. In all cases increasing midrange annual temperature, μ, leads to an increase in maximum abundance, κ (Figure 2.7 (a,b,f)). Similarly, increased amplitude of seasonal temperature fluctuations, λ, consistently leads to increased maximum abundance (Figure 2.7 (c,d,f)). All cases also show that maximum abundance increases as the peak temperature shifts later in the year (ϕ increases) within the studied range (Figure 2.7 (a,c,e)). In all cases the model shows high population growth late in the season, leading to a peak in adult abundance in mid-October. This is because decreasing larval numbers at the end of the year cause a release of density-dependence, resulting in higher larval survival, increased pupal numbers (Figure 2.6 (c)) and consequently high adult abundance. This effect would not be captured by host-seeking trapping methods as the emergent adults are programmed for diapause (Mitchell and Briegel 1989). Sulaiman and Service (1983) observed mosquitoes entering diapause throughout October in some years, lending some support to this hypothesis.

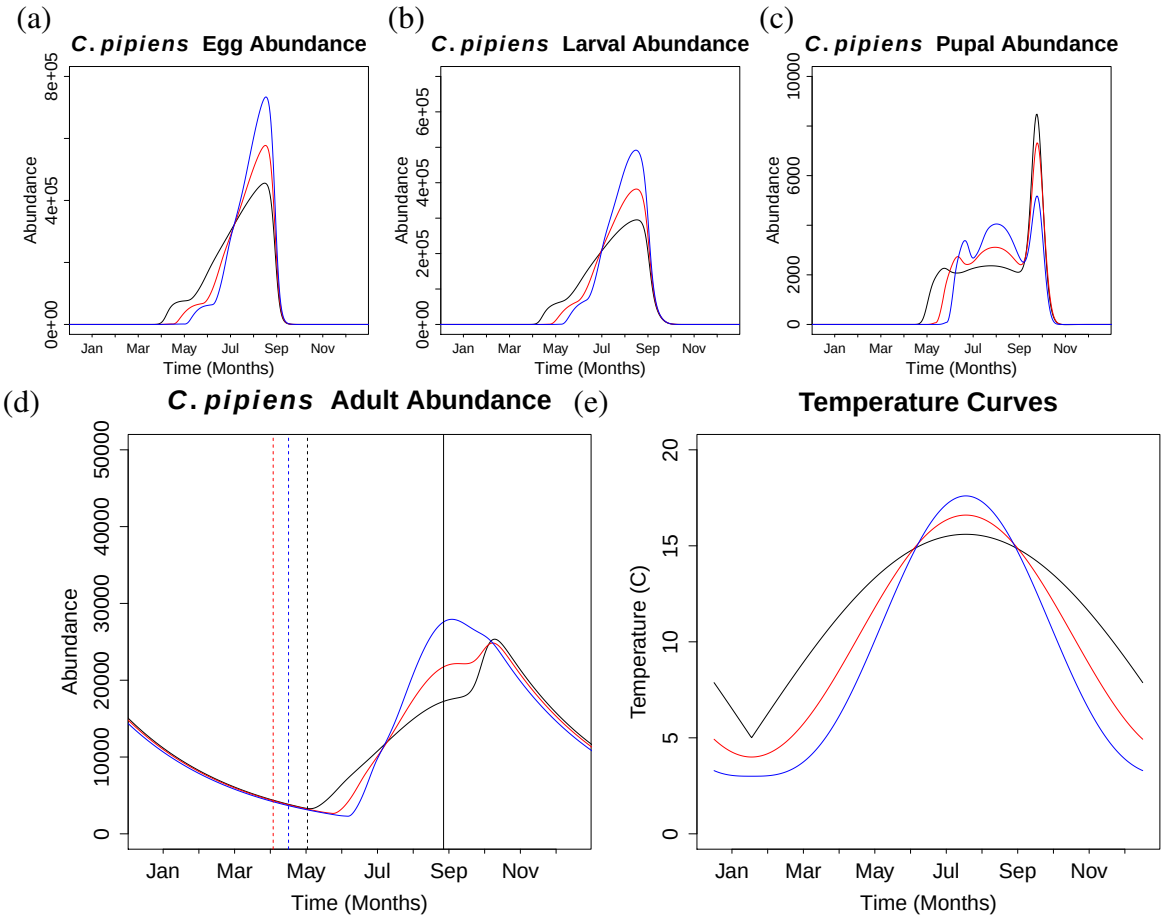

Figure 2.6: Season length and timing effects on abundance: Plots (a)-(d) show the abundance of eggs, larvae, pupae and adults for the three temperature scenarios shown in (e). On the adult plot, (d), the solid black line shows the diapause induction point and the dotted lines show the diapause termination points for each temperature regime.

Finally, for a given midrange annual temperature, amplitude of seasonal fluctuations or timing of peak temperature, decreased sharpness of the summer season (smaller values of γ), leading to longer periods of high temperature, gives larger maximum abundance (Figure 2.7 (b,d)). However, when sharpness of the summer season, γ, and amplitude, λ, are covaried, more sharply peaked temperature functions can lead to the larger abundances, even when mean annual temperatures are lower (Figure 2.6 & 2.7 (e)). In Figure 2.6, the highest abundance is shown by the blue line, despite the fact that it has the lowest mean annual temperature (mean temperatures are blue= $9.2\,^{\circ}$C, red= $10.3\,^{\circ}$C, black= $11.7\,^{\circ}$C).

2.3.2 Minimum abundance (θ)

The effect of environmental conditions on spring starting population size, θ, are shown in Figure 2.8. As with peak abundance, increasing annual midrange temperature or amplitude

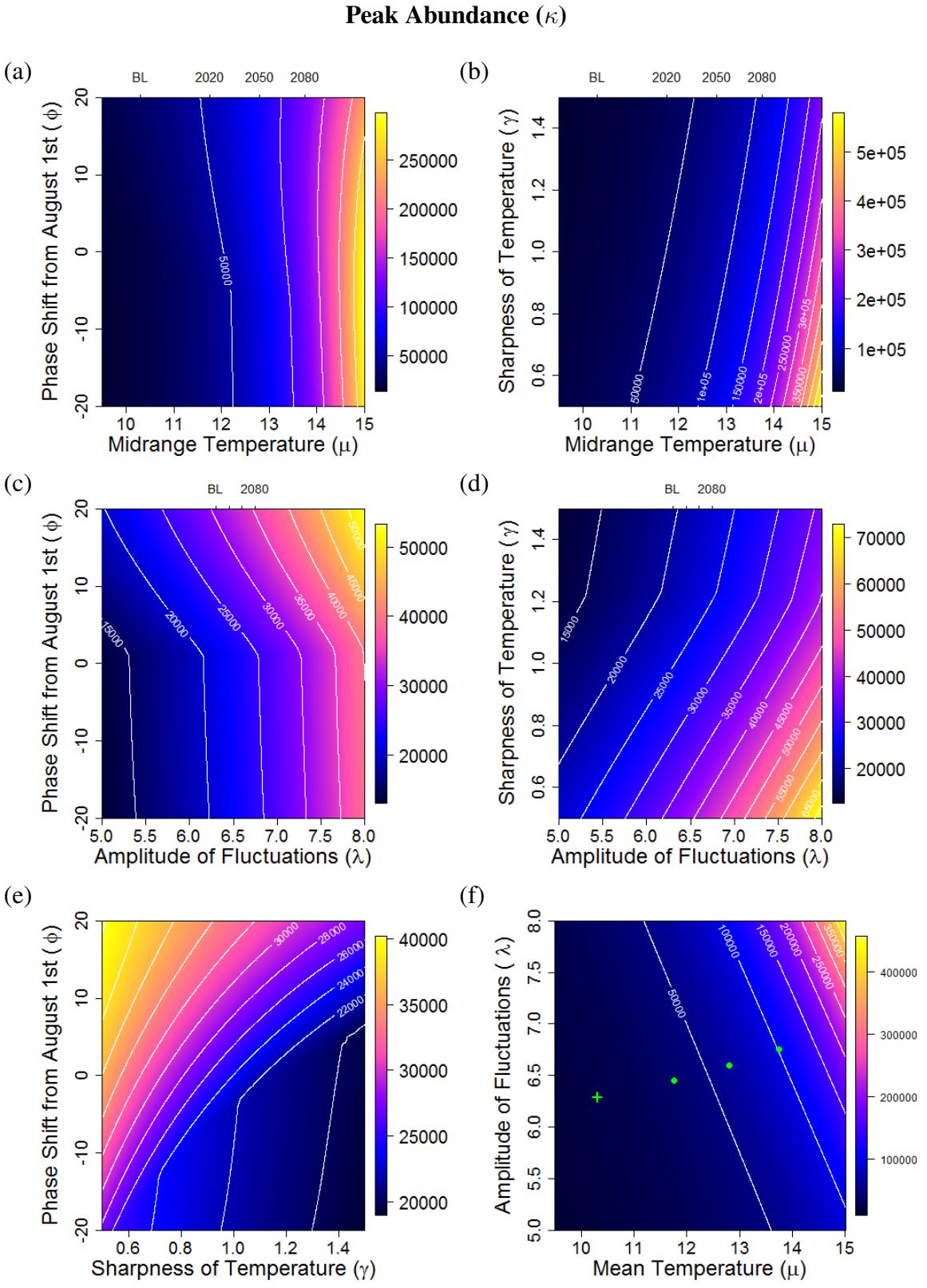

Figure 2.7: The effect of changing temperature variables on peak seasonal abundance of *Cx. pipiens* adults, κ. The axes atop figures (a-d) show the UKCIP projected values for μ and λ for the 2020s, 2050s and 2080s with the baseline (1961-1990) marked as BL. The white lines are contour lines. The green points on panel (f) show abundance given projected increases in both μ and λ by the 2020s, 2050s and 2080s relative to a 1961-1990 baseline (BL) shown by the green cross. There are no UKCIP projections available for shifts in μ or γ. When not varied, values are held according to the UKCIP baseline values for SE England (μ = 10.3 °C, λ = 6.3 °C, ϕ = +1.4 days and γ = 1.21).

of fluctuations always led to increased spring population, due to a combination of increased population growth in summer and decreased mortality over shorter winters (Figure 2.8 (a-d,f)). In co-varying midrange and peak temperature timing, the effects of changing peak time were relatively small and difficult to discern in comparison to those of increasing midrange but generally appeared to be negligible (Figure 2.8 (a)). When varying timing of peak temperature with amplitude increased spring populations were visible as amplitude increased and the temperature peak moved later in the year (Figure 2.8 (c)). Similarly, varying peak temperature timing with summer sharpness suggested that later temperature peaks tended to lead to larger spring populations (Figure 2.8 (e)). A trade-off between slightly earlier peak temperatures minimising the winter duration and slightly later peaks leading to larger summer populations is observable. Interestingly, conditions which led to higher summer abundance did not necessarily lead to a higher number of through-winter survivals. This was particularly evident in examining the relationship between timing of peak temperature and duration of high temperatures as lengthening summer, and correspondingly shortening winter, led to larger spring populations in some cases, whilst also giving smaller summer populations (Figure 2.7 (c) and 2.8 (c)).

2.3.3 Length of biting season (β)

The effect of environmental conditions on the length of the biting season, β, was investigated (Figure 2.9). All four temperature parameters can affect the biting season, provided either the termination or onset of diapause is governed by temperature, via cooler spring or autumn period, rather than via a photoperiodic queue. When photoperiod determines both the start and end of diapause, temperature has a negligible role in determining the length of biting season. Amplitude of seasonal fluctuations was seen to have a smaller effect on the biting season than the other parameters because it had the least potential to affect the duration over which the temperature exceeded $10\,^{\circ}\mathrm{C}$ (Figure 2.9 (c,d,f)). Increasing the midrange temperature led to notably longer seasons when the $10\,^{\circ}\mathrm{C}$ temperature threshold occurred within the range of the photoperiod thresholds (Figure 2.8 (a,b,f)). This can be seen in the divides between the yellow regions (governed by photoperiod) and the darker regions (governed at least partly by temperature). Shifting the peak temperature later in the year led to a decreased length of biting season because the onset of the season is delayed by low temperatures and the end of the season remains governed by photoperiod for the entire range explored (Figure 2.8 (a,c,e)). Decreasing the sharpness of the temperature peak consistently led to longer biting seasons because the $10\,^{\circ}\mathrm{C}$ thresholds move apart and development times generally decrease (Figure 2.8 (b,d,e)).

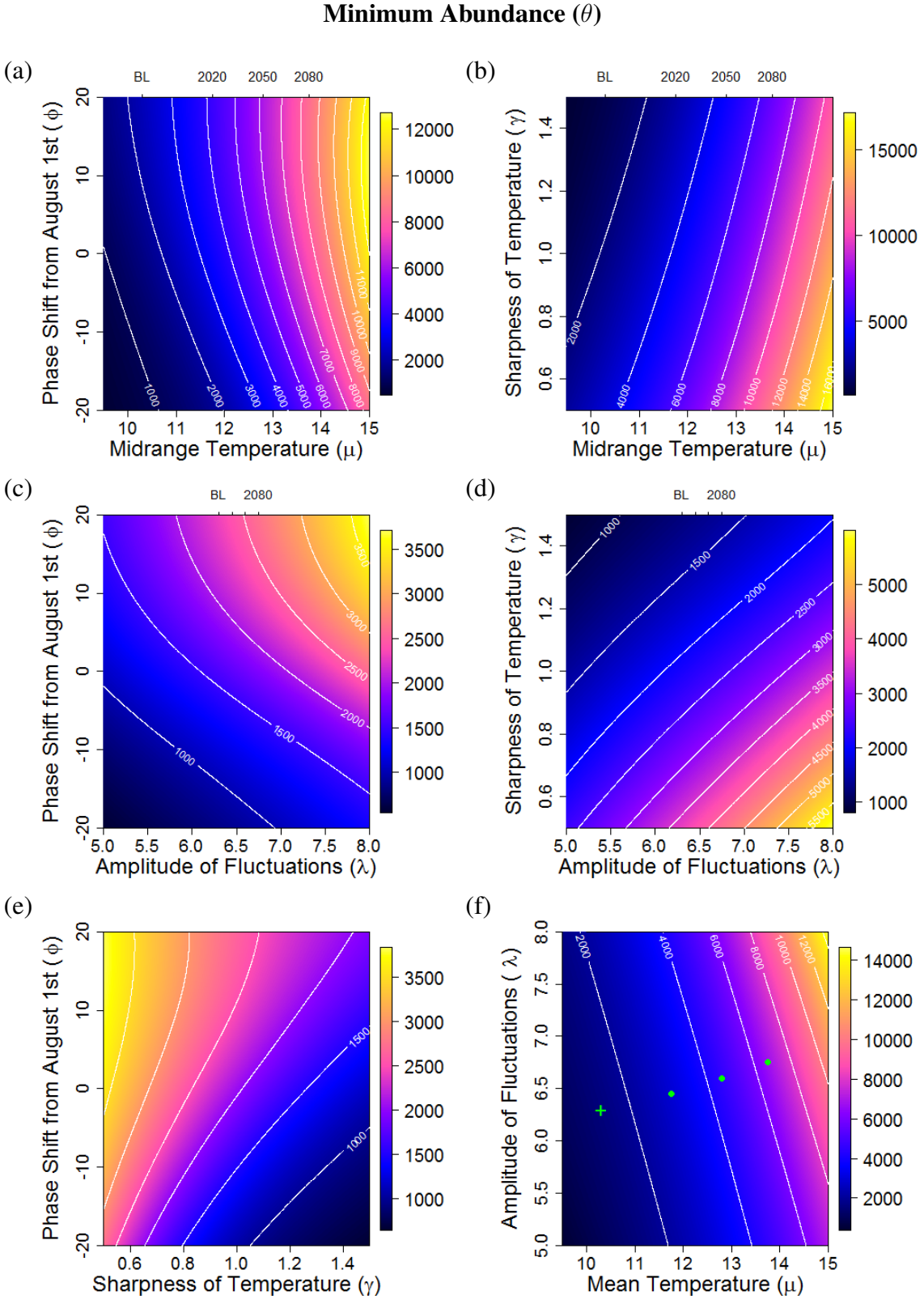

Figure 2.8: The effect of changing temperature variables on minimum seasonal abundance of *Cx. pipiens* adults, θ. The axes atop figures (a-d) show the UKCIP projected values for μ and λ for the 2020s, 2050s and 2080s with the baseline (1961-1990) marked as BL. The white lines are contour lines. The green points on panel (f) show abundance given projected increases in both μ and λ by the 2020s, 2050s and 2080s relative to a 1961-1990 baseline (BL) shown by the green cross. There are no UKCIP projections available for shifts in μ or γ. When not varied, values are held according to the UKCIP baseline values for SE England (μ = 10.3 °C, λ = 6.3 °C, ϕ = +1.4 days and γ = 1.21).

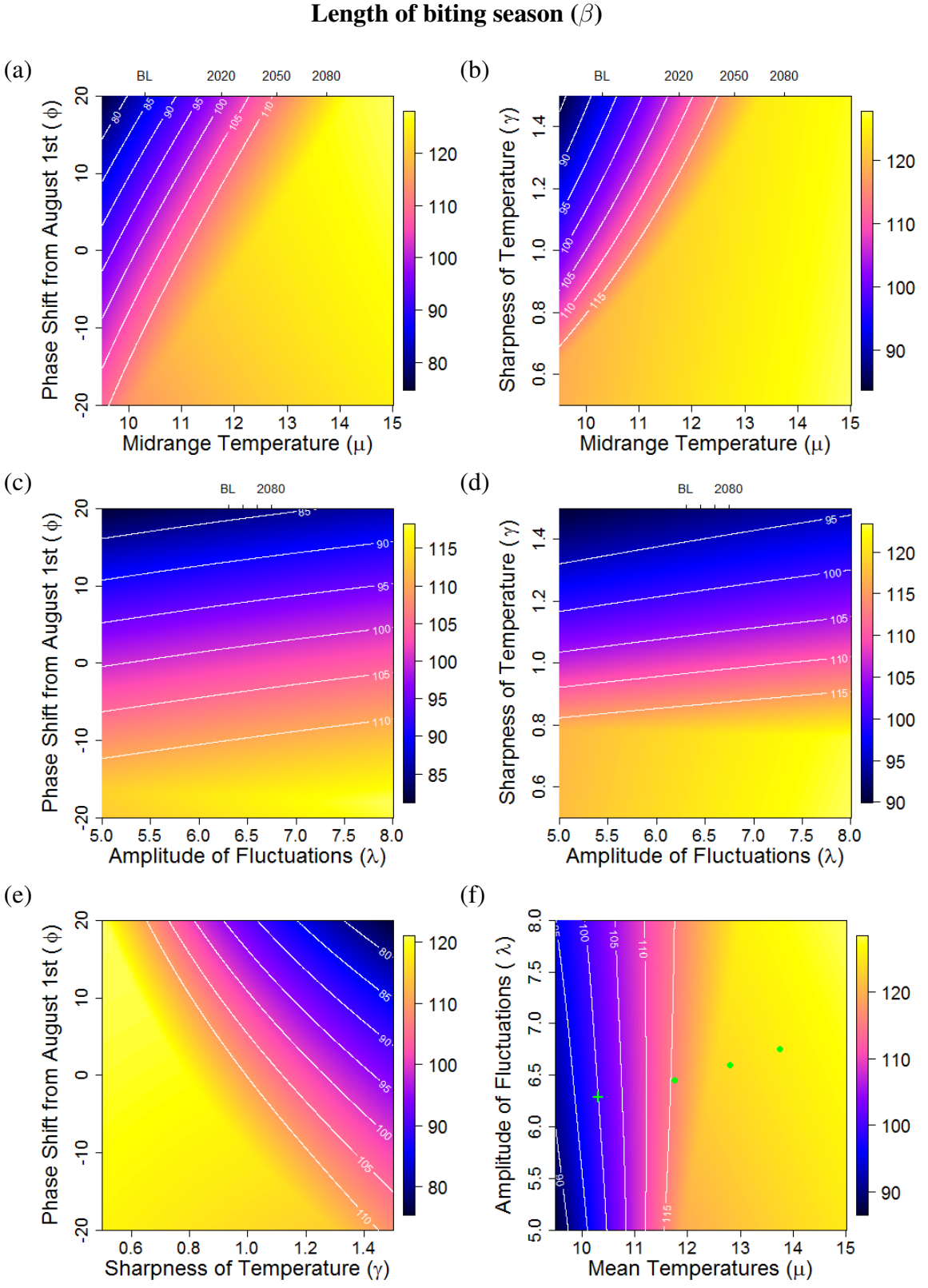

Figure 2.9: The effect of changing temperature variables on the length of the biting season of *Cx. pipiens* females, β. The axes atop figures (a-d) show the UKCIP projected values for μ and λ for the 2020s, 2050s and 2080s with the baseline (1961-1990) marked as BL. The white lines are contour lines. The green points on panel (f) show abundance given projected increases in both μ and λ by the 2020s, 2050s and 2080s relative to a 1961-1990 baseline (BL) shown by the green cross. There are no UKCIP projections available for shifts in μ or γ. When not varied, values are held according to the UKCIP baseline values for SE England (μ = 10.3 °C, λ = 6.3 °C, ϕ = +1.4 days and γ = 1.21).

2.3.4 Sensitivity Analysis

A sensitivity analysis was carried out to understand the effects of changes within the expected range of variability for each of the four parameters of the modified cosine wave (Figure 2.10). The coefficient of variation was calculated for each of the four temperature parameters according to the data from the North Kent marshes and the parameters were varied accordingly. The plots clearly show that peak mosquito abundance is most sensitive to changes in midrange of the annual temperature, μ. This is as expected because both development and survival of larvae increase rapidly with rising temperatures, relative to those currently experienced in the UK. Further, an increase in midrange temperature has a larger effect than an equivalent decrease because development rates are concave upwards (Figure 2.1). The effect of amplitude, λ, mirrors that of midrange, μ, but is less marked because this change does not result in as large an increase in summer temperatures and diapausing mosquitoes experience less sensitivity to small temperature changes. The effect of peak temperature timing, ϕ, is sensitive to which date the shift is relative to. However, in this instance shifting the timing of the peak temperature (a shift of approximately +/-6 days) affects peak mosquito abundance on a similar scale to varying amplitude within its range of variation. Sharpness of the summer season γ, has quite a substantial effect on peak abundance and, akin to the observations with temperature midrange, lengthening the summer period has a greater impact than an equivalent shortening.

The effects of midrange, amplitude and sharpness on spring population size, θ, mimic their effects on peak abundance, as κ and θ are highly correlated (r_p = 0.968). Timing of peak temperature, ϕ, is slightly more influential in determination of post-winter population size than on peak abundance because it has a notable effect on the length of the biting season. This is because earlier peak temperatures tend to lead to an earlier biting season start date but the termination of the season occurs as a result of photoperiod. Biting season is affected almost equally by an increase in midrange temperature or by a lengthening of the summer season, though decreasing the midrange temperature has a larger impact than an equivalent shortening of the season. Both amplitude and timing of peak temperature have quite small effects on the length of the biting season, producing changes of about 5% or lower. Again, the peak abundance κ and the length of the biting season, β, are strongly correlated (r_p = 0.854).

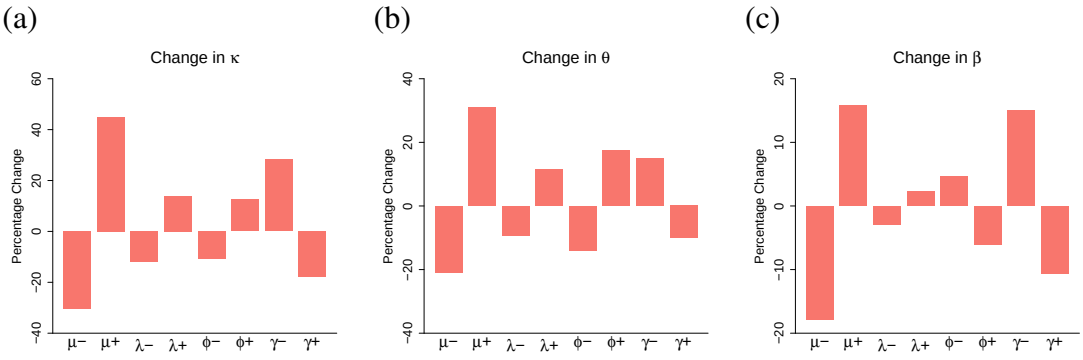

Figure 2.10: (a - c) Show the effect of a change in each of midrange temperature, μ, amplitude of fluctuations, λ, phase shift, ϕ and sharpness, γ, on peak abundance, κ, minimum abundance, θ and length of biting season, β, respectively. The size of the changes shown are chosen according to the magnitude of the coefficient of variation (+/- $10.6\%, 11.8\%, 17.1\%$ and 28.1% for midrange temperature, amplitude of fluctuations, timing of peak temperature and sharpness of summer period, respectively).

2.3.5 Exploring modified cosine temperature approximation

The mosquito summary statistics (maximum abundance, κ, minimum abundance, θ, and length of biting season, β) were calculated for each year, interpolating between exact temperature values and using cosine waves which either included or excluded inter-annual variability (Figure 2.11 (a-c)). It is clear from Figure 2.11 (a) that the cosine wave incorporating inter-annual variability generally predicts a peak abundance, κ, closer to that estimated using the interpolation method than the cosine wave which is fixed across the years. The observation is supported by the fact that the mean absolute percentage difference between the interpolation prediction and the modified cosine prediction is 8.6% (95% CI $(5.5\%, 11.6\%)$) when inter-annual variability is included and 14.7% (95% CI $(11.0\%, 18.5\%)$ when excluded. A Wilcoxon signed ranks test shows that this difference is statistically significant (p = 0.006). The differences in minimum abundance, θ, estimation are less pronounced with an average mean absolute difference of 6.7% (95% CI $(5.3\%, 8.1\%)$) when incorporating inter-annual variability and 8.8% (95% CI $(6.6\%, 11.0\%)$) in the fixed case, which was not found to be statistically significant (p=0.066). When comparing the length of the biting season for the three methods it is clear that the interpolation method leads to greater predictions for the length of the biting season. This is because, when the true temperature values are smoothed over by fitting a cosine wave, the date at which the season begins is pushed later. There was no statistically significant difference found between the estimated lengths of the biting season for the two cosine waves (p=0.915). The residual sum of squares for each cosine fit was not found to be linked with the magnitude of the changes between the interpolation predictions and those from the modified cosine waves. Similarly there was no statistical evidence of a link between any of the individual modified cosine parameters and the percentage

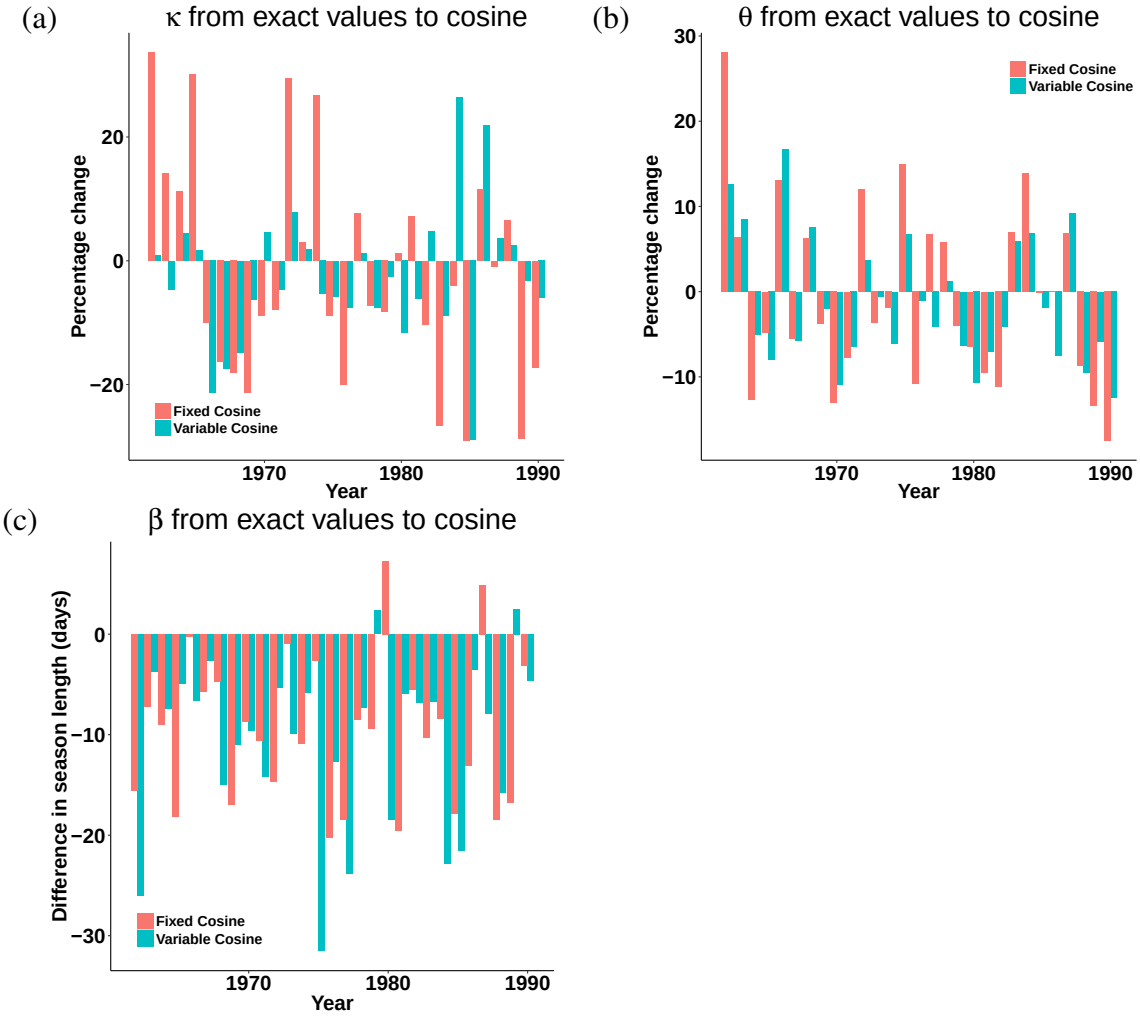

Figure 2.11: (a) and (b) show percentage changes, in peak abundance, κ, and minimum abundance, θ, respectively, in predictions from interpolation between mean daily temperatures and from the two modified cosine waves (pink - fixed, blue - variable). (c) shows the actual change in the length of the biting season in moving from the interpolation between mean temperature values and the two cosine waves.

changes in abundance.

2.4 Discussion

Whilst it has long been understood that a range of environmental drivers, including temperature, have a large impact on mosquito physiology and thus on development, recruitment and death rates (Couret et al. 2014; Ciota et al. 2014; Lyimo et al. 1992), the effect of changing climate on seasonal dynamics has been unclear (Semenza and Menne 2009). Development of a mechanistic model which explicitly incorporates the effects of temperature on each of

the mosquito life stages takes important steps towards understanding how predicted warming can be expected to influence seasonal population abundance of temperate mosquitoes. The model supports expectations that increased temperatures could lead to substantial increases in mosquito numbers and estimates that, given predicted increases in both mean annual temperature and amplitude of seasonal temperature fluctuations for the UK, *Cx. pipiens* abundance will increase in coming years. The results also indicate that even small changes in seasonal temperature, in particular mean annual temperature, could lead to sizeable changes in mosquito seasonal abundance and phenology (Mirski et al. 2012). This sensitivity highlights the need for detailed incorporation of the effects of environment on vector dynamics in epidemiological modelling. In interpreting these findings, it is important to be aware that hydrological processes, such as the effects of rainfall and humidity on adult and larval survival, have not been incorporated into the model. Inclusion of these processes will be crucial to fully understand vector seasonality, as high temperatures in temperate climates often lead to lower humidity and rainfall, which could counteract the positive effects of temperature on abundance.

These results show that the size, both of peak mosquito populations and of populations surviving over winter, will increase with increasing amplitude of seasonal temperature fluctuation. One may have expected that, with increasing amplitude causing both higher summer temperatures and cooler winters (when annual mean temperature remains fixed), effects on peak vector abundance would trade-off against one another. This trade-off is not observed because the model is much more sensitive to temperature changes in the summer months than through the winter. This is partly because there is little empirical data on responses of mosquitoes to cold temperatures, though diapausing mosquitoes are believed to be relatively insensitive to temperatures changes within the region of 0 to $10\,^{\circ}\mathrm{C}$, which is typical for the UK winter. Extreme cold and very low relative humidities have been shown to drastically increase mortality in diapausing *Cx. pipiens* (Rinehart et al. 2006) but these effects are not included in our model (Equation 2.14) because adults typically overwinter in protective shelters and are therefore likely to be buffered against extreme temperatures and humidities. This buffering was seen in populations of *Cx. pipiens*, which thrive through much of Russia, where external temperatures ranged from -22 to $-4\,^{\circ}\mathrm{C}$ whilst temperatures in diapause shelters ranged from -11 to $-1.1\,^{\circ}\mathrm{C}$ (Vinogradova 2000). It is rare for temperatures cold enough to induce exceptionally high mortality rates to occur in the UK (3 consecutive days below $-5\,^{\circ}\mathrm{C}$ in (Rinehart et al. 2006)). However, even subtle effects of low temperature on overwinter survival have altered disease persistence in the US (Wimberly et al. 2014). Very low temperatures may be limiting for key transmission processes, though further research is required to improve understanding, and allow parameterisation, of these processes.

The model also shows that a “late" summer, where temperatures peak in mid-to-late August, leads to a larger peak mosquito abundance than an “early" summer, with peak temperatures in July. I expect this is due to the peak temperature aligning with the development of a larger number of mosquitoes, since abundance in the model steadily increases through the summer months. Further, it was observed that maximum temperatures and the timing of these temperature peaks can be more influential in determining mosquito abundances than mean annual temperatures (Figure 2.6). This is an important finding as it is often assumed that predicted increases to mean annual temperature will cause increases in mosquito population size. Whilst this is likely to be true, this result suggests that periods of extreme high temperatures may cause more severe increases to mosquito population size than general temperature increases spread across an entire season.

Many standard approaches model seasonality using sinusoidal seasonal forcing to describe parasite transmission and thus fail to capture daily and inter-annual variability (Altizer et al. 2006). Here, seasonal abundance predictions using an interpolation between mean daily temperatures were compared with a series of annually fitted modified cosine waves, and a series of cosine waves ignoring inter-annual variability. This highlighted that mosquito populations can be very sensitive to small changes in the seasonal temperature profile. The results obtained using the observed daily temperatures more closely mimic the results when incorporating inter-annual variability in cosine curve parameters than when excluding such variability (Figure 2.11 (a)). This finding is crucial because current climate projections for the UK suggest that inter-annual variability in weather patterns will increase in coming years (Jones et al. 2009). No evidence was found that failure to either capture temperatures at a daily scale or to include inter-annual variability would lead to systematic over- or under-prediction of seasonal abundance. This contrasts with what may be expected from Jensen’s inequality (Jensen 1906), which would suggest that smoothing through the points with a cosine wave would result in overestimate development times. Given these results it seems that the approximation of a modified cosine can still be reasonable for a simulation-based experiment, as presented here, because it shows the response to environmental changes in a clear way and does not appear to show bias in results. Indeed, such approaches are necessary to understand the impacts of specific seasonal temperature characteristics, such as late summers or particularly short summers, as these effects can be difficult to tease out when using observed temperature values. This technique is also useful for forecasting future changes, when precise daily variability in temperatures will be unknown but predictions of how annual means and timings of peak temperatures may shift are available. However, when using the modified cosine wave, estimates of peak mosquito abundance may regularly differ from

those one would obtain interpolating between mean daily temperature values by as much as 20% and these margins of error should be considered in the formulation of any transmission model that uses these values as input.

Rainfall patterns are likely to have a direct effect on the number and size of larval habitats, which will affect larval density. Many studies have shown that intra-specific competition, as well as predation, impacts larval development and death rates (Alto et al. 2012; Loetti et al. 2011; Peters and Barbosa 1977; Beketov and Liess 2007), with recent work showing that the interaction between temperature and competition may strongly influence seasonal dynamics (Amarasekare and Coutinho 2014). These impacts will be strongly linked to hydrology and can be included in models using a variety of functional forms discussed by White et al. (2011). The importance of such processes on seasonal abundance was clearly displayed by Morin and Comrie (2013), who showed that both abundance and timing of biting season of *Cx. quinquefasciatus* across the Southern United States was strongly latitude- and longitude-dependent, due to the interaction of temperature and rainfall throughout the season. The model results indicate that population growth is strongly affected by the assumption of a fixed larval habitat, as increased larval density in midsummer causes population growth to level off, due to predation rates approaching their maximum, before increasing again in the latter part of the season, particularly when there is a long summer (Figure 2.6 (d) black line). As larval numbers dwindle in the late summer months, density decreases and larval survival increases again, leading to a late season abundance increase. In the field, due to contraction of breeding sites as they dry out over the summer, the crash in larval survival due to predation, and in future extensions of the model competition, may continue into the late summer period. However, human creation of larval habitats, such as people storing water butts in their gardens or using hosepipes, may also be key when considering abundance of *Cx. pipiens* in the UK, due to the decreased dependence on rainfall for larval habitat through the drier months, particularly in urban settings (Townroe and Callaghan 2014). To account for these effects a similar approach to that taken by Tran et al. (2013) could be taken where larval habitat was composed of both permanent and temporary reservoirs. For these reasons, in the future hydrological processes must be explicitly incorporated into the model if understanding of how changing climate may influence seasonal abundance of temperate mosquitoes is to be improved.

This work shows that DDEs can be an effective and flexible tool in modelling mosquito seasonal dynamics. To develop and refine this work, advancements must be made in three key areas of research. Firstly, understanding of how predation on larvae and competition between larvae interact to regulate population size must be improved, as these areas have, to

date, been studied in isolation of one another (Quiroz-martinez and Rodriguez-Castro 2007; Madder et al. 1983b; Agnew et al. 2000; Alto et al. 2012). Secondly, humidity has been shown to have an effect on mosquito populations (Lebl et al. 2013; Carrieri et al. 2014), however the impacts on individual mosquitoes are poorly understood, which restricts model parametrisation. Finally, the interaction between temperature and photoperiod and its effect on diapause behaviour are strongly dependent on region and rearing conditions (Tauber et al. 1986) and whilst numerous investigations have been carried out to understand these processes in *Cx. pipiens* populations in Russia and surrounding countries (Vinogradova 2000) and in North America (Spielman 2001; Bailey et al. 1982; Madder et al. 1983a; Sanburg and Larsen 1973), this work remains to be done for European populations.

Vector-borne disease models can only be effective if the estimates of vector density, required as inputs, are accurate (Lord 2004). The extrinsic incubation period (EIP) of a pathogen, mosquito biting rate and vector competence may all vary substantially with temperature (Ciota and Kramer 2013), meaning the identification of periods where peaks in vector abundance may overlap with high biting rates and short EIPs will be crucial in determining transmission risk. My model predicts these timings given environmental conditions and shows that vector abundance and phenology are highly variable, which could interact positively or negatively with disease dynamics, causing sporadic disease outbreaks. By explicitly modelling the vector population in all its life stages and incorporating the effects of environmental variability on the vector life cycle, I have developed a tool which can be used in tandem with existing epidemiological models to improve seasonal predictions of vector-borne disease transmission, using R_0 models like that presented by Hartemink et al. (2011). Recent studies investigating the risk of WNV introduction or spread, such as Bessell et al. (2014), have been forced to make the assumption that mosquito populations are fixed, without accounting for the effects of environment on mosquito seasonality and behaviour. By coupling predictions of seasonal vector abundance with these epidemiological models, one could substantially improve model predictions and our understanding of disease transmission risks (this idea is explored in detail in Chapter 5). In particular, by applying a 1:1 sex ratio and including diapause dynamics in our model, one can specifically estimate the population of host-seeking females, which is the key subset of adults required by epidemiological models. Furthermore, age-dependent (Bellan 2010) or infection-status dependent mortality, or behavioural alteration of adults (Alto et al. 2014; Ciota and Kramer 2013; Ciota et al. 2013) have been shown to be very influential in models of mosquito-borne disease transmission and control (Bellan 2010), and these effects could be incorporated in this model. By explicitly including the effects of temperature on vector seasonal dynamics, I have developed a tool which can be combined with our understanding of pathogen transmission to improve predictions on the

risk of disease transmission and spread.

Chapter 3

Cx. pipiens seasonal abundance data collection

3.1 Introduction

Multiple interacting ecological processes underpin seasonal dynamics of insect vectors. Density-independent effects, in particular temperature, can influence a range of processes in insects, including development, fecundity and mortality (Brown et al. 2004). Temperature can often have opposing impacts on population dynamics, with high temperature having a negative effect on adult survival (Andreadis et al. 2014) but a positive effect on immature development (Ciota et al. 2014). Density-dependent effects, such as intra-specific competition, can also impact population dynamics and patterns of abundance, as limited access to food or other resources has been shown to induce multiyear population cycles, or chaotic behaviour (Klomp 1964). Inter-specific interactions, which are also density-dependent, such a predator-prey interactions or competition between species can have similar affects on insect phenology (Connell 1983; Schoener 1983). The relative roles of these processes remain uncertain in most insect vector systems, hampering our ability to predict transmission seasons and persistence between years. Due to the complexities associated with modelling multiple such drivers, most model systems still focus on single drivers. However, to capture insect population dynamics accurately, it is often necessary to incorporate both density-dependent and density-independent processes (Bewick 2016), as in Chapter 2.

Density-dependence has been shown to limit population sizes in numerous ways, including through competition for food resources and both conspecific and heterospecific predation. This regulation can cause a range of abundance patterns, including stable states, population

cycles and chaotic behaviour (Sinclair and Pech 1996). Understanding the relative contributions of density-dependent and density-independent factors on mosquito abundance is crucial because different life stages inhabit different ecological niches. Consequently, vector control measures either target the larval stage, which is known to be density-dependent (Alto et al. 2012), or the adult stage, where evidence of density-dependence is scarce (Smith et al. 2013), with important impacts on control efficacy. Understanding the relative contributions of these biotic, density-dependent processes, when presented alongside abiotic processes, requires that models incorporate both factors (Benton et al. 2006). Such approaches are becoming more common, with a mark-release-recapture field study by Nowicki et al. (2009) monitoring butterfly abundance trends at a 2.9 hectare site in northern Italy showing that density-dependence appeared to be significantly more influential than abiotic factors. Tamburini et al. (2013) showed, using a long term dataset, whilst summer temperature and rainfall significantly affected population growth rate of an alpine moth species, density-dependence was the most important factor in determining population dynamics. Chaves et al. (2012) showed that population dynamics of the mosquito, *Aedes aegypti*, exhibited both substantial density-dependent regulation and sensitivity to temperature and rainfall.

In the case of *Cx. pipiens*, low temperature over the winter months creates conditions unsuitable for development and survival of immature mosquitoes, causing a cessation of breeding activity as adults enter a diapausing state (Denlinger and Armbruster 2014). During the active mosquito season, both adult and immature population dynamics are strongly driven by temperature (Bisanzio et al. 2011; Mulatti et al. 2014; Rosà et al. 2014), which influences immature development rates (Loetti et al. 2011), survival of all stages (Ciota et al. 2014) and consequently abundances of each life stage. Further, inter- and intra-specific competition (Madder et al. 1983b; Costanzo et al. 2005; Ruybal et al. 2016) and predation (Onyeka 1983; Mogi and Okazawa 1990) have been observed to affect development and survival of the larval stage of *Cx. pipiens* in laboratory and field studies, across its geographical range. Statistical models have also used these mechanisms to successfully explain regulation of population sizes during the biting season (Costanzo et al. 2005; Mulatti et al. 2014). Substantial uncertainty remains around the relative contributions of density-dependent and density-independent factors to abundance patterns in field populations.

Diapause is a mechanism widely used by insect species to survive adverse seasons (Sim and Denlinger 2013). Diapause behaviour is highly variable across mosquito species, dependent on the environmental conditions faced. Many tropical mosquito species may not diapause, when conditions remain favourable for development all year round. Temperate species, however, have adapted a range of strategies to survive poor winter conditions, with

diapause occurring in different life stages for different species (Denlinger and Armbruster 2014).

Mosquito dispersal to different habitats has resulted in evolution of variability in diapause behaviour within species. For example, Lounibos et al. (2003) show that *Aedes albopictus* does not diapause in tropical regions but does in response to low photoperiods in temperate climates. Consequently, expansion of *Ae. albopictus* across the USA has led to diapause incidence being positively correlated with latitude due to differences in photoperiods experienced. This correlation is consistent with findings across a range of mosquito species where the length of the growing season declines as one moves north, leading to earlier diapause induction due to the earlier arrival of winter at more northerly locations (Denlinger and Armbruster 2014). The decline in growing season length at more northerly locations has been shown to lead to a decreased voltinism (number of generations in a year) in insect species (Zeuss et al. 2017), which will affect opportunities for disease transmission in vectors. These results have been reflected in *Cx. pipiens* populations, for which diapause induction has been shown to occur in response to low photoperiods (Sanburg and Larsen 1973; Madder et al. 1983b; Spielman 2001), with relatively low rates of diapause at more southerly locations (Nelms et al. 2013). There is some evidence that higher temperatures may also delay diapause induction (Sanburg and Larsen 1973; Madder et al. 1983b; Spielman 2001) and bring forward diapause termination (Ciota et al. 2011) in *Cx. pipiens*, however these effects are believed to be secondary to photoperiod (Sim and Denlinger 2013; Denlinger and Armbruster 2014). A clear understanding of diapause induction and termination queues is central to our ability to predict mosquito biting and disease transmission seasons (Armbruster 2016), as well as pathogen persistence overwinter (Nelms et al. 2013).

A recent review paper by Reiner et al. (2013) highlights that 82% of mechanistic models of mosquito-borne pathogen transmission between 1970-2010 either did not use data, or used data to estimate only one or two parameters ($N_{models} = 388$). This marriage of mechanistic models and field data is crucial in capturing and understanding interacting ecological processes and their implications for population dynamics (Bewick 2016). Such attempts to combine mechanistic models of mosquito dynamics with data have become more popular in recent years. Jian et al. (2014b) investigate the relative importance of biotic and abiotic processes in determining population size of *Cx. pipiens* in Northern Italy. Alongside important abiotic factors such as temperature, daylight hours and soil moisture, the authors find significant density dependence at a time scale related to the length of larval development. These findings are echoed by those of Marini et al. (2016), who find that observed interseasonal abundance patterns can largely be explained by different temperatures and larval

carrying capacities, which the authors estimate by applying maximum likelihood methods to 12 years of field capture data. As larval carrying capacity will directly affect density-dependent processes, this finding again suggests that inclusion of density-dependent and density-independent processes will be key.

As previously discussed, mosquitoes are known to show geographic variability in diapause initiation and termination, in response to shorter growing seasons at increasing latitudes (Denlinger and Armbruster 2014). To determine how aspects of mosquito phenology, including diapause, may vary in response to different environmental drivers experienced across their range, analyses incorporating the range of environmental conditions experienced across their geographic range are required. Such analyses have been used to understand the effect of environmental queues on continental-scale avian migration phenology using weather data and citizen science bird data (Kelly et al. 2016). In insect populations, Zeuss et al. (2017) showed that voltinism decreased with increasing latitude in lepidopterans and odonates across Europe. On smaller scales, variations in phenology of *Culicoides* have been attributed to land cover and climatic variables in Scotland (Searle et al. 2013). In Spain the environmental factors underlying the spatial variability of appearance of the honey bee have been investigated (Gordo et al. 2010), revealing a strong link between temperature and latitude, and emergence dates. Given sufficient data of a high temporal resolution and enough sampling effort at the start and end of the vector season it would be possible to conduct similar analyses for mosquito species. Such analysis would improve understanding of how environmental factors drive phenology across the range.

To improve understanding of these key processes affecting population dynamics and to further develop the mathematical model, presented in Chapter 2, by identifying aspects of seasonal abundance which were captured particularly well or poorly, an extensive period of fieldwork was taken. I monitored abundances of all *Cx. pipiens* life stages in the field at a high temporal resolution to determine:

1. What roles do density-dependent and abiotic factors play in the regulation of abundance patterns in the field? Are the relative importances of these biotic and abiotic factors consistent across the season?
2. What are the observed diapause induction and termination times for a UK population of *Cx. pipiens*? Can patterns in diapause timings across *Cx. pipiens* geographical range be predicted from environmental variables?
3. How does the voltinism of UK field populations of *Cx. pipiens* compare to *Cx. pipiens*

in other parts of its range? Are the patterns of abundance consistent across all life stages?

4. Given the temperatures observed in the field, does the mathematical model, presented in Chapter 2, accurately predict seasonal abundance in each life stage?

I discuss the answers to questions 1-3 in this Chapter and perform a full comparison of the model with the observed field data to answer question 4 in Chapter 4. In the latter part of this Chapter, this data is then discussed in the context of the wider range of *Cx. pipiens* seasonal abundance data found across the literature, to determine if geographical patterns in diapause behaviour can be predicted from environmental drivers.

3.2 Methods

3.2.1 Field data collection

Intensive sampling of adult and immature mosquitoes was carried out from the 2nd of March until the 2nd of October, 2015. The start date coincided with the first full week in March, a minimum of one month earlier than previous UK fieldwork start dates (Hutchinson et al. 2007; Townroe and Callaghan 2014; Townroe and Callaghan 2015) and was chosen to ensure that the start of the *Cx. pipiens* season would be captured by my field data. Collections were stopped at the beginning of October in response to five consecutive sampling occasions where no eggs or adults were observed. Ending sampling in October is consistent with other UK monitoring programmes (Hutchinson et al. 2007; Townroe and Callaghan 2014; Townroe and Callaghan 2015). The field study was carried out on the grounds at the Centre for Ecology $\&$ Hydrology (CEH) site in Wallingford (51° 36' 9.0144" N, 1° 6' 45.7344" W) (Figure 3.1).

3.2.2 Immature sampling

Immature *Cx. pipiens* were monitored using four 450 litre circular water butts (Figure 3.2(a)) placed at the locations shown in Figure 3.1. Butts number 1 and 2 were placed in exposed locations with some cover from bushes on the north side but all other sides open and no overhanging vegetation. These butts received direct sunlight throughout the majority of the day. Butt number 3 was more sheltered with no overhanging vegetation but cover on the north and west sides and direct sunlight until late afternoon or early evening dependent on

Figure 3.1: Field site: Red markers show the locations of water butts 1-4. Yellow markers show the locations of adult traps 1-4. The blue marker shows the location of the meteorological site (not present at the time the satellite image was taken).

(a)  (b) 

Figure 3.2: Mosquito traps: One of the four water butts used as larval habitat is shown in (a). Image (b) shows an adult trap.

the time of year. Butt number 4 was sheltered under a tree and only received direct sunlight in the morning. Consequently, the four butts were subjected to different biotic and abiotic environments. All butts were located within 20 yards of each other. In January the butts were filled with clean water, which was then infused with hay by suspending 2kg of hay in a net bag in each butt. The hay infusion was used because adult female *Cx. pipiens* are known to favour breeding sites with a high organic content and hay infusions have been shown to be effective attractants (Tate and Vincent 1933; Jobling 1938; Vinogradova 2000). The bags of hay were left in the butts until the end of March and then removed for ease of sampling to avoid the larvae hiding in the hay bags. A HOBO temperature logger, floating on the surface of the water, was set to record surface water temperature at hourly intervals in each butt, as *Cx. pipiens* spend most time at the surface (Yee et al. 2004).

The number of egg rafts in each butt was counted at 10am on Mondays, Wednesdays and Fridays, allowing abundance changes to be tracked at a high temporal resolution. Samples were taken from the 2nd of March until the 5th of October 2015, by which time six consecutive sampling occasions showed zero egg rafts (Figure 3.3 (a)) (note that in three weeks only two counts were made due to logistical issues). On each sampling occasion, after the egg rafts were counted a 500ml dip was taken from each of the north, south, east and west edges of each water butt using the standard dipping procedure (described in Additional File 2 of Fillinger et al. (2008)). No dips were taken from the middle of the butt as both larvae and pupae were observed to congregate at the edges. The dips were transferred into one or more white plastic trays for counting (Figure 3.3 (b)). When numbers were less than approximately 20, numbers of 1st/2nd instar larvae, 3rd/4th instar larvae, and pupae were counted in the field at the time of collection. In most cases this was not possible due to the large number of individuals in each sample, so photographs were taken of the contents of each tray. The samples were then counted manually on the computer using Microsoft Paint. The validity of counting from photos was checked by comparing direct counts from the tray with counts from photos on the first two days of sampling. Image recognition software could not be reliably used to count the larvae both due to the poor contrast between the water colour and the larvae, and to the inability to distinguish between different larval instars and life stages. All samples were returned to the water butts after photographing to prevent removal effects from one catch to the next. Twenty 4th instar larvae were taken from each water butt (when abundances were high enough that the number removed was a small proportion of the total population) monthly for morphological identification to species level (Becker et al. 2003). Those 4th instar larvae taken for identification were examined by microscopy in the laboratory using the identification keys in Becker et al. (2003). Larvae were killed prior to examination by submersion in boiling water. Identification of earlier instars is not possible because they are morphologically indistinguishable from larvae from a number of other species (Becker et al. 2003).

3.2.3 Adult sampling and identification

To sample the adult population four John W. Hock Miniature Downdraft Blacklight (UV) traps (also referred to as CDC light traps) (Figure 3.2 (b)) were run nightly from the 14th of April until the 2nd of October, when there had been 5 consecutive empty collections, in the yellow locations indicated on Figure 3.1. The traps were baited with dry ice to attract female adult mosquitoes and were run 4 times a week overnight from Monday to Thursday throughout the year (though seven nights were missed due to logistical issues). These traps

(a)  (b) 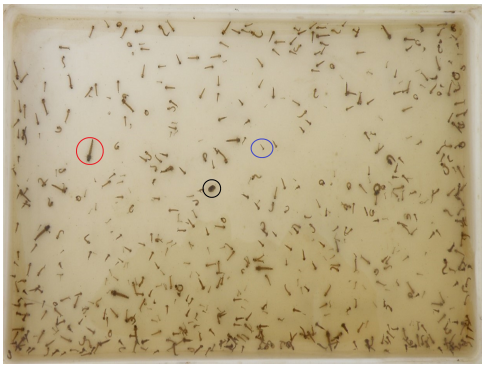

Figure 3.3: A group of egg rafts floating on the water surface is shown in (a). Image (b) shows an example sample of larvae and pupae. A 1st/2nd instar larva is circled in blue, a 3rd/4th is circled in red and a pupa is circled in black.

are widely used in sampling adult *Cx. pipiens* as they are relatively inexpensive and reliable, and have been shown to be effective in attracting *Cx. pipiens* (Lee and Rowley 2000; Hutchinson et al. 2007; Loss et al. 2009; Ciota et al. 2011; Kemenesi et al. 2014; Montarsi et al. 2015). Adult trapping started later than immature trapping due to logistical issues with the supply of dry ice. Trap 1 was hung amongst some trees adjacent to the water butts and traps 2 to 4 were hung in the tree line at the side of an adjacent field used to graze cattle at distances of approximately 80m, 140m and 200m from the water butts (Figure 3.1). The traps were run from 1700 each day until 0900 the following morning, as *Cx. pipiens* biting is known to peak just after sunset and during sunrise (Meillon et al. 1967). Adults were placed in the freezer immediately after collection and left for at least one hour before identification. All mosquitoes caught were identified to species level by microscopy in the laboratory using the identification keys in Becker et al. (2003) and the number of females of each species was recorded. Males were not recorded as they do not blood feed or contribute to disease spread and so are not present in substantial numbers in the traps. Minimum and maximum daily ambient air temperature, cumulative daily rainfall, daily sunlight hours and mean daily wind speed were recorded throughout the sampling period at a CEH weather station in the adjacent field.

3.2.4 Analysis of field data from the CEH Wallingford site

Relationship between adult abundance, month and daily meteorology

A quasi-poisson GLM (Nelder and Wedderburn 1972; Wooldridge 1999) was fitted to the daily abundance of adult female *Cx. pipiens* to determine which environmental variables were key determinants of adult catch on a particular day and to determine when adult catch

size was observed to decrease late in the season as a result of diapause induction. A quasi-poisson model was chosen because the poisson distribution is appropriate for count data but the data was found to be overdispersed (dispersion parameter 3.35). The explanatory variables included were; rainfall in the 24 hours prior to collection, sunlight hours, mean wind speed, maximum and minimum air temperature in the 24 hours prior to collection, cumulative rainfall in the three weeks prior to collection and average maximum air temperature in the three weeks prior to collection. Three weeks was chosen because this is the estimated time from egg hatch to adult abundance at $15\,^{\circ}\mathrm{C}$ (Loetti et al. 2011), which is the mean water temperature across the summer of the butt with the highest immature abundance. Finally, month of the year was included as a factor variable to account for changes in the population size throughout the season.

In particular, it was hypothesised that

- Rainfall variables will have a positive impact on abundance due to increased habitat availability (Wang et al. 2011; Mulatti et al. 2014).
- Positive impacts of air temperature, such as increased biting and immature development rates (Loetti et al. 2011), will outweigh potential negative impacts, such as decreased adult longevity (Ciota et al. 2014), leading to increased catch sizes .
- Month of the year would affect catch size as the mosquito population size would increase throughout the biting season, before decreasing in autumn as adult females enter diapause.

Variable selection was carried out using a variant of the Akaike information criterion (AIC) (Akaike 1973), the quasi-AICc (qAICc). QAICc values were calculated using the dredge function in R (Barton 2016), which fits models containing all possible combinations of the explanatory variables and ranks those models by qAICc and the model with the lowest qAICc was chosen. The qAICc is a version of the AIC, a commonly used model selection tool, which is appropriate for overdispersed count data when the sample size is small (Anderson et al. 1994). The qAICc was selected because the sample size was relatively small, with the number of samples per parameter below 40. A quasi-AIC was required because the quasi-poisson GLM was fitted. The model residuals were tested for normality and for temporal autocorrelation at lags of up to 50 observations, which includes the predicted egg-laying to adult emergence times for any water temperatures observed during the active season.

The role of developmental processes and mortality rates in explaining immature abundance patterns

Sampling each of the immature life stages in water butts allowed me to assess the relative contributions of biotic and abiotic processes to *Cx. pipiens* development and survival. Predictions of density-dependent larval survival were obtained by solving Equation 2.3 for $S_L(t)$, given the hourly water temperatures experienced in butt 4 at the field site. Density-independent larval survival was calculated in the same way, with $\delta_\pi(t)$, the larval mortality due to predation, set to zero. Similarly, predictions of larval stage duration were obtained by solving Equation 2.4 for $\tau_L(t)$, using hourly temperatures from butt 4. The resulting outputs are time series giving larval survival and stage duration at all times through the year. Predicted pupal abundance at time t, $\hat{P}_j(t)$, was generated using my field observations of egg abundance, $E(t)$, with the model predictions for generation time and survival, such that

$$\hat{P}_j(t) = E(t - \tau_L(t))S_L(t), \tag{3.1}$$

where $j = d, i$ correspond to using density-dependent and density-independent larval mortality respectively. These predicted pupal abundances, $\hat{P}_j(t)$, were compared against my field observations of pupal abundance, $P(t)$. In this way, the accuracy of predicted stage duration ($\tau_L(t)$) and survival ($S_L(t)$) through the larval stage was tested. By generating predictions of pupal abundance using both density-dependent and density-independent survival, it was also possible to assess the relative contribution of both mortality sources to abundance patterns. The field-observed and predicted pupal abundances were scaled by their maximum value, due to the unknown difference between egg and pupal detectability and the variability in egg raft sizes. Due to the required scaling of observed and predicted abundances, it was not possible to assess the magnitude of survival estimates. However, patterns of variation in survival through the season could be assessed.

The detectability of each life stage determines the probability that an individual of that stage would appear in a field sample. Detectability of egg rafts was assumed to be very high because they float on the surface of the water and are immobile, making them easy to see and count. Both larvae and pupae have been shown to effectively evade predators, suggesting they may be able to avoid the dipper (Awasthi et al. 2012). Increased buoyancy of pupae means that they spend more time at the water surface than earlier instars suggesting they may have a higher detection probability that larval stages (Futami et al. 2008; Awasthi et al. 2012). Crucially, it was assumed that relative detectability of each stage remained constant across the season, meaning that detectability may only affect total estimated population size

and not observed patterns of abundance. Given this assumption, patterns of survival through the season could be interpreted, despite uncertainty in absolute survival values.

3.2.5 Continental scale patterns in *Cx. pipiens* phenology based on existing literature

To investigate the ability of environmental variables to predict geographical trends in diapause behaviour I exhaustively searched the literature for existing *Cx. pipiens* datasets. I searched the first twenty pages of Google scholar and Web of Science results using the search terms "*Culex pipiens* seasonal abundance", "*Culex pipiens* dataset", "*Culex pipiens* monitoring", "*Culex pipiens* trapping", "*Culex pipiens* activity patterns" and "*Culex pipiens* diapause timing". Using this information I compiled a database of 44 studies with information regarding; which life stages were monitored, study length (in years), the number of regions for which data was presented, the temporal resolution of the dataset, the location of the study, the elevation of the study site, the dates on which *Cx. pipiens* was first recorded and last recorded, and the date of the highest recorded abundance. I restricted my search to include only studies monitoring adult female abundance. The possible effects of adult population size on diapause timings were not considered due to the range of different trapping procedures used across studies. It is known that differences in trap type and trap height can have substantial impacts on catch sizes and consequently on population size predictions (Anderson et al. 2004; Hutchinson et al. 2007).

Studies were then considered for inclusion in the analyses according to the following criteria:

- Only studies presenting adult capture data were included in the analyses, to maintain consistency in results and in response to the low number of studies monitoring immature stages.
- Only the European and North American studies were included in the analyses due to the substantially different latitude and climate in South Korea and the Middle East (where *Cx. pipiens* have been found to remain active all year round (personal communication with Dr. Laor Orshan)).
- I removed those studies which presented abundance at a monthly timescale from my analysis, as the accurate estimation of season start and end dates was impossible at such a coarse temporal resolution.
- Studies which used traps spread over a large area (>10km between sites) were excluded, unless the data was presented for each trapping location individually, as there

was no way to determine temperatures or timings at individual sites, which are likely to show geographic variability.

Nine datapoints remained for the analysis of continental scale relationships between phenology and environment. Air temperature data for each study area was found using Fetch Climate (Microsoft 2014) (query date: 16/01/2017), with average daily air temperatures for the studied years at each trapping site queried. Fetch Climate is a geotemporal information retrieval service which gives data about a range of environmental variables by searching a range of data sets and selecting the most appropriate by minimising uncertainty in the dataset, as described in Grechka et al. (2016). By supplying Fetch Climate with a query date it is possible to ensure reproducibility of results as the temperature datasets provided will be those deemed most appropriate on the query date. The accumulated degree days were calculated for each remaining site by subtracting $10\,^{\circ}\mathrm{C}$ (the lower thermal development threshold (Almirón and Brewer 1996; Loetti et al. 2011)) from each average daily air temperature and taking the sum of the positive values from the 1st of January until the end of April, each trapping year. The end of April was chosen as the majority of studies across *Cx. pipiens* range suggest that diapause emergence occurs in May, though varies geographically. In cases where mosquito counts were presented as either cumulative values or averages over a number of years, I took the average degree days across those years. For each site spring and autumn photoperiod measures were calculated by determining the day of the year upon which the photoperiod moved above 14 hours and the day upon which the photoperiod decreased below 13 hours respectively, as these were the estimates of season start and end photoperiods used in the model in Chapter 2.

Using this data from the literature, I investigated the following expectations about the effects of photoperiod and air temperature on diapause timings:

- Higher latitudes, with the spring photoperiod threshold being passed earlier in the year, were expected to exhibit earlier diapause termination (Denlinger and Armbruster 2014).
- Similarly, passing the autumn photoperiod threshold earlier in the year was expected to cause earlier diapause induction (Denlinger and Armbruster 2014).
- Particularly high accumulated degree days was anticipated to lead to earlier diapause termination (Ciota et al. 2011).

An exploratory correlation analysis of this data, to examine collinearity between environmental variables and the season start, season end, season length and peak abundance timings, was carried out by calculating Pearson's correlation values. Multiple linear regressions, assuming a gaussian error distribution, were also fitted, with accumulated degree days, the photoperiod thresholds and elevation included as independent variables and the phenology metrics as dependent variables. Only the season start date model satisfied model assumptions.

3.3 Results

3.3.1 Analysis of data collected at CEH Wallingford field site

Species composition of adult and immature mosquito communities

Only the adult trap (trap 1) next to the water butts reliably caught *Cx. pipiens* (trap 1 averaged 4.96 ± 6.42 mosquitoes per night, traps 2-4 averaged 0.36 ± 0.84 mosquitoes per night), so I only presented catch data from trap 1. A possible reason that traps 2-4 showed substantially lower catch sizes is their increased distance from the breeding site (Figure 3.1). Immature *Cx. pipiens* were not evenly distributed between the four water butts. In the initial immature population peak in April, the population was spread quite evenly between the four butts (Figures 3.4a-3.4d). After this initial peak in abundance, the population becomes concentrated in butt 4, with the vast majority of eggs laid there.

Adult trap 1 caught a total of 481 mosquitoes over the trapping period with 452 *Cx. pipiens* (94.0%), 26 *Culiseta annulata* (5.4%), 2 *Anopheles maculipennis* (0.4%) and 1 *Aedes geniculatus* (0.2%). Over the course of the sampling I performed morphological identification on 300 4th instar larvae from across the 4 water butts, all of which were *Cx. pipiens*. Since all final instar larvae identified were *Cx. pipiens* it was assumed that earlier instars were also *Cx. pipiens*. Given that *C. annulata* and *Cx. pipiens* favour similar larval habitats (Medlock et al. 2005) it is possible that there were also some *C. annulata* larvae present in the butts. However, as none appeared in the 4th instar larval samples and they accounted for only 5.4% of the adult catch it is unlikely that the seasonal abundance patterns of *Cx. pipiens* will be impacted significantly by co-occurrence with low populations of *C. annulata*.

Seasonality in immature stages

The egg data shows two clear generational peaks in late April and late June (Figure 3.4a). A similar pattern is observed in 1st/2nd instar larvae, with the peaks occurring a few days after the peaks in egg abundance (Figure 3.4b). The 1st/2nd instar larvae also show signs of a small third peak in August. The time series for 3rd/4th instar larvae and pupae both clearly show three peaks in abundance through the year, with a third peak in late August/September which is not obvious in the earlier life stages (Figures 3.4c-3.4d).

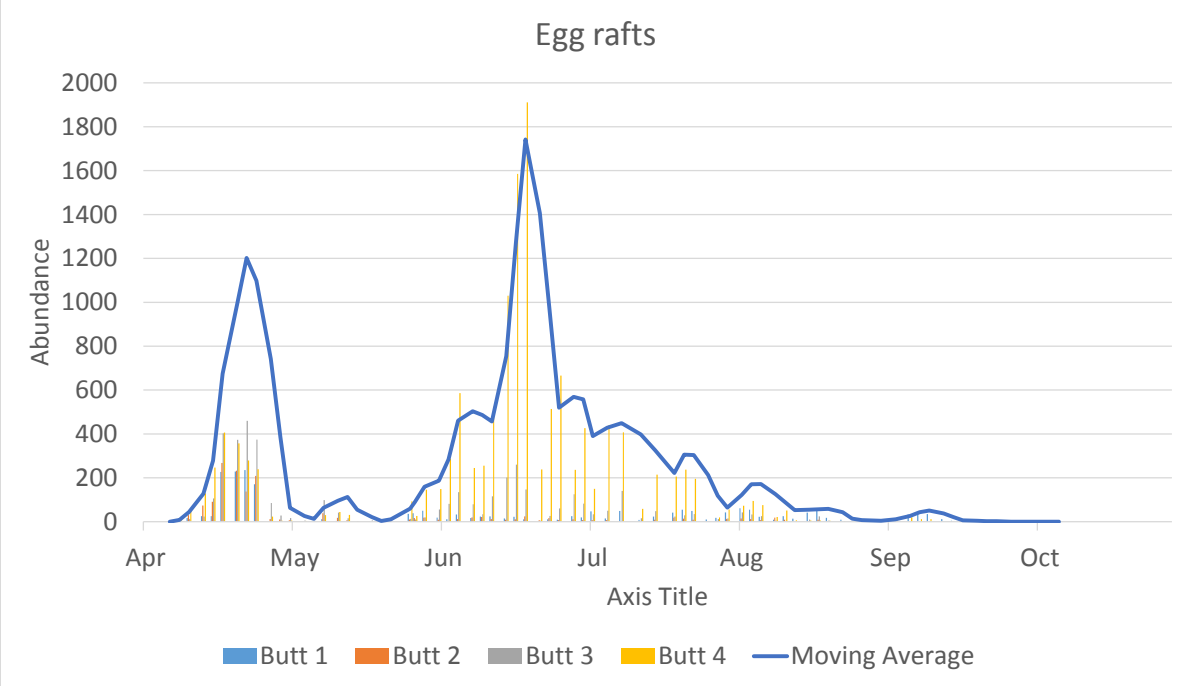

(a) Egg data: First recorded on 6th of April and last recorded on 21st of September.

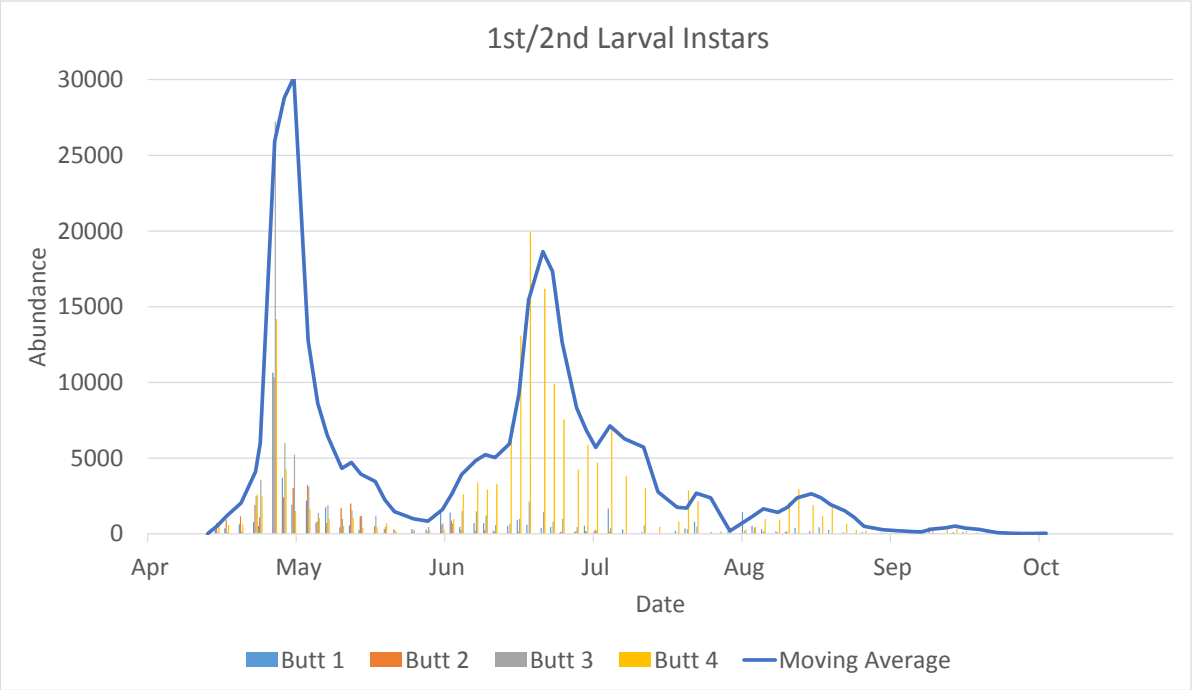

(b) 1st and 2nd larval instar data: First recorded on 15th of April and last recorded on 5th of October.

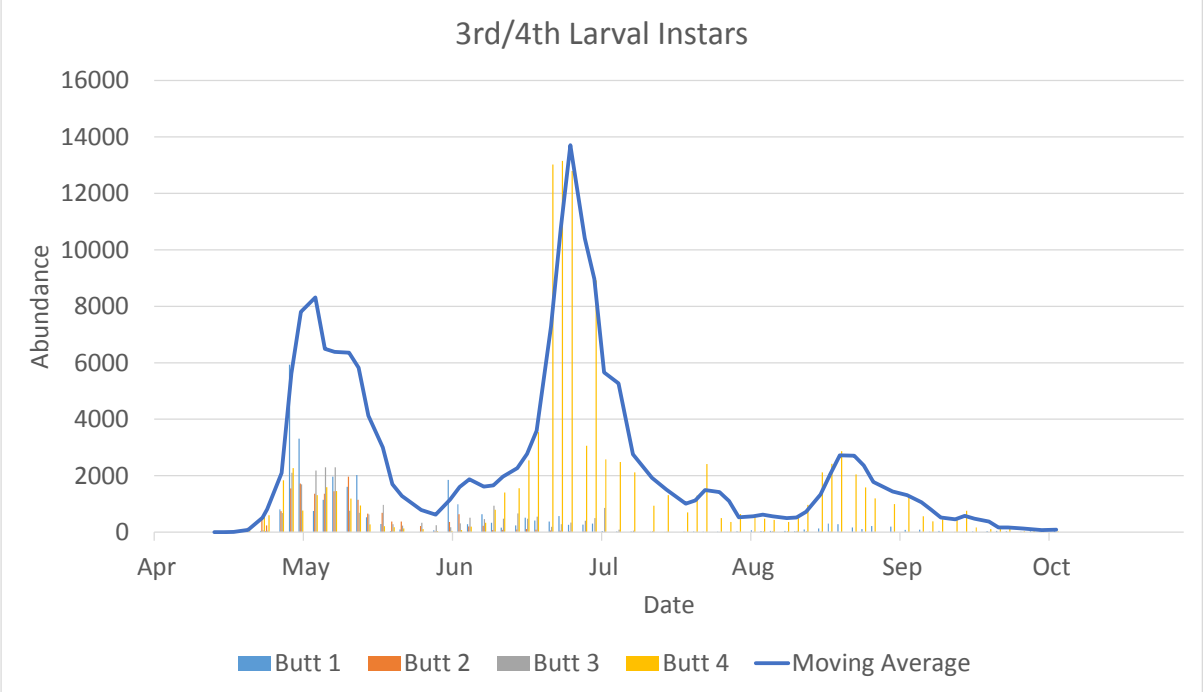

(c) 3rd and 4th larval instar data: First recorded on 17th of April and last recorded on 5th of October.

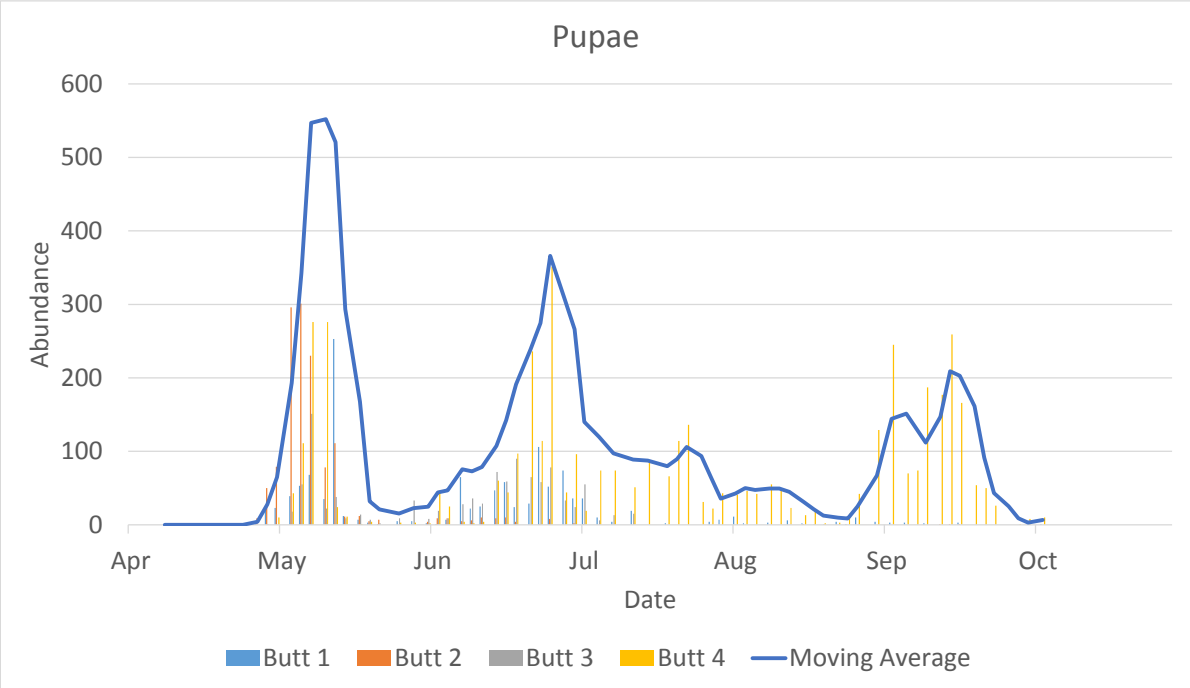

(d) Pupal data: First recorded on 24th of April and last recorded on 5th of October.

Figure 3.4: Immature population numbers displayed by water butt. The solid blue line shows a 3-day moving average of abundance. The coloured bars show the contribution of each water butt to the total immature count. In plot (a) only egg rafts were counted, rather than individual eggs.

I hypothesise that the gap in time between the early-season and mid-season immature peaks is caused by the time required for egg-to-adult development of the first spring generation, rather than the duration of the adult gonotrophic cycle causing a delay between egg-laying events of adult females that had overwintered. It has been shown that survival throughout the winter months has a negative consequence on adult fitness, resulting in weakened adult mosquitoes (Hahn and Denlinger 2007), which could result in adult females dying immediately after egg-laying. This is supported by high numbers of dead adult *Cx. pipiens* which were observed floating on the surface of the water butts in the early part of the season. Mortality of post-diapause females after laying one egg raft would explain the approximate 2 month delay between the first and second immature peaks (Figures 3.4a-3.4d), as this delay would stem from the time required for the spring generation to complete devleopment. Estimates of the stage durations calculated by the Chapter 2 DDE model, using field observed water temperatures, suggest that the time required for development through all life stages in the spring is $40 - 70$ days (Figure 3.5 b). This time delay coincides with the duration between the first and second egg peaks in the data (Figure 3.4a). The time between egg peaks cannot be explained by the time required for adults to locate a blood meal and complete a gonotrophic cycle between egg-laying events. Figure 3.5 (a), shows that the gonotrophic

cycle is estimated to take less than 20 days for the spring air temperatures experienced in the field, whilst the time delay between egg peaks is approximately two months.

The final peak in pupae is very large in comparison to the number of eggs present. This is clear from the fact that, unlike in the first two pupal peaks, there is no discernible peak in egg abundance corresponding to the final pupal peak (Figures 3.4a & 3.4d). Using the observed egg abundance and the mathematical model predictions of larval development time and larval survival including density-dependence, as described in Section 3.2.4, it was possible to estimate the pupal abundances, for comparison with the field data (Figure 3.6). Figure 3.6 shows that, in the final generation, the larval stage duration predicted using the model is longer than that observed in the field, as the final model-predicted peak (black line) occurs after the peak observed in the field (red line). This leads to a mismatch in timings of the peaks between using the generation time from the model and observed data (black and red lines respectively). However, at other points in the season, the development and survival from egg to pupa can be well explained by the predictions of stage duration and survival, as included in the mathematical model. Further, the relative sizes of the predicted and observed peaks match well throughout the season when density-dependence is included.

The relatively large pupal peak at the end of the season can be considered to occur as a result of a reduction in the density-dependent mortality rate due to predation, particularly as the predictions ignoring predation do not capture the final peak whilst those including predation do (Figure 3.6 black line and blue line, respectively). As the larval population size in the water butts dwindles, the number of predators decreases in response to the reduction in prey number, leading to a slight increase in larval survival and a relatively large pupal peak (Figure 3.7). The impact of density-dependence on survival is particularly evident when comparing simulations carried out by the DDE model described in Chapter 2, both including and excluding density-dependence. Figure 3.8 shows that exclusion of density-dependence leads to continuously increasing pupal population size through the year, as density-independent mortality is insufficient to regulate population size.

Adult data from CEH Wallingford traps

The adult data shows less defined generations than the immature data (Figure 3.9) with a small peak early in the season upon emergence from diapause, followed by a drop in numbers before a general increase throughout late May and June. High numbers are sustained throughout July before catch sizes decrease again throughout August. There is evidence from the data that adult activity reaches a small peak in April, immediately after diapause

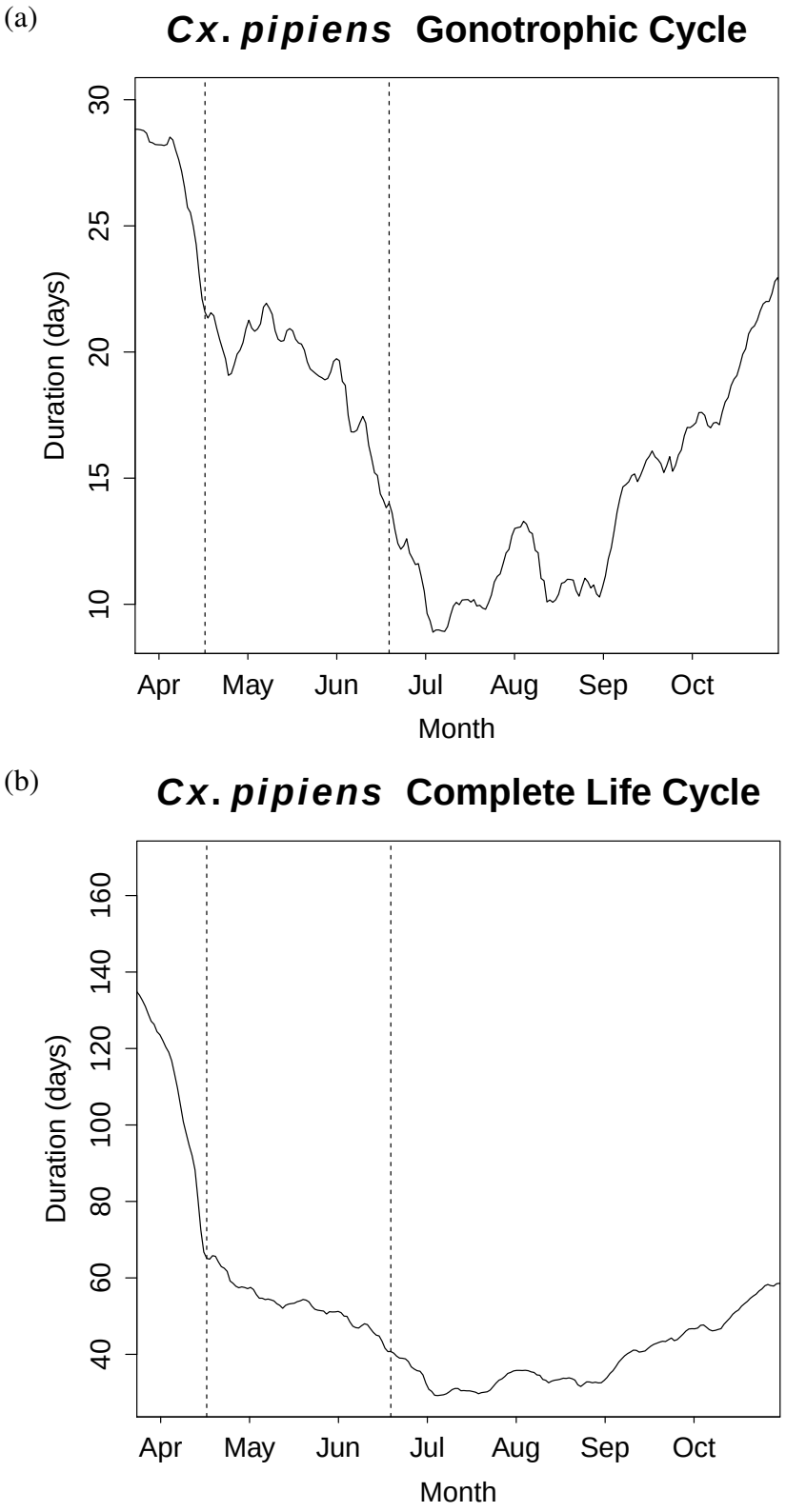

Figure 3.5: Gonotrophic Cycle vs Life Cycle: Plot (a) shows the duration of the gonotrophic cycle, as estimated by the Chapter 2 DDE model, using the air temperatures observed at the field site. Plot (b) shows the duration of the complete *Cx. pipiens* life cycle (eggs+larvae+pupae+gonotrophic cycle), estimated using the Chapter 2 DDE model, the air temperatures recorded at the field site and the water temperatures recorded in butt 4. In both plots the timings of the first and second egg peaks are shown by the dotted lines.

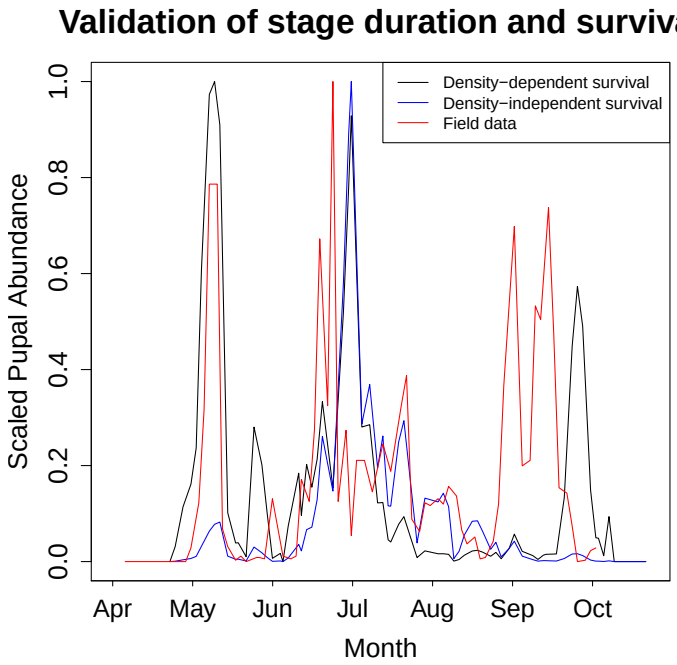

Figure 3.6: Comparison between observed and predicted pupal abundance patterns: The red line shows the pupal abundance recorded in butt 4. The black line shows the predicted pupal abundance including density-dependent larval mortality, $\hat{P}_d(t)$, given the observed egg abundance and water temperatures in butt 4 and the Chapter 2 DDE model predictions of stage duration and density-dependent survival. The red line shows the predicted pupal abundance excluding density-dependent larval mortality, $\hat{P}_i(t)$, given the observed egg abundance and water temperatures in butt 4 and the Chapter 2 DDE model predictions of stage duration and density-independent survival. The full process by which $\hat{P}_d(t)$ and $\hat{P}_i(t)$ are calculated is described in Section 3.2.4.

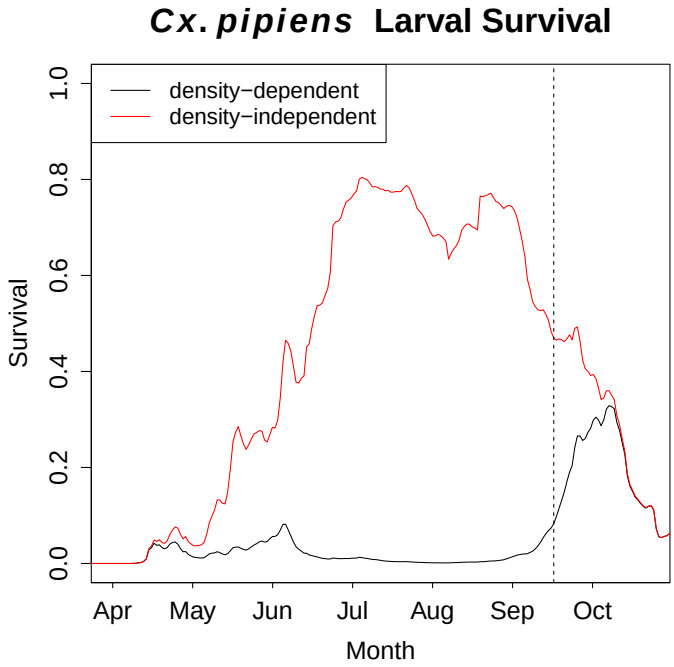

Figure 3.7: Larval Survival: The survival of the density-dependent larval stage, as estimated by the mechanistic model, is shown. The black line represents the observed survival including density-dependence, while the red line shows the predicted survival in the absence of density-dependence. The dotted line shows the time of the final observed pupal peak.

emergence, before dying back again until late-May and June. This feature is mirrored in the immature data (Figure 3.4a-3.4d) which also shows a strong peak in eggs laid in late April followed by a period of low abundance until late-May into June.

Considering environmental predictors of patterns in adult abundance, the difference between the QAICc value of the selected model and the intercept-only model (which includes no environmental predictors) was 108.13, showing substantial improvements over the intercept-only model. Table 3.1 shows the three models with the lowest QAICc. The top model was chosen because it had the lowest QAICc and incorporates fewer parameters than the next best option. In this final GLM, month of the year was a highly significant predictor of catch size (Table 3.2). Maximum air temperature in the 24 hours prior to collection and the quadratic air temperature terms were also significant at the 5% level, though the difference in QAICc between models including and excluding the quadratic air temperature term was very small. The model coefficients are shown in Table 3.3, which shows that increasing air temperature increases the expected catch size over the study period. The model assumptions were checked by examining the residuals for temporal autocorrelation and normality and there was no sign that either assumption was violated (Figures 3.10-3.11). The explanatory variables were checked for collinearity (correlation between two explanatory variables) by

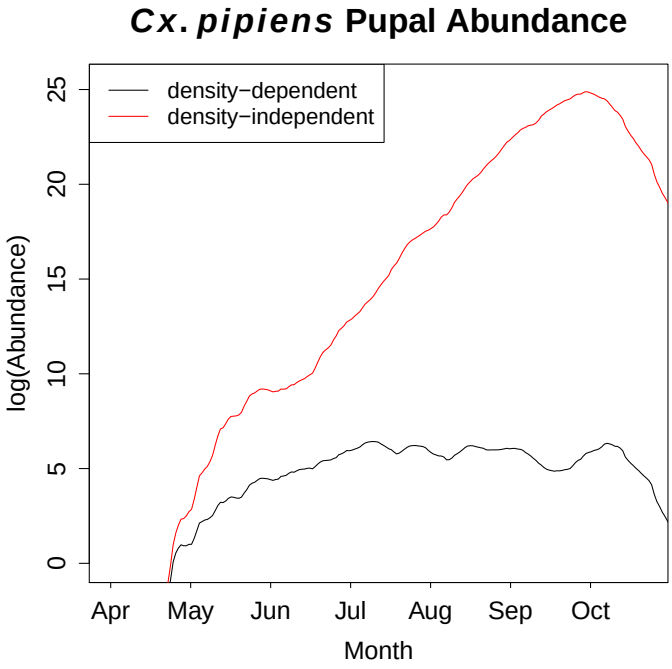

Figure 3.8: Effect of density-dependence on pupal populations: The black line represents the pupal population predicted by the DDE model, described in Chapter 2, when incorporating density-dependence, whilst the red line shows the pupal abundance predicted in the absence of density-dependence. The plots are shown on the natural log scale due to the differences in the scale of abundance predictions between the two methods.

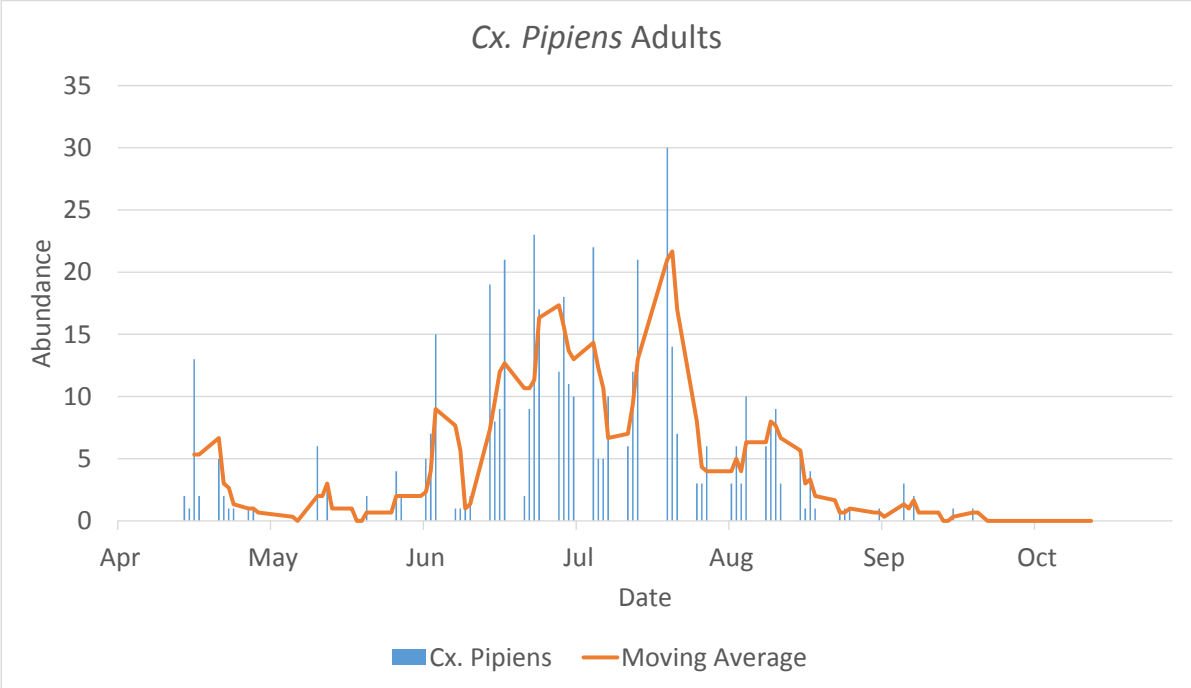

Figure 3.9: Adult data: The blue bars show adult female *Cx. pipiens* catch numbers collected by trap 1. The orange line shows a 3-day moving average of catch numbers.

Variables	logLik	QAICc	delta
Month + Max Temp + Max Temp^2	-252.042	164.4	0.00
Month + Max Temp.+ Max Temp^2 + Min Temp	-248.428	164.9	0.50
Month + Max Temp	-258.863	165.8	1.36
Intercept only	-476.722	272.5	108.13

Table 3.1: Model selection: The three models with the best QAICc are shown, alongside the intercept only model.

	Df	Sum Sq	F value	Pr(>F)
Max air temperature (24h)	1	19.722	5.8839	0.01728
Month	6	148.514	7.3849	1.928×10^{-6}
Quadratic max air temperature (24h)	1	13.642	4.0700	0.04663
Residuals	90	301.666		

Table 3.2: ANOVA applied to quasipoisson GLM: An ANOVA showing the variance explained and p-value for each of the variables included in the quasipoisson GLM.

calculating the variance inflation factors (VIFs) and none of the variables included in the final GLM showed signs of collinearity (month of the year and average daily maximum air temperature in the 2 weeks prior to collection showed moderate collinearity but average daily maximum air temperature was not included in the final model). The fit of the quasi-Poisson GLM model to the adult catch data can be seen in Figure 3.12. A pseudo R-squared value was calculated for the quasi-poisson GLM by taking one minus the residual deviance over the null deviance and the model was seen to have good explanatory power (R^2 = 0.616).

The pairs of months of the year between which significant differences in adult female catch size were found at the 5% level are shown in Table 3.4. Catch sizes were significantly higher in July than in August, having accounted for environmental conditions. I propose that this is indicative of diapause initiation in adult females occurring in August because diapausing females will not be caught by the host-seeking traps (Engler et al. 2013; Madder et al. 1983a). This is supported by Figure 3.13, which shows the adult abundance predicted by the Chapter 2 DDE model, for the temperatures experienced in the field experiment. Low immature survival in the middle of the season (Figure 3.7) is not thought to be sufficient to explain the drop in adult numbers throughout August (Figure 3.13 black line). However, diapause initiation during August would explain this drop in catch sizes (Figure 3.13 red line).

Coefficient	Estimate	Standard Error	t value	Pr(>|t|)
Intercept	-4.4923	2.2510	-1.996	0.0490
August	-0.1569	0.4338	-0.362	0.7185
July	0.8189	0.4000	2.047	0.0435 *
June	0.5756	0.4050	1.421	0.1587
May	-0.5201	0.5639	-0.922	0.3589
October	-2.9636	1.8637	-1.590	0.1153
September	-1.8477	0.7314	-2.526	0.0133 *
Max Temp	0.4536	0.1973	2.299	0.0238 *
Quadratic Max Temp	-0.0079	0.0041	-1.923	0.0577 .

Table 3.3: Regression coefficients quasi-poisson GLM: A summary of the regression coefficients for the quasi-poisson GLM of environmental variables on daily catch of adult female *Cx. pipiens*.

Hypothesis	Estimate	Standard Error	z value	Pr(>|z|)
Jul-Aug=0	0.9758	0.2752	3.545	0.00553
Sep-Jul=0	-2.6667	0.678	-3.933	0.00116
Sep-Jun=0	-2.4233	0.6804	-3.561	0.00479

Table 3.4: Tukey tests: The Tukey highest significant difference test (Tukey 1949) highlighting which means which are significant at the 5% level, showing between which months there is a significant difference in predicted catch size.

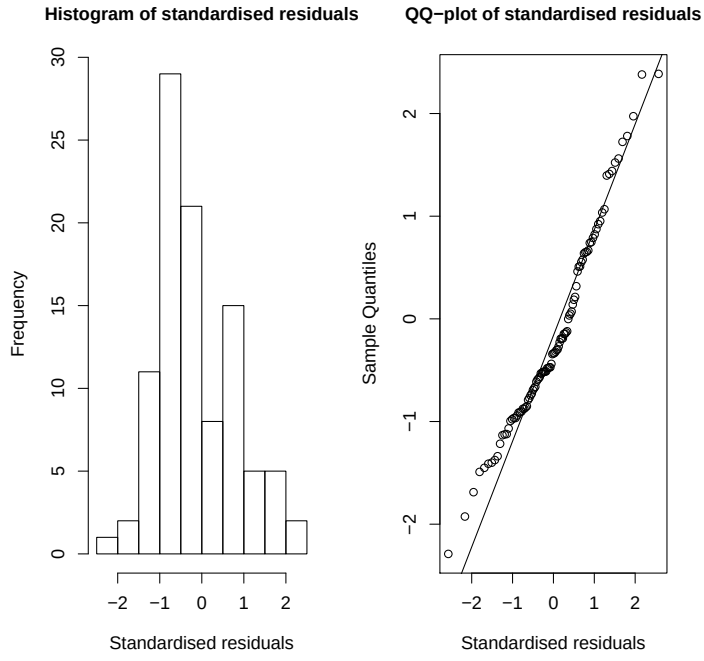

Figure 3.10: A histogram and QQ-plot showing normally distributed residuals for the quasipoisson GLM fitted to the adult catch data.

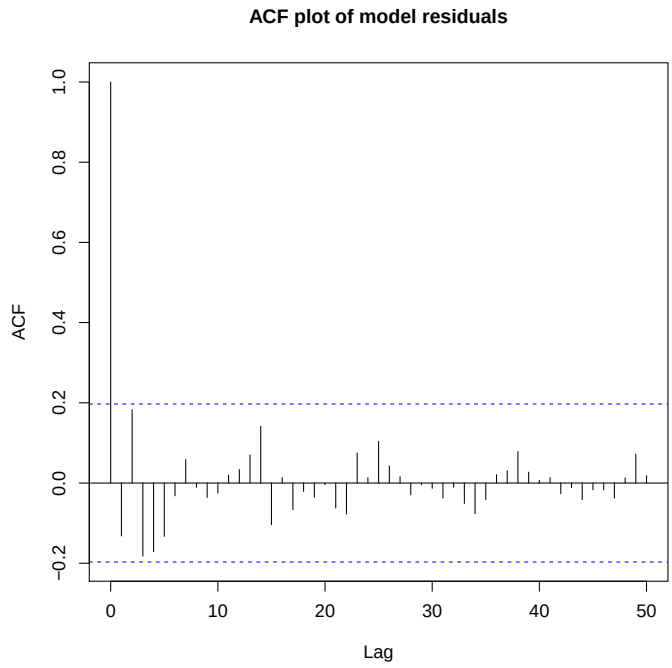

Figure 3.11: ACF plot: An autocorrelation function (ACF) plot showing no evidence of temporal autocorrelation in the residuals of the quasipoisson GLM fitted to the adult catch data. Autocorrelation is tested at lags of up to 50 observations, with $1-4$ nights between observations.

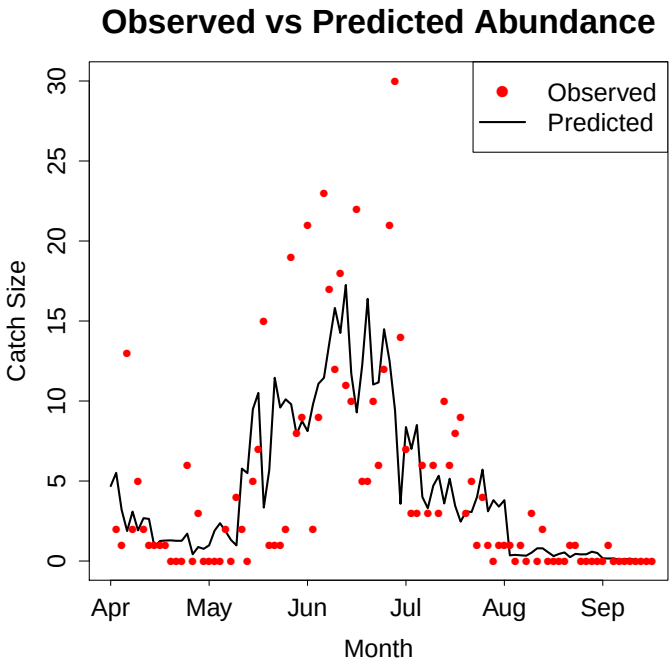

Figure 3.12: Quasi-poisson GLM predictions: a plot showing a the predicted catch sizes from the quasi-poisson GLM (Table 3.3) compared to the observed catches.

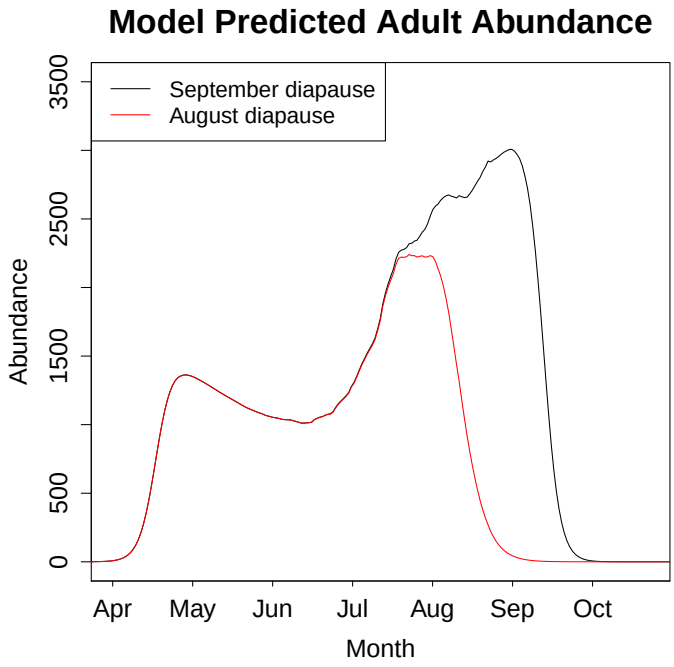

Figure 3.13: Diapause initiation: Seasonal abundance of active adult female *Cx. pipiens*, as predicted by the Chapter 2 DDE model, is shown. The active population is determined by multiplying the total predicted adult population by the proportion of the population which is active at time t, $\zeta(t)$ (Equation 2.17). The black line shows diapause initiation in September and the red shows diapause initiation in August.

3.3.2 Analysis of *Cx. pipiens* meta-analysis data

Patterns in European and North American *Cx. pipiens* phenology

In total I found 44 papers which described a *Cx. pipiens* seasonal abundance dataset (Table 3.5), at the locations shown in Figure 3.14). In 20 cases the data was presented at a monthly resolution, meaning the start and end dates for each season could not be interpreted clearly. In these cases, it was not made clear within the paper whether first and last recorded non-zero catches were the first and last nights of trapping, or whether trapping had extended beyond these dates. This is an important distinction because mosquitoes caught on the first night of trapping would imply that the season had likely begun prior to trapping starting. Removing those studies presenting data at a monthly resolution (n = 20), amalgamating data over a large geographic area (> $10km$ between traps) (n = 30) or sampling only non-adult stages (n = 9), left only 9 abundance profiles meeting all criteria required for inclusion in the analyses.

Paper	Life stage(s)	No. sites	Combined over >10km	No. years	Combined over years	Resolution	Location	Included
Helbing et al. (2015)	Adult	14	Yes	31	Yes	Daily	USA	No
Madder et al. (1983b)	Adult	1	No	1.5	No	Weekly	Canada	Yes
Balenghien et al. (2006)	Adult	2	No	1	No	Weekly	France	Yes
Anderson et al. (2004)	Adult	1	No	1.5	No	Weekly	USA	Yes
Wang et al. (2011)	Adult	1	Yes	8	No	Weekly	Canada	No
Chaskopoulou et al. (2013)	Adult	28	Yes	1	No	Weekly	Greece	No
Rosà et al. (2014)	Adult	44	Yes	11	Yes	Weekly	Italy	No
Carrieri et al. (2014)	Adult	16	Yes	14	Yes	Weekly	Italy	No
Jian et al. (2014b)	Adult	15	Yes	1	No	Weekly	Italy	No
Andreadis et al. (2001)	Adult	148	Yes	1	No	Weekly	USA	No
Geery and Holub (1989)	Adult	40	Yes	1	No	Weekly	USA	No
Bogojević et al. (2009)	Adult	1	No	10	Yes	Bi-monthly	Croatia	Yes
Votýpka et al. (2008)	Adult	1	No	3	Yes	Bi-monthly	USA	No
Ponçon et al. (2007b)	Adult	2	No	1	No	Bi-monthly	France	Yes
Montarsi et al. (2015)	Adult	1	No	1	No	Bi-monthly	Italy	Yes
Bolling et al. (2009)	Adult	20	Yes	2	Yes	Bi-monthly	USA	No
Dehghan et al. (2011)	Adult	2	Yes	1	No	Monthly	Iran	No
Orshan et al. (2008)	Adult	1	Yes	5	Yes	Monthly	Israel	No
Bisanzio et al. (2011)	Adult	36	Yes	7	No	Monthly	Italy	No
Toma et al. (2008)	Adult	14	Yes	5	Yes	Monthly	Italy	No
Kim et al. (2003)	Adult	29	Yes	2	Yes	Monthly	Korea	No

Paper	Life stage(s)	No. sites	Combined over >10km	No. years	Combined over years	Resolution	Location	Included
Kim et al. (2007)	Adult	29	Yes	1	No	Monthly	Korea	No
Kim et al. (2009)	Adult	19	Yes	1	No	Monthly	Korea	No
Kim et al. (2010)	Adult	19	Yes	1	No	Monthly	Korea	No
Ventim et al. (2012)	Adult	4	No	1	No	Monthly	Portugal	No
Kemenesi et al. (2014)	Adult	13	Yes	1	No	Monthly	Serbia	No
Schaffner and Mathis (2013)	Adult	2	Yes	2	Yes	Monthly	Switzerland	No
Alten et al. (2000)	Adult	4	Yes	1	No	Monthly	Turkey	No
Gündüz et al. (2009)	Adult	7	Yes	1	No	Monthly	Turkey	No
Barker et al. (2010)	Adult	NA	Yes	10	Yes	Monthly	USA	No
Bolling et al. (2007)	Adult	14	Yes	2	Yes	Monthly	USA	No
Costanzo et al. (2005)	Adult	5	Yes	1	No	Monthly	USA	No
Ibanez-Justicia et al. (2015)	Adult	778	Yes	4	Yes	Sporadic	Netherlands	No
Townroe and Callaghan (2015)	Adult	110	Yes	1	No	Sporadic	UK	No
Becker and Ludwig (1983)	All	NA	Yes	NA	NA	Unknown	Germany	No
Madder et al. (1983b)	Egg	1	No	2	No	Daily	Canada	No
Jackson and Paulson (2006)	Egg	9	Yes	2	No	Weekly	USA	No
Lampman et al. (2006)	Egg	16	No	11	No	Bi-monthly	USA	No
Madder et al. (1980)	Egg/Adult	1	No	1	No	Weekly	Canada	No
Lalubin et al. (2013)	Egg/Adult	1	No	2	No	Monthly	Switzerland	No
Spielman (2001)	Larvae	2	No	1	No	Weekly	USA	No
Rydzanicz and Lonc (2003)	Larvae	12	No	3	Yes	Monthly	Poland	No

Paper	Life stage(s)	No. sites	Combined over >10km	No. years	Combined over years	Resolution	Location	Included
Aldemir et al. (2009)	Larvae	31	Yes	2	No	Monthly	Turkey	No
Townroe and Callaghan (2014)	Larvae/Pupae	20	Yes	2	Yes	Monthly	UK	No

Table 3.5: *Cx. pipiens* seasonal abundance datasets: The study by Votýpka et al. (2008) was not included, despite meeting the other criteria, due to a late start to trapping.

Figure 3.14: A map showing the distribution of data sources on *Cx. pipiens* seasonaility. The yellow marker shows the location of the Wallingford field site. The blue markers show the locations of the field sites for which there was appropriate data for the final analysis. The red markers show the studies which were excluded from the analysis.

Coefficient	Estimate	Standard Error	t value	Pr(>|t|)
Intercept	-209.03	102.6563	-2.036	0.0973
Spring Photoperiod	2.98	0.88307	3.370	0.0199
Degree days	-0.29	0.18293	-1.606	0.1692
Elevation	0.09	0.03956	2.267	0.0728

Table 3.6: Regression coefficients for season start: A summary of the regression coefficients for the model of environmental variables on season start date.

A multiple linear regression was fitted to understand any relationships between the observed season start dates and environmental conditions (Table 3.6). The model assumptions were checked and the assumptions of independence, normal residuals, constant error variance and linearity were satisfied. The model R^2 value showed that the linear model explained the majority of the variation in the meta-analysis data (R^2 = 0.824). These results suggest that the timing at which the spring photoperiod threshold is passed appears the most likely driver of diapause termination, with diapause termination occurring earlier in locations where day length is high early in the year. Consequently, more northerly populations will be expected to exit diapause earlier in the year, as has been shown for other species (Denlinger and Armbruster 2014).

None of the environmental variables included were found to have a relationship with the timing of peak abundance, as the intercept-only model had the lowest AIC. Statistical models investigating season length and season end dates were unreliable due to violation of model assumptions. Figure 3.15 shows that timing of the mid-season abundance peak is well correlated with the timing of the season start but poorly correlated with the timing of the season end. This supports the notion that the end of the season may be less predictable than the start because, as more egg cohorts accumulate, generations will overlap as they will develop and survive at different rates.

3.4 Discussion

3.4.1 Implications of the UK fieldwork observations on *Cx. pipiens* phenology

The field data collected shows strong generational peaks in the immature life stages, accompanied by a more gradual build-up of adults through the biting season (Figures 3.4a-3.9). Figure 3.4d shows that three distinct immature generations were observed throughout the

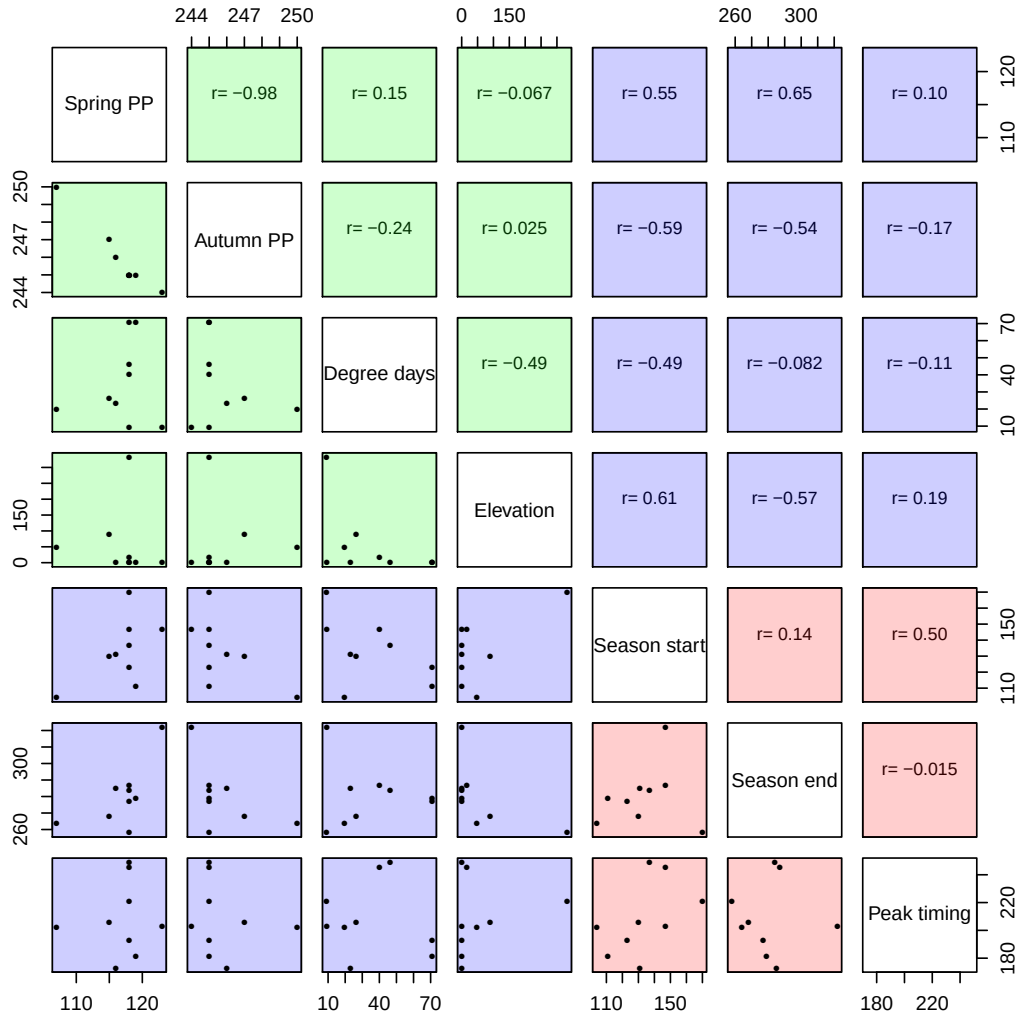

Figure 3.15: Correlations between variables: Plots showing correlations between environmental variables and season timings. PP stands for photoperiod. The r values given are the pearson correlation values. Plots are colour-coded such that green represents environment-environment correlations, blue represents environment-phenology correlations and red represents phenology-phenology correlations. The plot is symmetric, with data in the bottom left and r-values in the top right.

season. Zeuss et al. (2017) showed that voltinism across a range of 943 insect (lepidopteran and odonate) populations decreased with increasing latitude in the northern hemisphere, in response to decreased growing seasons. This is reflected in the fact that Madder et al. (1983b) observed one more generation of *Cx. pipiens* than was observed at CEH Wallingford, at a latitude 8° south of my field site. These patterns of abundance in the immature stages can be well explained by the estimates of larval stage duration and survival from the mathematical model (Figure 3.6). In particular, regulation of the larval population through predation appears to be high in the middle of the active season, though a decrease in predator numbers late in the year may lead to an increase in the size of the diapausing population (Figure 3.7). By tracking adult abundance at a high temporal resolution, further information about *Cx. pipiens* diapause timings was obtained, with diapause induction occurring in August in the field. Further similar studies, across the geographical distribution of *Cx. pipiens*, are required to increase the range of environmental conditions in which phenological patterns are measured, allowing for more robust inferences about the influence of environmental variation on patterns of abundance and diapause behaviours.

The autumn pupal peak, in late August/early September, is likely to be due to the fact that the reduction of egg-laying by adults leads to a clearing of the egg and larval stages, with low abundance during late July and early August. This reduction in the larval population is believed to cause a drop in predator numbers, as in classical predator-prey systems (Lotka 1925; Volterra 1926), causing an increase in larval survival and pupal population size at the end of the season. The hypothesis of a decreased predator population is supported by observations made whilst conducting the fieldwork, that predator numbers appeared to decrease in the late part of the mosquito active season. Further, Figure 3.6 shows that the pupal abundance can be well estimated using the observed egg abundance and the model estimates of stage duration and survival. This lends support to the idea that the autumn pupal population peak can be explained by a reduction in the predator population size and a corresponding increase in larval survival, as predicted in the mathematical model. The mathematical model appears to underestimate the development rate of the final generation (Figure 3.6). Density-dependence is known to affect development rates as well as survival (Madder et al. 1983b), so it is likely that this discrepancy between model predictions and field observations is due to decreased density-dependence leading to faster development in the autumn generation.

The influence of density-dependence suggests that population size and abundance patterns may be strongly regulated by breeding habitat availability. This importance of density-dependence can be seen in Figure 3.8, where predictions of the pupal population can be seen to steadily increase in the absence of density-dependence. The comparison in Figure

3.8 highlights the impact of density-dependence on survival, however numerous studies have shown that density-dependence also influences development rates (Couret et al. 2014), adult body size (Madder et al. 1983b; Alto et al. 2012; Muriu et al. 2013) and population sizes (Jian et al. 2014b) across a range of mosquito species and breeding sites. The increase in pupal numbers observed in the field data has not led to an obvious increase in adult catch sizes, as this final generation of pupae would be programmed for diapause, meaning they would not appear in traps (Mitchell and Briegel 1989). However, this increased population of diapausing adults may influence population size in the following season.

Monitoring populations in water butts means that catch size for each immature stage on a particular day is not generally dependent on environmental conditions at that time but rather on the number of eggs laid a certain time ago and the development rates and survival since then. The number of eggs laid a given time ago was unknown, as only the total abundance of egg rafts was counted on each day. This means that there is substantial temporal autocorrelation in the immature abundance data (Figures 3.4a-3.4d). This autocorrelation was not observed in the adult samples (Figure 3.11), likely because adults can disperse over a much wider area. I had intended to analyse the patterns of abundance in each water butt alongside the observed water temperatures to determine generation times and survival values based on observed peaks in the data. However, the tendency of adults to oviposit almost exclusively in butt 4, after the initial population peak, meant that such an analysis was not possible due to the lack of data across the butts.

Several factors may explain why the strong generational peaks observed in the immature stages are not evident in the adult time series. Firstly, female mosquitoes developing late in the year are programmed to mate and enter diapause upon emergence rather than seeking a blood meal (Mitchell and Briegel 1989). This means they are not caught by adult traps that target host-seeking individuals. Consequently, the adult population produced by the late summer pupal peak would not be visible in the trap data. A further contributing factor is likely to be the increased longevity of the adult stage, when compared to the immature stages. This means that adults of different generations can overlap and are more likely to do so later in the season. Adult longevity depends on the air temperatures experienced, similarly to immature development, however the adult lifespan is substantially longer than the time required for development through the immature stages, for both *Cx. pipiens* and *Aedes albopictus* (Alto and Juliano 2001; Loetti et al. 2011; Brady et al. 2013; Ciota et al. 2014).

My finding that generational peaks are much less clear in adult population data than in immature population data has several potential biological explanations. According to both laboratory observations and my model predictions, the adult stage of *Cx. pipiens* lasts over twice as long as the immature stage on average. Ciota et al. (2014) estimate the mean adult lifespan ranges from approximately 75 days at $16\,^{\circ}\mathrm{C}$ to 25 days at $28\,^{\circ}\mathrm{C}$ (errors not given). This is more than twice the development time from egg hatch to adult emergence estimated by Loetti et al. (2011) at similar temperatures, with development time of $21.6(\pm 1.6)$ days at $15\,^{\circ}\mathrm{C}$ and $8(\pm 1)$ days at $30\,^{\circ}\mathrm{C}$. The relatively long adult lifespan leads to considerable overlap in cohorts of adults arising from batches of eggs laid by different females, particularly in the middle to the end of the adult season (i.e. 2nd and 3rd generation individuals per year). Each of these adult cohorts develops and survives at different rates depending on the fluctuating environmental conditions to which they have been subjected during their lifetimes. This blurring of generational peaks generally observed in adult *Cx. pipiens* datasets is further exacerbated by the fact that adults only visit the traps when host seeking (roughly one twentieth to one tenth of their lifetime depending on air temperature effects on the reproductive cycle (Hartley et al. 2012)) and will disperse following emergence. By contrast, immatures are being sampled in a closed system in which they are present until death or emergence.

The immature population was evenly distributed between the four water butts in the initial peak, after which adult females preferred to oviposit in butt 4 (Figure 3.4a-3.4d). I hypothesise that after the initial peak had cleared, butt 4 became the favoured butt because it was observed to maintain a higher organic content, which *Cx. pipiens* are known to favour (Vinogradova 2000). Butt 4 was seen to host a high concentration of rat-tailed maggots which are an indicator species for water with a high organic content (Campbell 1939), butt 3 was colonised by duckweed which is known to repel *Cx. pipiens* (Eid et al. 1992) and butts 1-3 all hosted may fly larvae which are indicator species of clean water (Campbell 1939). It was also observed that the mean surface temperature of butt 4 was $2\,^{\circ}\mathrm{C}$ cooler than butts 1 and 2 and $1.2\,^{\circ}\mathrm{C}$ cooler than butt 3 across the summer. This temperature difference was due to the fact that butt 4 experienced the smallest amount of direct sunlight, whilst butts 1 and 2 experienced the most. The possibility that occasional damagingly high temperatures in butts 1-3 could also explain the difference in *Cx. pipiens* populations between the butts is explored in detail in Chapter 4.

Adult catch sizes from my traps were significantly larger in July than in August (Table 3.3). This implies that either the total size of the population is smaller in August than July or a decreased proportion of the population is host-seeking in August, as adults are preparing for diapause and the traps catch only host-seeking adults. Figure 3.13 shows that high larval

mortality in the summer months (Figure 3.7) could not explain this drop, however diapause initiation in August did. Sulaiman and Service (1983) and Onyeka and Boreham (1987), who counted adults resting in overwinter shelters, observed the majority of mosquitoes arriving at shelters during September, rather than August. I propose that this apparent mismatch in timings is due to the fact that *Cx. pipiens* are known to cease blood-feeding and commence nectar feeding to build up fat reserves in preparation for diapause (Mitchell and Briegel 1989; Robich and Denlinger 2005). Mitchell and Briegel 1989 showed that mosquitoes which had fed on sugar for $7 - 10$ days prior to hibernation survived for 6 months with 50% mortality, whereas those which had blood-fed before being placed in hibernation reached 50% mortality within 20 days. As the traps only attract host-seeking females, no nectar-feeding individuals will appear either in our data or in diapause shelters. This time spent nectar-feeding, combined with the results shown in Figure 3.9 would support initiation of diapause in August, with appearance in shelters occurring in September, as observed by Sulaiman and Service (1983) and Onyeka and Boreham (1987).

Some studies have shown that rainfall appears to influence population size through habitat availability (Wang et al. 2011; Mulatti et al. 2014). Others have shown a lack of rainfall dependence, in cases where breeding habitat is provided by other means, such as irrigation (Jian et al. 2014b). Wimberly et al. (2014) showed that the impacts of precipitation on WNV cases exhibited substantial geographic variability, dependent on local hydrology. The analysis of the adult field data suggested that rainfall did not affect the catch sizes of *Cx. pipiens* and should be excluded from the final model. This finding is likely a product of the field set-up, as there was a stable amount of larval habitat provided by the four water butts. Further, one may also have expected that high wind speeds would have interfered with *Cx. pipiens* flight causing a reduction in catch sizes (Meillon et al. 1967). I believe that this was not observed due to the relatively small sample size and the low wind speeds observed (maximum observed daily average wind speed was 10mph).

3.4.2 Geographical trends in *Cx. pipiens* dynamics observed from current literature

National scale geographical patterns in phenology of a range of insect species, have been explained by environmental drivers in recent studies (Gordo et al. 2010; Searle et al. 2013; Ernst and Buddle 2015). Gordo et al. (2010) found that air temperature and altitudinal gradients explained most of the spatial variability in the emergence times of bee populations in

Spain. In analysing the relationship between available *Cx. pipiens* data from across its geographical range the objective was to determine whether geographical patterns in diapause behaviour could be predicted using environmental variables. In doing so, I found some evidence that quantifiable relationships may exist, particularly between photoperiod and diapause termination. However, this analysis must be interpreted with caution as it contains only 9 data points, meaning it will be underpowered to detect relationships between environmental variables and season start timings. Further, 9 data points is insufficient to represent the full range of environmental variables across *Cx. pipiens* range.

It has been shown for a range of temperate mosquitoes that diapause termination and initiation generally occur earlier in the year at higher latitudes, in response to shorter growing seasons (Denlinger and Armbruster 2014; Lounibos et al. 2003). *Cx. pipiens* has a wide range, spanning the entire holarctic (Vinogradova 2000), meaning populations across its distribution will be expected to diapause in response to different photoperiod and temperature queues. This is reflected in the fact that populations in California have shown low rates of diapause during winter (Nelms et al. 2013), whilst those in more northerly regions diapause for several months of the year (Madder et al. 1983a; Spielman 2001). Temperature has also been shown to influence diapause incidence in laboratory (Sanburg and Larsen 1973; Madder et al. 1983b) and field populations (Ciota et al. 2011), though photoperiod is believed to be the primary driver (Denlinger and Armbruster 2014). If *Cx. pipiens* diapause behaviours could be predicted from environmental drivers then this would allow for improved predictions of seasonal abundance. By improving knowledge of geographical trends in *Cx. pipiens* diapause timings, voltinism and its potential impacts on disease transmission across the species range could be better understood.

I found some evidence that *Cx. pipiens* emergence may occur earlier in the year at higher latitudes (Table 3.6). No evidence of air temperature or elevation effects were found in my study. The lack of any relationship between air temperature and season start dates across the *Cx. pipiens* range may stem from the fact that photoperiod is believed to be the dominant driver of diapause behaviour, making temperature effects more difficult to detect (Sim and Denlinger 2013; Denlinger and Armbruster 2014). Further, the prohibitively small sample size means that the statistical analysis will be underpowered to detect relationships between environmental variables and diapause termination. There was no evidence of a relationship between any environmental variables and diapause induction or peak abundance in my study, as the small sample size led to the assumptions of the multiple linear regression being violated. The range of elevations represented in the data, in particular, were very restricted, varying from 0.1-332.8m, where only the maximum observation exceded 90m.

In carrying out and interpreting these analyses it is important to emphasise that access to data of sufficient temporal resolution is very limited. Mosquito surveillance programmes are often restrained by available resources, meaning that trapping efforts are focussed at the centre of the biting and pathogen transmission seasons. This is reflected in European Centre for Disease Control (ECDC) surveillance guidelines which suggest that to understand presence, distribution, abundance or seasonal activity of native mosquito species, trapping should be carried out twice per month (Schaffner et al. 2014). Of those studies found to report on seasonal abundance of adult *Cx. pipiens*, the data was most frequently presented as cumulative monthly totals (Table 3.5). Without access to the raw data, this does not allow for an accurate estimate of season start or end date, as the time within the month at which *Cx. pipiens* was first or last recorded is unknown. In my analyses, I chose to include bi-monthly data due to the small sample size collected, however data at a weekly or daily time scale would be more appropriate for an analysis of this type. Further, data is often presented cumulatively over a large geographical area. In the absence of data for each individual trapping location it is not possible to determine environmental effects on diapause timings.

Further, studies often do not report the start and end dates of their trapping procedures, or do not start trapping until well into the mosquito season. The lack of information about trapping start and end dates means that it is unclear whether the first or last recorded date of *Cx. pipiens* capture was also the first or last night of trapping. This information is important because the presence of *Cx. pipiens* on the first or last trapping occasion would suggest that the mosquito season extends beyond the recorded dates. In absence of this information it was necessary either to exclude the data or to assume that the first or last recorded capture signals the start or end of the active season. This problem could be solved by authors providing more detailed information about the trapping schedule of the studies. Without access to the original dataset, accurately estimating season end point can also be difficult because, whilst there may be incidents of *Cx. pipiens* captures late in the year, the vast majority of the population may have entered diapause shelters long before the last capture. Access to data of a high temporal resolution would be required to make more informed estimates about the rate at which the population enters diapause and around which point in time this entry into diapause is centred.

A centralised database pooling together collected datasets from a wide range of vector researchers with a minimum required temporal resolution of observations and standardised reporting of key metrics such as first and last date of recorded adult females would allow questions regarding environmental drivers' effects on species phenology across a large range to be answered. Historically, pathogens and vectors have been sparsely recorded, with recording generally restricted to only presence/absence data (Purse and Golding 2015). However, large scale projects to bring together knowledge on vector seasonality from a wide spatial range are now being proposed and implemented. Rund and Martinez (2017) propose a roadmap for a US National Vector Surveillance System, which would bring together data from ~ 1000 US mosquito control agencies and would report findings in a standardized way. This data would allow researchers to answer key questions on a wide range of topics related to vectors and vector-borne disease. Hoekman et al. (2016) describe a new project from the National Ecological Observatory Network to monitor mosquito populations across a broad geographical range of 60 sites across 20 ecoclimatic regions in the USA for the next 30 years. These initiatives would allow geographic patterns in mosquito phenology to be examined and understood, improving model parameterisation and giving valuable insights into disease transmission risks. Similar initiatives are beginning to be put into place across Europe to inform on differences between phenologies across the two continents (ECDC 2017), however such programmes remain in their infancy.

Chapter 4

Understanding how biotic and abiotic factors interact with life cycle behaviour to produce adult mosquito phenology: insights from combining models and empirical data

4.1 Introduction

In studying mosquito-borne disease models developed in 1970-2010, Reiner et al. (2013) found that 82% of models either did not use empirical field or laboratory data, or combined the model with such data to estimate only one or two model parameters (N_{models} = 388). Further, less than 4.5% of all models explicitly modelled both aquatic and adult mosquito stages, whilst allowing seasonal abundance to vary either sinusoidally or based on a pattern derived from field data. In recent years, increases in the volume of field data available, increased computational power, and advances in ecological and statistical modelling techniques have led to a shift towards more reliance on data and less reliance on theoretical model frameworks (Luo 2011). This trend has been reflected in vector-borne disease research, where initial work focussed on the analysis of mathematical models of malaria transmission in the early and mid-1900s (Smith et al. 2012). Recently a greater emphasis has been placed on the importance of the direct use of empirical field data to develop and inform mechanistic (Barker et al. 2013) and statistical models (Wimberly et al. 2014), particularly large computer simulation models such as CIMSiM and Skeeter Buster (Focks et al. 1993a, 1993b,

1995; Magori et al. 2009).

Species distribution models, which use data to assess climatic impacts on *Cx. pipiens* populations or WNV outbreaks have become increasingly popular in recent years (Mulatti et al. 2014; Rosà et al. 2014; Wimberly et al. 2014; Jian et al. 2014b; Montarsi et al. 2015). These models have identified a number of key drivers linked to *Cx. pipiens* phenology and WNV outbreaks, such as temperature and habitat availability. In particular, these models highlight the spatial variability and interactions of climatic factors on abundance measures and the probability of outbreaks (Wimberly et al. 2014). However, whilst instances are becoming more common (Barker et al. 2013; Lončarić and Hackenberger 2013; Marini et al. 2016), the expensive and time-consuming nature of collecting mosquito abundance data across numerous locations means the majority of mechanistic models investigating *Cx. pipiens* or WNV are not challenged with empirical field data (Wonham et al. 2004; Bowman et al. 2005; Cruz-Pacheco et al. 2005; Liu et al. 2006; Bergsman et al. 2015; Marini et al. 2017). Some recent models have begun to address this knowledge gap. Marini et al. (2016) developed a temperature- and density-dependent ODE model to predict abundance of *Cx. pipiens* populations, which the authors validated against adult female capture data from Northern Italy. The results were promising, as more than 90% of the weekly trap records lie within the 2.5-97.5% quantiles of the model predictions. Pawelek et al. (2014) develop a model, validated against capture data from South Carolina, to assess the efficacy of control strategies applied to *Cx. pipiens* populations.

Accurate seasonal predictions of vector density are essential, if vector population models are to be coupled with epidemiological models with confidence (Lord 2004). Calculations of important disease transmission metrics, such as R_0 values, rely on accurate estimation of parameters such as vector-to-host ratios and adult longevity (Rogers and Randolph 2006). By challenging mechanistic models of vector seasonality with data, key model shortcomings can be identified for further development, or confidence in the model can be built before using it to make policy decisions.

Figure 4.1 shows that the DDE model developed in Chapter 2 does not accurately capture all features of the *Cx. pipiens* seasonal abundance data collected in Chapter 3. In Section 3.3.1, it was shown that the model estimates of larval stage duration and survival captured field-observed rates well (Figure 3.6). However, when comparing Chapter 2 model estimates of abundance of all life stages with the Chapter 3 data, the active mosquito season is predicted to both start and end later in the season than was observed in the data. Further, there are

clear peaks observable in the abundance data that are not present in the model predictions, which increase more steadily throughout the season (Figure 4.1). Given these discrepancies between the model predictions and the data, I revisit some of the assumptions made in Chapter 2 and incorporate additional complexities in the model, in order to better capture the observed seasonal dynamics.

4.1.1 Diapause dynamics

The analysis of the data collected in Chapter 3 found that diapause initiation in the monitored *Cx. pipiens* population occurred in August. This contrasts with the model parameterisation in Chapter 2 (Equation 2.17), where diapause initiation was centred around a photoperiod corresponding to the 10th of September at the field site. Figure 4.1 highlights this mismatch in timings as Chapter 2 model predictions of abundance, of all life stages, exceed the abundances observed in the data in September. In Chapter 2, the September photoperiod value was chosen to reflect the fact that UK mosquitoes have been observed to enter diapause shelters throughout the month of September (Sulaiman and Service 1983). The discrepancy in timings with the field data stems from the fact that adult female *Cx. pipiens* emerging programmed for diapause, have been shown to feed on nectar in advance of entering diapause shelters (Mitchell and Briegel 1989). Consequently, appearance in shelters is not a reliable signal of diapause induction.

Further, in the field study, eggs were first observed on the 6th of April, however in Chapter 2 (Equation 2.17) diapause termination in spring was set to occur at a photoperiod corresponding to the 17th of April (Figure 4.1). The spring photoperiod value was chosen as an average to reflect the fact mosquitoes were observed to exit diapause shelters throughout the entirety of April and into May (Sulaiman and Service 1983). However, the field data suggest that those eggs which emerge very early in the season may be particularly influential due to the abundance of predator- and competition-free habitat.

Changing the diapause initiation and termination times resulted in an increase to the length of the diapause period, requiring that the overwinter mortality rate be reduced to give similar adult mosquito survival. Further, overwinter survival of temperate mosquitoes may affect both pathogen persistence and seasonal patterns of the abundance the following year. Estimates of *Cx. pipiens* overwinter survival from the literature show substantial variability between sites and years: $2-60\%$ (Sulaiman and Service 1983), 35% (Onyeka and Boreham 1987), $3-60\%$ (Bailey et al. 1982). This variability may stem from a range of factors such as

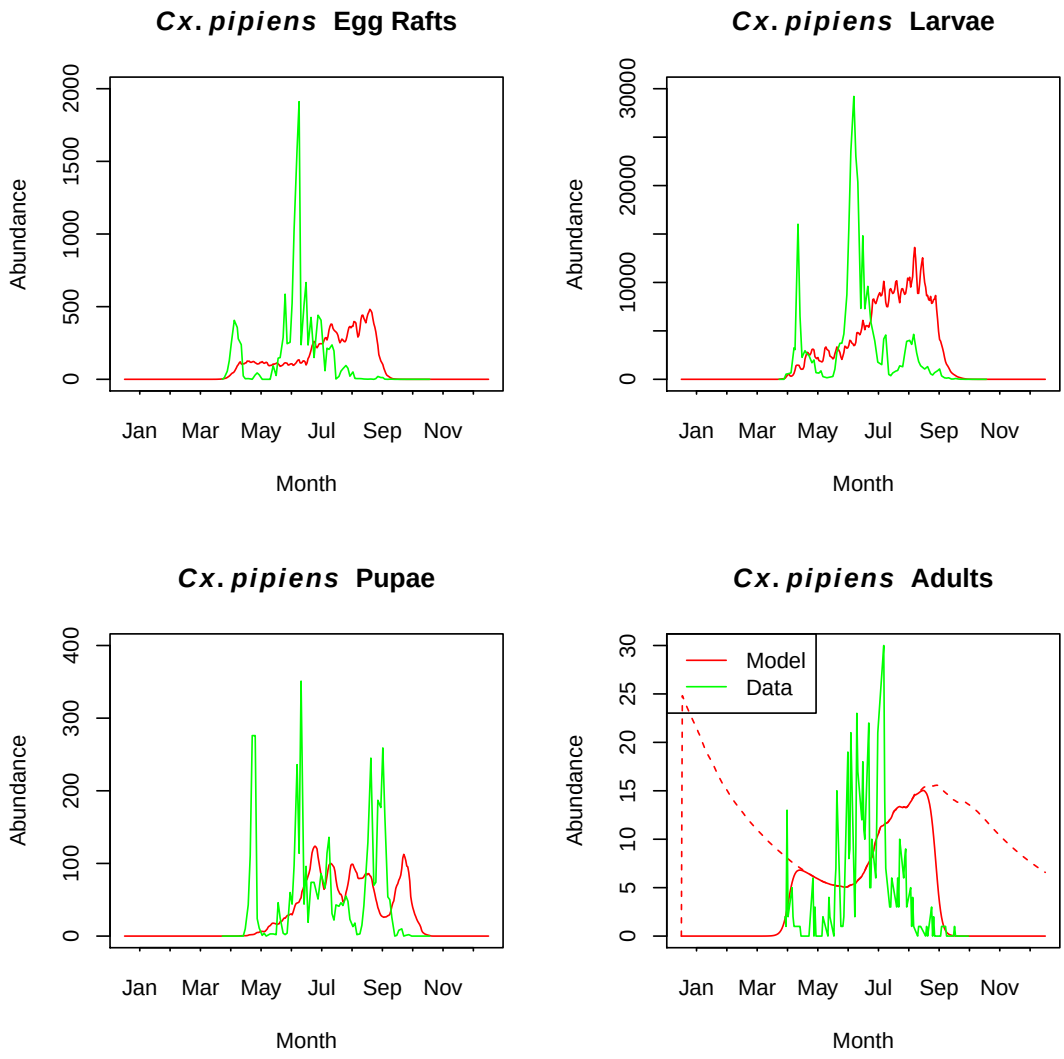

Figure 4.1: Chapter 2 model fit to data: The model predictions (red) and observed (green) abundance of each life stage are shown. All model parameters are defined in Table 2.1. Hourly water temperature values for butt 4 were used alongside minimum and maximum daily air temperature values when running the model. In the adult plot the dashed line shows all adults and the solid line excludes those in diapause by multiplying the adult abundance by the proportion of active adults $\zeta(t)$, at time t. This simulation (and other simulations in this Chapter) was run in the absence of the 18 month "burn-in" period described in Section 2.2.1, to allow for comparison across model runs with the same starting population size in the year displayed.

the level of predation experienced, possible fungal infection in the population (Service 1969) and the temperatures and humidity in diapause shelters (Rinehart et al. 2006).

The seasonal abundance data shown in Figure 4.1 also displays a clear drop in adult activity immediately after depositing the first egg raft of the season. Surviving winter demands 80% of a female's fat reserves on average (Onyeka and Boreham 1987). This loss of fat reserves has been shown to impact on reproductive fitness, with egg raft sizes laid by females in summer being 61% larger than those laid immediately following diapause (Madder et al. 1983b). I hypothesise that this drop in adult activity corresponds to high mortality of adults immediately after overwintering and laying an egg raft. When carrying out the fieldwork, support was given to this theory, as a large number of dead *Cx. pipiens* adults were seen floating on the surface of the oviposition sites only in the early part of the mosquito active season. As discussed in Section 3.4.1, the dip in activity could not be explained by adults undergoing a gonotrophic cycle, as the delay between periods of activity was too long. This process of post-oviposition mortality was not modelled in Chapter 2 and will be included in the new model presented in this chapter.

4.1.2 Synchronicity of predator and mosquito populations

Cx. pipiens is opportunistic in its egg-laying behaviour, regularly ovipositing in a variety of breeding sites such as small (Vezzani and Albicocco 2009) and large container habitats (Yee et al. 2004) and natural water bodies, including temporary pools and permanent ponds (Vinogradova 2000). The wide range of different habitats utilised for immature development means that *Cx. pipiens* are thought to be most at risk from a range of generalist predators (Juliano 2007). In Southern England a very wide range of species have been shown to act as mosquito larval predators (Medlock and Snow 2008), including dragonfly and damselfly nymphs, predatory beetle larvae (Onyeka 1983), ditch shrimp and numerous fish species (Golding et al. 2015). In the fieldwork detailed in Chapter 3 both beetle larvae and mayfly larvae, which are known predators of mosquito larvae (Medlock and Snow 2008), were observed in the water butts. It has been shown for a wide range of mosquito larval predators that a Holling type II function accurately describes consumptive behaviour (Onyeka 1983; Marti et al. 2006; Fischer et al. 2013). However, different predators will consume different volumes and may be active over different parts of the year (Onyeka 1983).

In Chapter 2, I assumed that the predator population size was a fixed proportion of the larval population size at all points of the year. However, the wide range of generalist predators

of *Cx. pipiens* larvae means that mismatch in timings between predators and mosquitoes may occur if mosquito larvae are relatively unimportant prey resources of certain predator species at certain locations. Further, it is possible that climate impacts may have differential effects on the prey and predator populations, which may cause misaligned timings of the populations' active seasons. Classical predator-prey systems have shown that, in the case of specialist predators, predator numbers peak slightly after the peak in prey numbers (Billard 1977), rather than at the same time as in Chapter 2. Consequently, in this Chapter I relax the assumptions of the Chapter 2 model by allowing the ratio of predators to prey to change through the year.

4.1.3 Impact of temperature data resolution on model predictions

A wide range of insect species' life cycles are composed of multiple stages that occur in different environments (Resh and Cardé 2009). For example, the immature life stages of mosquitoes, damselflies, dragonflies and hoverflies all live in aqueous environments, whilst the adult life stage is airborne. The pre-adult stages of midges live in semi-aquatic substrates, such as moist soil and cow pats (Walker 2001). This shift in environment during the species' life cycle means that development is dependent on different environmental variables at different times. Pre-adult development of midges is dependent on moisture levels and soil temperature (Searle et al. 2014), whilst pre-adult development of insects with aqueous immature stages is dependent on water temperature. Despite this, many models of insect seasonality approximate temperatures of aquatic and semi-aquatic life stages by air temperature (Shaman et al. 2006; Wang et al. 2011; Cailly et al. 2012; Beck-Johnson et al. 2013; Tran et al. 2013; Lončarić and Hackenberger 2013; Searle et al. 2014; Marini et al. 2016).

It has recently been shown in a tropical mosquito habitat that using air temperatures as a proxy for water temperatures can result in substantial over- or under-estimation of mosquito abundance (Paaijmans et al. 2010). Observed air and water temperatures in the field experiment, detailed in Chapter 3, regularly differed by more than $3\,^{\circ}\mathrm{C}$, as shown by the relationship in Figure 4.2. Therefore, it is expected that the impacts of the temperature difference on mosquito development and survival, and consequently abundance, may be large. Specifically, development rates will be underestimated (Equation 2.12), however the effect on survival will depend on the temperatures experienced (Equation 2.13) (Loetti et al. 2011). The profound effects of using air temperature as a proxy for water temperature when estimating immature stage durations are shown in Figure 4.3, where the total estimated duration of all

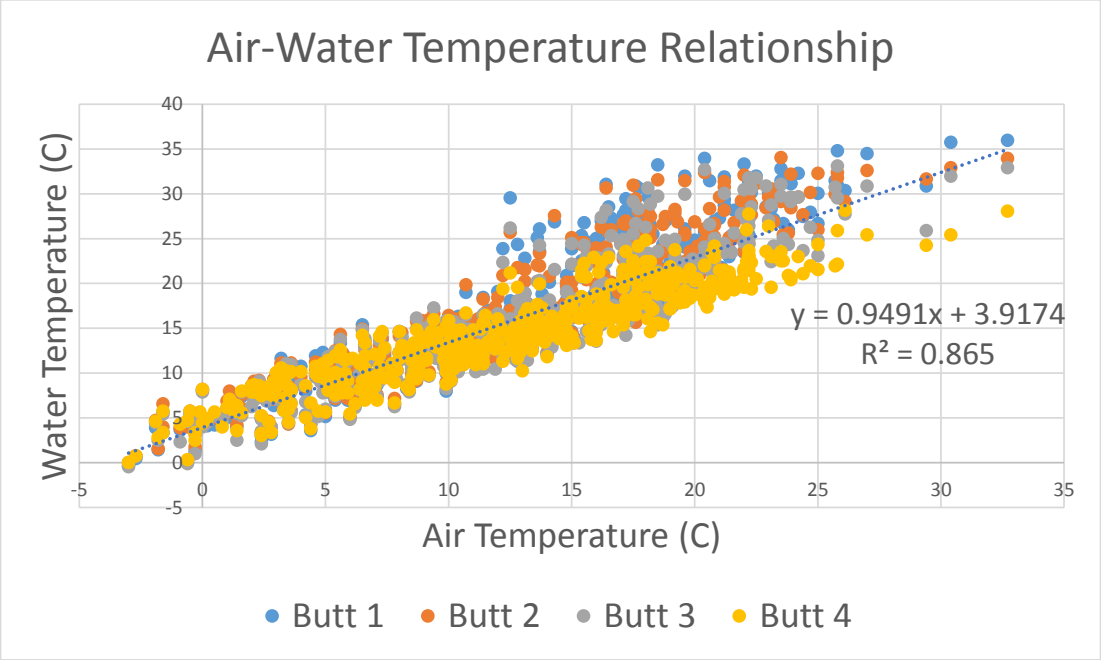

Figure 4.2: Air-water temperature relationship: The relationship between water temperatures measured across the four water butts monitored in Chapter 3 and air temperatures recorded at the CEH weather station is shown.

immature stages differs by up to two weeks, dependent on the temperature used in the model.

The use of air temperature when modelling aqueous life stages stems from the fact that water temperatures are less readily available than air temperatures and there is not a straightforward relationship between the two across the range of mosquito habitats. Exposure to direct sunlight will increase water temperatures in small water bodies, larger water bodies will heat and cool more slowly than smaller ones and both artificial and natural containers will have a range of different thermodynamic properties (Preud'homme and Stefan 1992). This is made clear by the range of temperatures shown in Figures 4.2 and 4.4, where the recorded water temperatures showed substantial variability across four water butts, which were of equal size and differed only in terms of sun and wind exposure (mean temperatures were: butt 1 = 17.2 °C, butt 2 = 17.2 °C, butt 3 = 16.4 °C, butt 4 = 15.2 °C for April to September). These water temperatures also differ substantially from the air temperatures taken in the adjacent field (mean air temperature was 13.6 °C for April to September). Water temperatures were not available for the Chapter 2 simulations, however the data collection in Chapter 3 means that they can be included in this Chapter.

Outwith the issue of using water temperature versus air temperature, many studies into

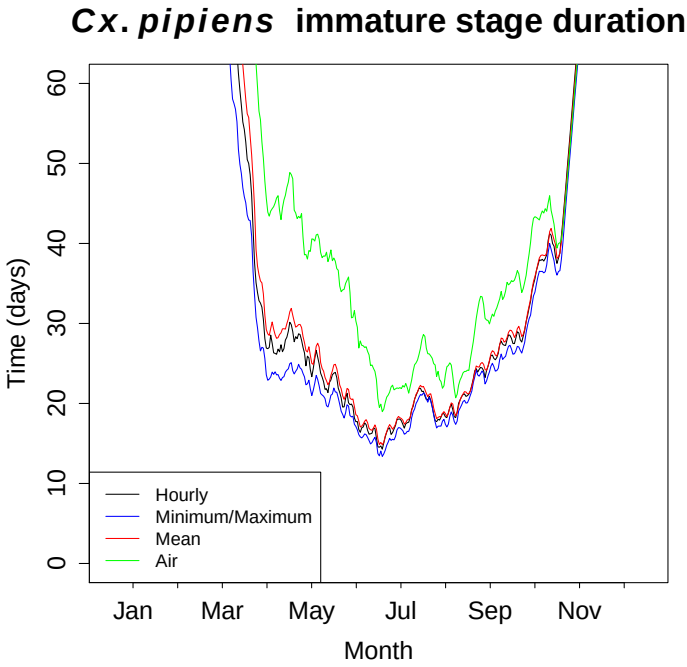

Figure 4.3: Immature development times: The DDE model predictions of the total duration from egg-laying to adult emergence are shown for different water temperature input scenarios. Water temperatures are for butt 1 in all cases and minimum and maximum daily air temperature values are used for the adult processes in all cases. The water temperatures used are as follows: Hourly - hourly water temperature data, Minimum/Maximum - minimum and maximum daily water temperatures, Mean - mean daily water temperatures, Air - minimum and maximum daily air temperatures were used as a proxy for water temperature.

mosquito population dynamics have considered constant temperatures, or mean daily temperatures, however it has recently been shown that diurnal temperature range can have a large impact on mosquito life history traits and on the ability of mosquitoes to transmit disease (Paaijmans et al. 2010). Specifically, Lambrechts et al. 2011 showed in a laboratory study that, *Aedes aegypti* died more quickly and were less susceptible to virus infection when exposed to larger diurnal temperature range, around the same mean temperature. Similarly, a laboratory experiment by Carrington et al. 2013 found that, with a mean daily temperature of $26\,^{\circ}\mathrm{C}$, a large diurnal temperature range ($18\,^{\circ}\mathrm{C}$) extended immature development, lowered larval survival and reduced reproductive output of *Ae. aegypti*, a tropical mosquito species. Brady et al. (2013) included diurnal temperature range when modelling adult survival of *Ae. aegypti* and *Ae. albopictus* in both laboratory and field settings, however diurnal temperature range remains widely neglected in models of temperate mosquito dynamics.

During the fieldwork, the immature mosquito population was observed to be congregated almost exclusively in one of the four water butts (butt 4) in the summer and autumn months.

This butt was observed to be the coolest of the four, whilst temperatures in the other three butts reached highs of approximately $36\,^{\circ}\mathrm{C}$, which is a damagingly high temperature for *Cx. pipiens* larvae (Loetti et al. 2011). Further, due to decreased sun exposure, butt 4 showed a smaller diurnal temperature range (Figure 4.4 (b)) than was observed in butts 1-3. These differences in temporal resolution of temperature inputs will affect calculation of vital rates, like development, as shown in Figure 4.3. Hence, I aimed to understand if these higher water temperatures were likely to induce a high mortality rate in butt 1, explaining the much smaller mosquito population found throughout the summer.

4.2 Aims

In response to the Chapter 2 model failing to capture the diapause timings and patterns of abundance observed in the field data (Figure 4.1), I update the model to reflect the observations discussed in Section 4.1.1. I then run simulations to understand the effects of seasonally varying predation (Section 4.1.2) and the effects of using different temporal resolutions of temperature input data (Section 4.1.3). The aims of these updates and consequent simulations are as follows:

1. **Diapause timing:** The timings of entry to and exit from diapause were not well captured by the Chapter 2 model. I update the model parameters governing diapause initiation and termination in light of the new data collected in Chapter 3 and discuss the implications of these changes on the model fit to data.

2. **Adult overwinter survival:** The updates to diapause timings, and the consequent increase to the duration of the overwinter period, required that the adult overwinter mortality rate be reduced. I update and investigate the effects of varying the minimum adult death rate, which acts over winter, on the ability to capture patterns of seasonal abundance.

3. **Post-diapause mortality:** I hypothesise that old, post-diapause females experience an increased mortality due to the negative costs which diapause can exert on fitness. I introduce a seasonal adult death rate term which acts immediately after emergent females complete egg-laying in the spring and examine the impact of this term on the ability of the model to accurately predict field data.

4. **Seasonal variation in predation:** Changes in synchronicity between the mosquito and predator populations are likely to impact seasonal abundance patterns. I explore the effects of variable predator numbers by subjecting the predator population to sinusoidal seasonal forcing. I compare this scenario with a constant predation scenario,

(a)

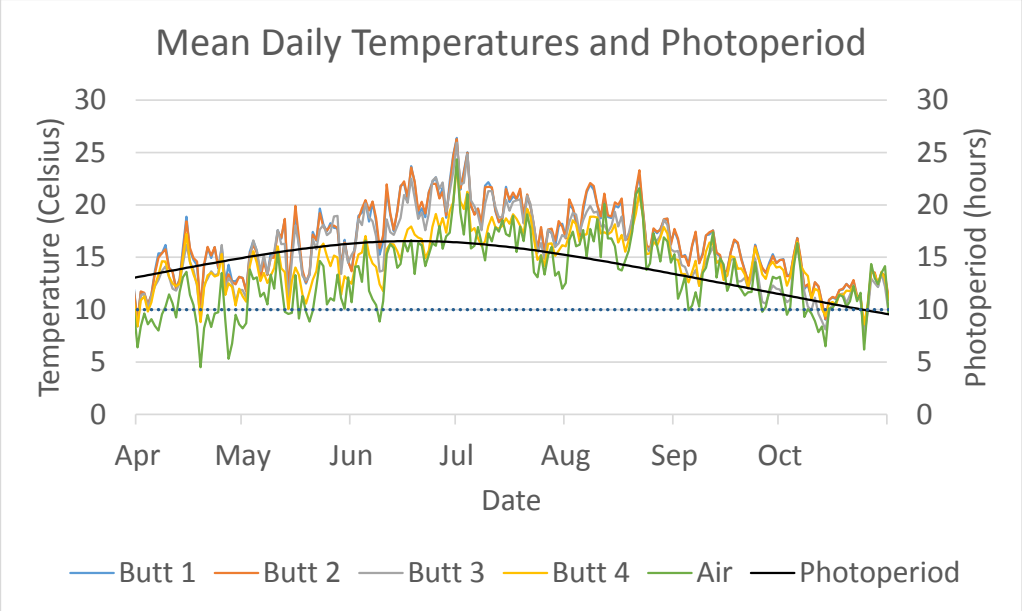

(b)

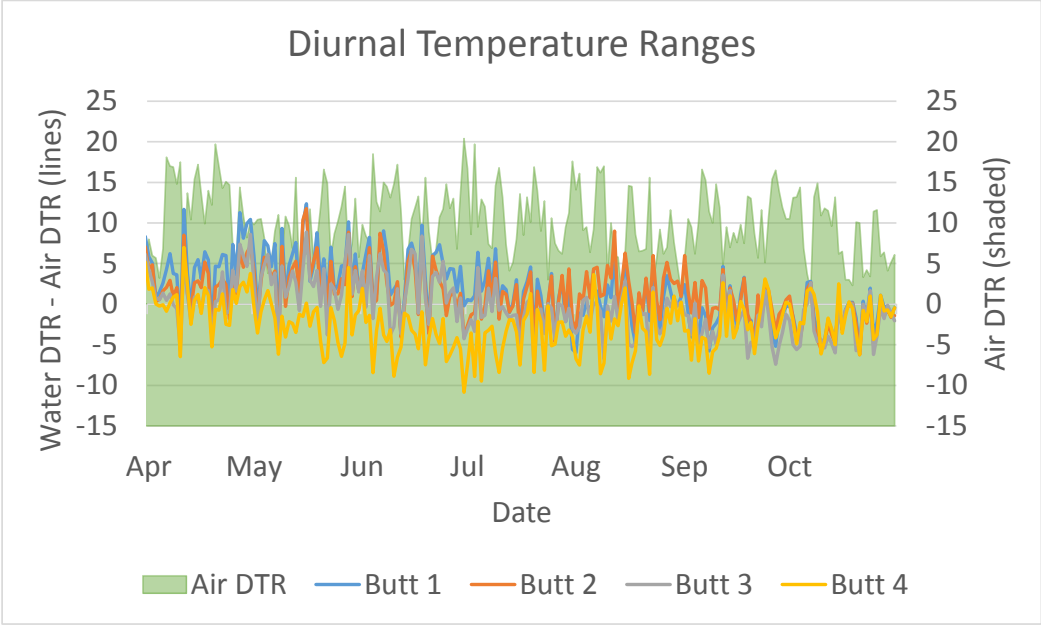

Figure 4.4: Temperature data: (a) shows mean daily temperatures for each of the four water butts, air temperature, and photoperiod. In (b) the lines show the difference between the DTR of the water temperature for each butt and the DTR of the air temperature. The DTR of the air temperature is shown by the shaded area.

where predator numbers remain directly proportional to larval numbers without seasonal forcing, as in Chapter 2.

5. The effects of the temporal resolution of temperature input data on model predictions are studied.

   5.1. **Water temperature temporal resolution:** Diurnal temperature range has been shown to affect mosquito vital rates (Lambrechts et al. 2011; Carrington et al. 2013). The impacts of including fine resolution daily temperature variables are examined, using hourly temperature measurements taken for two of the four water butts (butts 1 and 4). These results are compared with those observed when using mean temperatures, and minimum and maximum daily temperatures, to understand the effects on abundance predictions of including diurnal water temperature range.

   5.2. **Water butt temperature comparisons:** Damagingly high temperatures for immature mosquito development were observed to occur in butts 1-3. I investigate whether these higher temperatures, and often larger diurnal temperature ranges, would lead to increased mortality, explaining the substantially smaller number of mosquitoes seen in these butts (beyond the initial spring population peak) compared to butt 4.

   5.3. **Air temperature temporal resolution:** As with water temperatures above, I investigate the effects of both including and excluding diurnal temperature range in air temperature and compare the effects on abundance predictions.

   5.4. **Air temperature as a proxy for water temperature:** Models of mosquito seasonality often use air temperature as a proxy for water temperatures (Cailly et al. 2012; Tran et al. 2013; Lončarić and Hackenberger 2013). The implications for seasonal abundance of approximating water temperatures with air temperatures are explored.

4.3 Methods

I will now recap the DDE model described in detail in Chapter 2, followed by those functional forms which are unchanged. Afterwards I will discuss in detail those functional forms which have been changed, or for which the parameterisation has been updated in light of the field data. With the availability of water temperature collected in the field study, I now use

$T(t)$ to refer to water temperature for immature aquatic processes and air temperature for adult processes.

4.3.1 Modelling framework

Here I present a brief recap of the mosquito model framework, discussed in detail in Chapter 2. The four state equations which correspond to eggs, $E(t)$, larvae, $L(t)$, pupae, $P(t)$ and adults $A(t)$ at time t, are

$$\begin{aligned}
\frac{dE}{dt} &= R_E(t) - M_E(t) - \delta_E(T(t))E(t),\\
\frac{dL}{dt} &= R_L(t) - M_L(t) - (\delta_L(T(t)) + \delta_\pi(L(t)))L(t),\\
\frac{dP}{dt} &= R_P(t) - M_P(t) - \delta_P(T(t))P(t),\\
\frac{dA}{dt} &= R_A(t) - \delta_A(T(t))A(t),
\end{aligned} \tag{4.1}$$

where $\delta_i(T(t))$ ($i = E, L, P, A$) represents the stage-specific, density-independent, temperature-driven, mortality rate, $\delta_\pi(L(t))$ represents the larval mortality rate due to external predation and $R_i(t)$ and $M_i(t)$ represent the rate of recruitment into and maturation out of stage i, respectively. The maturation equations are defined by

$$\begin{aligned}
R_E(t) &= b(t)A(t),\\
M_E(t) = R_L(t) &= R_E(t-\tau_E(t))S_E(t)\frac{g_E(T(t))}{g_E(T(t-\tau_E(t)))},\\
M_L(t) = R_P(t) &= R_L(t-\tau_L(t))S_L(t)\frac{g_L(T(t))}{g_L(T(t-\tau_L(t)))},\\
M_P(t) = R_A(t) &= R_P(t-\tau_P(t))S_P(t)\frac{g_P(T(t))}{g_P(T(t-\tau_P(t)))},
\end{aligned} \tag{4.2}$$

with $b(t)$ as the egg-laying rate at time t, $\tau_i(t)$ and $S_i(t)$ as the stage duration and survival of individuals in stage i ($i = E, L, P$) at time t respectively and $g_i(T(t))$ as the development rate of individuals in stage i at temperature $T(t)$. The proportion of individuals which survive from recruitment into one class, to maturation to the next, is defined by the following

sequence of DDEs,

$$\begin{aligned}
\frac{dS_E}{dt} =& S_E(t)\left(\frac{g_E(T(t))\delta_E(T(t-\tau_E(t)))}{g_E(T(t-\tau_E(t)))} - \delta_E(T(t))\right),\\
\frac{dS_L}{dt} =& S_L(t)\Bigg[\left(\delta_\pi(t-\tau_L(t)) + \delta_L(T(t-\tau_L(t)))\right)\left(\frac{g_L(T(t))}{g_L(T(t-\tau_L(t)))}\right)\\
&- \delta_\pi(L(t)) - \delta_L(T(t))\Bigg],\\
\frac{dS_P}{dt} =& S_P(t)\left(\frac{g_P(T(t))\delta_P(T(t-\tau_P(t)))}{g_P(T(t-\tau_P(t)))} - \delta_P(T(t))\right).
\end{aligned} \tag{4.3}$$

The rate of change of the duration of the three immature life stages and the gonotrophic cycle are given by

$$\frac{d\tau_i(t)}{dt} = 1 - \frac{g_i(T(t))}{g_i(T(t-\tau_i(t)))}, \tag{4.4}$$

where $i = E, L, P, G$. Here the development rate, $g_i(T(t))$, is dependent on temperature.

4.3.2 Inoculation and history

The inoculation and history processes remain unchanged from those used in Section 2.2.1. For historical values, $t < 0$, it was assumed that temperatures were constant and equal to the first temperature observation corresponding $t = 0$. The adult population was inoculated on the 1st of January 2015 with 5000 individuals. Simulations were carried out over 12 months, with no “burn-in" period, as was used in Chapter 2, to understand the effects of model or temperature inputs on the first season, rather than the combined effects over multiple seasons. This allowed the effects of changes within a season to be studied using a common population size at the start of that season.

4.3.3 Recap of unchanged functional forms and parameterisations

I briefly recap those functional forms that are unchanged from Chapter 2.

Development rates

Growth rates for the immature stages were modelled using a power function,

$$g_i(T(t)) = \begin{cases} \alpha_i T(t)^{\eta_i}, & T(t) > \left(\frac{b_m}{\alpha_i}\right)^{\frac{1}{\eta_i}}, \\ b_m, & \text{otherwise} \end{cases}. \tag{4.5}$$

Here $i = E, L, P$ correspond to the egg, larval and pupal stages respectively, with α_i and η_i as parameters fitted to data.

Immature death rate

Death rates for the immature stages were modelled using a modified Gaussian functional form

$$\delta_i(T(t)) = \begin{cases} \nu_{0i} \exp\left(\left(\frac{T(t)-\nu_{1i}}{\nu_{2i}}\right)^2\right), & \nu_{1i} + \frac{\nu_{2i}}{2}\ln\left(\frac{b_{di}}{\nu_{0i}}\right) < T(t) < \nu_{1i} - \frac{\nu_{2i}}{2}\ln\left(\frac{b_{di}}{\nu_{0i}}\right), \\ b_{di}, & \text{otherwise}, \end{cases} \tag{4.6}$$

for $i = E, L, P$, which leads to expected survival times following a bell-shaped curve centred at ν_{1i} and bounded to be greater than or equal to $\frac{1}{b_{di}}$.

Egg-laying rate and gonotrophic cycle

The functional form of the gonotrophic cycle development is given by

$$g_G(T(t)) = q_1/(1 + q_2 \exp(-q_3 T(t))), \tag{4.7}$$

where $g_G(t)$ is the rate of progression of the gonotrophic cycle at time t, with q_1, q_2 and q_3 as fitted constants. The egg-laying rate, $b(t)$, was then calculated according to

$$b(t) = \frac{\zeta(t)R}{2\tau_G(t)}, \tag{4.8}$$

where $R = 200$ is the average egg raft size from the literature (Jobling 1938; Vinogradova 2000) and $\zeta(t)$ is the proportion of adults which are non-diapausing.

4.3.4 New and updated functional forms and parameterisations

Now I discuss cases where model assumptions have been updated in light of new data collected in Chapter 3. Changes to parameters are discussed in the order they were applied to the model. The full list of parameter values used in this Chapter, with new or updated parameter values highlighted in red, is presented in Table 4.1.

Diapause initiation and termination

Figure 4.1 shows that the model presented in Chapter 2 does not capture the start and end dates of the active mosquito season well. The proportion of active adults at any point in time, $\zeta(t)$, is dependent on photoperiod, $\psi(t)$, such that

$$\zeta(t) = \begin{cases} \frac{1}{1+\exp(\omega_S(\xi_S - \psi(t)))} & : \psi(t) \text{ increasing}, \\ \frac{1}{1+\exp(\omega_A(\xi_A - \psi(t)))} & : \psi(t) \text{ decreasing}, \end{cases} \tag{4.9}$$

where ξ_S is the spring photoperiod threshold for which greater than 50% of the population becomes active and ξ_A is the opposite threshold for when 50% of the population enters diapause. The constant parameters ω_S and ω_A define the rate with which the transition between diapausing and active states occurs. The quasi-poisson GLM fitted to the adult capture data in Section 3.3.1 showed that diapause occurred in August, while the Chapter 2 estimate assumed diapause initiation in September. Consequently, the photoperiod threshold, ξ_A, was updated to 15 hours, which occurs exactly one month earlier in the season than the previous estimate from Chapter 2. The rate at which mosquitoes enter diapause, ω_A, was also decreased to give a more gradual transition between active and diapausing adults (Table 4.1), reflecting the observation that diapause initiation appears to be less synchronous than termination (Figure 4.1). In the field study, eggs were observed to appear on the 6th of April, so the 50% photoperiod threshold was moved to early April ($\xi_S = 13.7$) rather than late April.

During- and post-diapause adult death rate

Motivated by the field observations, I hypothesise that old, post-diapause females experience an increased mortality due to the negative costs which diapause can exert on fitness (Section

Parameter	Definition	Value	Eqn	Reference
α_E	Fit parameter in egg maturation	2.20×10^{-3}	4.5	Figure 2.1 (a)
β_E	Fit parameter in egg maturation	1.77	4.5	Figure 2.1 (a)
α_L	Fit parameter in larval maturation	3.15×10^{-3}	4.5	Figure 2.1 (b)
β_L	Fit parameter in larval maturation	1.12	4.5	Figure 2.1 (b)
α_P	Fit parameter in pupal maturation	7.11×10^{-4}	4.5	Figure 2.1 (c)
β_P	Fit parameter in pupal maturation	1.89	4.5	Figure 2.1 (c)
$\mu_{0E}, \mu_{0L}, \mu_{0P}$	Baseline immature death rate	0.0157	4.6	Figure 2.2 (a)
$\mu_{1E}, \mu_{1E}, \mu_{1P}$	Optimum temperature for immature survival	20.5	4.6	Figure 2.2 (a)
$\mu_{2E}, \mu_{2E}, \mu_{2P}$	Width parameter for immature death rate	7	4.6	Estimated from laboratory data
α_A	Fit parameter in adult death	2.17×10^{-8}	2.14	Ciota et al. (2014)
β_A	Fit parameter in adult death	4.48	2.14	Ciota et al. (2014)
b_m	Baseline maturation rate	$\frac{1}{60}$	4.5	Almirón and Brewer (1996) and Loetti et al. (2011)
b_{di}	Threshold immature death rate	1	4.6	Time-scale of model
b_{da}	Baseline adult death rate	0.003	2.14	Sulaiman and Service (1983), Onyeka and Boreham (1987), and Bailey et al. (1982)
a	Attack rate of predators	1	4.11	From simulation
h	Handling time of predators	0.002	4.11	From simulation
r	Max no. of predators per larva	0.001	4.12	From simulation
V	Volume of larval habitat	20l	4.11	By calculation
R	Egg raft size	200	2.19	Vinogradova (2000)
q_1	Gonotrophic cycle fit parameter	0.202	4.7	Figure 2.3 (b)
q_2	Gonotrophic cycle fit parameter	74.5	4.7	Figure 2.3 (b)
q_3	Gonotrophic cycle fit parameter	0.246	4.7	Figure 2.3 (b)
ξ_S	Spring diapause threshold	13.7	4.9	From fieldwork
ξ_A	Autumn diapause threshold	15	4.9	From fieldwork
ω_S	Spring diapause transition	5	4.9	From fieldwork
ω_A	Autumn diapause transition	3.5	4.9	From fieldwork
Γ	Post-diapause mortality mult.	8	2.14	From simulation
σ^2	Post-diapause mortality duration	4	2.14	From simulation
$\mathcal{D}$	80% diapause exit threshold day of year	109	2.14	From fieldwork
υ	Predation timing parameter	31	4.12	From simulation
χ	Predation sharpness parameter	2	4.12	From simulation
φ	Latitude	51.6		Latitude of Wallingford field site

Table 4.1: Parameter values used for running the model with changes from the previous chapters in red.

4.2 point 3) (Hahn and Denlinger 2007). The functional form for the adult death rate, $\delta_A(t)$, has been modified to incorporate an additional post-diapause death term, which is supported by the decreased adult abundances observed in May, following the initial peak in abundances upon diapause emergence (Figure 4.1). This term was added to the existing Gaussian function from Chapter 2 (Equation 2.13). It can be seen from Figure 4.5, which compares the adult death rate with and without the additional mortality, that the additional term only has an affect in the post-diapause phase of the year. The updated adult death rate function is given by

$$\delta_A(t,T(t)) = \begin{cases} \overbrace{\alpha_A T(t)^{\eta_A}}^{\text{old}} + \overbrace{\left(\frac{\Gamma}{\sqrt{2\pi\sigma^2}}\exp\left(-\frac{(t-\tau_G(t)-\mathcal{D})^2}{2\sigma^2}\right)\right)}^{\text{new process}}, & T(t) > \left(\frac{b_{da}}{\alpha_A}\right)^{\frac{1}{\eta_A}} \\ \underbrace{b_{da}}_{\text{updated parameter}}, & \text{otherwise} \end{cases}. \tag{4.10}$$

Here α_A and η_A are constants fitted to data from the literature regarding the temperature dependence of adult longevity, as in Section 2.2.2. Γ is a scaling parameter defining the strength of the post-diapause mortality effect, σ^2 controls the length of time over which this post-diapause mortality acts and $\mathcal{D}$ is the day of the year on which an arbitrary threshold value (80%) of adults have exited diapause. The death rate was constrained not to drop below a base death rate of b_{da}, which determines the mortality of diapausing females. The shift in the diapause thresholds, previously discussed, increased the length of the overwinter period, meaning that a reduced b_{da} was required to give a similar overwinter survival percentage to that used in Chapter 2 (b_{da} = 0.01 to b_{da} = 0.003) (Bailey et al. 1982; Onyeka and Boreham 1987). The value for Γ was chosen such that the post-diapause death rate was sufficient to wipe out the adult population. In Section 4.4.2 it is shown that the value chosen is sufficient to kill off the population, with further increases to Γ having negligible effect on abundance patterns. The mortality duration parameter, σ^2, was chosen to maximise the correlation between the adult field data and the model-predicted adult abundance by increasing σ^2 in increments of 0.1 and choosing the strongest correlation. The diapause exit parameter, $\mathcal{D}$, was chosen to coincide with the end of the first adult abundance peak in the field data, when it was assumed that the majority of the population had left diapause.

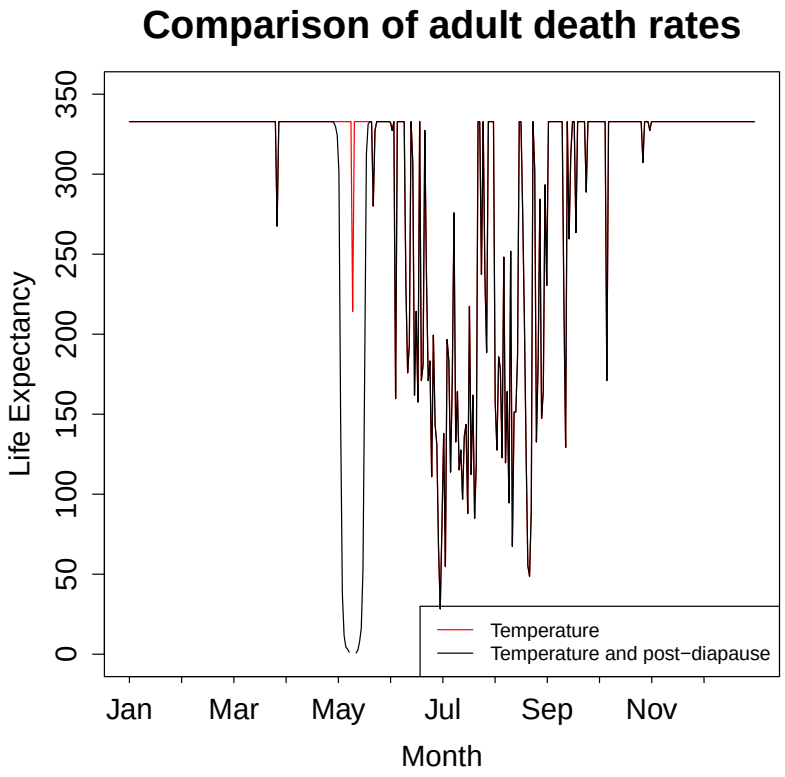

Figure 4.5: Adult death rates: the red line shows the adult death rates predicted under the Chapter 2 model, in the absence of the post-diapause mortality term (only temperature dependence). The black line shows the adult death rates predicted under the updated model, including the post-diapause mortality term.

Seasonally varying predation

The strength of seasonal predation is affected by the ratio of predators to prey, the attack rate of predators and the predators' handling time. The three parameters have high uncertainty, as attack rates and handling times will vary greatly between predator species (Quiroz-martinez and Rodriguez-Castro 2007) and the ratio of predators to prey will vary seasonally, by location, and by species (Medlock and Snow 2008). Similar to mosquito development and survival, predator attack rates and handling times may also be affected by temperature. I investigate the effects on seasonal abundance of altering the maximum number of predators per larva, r. As in Section 2.2.2, the larval death rate due to predation is given by the Holling type II function (Marti et al. 2006; Fischer et al. 2013)

$$\delta_\pi(L(t)) = \frac{a\mathcal{P}(t)}{V + ahL(t)}. \tag{4.11}$$

where a is the attack rate, h is the handling time, V is the volume of habitat and $\mathcal{P}(t)$ is the predator density at time t. In Section 2.2.2 it was assumed that $\mathcal{P}(t) = rL(t)$, such that the predator density was equal to a constant proportion of the larval density. Now I make the extension that the proportion of predators to larvae, r, varies seasonally. This allows the effects of varying the synchronicity of predator and mosquito populations to be investigated. Consequently, r is replaced by $r(t)$ and predator density is related to larval density, according to

$$\mathcal{P}(t) = \mathcal{R}(t)L(t) = r_{max}\left(\frac{1}{2} + \frac{1}{2}\sin\frac{2\pi(t-\upsilon)}{365}\right)^{\chi} L(t), \tag{4.12}$$

where $r(t)$ is the number of predators per larva at time t, r_{max} is the maximum number of predators per larva, υ defines the time at which the predation peak occurs and χ defines the time period over which predation is high, as displayed in Figure 4.6. I assume a fixed volume of larval habitat for simplicity. As larvae are believed to experience predation by generalist predators, I run simulations to investigate the effect of moving the predation peak either earlier or later in the year.

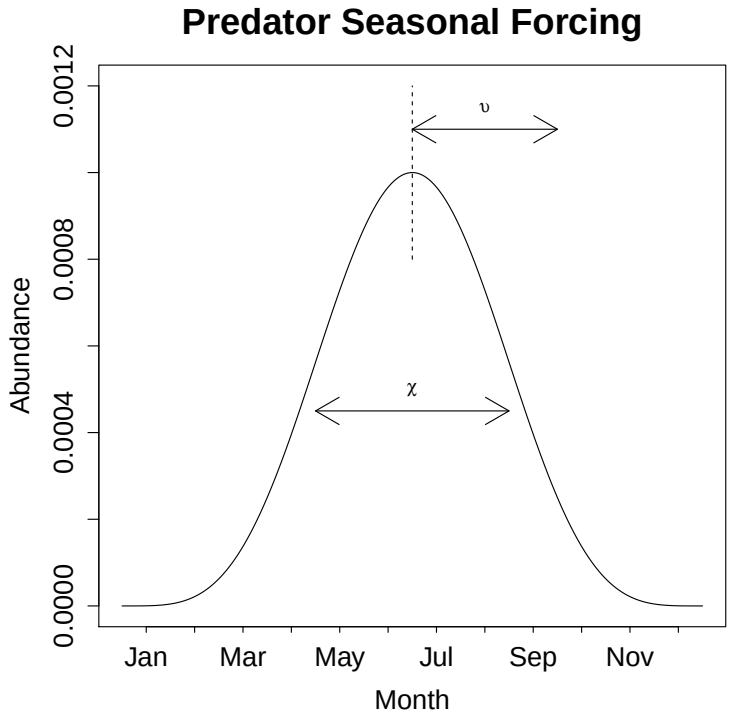

Figure 4.6: Predator seasonal forcing: The seasonal forcing function, $\mathcal{R}(t)$, is shown, highlighting how changes to υ and χ affect the ratio of predators to larvae throughout the season.

4.3.5 Air and water temperature temporal resolutions

One of my objectives was to understand whether including diurnal temperature variability substantially influenced model results. Further, I investigated whether including diurnal temperature variability would be accurately capture seasonal abundance patterns or if increasing temporal resolution by including the hourly measurements substantially improved accuracy. To understand the effects of temporal resolution of water temperature data on seasonal abundance, I considered three scenarios where I used mean daily, minimum and maximum daily, and hourly temperature values. Figure 4.7 shows the temperature profiles created under these three different temporal resolution scenarios for the first 20 days of April at the field site in 2015, highlighting that using mean daily temperatures results in large differences between actual and estimated temperatures throughout the day. In considering air temperature, only mean daily and minimum and maximum daily resolutions were considered, as hourly temperature measurements were not available:

- **Mean daily values -** Diurnal temperature variability was ignored by interpolating between mean daily temperature values, obtained by taking the mean of the hourly measurements recorded for each day. These mean daily values were assumed to be spaced exactly 24 hours apart and to occur at noon in all cases.

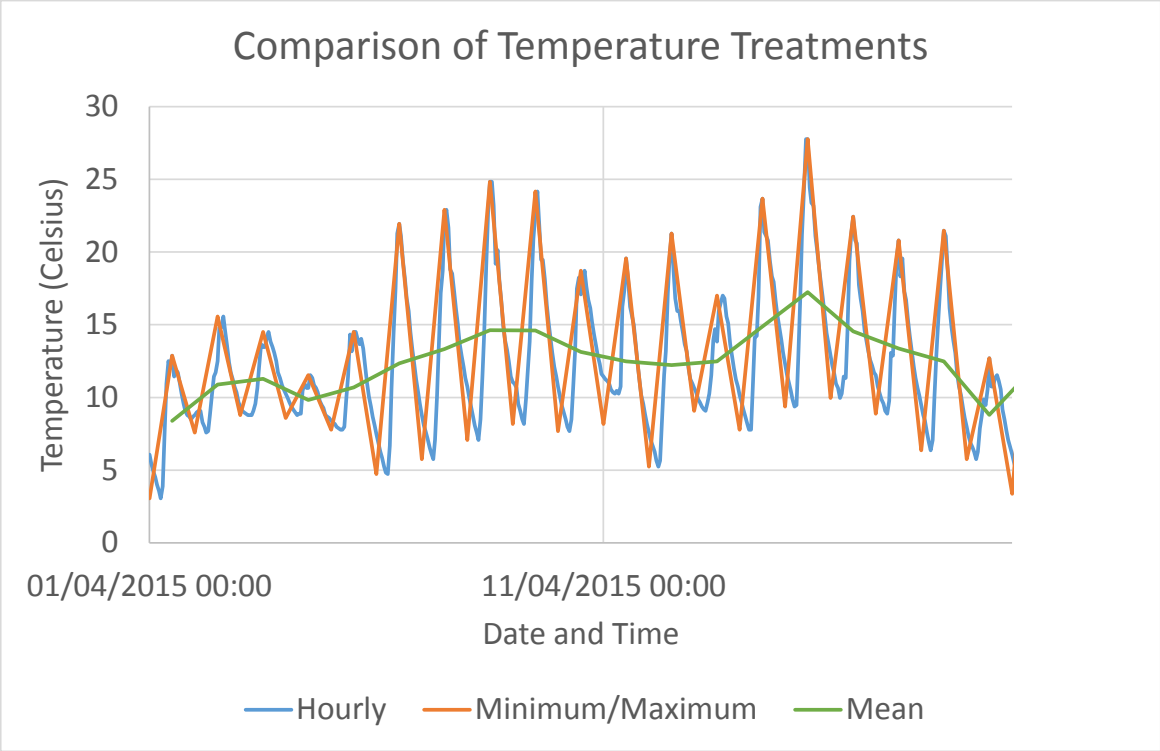

Figure 4.7: Comparison of temperature treatments: The three different water temperature treatments are plotted for the first twenty days of April - hourly values (blue), minimum/maximum values (orange) and mean daily values (green).

- **Minimum and maximum values -** Diurnal temperature variability was included by linearly interpolating between minimum and maximum daily temperature values, which were assumed to occur at midnight and noon.
- **Hourly temperature values -** Hourly temperature measurements were used, with linear interpolation between each measurement.

The effects of including or excluding diurnal temperature variability were investigated by comparing the observed abundance trends from the model with the trends from the field data. I present results using temperatures from both butt 1 and butt 4 separately because butt 1 was in direct sunlight and therefore reached temperatures potentially damaging for *Cx. pipiens*, unlike butt 4 which was cooler. Simulations accounting for the range of temperatures across the four water butts by splitting the immature equations to account for the four temperature profiles were not run because mosquitoes were observed to congregate in butt 4 beyond the spring abundance peak (Figure 3.4a-3.4d).

4.3.6 Comparing model predictions with data

A full description of the data collection procedure and fieldwork findings is given in Chapter 3. References to the updated model in future sections refer to the model described in this Section (Section 4.3). Simulations using this updated model were run using a set of baseline parameter values, listed in Table 4.1, unless explicitly stated otherwise. In the updated model, all vital rates related to processes ongoing in the immature aquatic stages (eggs, larvae and pupae) were estimated using hourly water temperature values from butt 4, unless otherwise stated. I used temperature recordings from butt 4 and compared updated model output for the pre-adult life stages to this butt, since other water butts did not contain sufficient numbers of individuals to inform seasonal patterns of abundance. Adult processes, such as development of the gonotrophic cycle, were governed by air temperature, for which I used recordings of the minimum and maximum daily temperature, unless otherwise stated.

Comparing model output to the collected data required estimation of both the usable volume of larval habitat in a water butt and the detection probability for larvae, pupae and adults, to allow scaling of the model output to the field data. The dipping set up is shown in Figure 4.8. It was estimated that 20% of the population in each water butt was sampled on each sampling occasion, given the following observations and assumptions:

1. Mosquito larvae were seen to use the outer 11cm of the 1.3m diameter water butts. This gave a usable surface area of 0.411m^2 per water butt.
2. Larvae were assumed to use the top 5cm of the water, giving a useful volume of 20 litres per butt.
3. The dipper was 11cm in diameter, meaning 4 dips gave a coverage of 17.67%, which was rounded up to 20% to account for the suction effect created by the dipper.

It was estimated that 0.5% of the adult population was caught by the light trap each night, based on the following assumptions:

1. A 1:1 sex ratio within the population (Vinogradova 2000), meaning that 50% of the total population could be included in the data because only females were recorded.
2. The gonotrophic cycle length was assumed to be 10 days, which corresponds to a temperature of $17.4\,^{\circ}\text{C}$ (Hartley et al. 2012), which was a commonly observed air temperature at the field site (Figure 4.4). This left only 10% of females host-seeking on a given night.

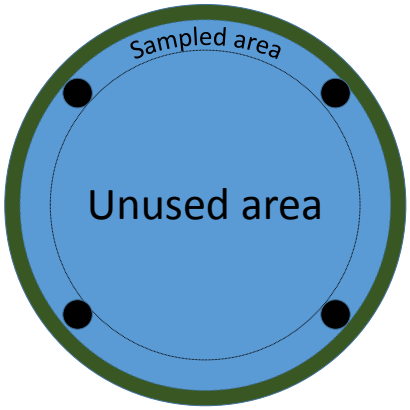

Figure 4.8: Dipping Coverage: A diagram showing the estimated coverage of the mosquito habitat in the water butt by the dipping procedure discussed in Section 4.3.6). The black circles show example dipping sites.

3. Traps were assumed to catch 10% of all active mosquitoes on a given night (Silva et al. 2005).

4.4 Results

In this section I present a comparison of the updated model, using the baseline parameter values in Table 4.1, and the Chapter 2 model, using the parameter values in Table 2.1, alongside the fieldwork data collected (Figure 4.9). After making a general comparison of these models I discuss the effects of varying the new parameters of the updated model.

4.4.1 Comparison of updated and previous models

A very distinctive feature of the empirical field data is that there is a clear double-peak in both egg and larval numbers, with the first peak in late-April and the second in June. The updated model captures the presence of the double peak in egg numbers, whilst the Chapter 2 model shows a steady increase in numbers throughout the season (Figure 4.9). The ability of the updated model to capture this double peak stems from the inclusion of the extra post-diapause mortality rate, which will be discussed fully in Section 4.4.2. However, whilst the updated model predicts the start of the initial peak well, the end of the first peak is predicted to occur later in the model than in the data. The temporal correlation between the updated model and the egg data across the season (Pearson's r_p = 0.31) is higher than that observed

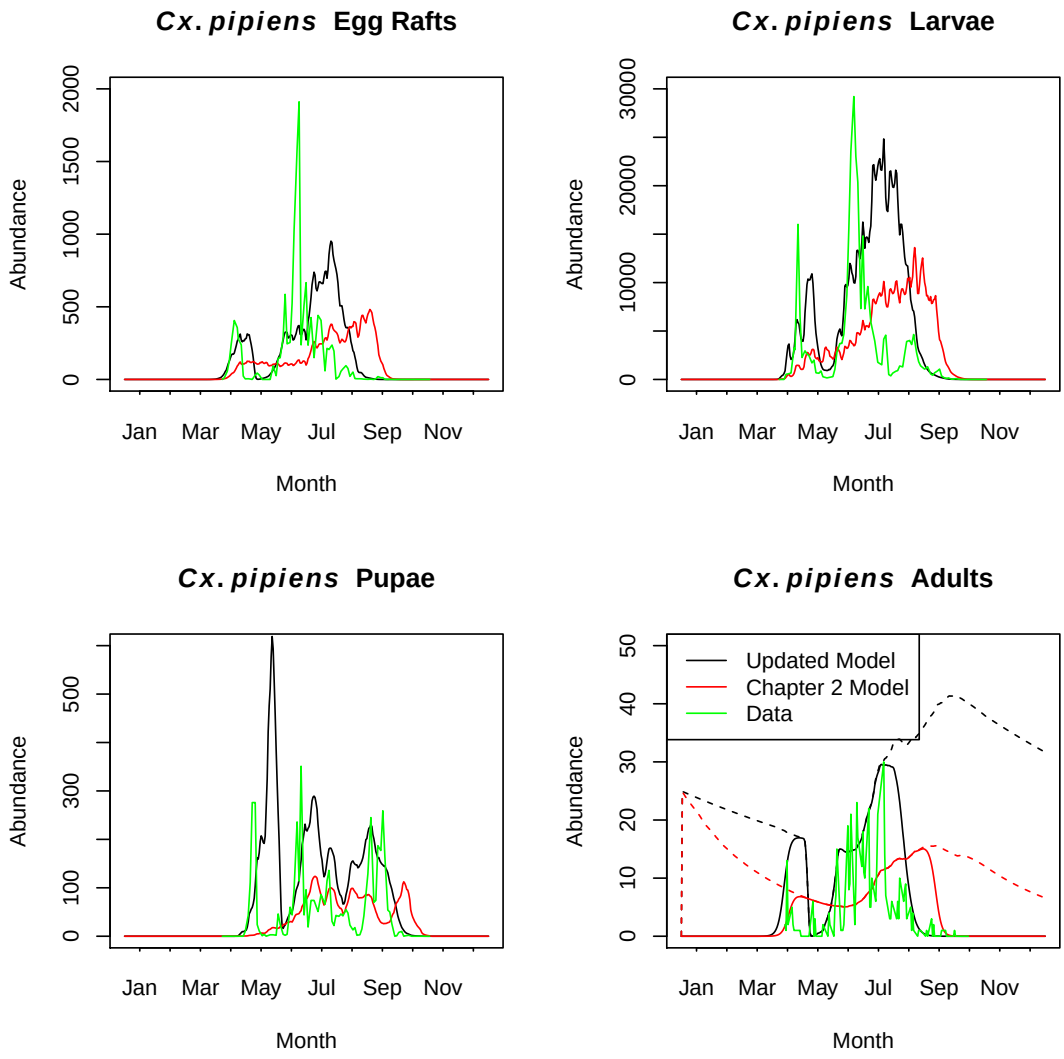

Figure 4.9: Model fit to data: The updated model predictions (black), Chapter 2 model predictions (red) and observed (green) abundance of each life stage are shown. All model parameters for the updated model (black) are defined in Table 4.1 and parameters for the Chapter 2 model are defined in 2.1. Hourly water temperature values for butt 4 were used alongside minimum and maximum daily air temperature values in both models. In the adult plot the dashed line shows all adults and the solid line excludes those in diapause.

under the Chapter 2 model (r_p = -0.04).

The updated model also predicts a longer summer peak than was observed in the data, with high egg and larval abundance continuing on throughout July, until mid-to-late August (Figure 4.9). However, the temporal correlation between the updated model and the larval data (r_p = 0.33) is still better than that observed using the Chapter 2 model (r_p = 0.07). The prolonged summer peak suggests that the egg-laying rate was lower than predicted by the model through this time period.

In the pupal data there are three clear peaks occurring in early May, late June and early September (Figure 4.9). As discussed in Section 3.3.1, this third peak in pupae is believed to stem from a release in density-dependence, causing improved survival at the end of the season. These three pupal peaks are replicated in the updated model predictions (r_p = 0.14) but not in the Chapter 2 model predictions (r_p = 0.08), though the temporal correlation between the updated model and data only shows slight improvement. The length of the first two pupal peaks is slightly greater in the fieldwork data than in the updated model predictions (Figure 4.9).

Figure 4.9 shows that the updated model fits the adult data well, with the timings of exit from and entry to diapause matching up with the data, giving good temporal correlation across the season (r_p = 0.57). The Chapter 2 model does not capture the season termination point well, with the population remaining active throughout late August (r_p = 0.15). Further, the season start in the Chapter 2 model appears to be too late, leading to a slower increase in the egg population. Again, there is a clear double peak in the field observed adult abundance, which is captured by incorporating the high post-diapause death rate in the updated model, but not captured in the previous model. The data shows substantially more daily variability in adult abundance than either model, however this is because the catch probability of the sampling method will be strongly influenced by weather conditions, whereas the model assumes a fixed catch probability. Given the observed data and the model predictions, the updated model correctly predicts that the bulk of female mosquito biting activity would occur in June and July, with a low biting rate in April, May and August.

4.4.2 Diapause dynamics

Mosquito overwinter survival effects on abundance patterns

Given the increase to the length of the overwinter season, the updated model was run for a range of updated values of b_{da}, which denotes the minimum adult death rate (other parameter values are the baseline values in Table 4.1). This allowed the effects of variation in overwinter survival on our ability to capture observed abundance patterns to be understood. Simulations were run for values of b_{da} from 0.003 to 0.01, corresponding to overwinter survival from 50% to 10%, consistent with the range of values in the literature (Bailey et al. 1982; Sulaiman and Service 1983; Onyeka and Boreham 1987). The field data is shown alongside the model simulations for reference (Figure 4.10). With only one year of capture data it is not possible to make accurate predictions about overwinter survival at the field site. Consequently, only comparisons between the parameter sets are discussed. I carried out simulations at regular intervals across the full range of parameter values. In each case I illustrate three model runs, corresponding to the minimum, central and maximum values, rather than using summary statistics, as in Chapter 2, as the other values within the range show consistent results. This approach better displays the abundance patterns throughout the season.

The results in Figure 4.10 show that increasing overwinter survival leads to increases in the abundance of all life stages, with the peak active adult population size increasing by approximately one third from low (10%) to high (50%) overwinter survival. In pupae, this increased abundance is most clearly seen in the initial population peak, whereas in the other stages the population is increased throughout the year. When overwinter survival is high, increases in the adult population upon diapause emergence lead to high egg and larval abundances early in the year. The inclusion of seasonally varying predation (Figure 4.10) means that density-dependent larval mortality is low at this time, so pupal numbers increase substantially. Later in the year, higher predation means that increases in the larval population are offset by increases in density-dependent mortality. Therefore, the predicted number of pupae does not increase late in the season. Nonetheless, increased spring population size, due to increased overwinter survival, causes an increase in the adult population throughout the entire year.

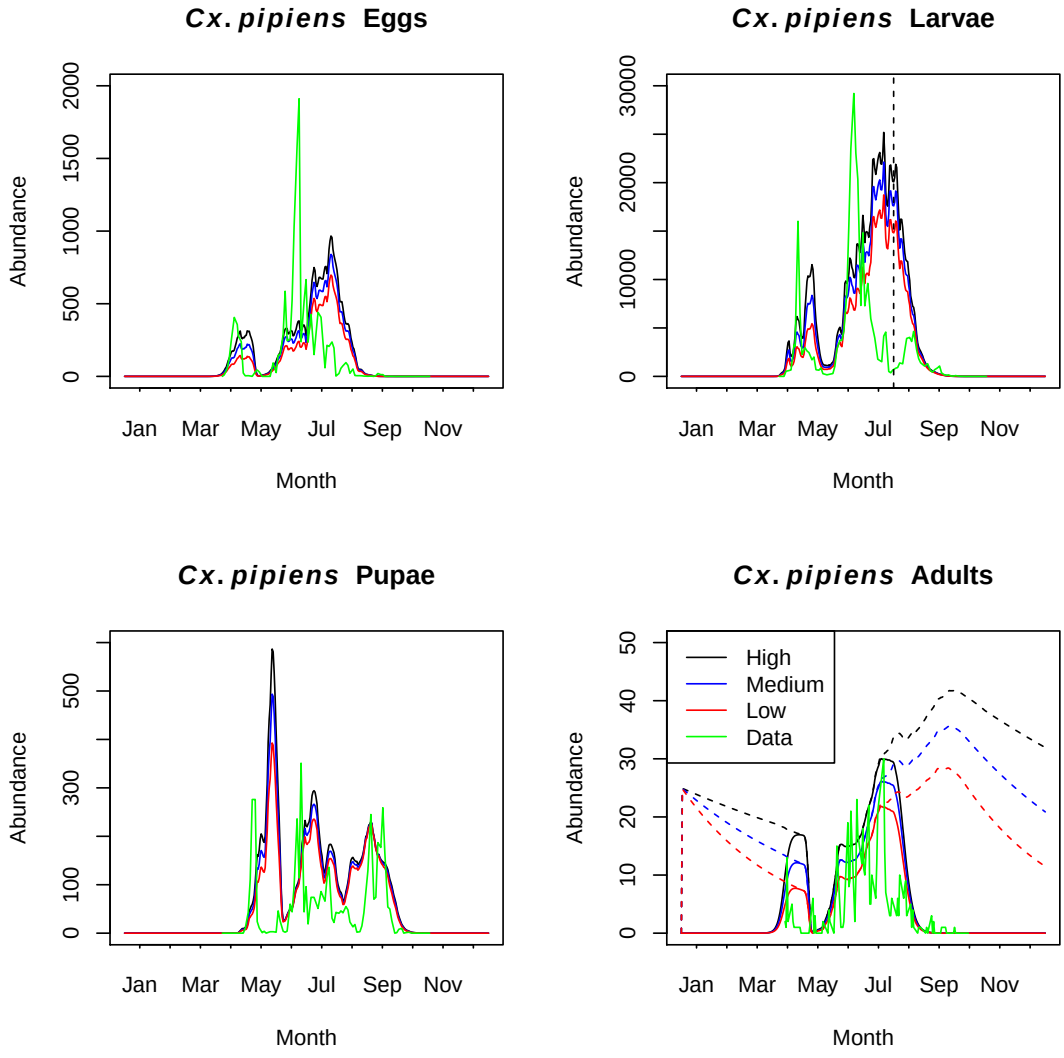

Figure 4.10: Overwinter survival impacts: A comparison of the updated model predictions for abundance of each life stage for three different values of b_{da} is shown. High (b_{da} = 0.003), medium (b_{da} = 0.006) and low (b_{da} = 0.01) refer to the minimum adult survival rates. The high survival scenario is the baseline value for b_{da} given in Table 4.1. Field collected air temperature is used, alongside water temperatures from butt 4. In the adult plot the dashed line shows all adults and the solid line excludes those in diapause. The dotted line in the larval plot shows the timing at which the peak predator-to-prey ratio occurs.

Impacts of post-diapause mortality on seasonal abundance dynamics and transmission season

Figure 4.11 demonstrates the updated model simulated for three different values of Γ, which determines the strength of the post-oviposition mortality rate (Equation 4.10) (other parameter values are the baseline values in Table 4.1). The double-peak in spring and summer across all life stages, shown in the fieldwork data, is only captured when including this post-diapause mortality (Figure 4.11, $\Gamma = 8, 16$). If post-diapause mortality is removed by setting Γ to zero then environmental conditions alone do not provide the drop in mosquito abundance observed. This provides support for the hypothesis of high post-diapause mortality of aged females. Figure 4.11 shows that inclusion of this death rate has a large impact on population size, suggesting an approximately 40% decrease in the peak annual abundance of active adults when this death rate is included, such that complete mortality of the adult stage occurs. Once post-diapause adult mortality is included, increasing the strength of the mortality rate beyond the arbitrary chosen value ($\Gamma = 8$) has little effect on population dynamics (Figure 4.11). Decreasing Γ leads to a gradual transition between the black line and the red (Figure 4.11). However, given the assumption made that the added mortality rate acts on all post-diapause adult females, there is no rationale for choosing a death rate which will result in mortality of only some proportion of the surviving population.

$\mathcal{D}$ determines the proportion of adults which exit diapause and lay a full egg raft before the post-diapause mortality occurs (Equation 4.10). The relatively synchronous exit of adults from diapause means that choosing values of $\mathcal{D}$ corresponding to 70%-90% of the population becoming active and laying an egg raft only varies the timing of the post-diapause mortality by 5 days. Consquently, simulations changing the parameter $\mathcal{D}$ within a sensible range are not shown, as the impact on results is negligible.

The parameter σ^2 determines the duration over which the post-diapause mortality acted (Equation 4.10). Values larger than the baseline ($\sigma^2 = 4$) were not considered, as this led to a wider period of high mortality than observed in Figure 4.11, resulting in mortality of emergent adults, which is unrealistic. Decreasing σ^2, causing a delay in the onset of the high mortality period, led to greater overestimation of the duration of the spring population peak by the updated model.

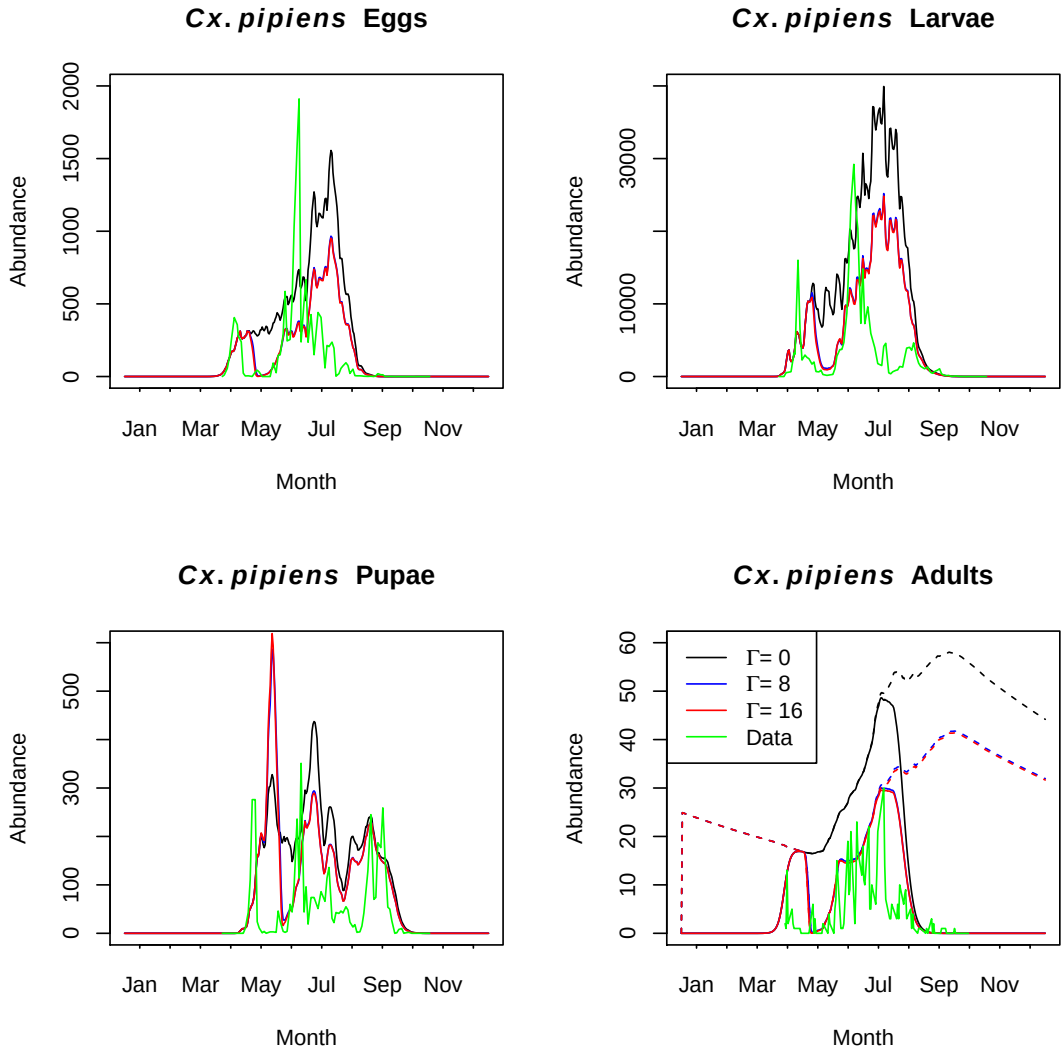

Figure 4.11: Impact of post-diapause mortality rate: A comparison of the updated model predictions for abundance of each life stage for three different values of Γ, which controls the strength of the post-diapause adult mortality effect. $\Gamma = 8$ is the baseline value used in other model simulations. Field collected air temperature is used, alongside water temperatures from butt 4. In the adult plot the dashed line shows all adults and the solid line excludes those in diapause.

4.4.3 Effects of variation in predator abundance and timing

Variations in the relative sizes of larval and predator populations may have substantial implications on larval mortality and consequently on abundance patterns across all life stages. Simulations simultaneously varying all combinations of two of the three predation parameters in the updated model (υ, χ and r) at small intervals (1,0.1 and 0.00005 respectively) across the full range were carried out. As previously, results are presented for the minimum, central and maximum values of the parameter range, for each parameter, as further results within the studied range were consistent with those shown. I compare each of the scenarios incorporating variable predator populations against a constant where predator density was assumed to be a constant proportion of larval density, with no additional seasonality, as in Chapter 2.

Synchronicity between predator and mosquito populations

The timing of the peak predator-to-prey ratio, determined by υ, corresponds to the 1st of August in the updated model. To explore the sensitivity of abundance patterns to the timing of predation, I then varied this timing between the 1st of July and 10th August (Figure 4.12). All other parameter values were as in Table 4.1. The red line, showing the latest peak in predator-to-prey ratio, appears to overestimate pupal abundance early in the year, and consequently abundance of the other stages from late May onwards. The simulations where the maximum predator-to-prey ratio occurs in early or late July ($\upsilon = 0, 20$), or where predator-to-prey ratio does not vary seasonally, show similar abundance profiles. Figure 4.12 shows that moving the effects of predation later in the year leads to very large abundance increases in the egg and larval stages from early summer until autumn. This is because survival is significantly improved in the initial generation, as can be seen by the large differences in the initial pupal peaks. Increased numbers of pupae lead to more adults by the end of May, which then proceed to lay more eggs. This causes the large number of eggs and larvae throughout the months of June and July. The late peak in predation results in a fivefold increase in the maximum abundance of host-seeking adults when compared to the earliest predation peak.

Shifting the predation curve in the updated model earlier in the year increases the predation experienced by the spring population peak (Figure 4.13). This leads to a smaller pupal peak in the spring and a larger pupal peak at the end of the year (Figure 4.12). This late pupal peak can have profound influences on the diapausing mosquito population. For example, the maximum active adult abundance under early predation (Figure 4.12, black line) is about two

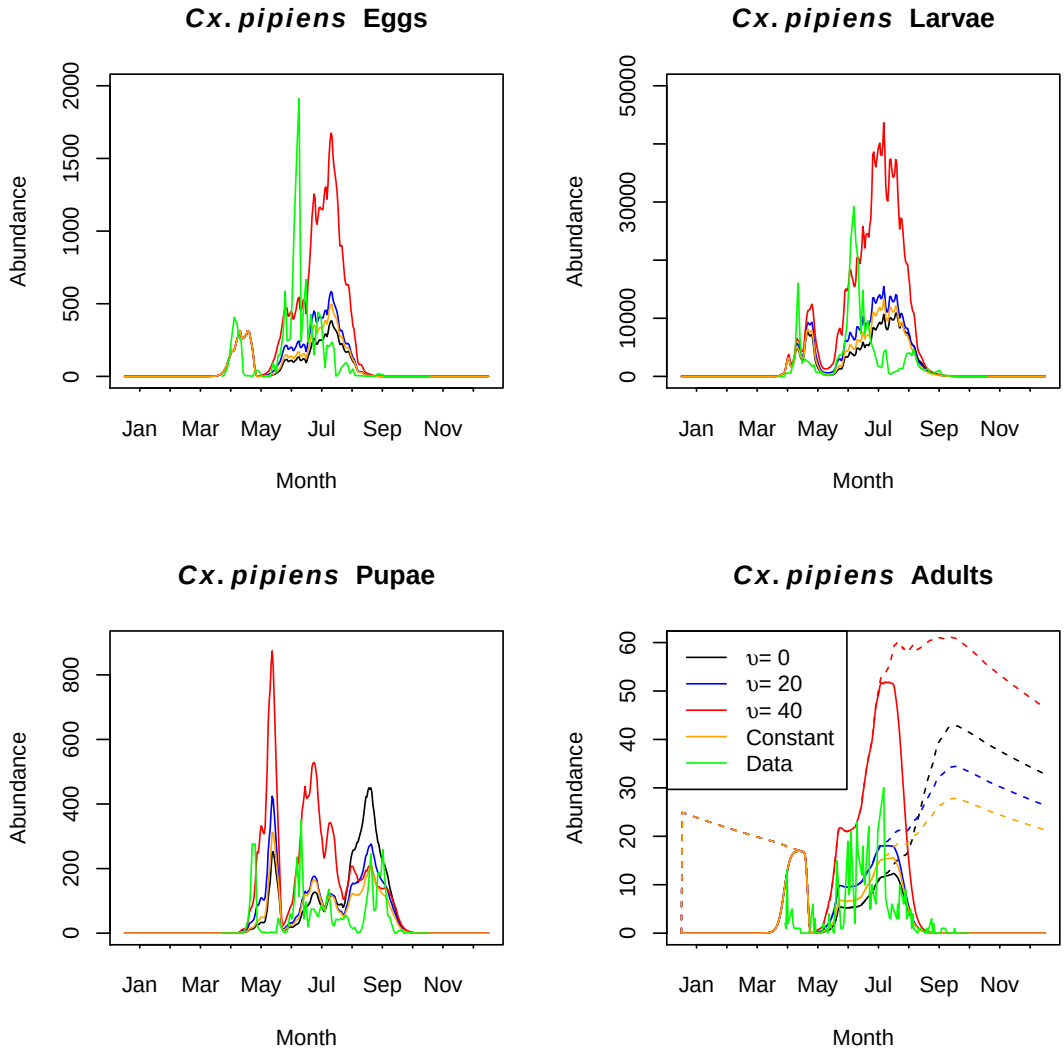

Figure 4.12: Predation timing impacts: A comparison of the updated model predictions for abundance of each life stage for three different values of υ, which determines of the timing of the peak value in the seasonal predation function: υ = 0 gives a 1st July peak, υ = 20 gives a 21st July peak and υ = 40 gives a 10th August peak. The “constant" line shows model results with no seasonal variation in predators. In the baseline updated model υ = 31, corresponding to the 1st August. Field collected air temperature is used, alongside water temperatures from butt 4. In the adult plot the dashed line shows all adults and the solid line excludes those in diapause.

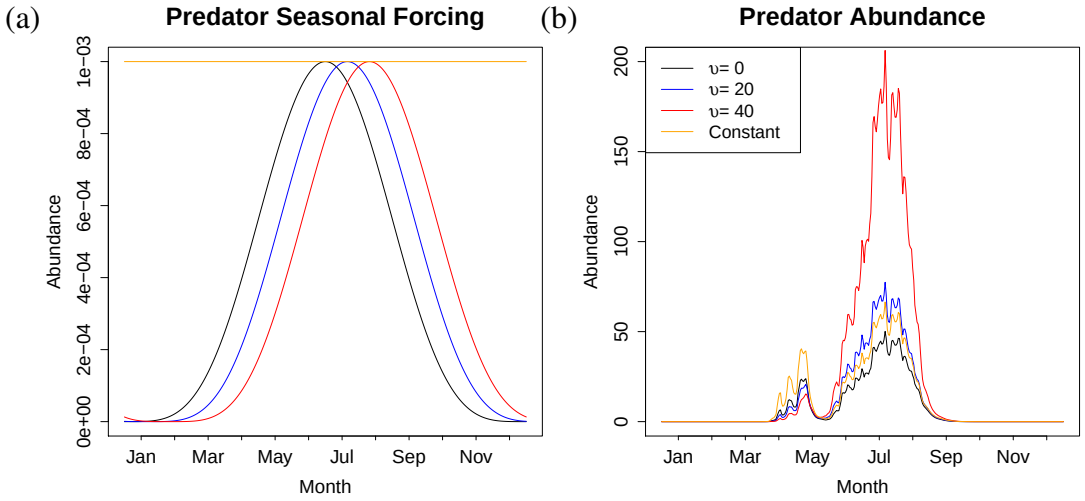

Figure 4.13: Predator seasonal abundance: (a) A comparison of the predator to prey ratios, $\mathcal{R}(t)$, (Equation 4.11) throughout the year for different values of υ, which determines the time at which $\mathcal{R}(t)$ is maximised: υ = 0 gives a 1st July peak, υ = 20 gives a 21st July peak and υ = 40 gives a 10th August peak. The "constant" line shows the case where $\mathcal{R}(t) = r$ and there is no seasonal forcing. (b) shows a comparison of the predator abundance throughout the year for the same three values of υ and the "constant" case.

thirds of the maximum active abundance under mid-season predation (Figure 4.12, blue line). However, under early predation, the diapausing population is approximately 25% larger than that under mid-season predation (Figure 4.12). If predator numbers are very high in the early part of the season and then decline, possibly in response to reduced numbers of prey as in classical systems, then we may see a very large overwintering mosquito population. This could lead to high mosquito abundance in the early part of the following year, with the implications discussed in Section 4.4.2.

The duration over which the period of high predation acts, determined by the sharpness, was also examined using the updated model. I altered the sharpness of the predation function by changing the parameter, χ, which denotes the power to which the sinusoidal function is raised (Equation 4.12 and Figure 4.6). Decreasing the period over which predation acts led to increases in the population size early in the year (Figure 4.14), similar to those observed when we shifted the predation peak later in the year (Figure 4.12). Results are similar because increasing the sharpness delays the onset of the higher predation period, decreasing predator numbers during the initial population peak (Figure 4.13). Increasing sharpness has little effect on abundance later in the season because adults start entering diapause before the effects of decreased predation are felt. Consequently, simulations with high sharpness show increased larval survival in the initial generation. This translates to increases in the adult population in late May and therefore increases in eggs and larvae following this.

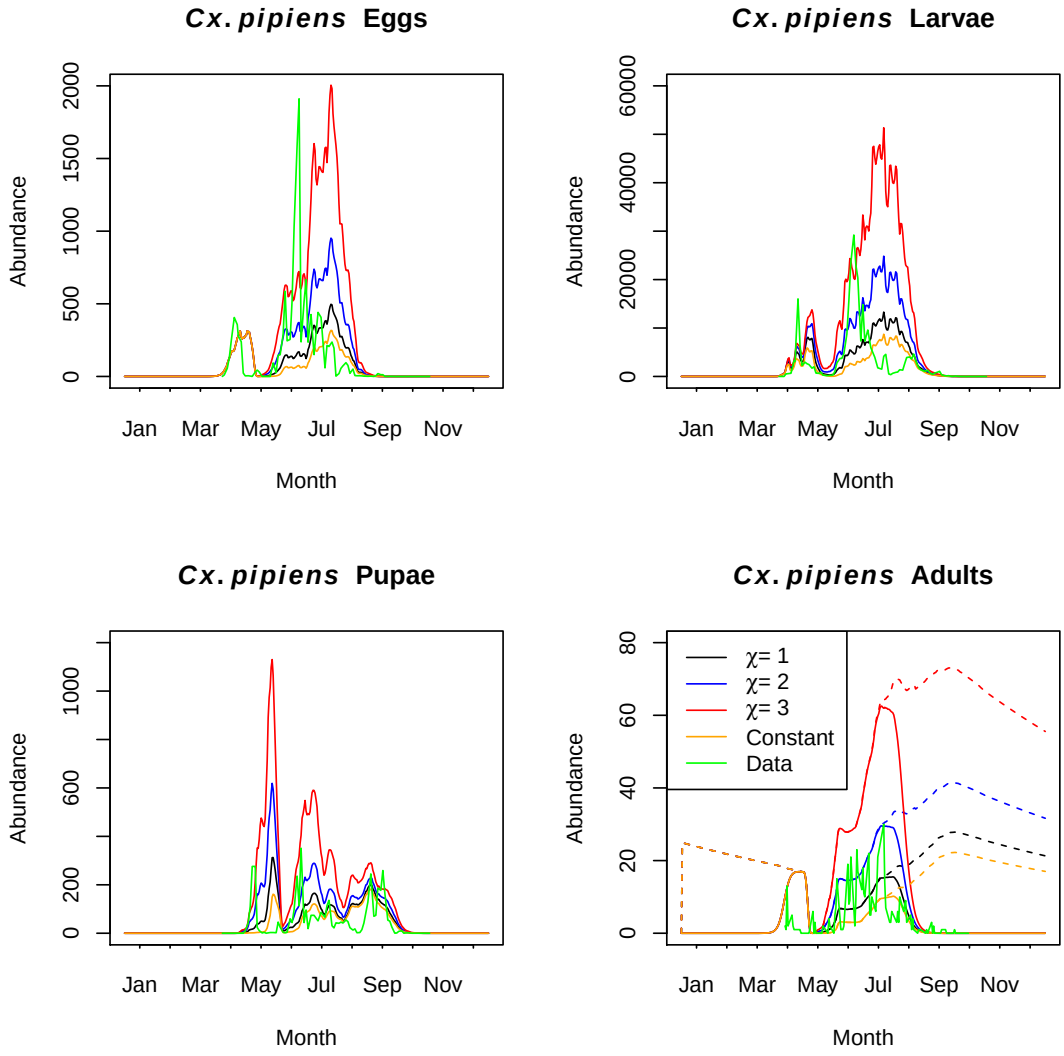

Figure 4.14: Effect of predation sharpness: A comparison of the updated model predictions for abundance of each life stage for three different values of χ, which determines of the sharpness of the seasonal predation function. In the baseline updated model $\chi = 2$. The “constant" line shows model results with seasonal variation in predators removed. Field collected air temperature is used, alongside water temperatures from butt 4. In the adult plot the dashed line shows all adults and the solid line excludes those in diapause.

Predation strength impacts

Increasing the number of predators per larva, r_{max}, in the updated model, led to decreases in the abundance of each life stage, as expected (Figure 4.15). The low predation case (black line) appears to overestimate abundance and the reduced density-dependence causes the final two pupal abundance peaks to merge. The simulation with no seasonality in predation (orange line) does not capture the relative sizes of peaks in abundance well, as the mid-season abundance is smaller than the spring abundance.

As the strength of predation increases the second population peak is substantially reduced in size, which leads to more pronounced peaks in abundance of the pupal stage than observed under low predation. As predation has been assumed to exhibit sinusoidal seasonal forcing, altering the strength of predation has much larger implications for the second peak in population abundance than for the early season peak. Upon removing the seasonality in predation, it can be seen that the abundance of all mosquito life stages decreases throughout the year, as this is equivalent to assuming the maximum value of r_{max} at all times in the year (Equation 4.12).

4.4.4 Effects of temperature treatment

The updated model was run using the baseline parameter values (Table 4.1) for a range of different temperature input data scenarios, to understand the impacts of both temperature data temporal resolution and using air temperature as a proxy for water temperature on abundance predictions.

Impacts of temporal resolution of temperature data

Comparing predictions from the updated model using hourly, minimum/maximum and mean daily water temperature values for butt 4, Figure 4.16 shows an approximate 30% increase in peak active adult abundance when using mean daily temperatures, as opposed to minimum/maximum or hourly temperatures. Using mean daily water temperatures leads to an overestimation of abundance, when compared with the field data. Simulations using mean temperatures, show a much larger initial pupal peak than those simulations at a higher temporal resolution. This larger pupal peak leads to a greater number of adults later in the season, causing increased egg and pupal numbers. These increases to egg and larval numbers after the initial peak are less strongly reflected in pupal numbers due to the increased density-dependent predation. There are no substantial differences between the abundance patterns

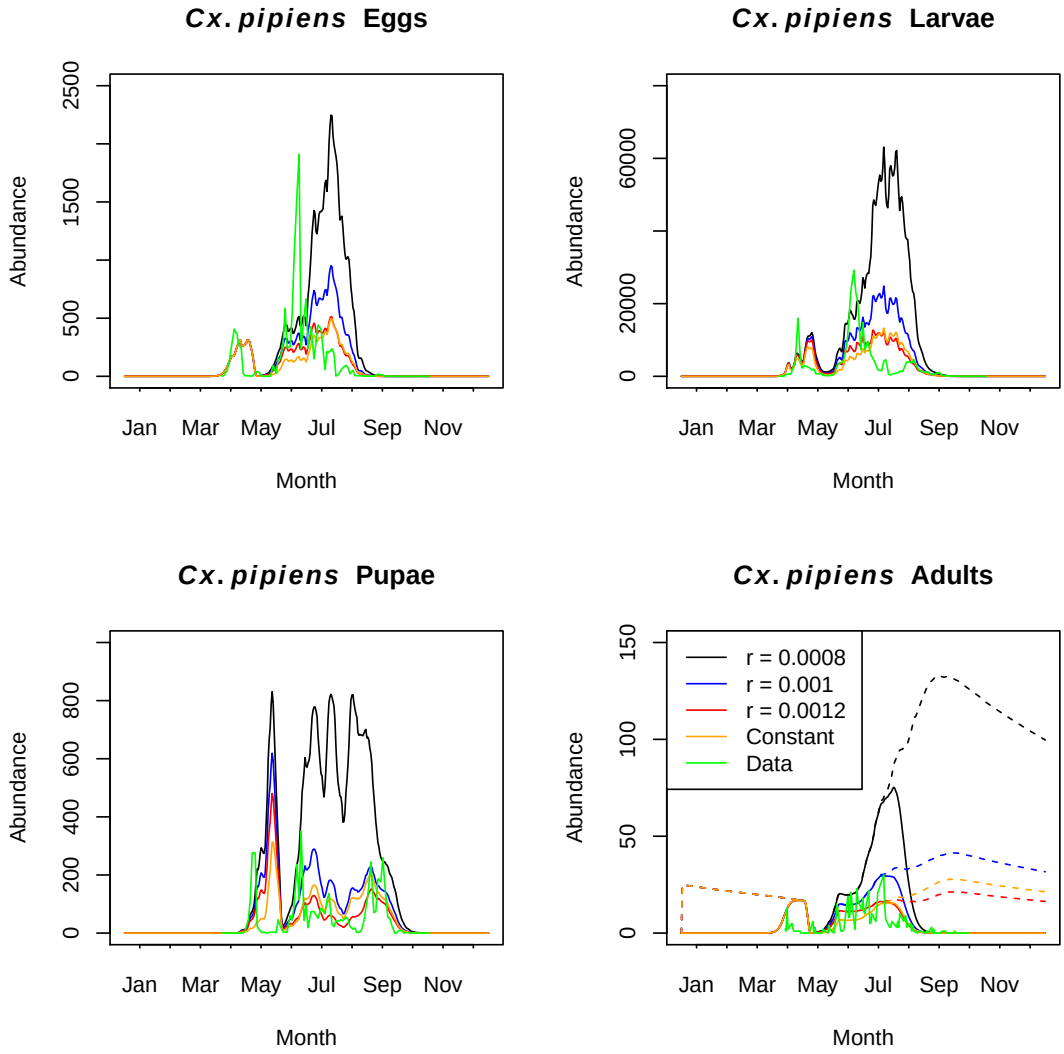

Figure 4.15: Effect of predation strength: A comparison of the updated model predictions for abundance of each life stage for three different values of r_{max}, which denotes the number of predators present per larva, is shown. r was varied in the range 0.0008-0.0012, as this was the range for which predation was sufficient to regulate the population without leading to extinction. In all other simulations the updated model uses a value of r_{max} = 0.001. The “constant" line shows model results with seasonal variation in predators removed. Field collected air temperature is used, alongside water temperatures from butt 4. In the adult plot the dashed line shows all adults and the solid line excludes those in diapause.

observed using minimum/maximum or hourly measures, as the small difference between the two temperature profiles results in a negligible impact on vital rates in this case.

The updated model was also run using the hourly water temperature values observed for butt 1 to understand if the higher temperatures observed explained the low numbers of larvae present. Figure 4.17 shows that for butt 1 there were substantial differences in abundance estimates under the three different temporal resolution temperature datasets. Using mean daily temperatures gave an approximate fourfold increase in the active adult peak abundance when compared to using minimums and maximums. Using daily minimum and maximum temperature, in turn predicted an approximately 50% increase in peak abundance when compared to using hourly temperature measurements. The predicted presence of a large mosquito population throughout the active season shows that the higher temperatures in butt 1 were not high enough to induce a sufficiently high immature death rate to explain the disappearance of *Cx. pipiens* from butts 1-3. As such, the strong preference for butt 4 seen in the data is more likely to be due to higher food availability than to avoidance of warmer habitats.

When investigating the effects of temporal resolution of air temperature (using butt 4 water temperatures for the immature stages), the differences in model predictions using minimum/-maximum and mean daily temperature were small for all life stages (Figure 4.18) with only slightly higher abundance predictions when using mean temperatures ($< 1\%$ difference in peak active adult abundance). Interestingly, Figure 4.4 (b) shows that diurnal temperature variability is often larger in air temperature than in butt 4 water temperature. However, exclusion of diurnal temperature variability in butt 4 led to the predicted peak in the active adult mosquito population doubling in size (Figure 4.16).

Consequences of using air temperature as a proxy for water temperature

Using air temperature as a proxy for water temperature resulted in population extinction under the updated model, strongly contrasting with the field observations and model predictions when water temperature was included (Figure 4.19 (a)). Extinction occurs because water temperatures were consistently higher than air temperatures, particularly in the early months of April and May (Figure 4.4 (a)). This led to shorter development times and higher survival when incorporating water temperature than in the air-temperature-only model (Figure 4.20). In the air-temperature-only model, the first batch of eggs laid after winter were unable to complete development and the population became extinct by the beginning of May.

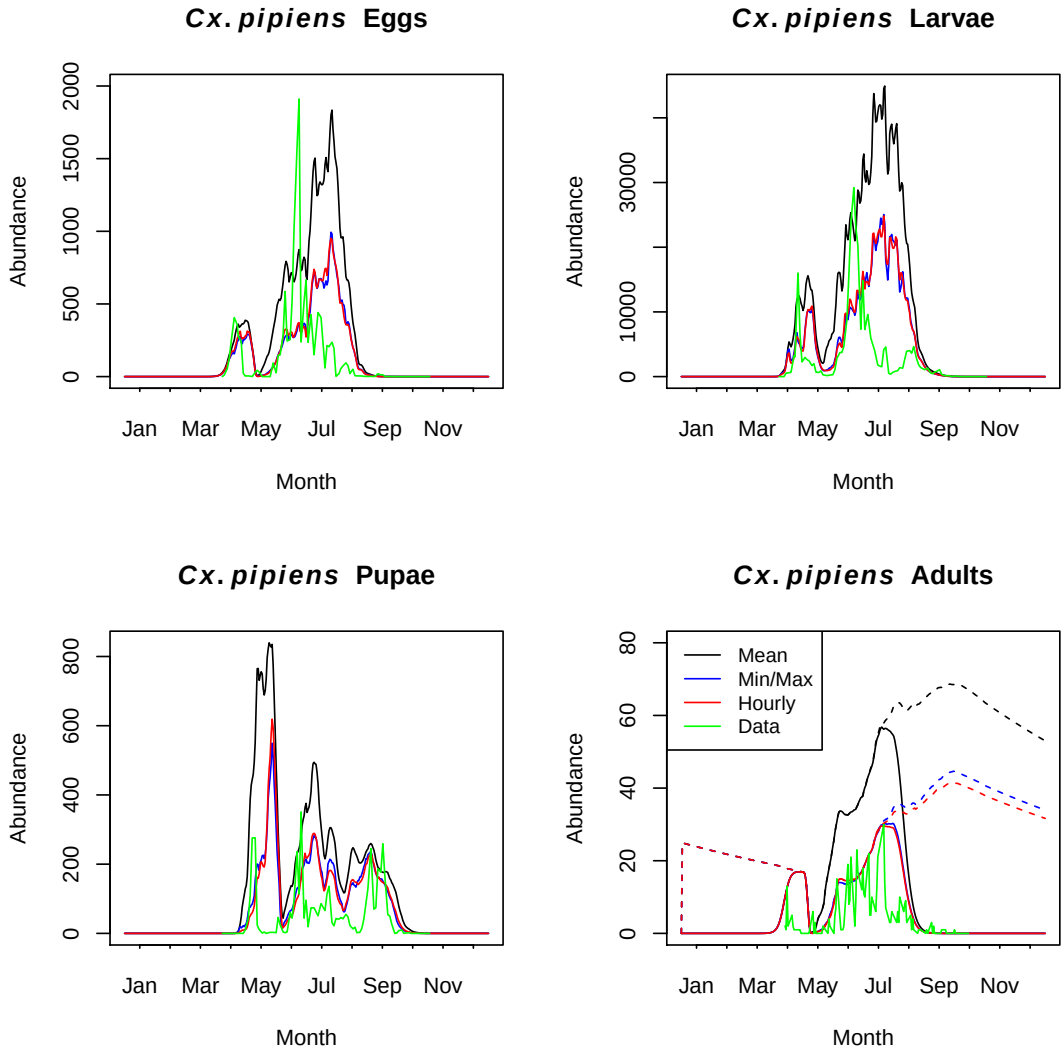

Figure 4.16: Effects of water temperature temporal resolution in shade: A comparison of the updated model predictions for abundance of each life stage in butt 4 using mean daily water temperature (black), minimum and maximum daily water temperature (blue) and hourly temperatures (red). In the adult plot the dashed line shows all adults and the solid line excludes those in diapause.

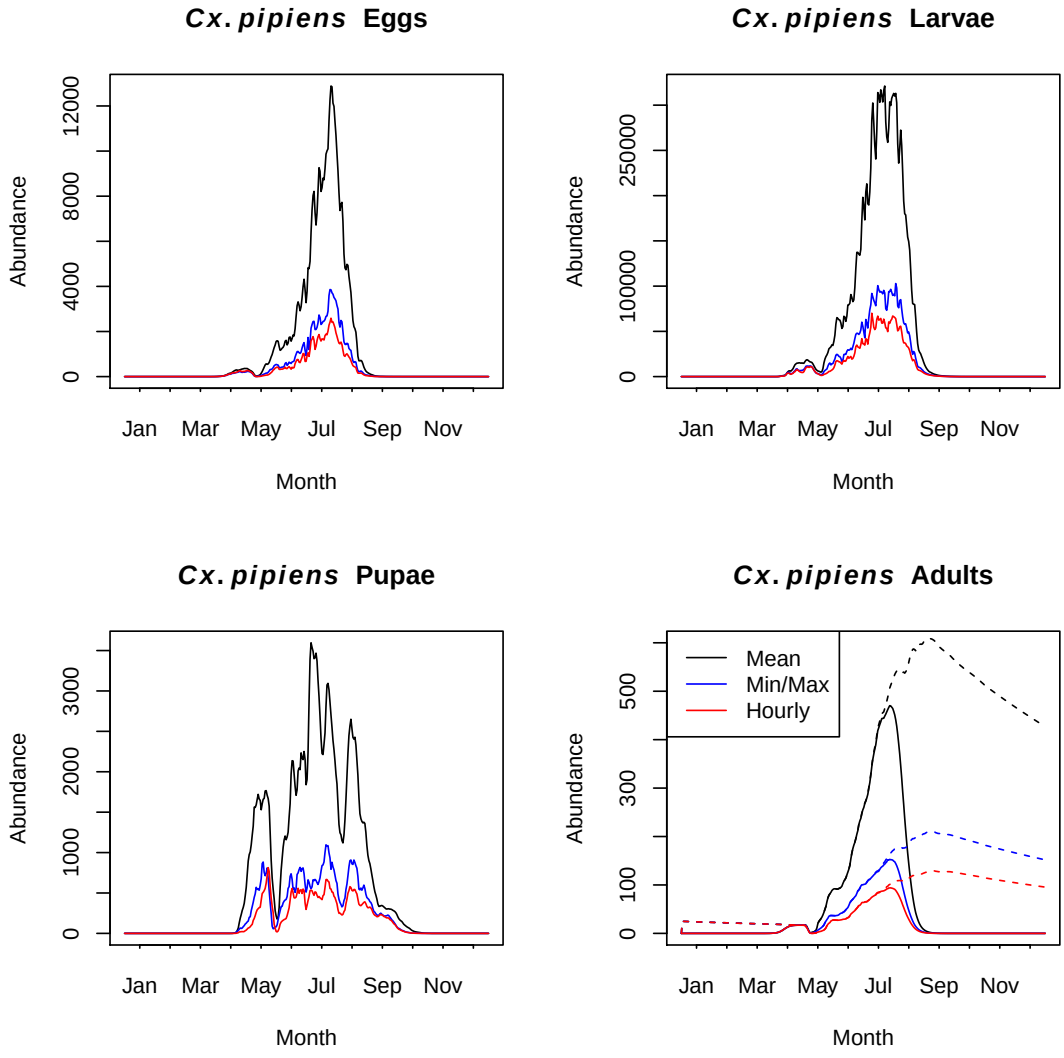

Figure 4.17: Effects of water temperature temporal resolution in sunlight: A comparison of the updated model predictions for abundance of each life stage in butt 1 using mean daily water temperature (black), minimum and maximum daily water temperature (blue) and hourly temperatures (red). In the adult plot the dashed line shows all adults and the solid line excludes those in diapause.

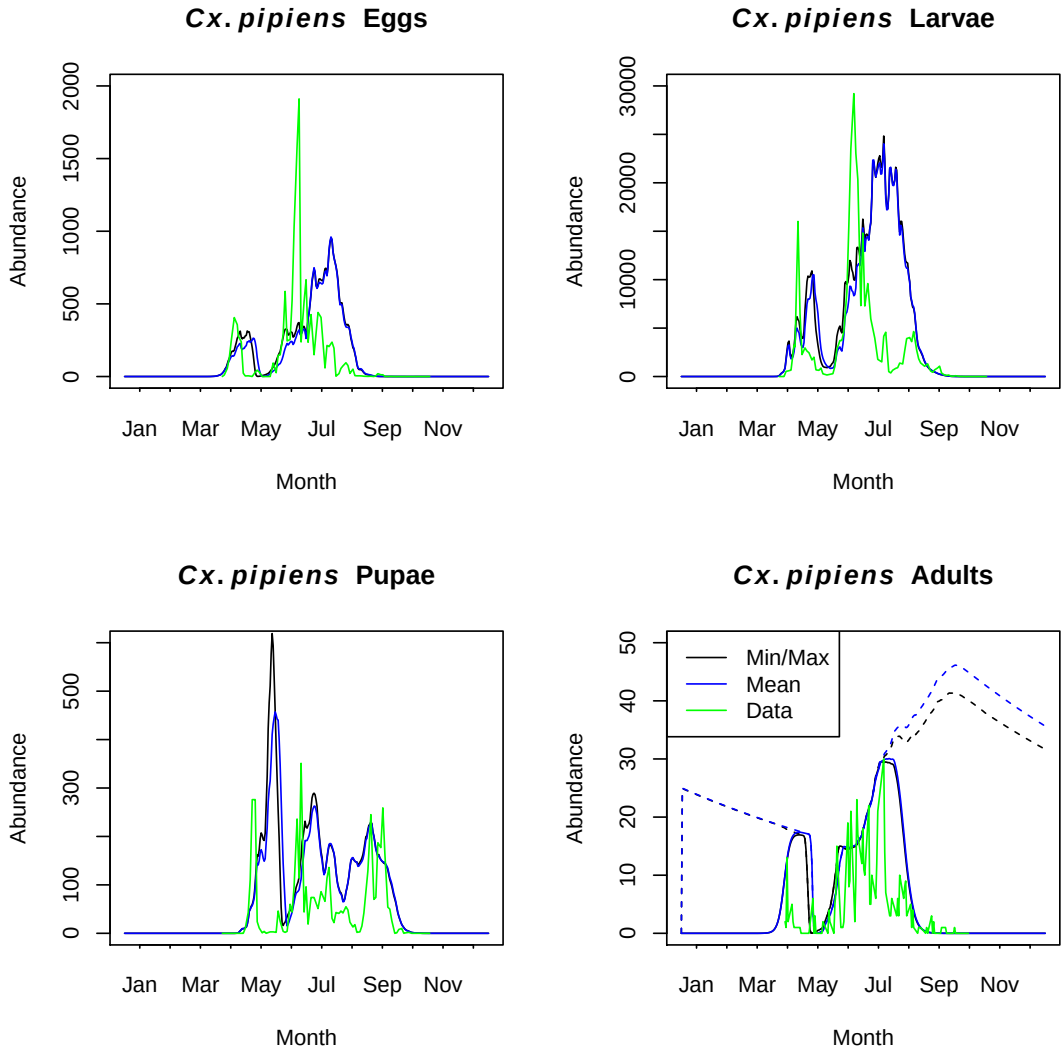

Figure 4.18: Effects of air temperature temporal resolution: A comparison of the updated model predictions for abundance of each life stage using mean daily air temperature (blue) and minimum/-maximum daily air temperature (black). The water hourly temperature values from butt 4 were used for the immature life stages. In the adult plot the dashed line shows all adults and the solid line excludes those in diapause.

Note that larval survival only increases in the air-temperature-only model after the larval population has become extinct (Figure 4.19), causing a release of density-dependence (Figure 4.20).

4.4.5 Mosquito overwinter survival effects on pathogen persistence

The number of females which survive the winter period will have a large impact on the probability of pathogen persistence between seasons (see Section 1.2.2). The possibility of pathogen persistence between seasons through vertical transmission will be strongly dependent on the minimum filial infection rate (MFIR), which gives the number of infected offspring produced per 1000 eggs laid by an infected parent. The MFIR values were calculated as

$$MFIR = \frac{1000}{A_F p_I}, \tag{4.13}$$

where A_F is the number of adult females at the end of winter and p_I is the prevalence of infection in the population. Using predictions for A_F obtained from the updated model, the required MFIR for pathogen persistence can be calculated. I used a value of $p_I = 1\%$ based on infection rates observed in field populations of *Cx. pipiens* in two different studies: Anderson et al. (2004) found 0.56% and 1.84% infection in two successive seasons in Connecticut and Hamer et al. (2009) found 1.8%, 0.74% and 0.81% infection in three successive seasons in Illinois. Running the updated model until stable annual population cycles had been reached (from year 2 of simulations onwards), the female population surviving to the end of winter, A_F, was 325, 992 and 2148 adult mosquitoes for minimum (10%), medium (30%) and maximum (50%) overwinter survival respectively. Given these abundance estimates and an estimate of 1% WNV prevalence, the required MFIR for disease persistence between seasons would be 307.2, 100.8 and 46.6, for minimum, medium and maximum survival respectively. The range of MFIR estimates from the literature (0.04-8.1) show that the field population was too small for virus persistence to be predicted for any of the tested overwinter survival scenarios and the climatic conditions experienced in 2015 at our study site.

If the prevalence of WNV in the population were to increase to 5.8% in the high survival scenario, then persistence would be expected at an MFIR of 8.1. Infection prevalences as high as 20.8% have been observed in *Cx. pipiens* field populations (Savage et al. 2006). In

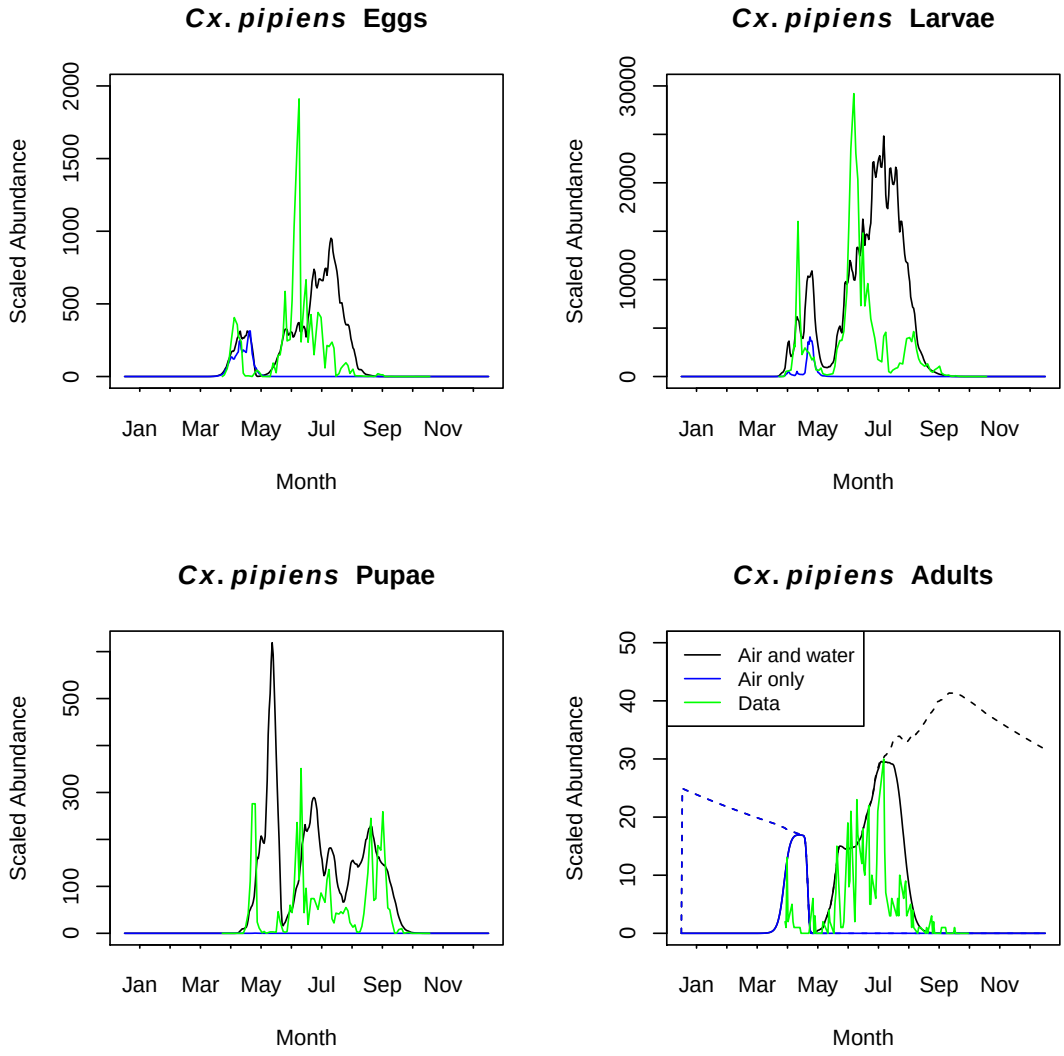

Figure 4.19: Effects of approximating water temperature using air temperature: A comparison of the updated model abundance predictions for each life stage using hourly water temperature values and daily minimum and maximum air temperature values (black line) and using only the daily minimum and maximum air temperature values (blue line). In the adult plot the dashed line shows all adults and the solid line excludes those in diapause.

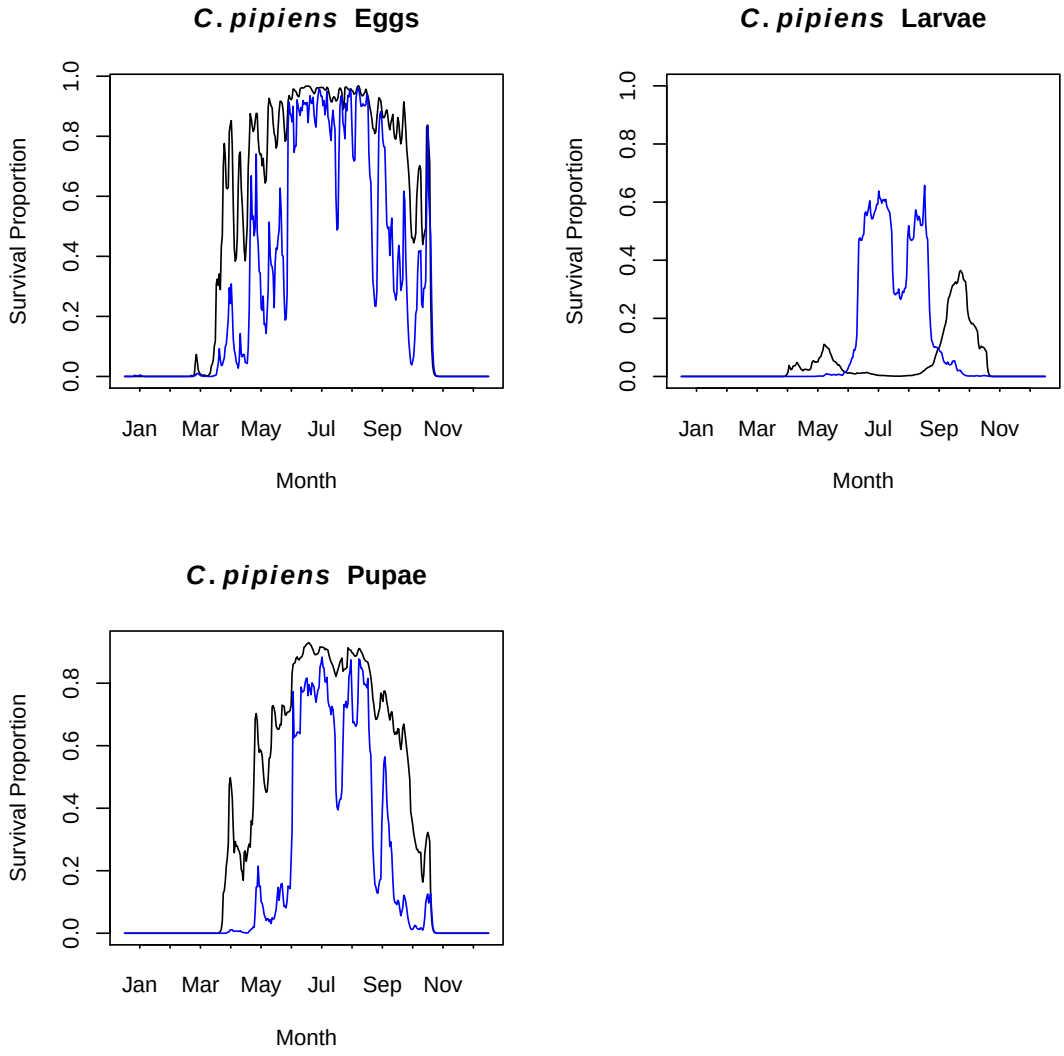

Figure 4.20: Effects of approximating water temperature using air temperature: A comparison of the updated model survival predictions for each life stage using hourly water temperature values and daily minimum and maximum air temperature values (black line) and using only the daily minimum and maximum air temperature values (blue line). There is no survival curve for adults as adults are not given a stage duration equation because there is no maturation from the adult class, only death. In the adult plot the dashed line shows all adults and the solid line excludes those in diapause.

the low survival scenario, prevalence of 38.0% would be required for persistence at an 8.1 MFIR, which seems unplausible. Persistence at the lower MFIR of 0.04 is not expected under any WNV prevalence or survival rate for this system. Increasing the amount of larval habitat to 375000 litres would be sufficient for pathogen persistence in the low (10%) overwinter survival scenario, with the lowest MFIR estimate of 0.04. This is an area equivalent to 18750 of the water butts used, given a depth of 5cm.

4.4.6 Conclusions

Here I present a brief summary of the conclusions of the investigations introduced in Section 4.2

1. **Diapause timing:** Bringing forward the diapause initiation and termination thresholds in the updated model gave better agreement with the data (r_p = 0.57 for adults) than was observed under the Chapter 2 model (r_p = 0.15 for adults) (Figure 4.9).
2. **Adult overwinter survival:** Simulations showed that overwinter survival can have profound impacts on seasonal abundance the following year, with peak active adult population size showing an approximate one third increase from the low to high survival scenarios (Figure 4.10).
3. **Post-diapause mortality:** Inclusion of the post-diapause adult mortality rate resulted in a better fit of the model predictions to the field data than was possible under the Chapter 2 model (Figure 4.11), which was not able to capture the peaks in the data (Figure 4.1).
4. **Seasonal variation in predation:** The timing of seasonal predation affected both the abundance patterns within a given year and the diapausing population, leading to implications for abundance in the following season (Figure 4.12).
5. The effects of the temporal resolution of temperature input data on model predictions were as follows.
    5.1. **Water temperature temporal resolution:** In water butt 1, where temperatures were generally highest, abundance predictions increased with decreasing temporal resolution of temperature data (Figure 4.17). In water butt 4, where temperatures were generally lower, abundance predictions were highest when using mean temperatures, however there was negligible difference between hourly and minimum and maximum daily temperatures (Figure 4.16).

5.2. **Water butt temperature comparisons:** Higher temperatures in butt 1 were not observed to cause prohibitively high immature mortality, with abundance predictions in butt 1 exceeding those in butt 4 (Figure 4.17). Thus, the concentration of immatures in butt 4 could not be explained by avoidance of lethal temperatures in butts 1-3.

5.3. **Air temperature temporal resolution:** Inclusion of diurnal temperature range of air temperature had negligible effects on abundance (Figure 4.18).

5.4. **Air temperature as a proxy for water temperature:** Approximating water temperature by air temperature led to population extinction for the system studied (Figure 4.19).

6. **Probability of pathogen persistence:** Pathogen persistence between seasons was not predicted to occur for the a population of the size observed in the field experiment.

4.5 Discussion

4.5.1 Relationship between abiotic factors, diapause timings and abundance patterns

The timing of diapause induction and termination will determine the length of the biting and pathogen transmission seasons, the overwinter survival of adults, and the likelihood of pathogen persistence between seasons (Lord 2004; Denlinger and Armbruster 2014). Having collected the fieldwork data I revised the model such that diapause termination occurred in early April and induction is centred around early August. These updated diapause thresholds gave improved agreement with the data, when compared with the predictions from Chapter 2 (Figure 4.9).

The sparsity of field studies investigating *Cx. pipiens* diapause behaviour, combined with the known geographic variability in response to diapause cues, means that photoperiod alone was considered to initiate and terminate diapause (Sim and Denlinger 2013; Denlinger and Armbruster 2014). However, more long term, spatially replicated mosquito seasonal abundance studies would increase power to detect and parameterise predicted effects of both temperature and photoperiod (Sanburg and Larsen 1973; Madder et al. 1983a; Spielman 2001) on diapause behaviour in *Cx. pipiens*. To understand diapause entry, this could involve combining adult catch data with studies monitoring populations in diapause shelters, as in Sulaiman and Service (1983), over a number of years to further our understanding of how photoperiod

and temperature interact to determine the end of the biting season and the start of mosquito diapause. Field studies pairing catch data with monitoring of overwinter shelters could be combined with laboratory studies, akin to those carried out in North America (Eldridge 1966; Sanburg and Larsen 1973; Spielman 2001), to further our knowledge of how environmental variables influence diapause entry.

The fact that the start of each abundance peak, with the exception of the autumn pupal peak, is well captured by the updated model across the life stages supports the finding in Chapter 3 that the temperature-dependent development rates have been captured well in the updated model. However, the end of the spring population peak is predicted to occur later in the updated model than in the data (Figure 4.9). The longer spring abundance peak observed in the updated model across the stages is most likely to stem from an overestimate of the gonotrophic cycle length in the early part of the season. The timing of the post-diapause mortality is dependent on the diapause exit time and the predicted length of the gonotrophic cycle (Equation 4.10). Given that the start of the peak is captured well, the timing of diapause termination seems likely to be accurate. It is most likely that overestimation of the gonotrophic cycle length would lead to a later mortality of adults, causing a longer initial period of egg-laying and a subsequent lengthening of the initial peak in abundance of each life stage, when compared with the field data.

The summer peak in the egg and larval populations is predicted by the updated model to be substantially longer than was observed in the field data (Figure 4.9). To explain this discrepancy in peak duration, it is useful to look at the results of the quasi-Poisson GLM fitted in Section 3.3.1, which predict a drop in adult catch sizes in early July (Figure 3.12), meaning that fewer host-seeking adults were predicted late in the season. However, in the updated model, high levels of egg-laying, leading to high larval abundance, are observed. Egg-laying and larval abundance in the data, show stronger generational peaks and a decreased egg population in mid-to-late July and early August. One possibility is that, because the study system was not closed, mosquitoes may have selected other oviposition sites outwith the study system. This would cause a drop in the number of *Cx. pipiens* observed at our field site, which would not be reflected in the model. Another possible reason for the discrepancy between the observed and predicted egg numbers is that the model assumes egg-laying is spread out over the length of the gonotrophic cycle (Equation 2.19), whilst in reality eggs should be laid in pulses at the end of each cycle (Vinogradova 2000; Lardeux et al. 2008). This pulsed egg-laying behaviour may explain the sharper generational peaks observed in the field data.

To allow egg-laying behaviour to occur only at the end of each cycle in the model, the adult stage would need to be divided into sub-stages according to the adult's current physiological state. This substantially increases the complexity of the model because each gonotrophic cycle would require two stages, one for cycle processes excluding egg-laying and a second for egg-laying. The single adult stage must therefore be split into a number of stages equal to twice the number of gonotrophic cycles a female can complete in her lifetime, which is temperature-dependent. This process of incorporating a series of nested delays, described in Section 2.2.1, is exceedingly cumbersome in this extended case. For these reasons, and to allow extension to explicitly include disease in Chapter 5, extension to multiple adult stages was not implemented here. However, splitting of the adult stage to better capture egg-laying would be a worthwhile future model development.

4.5.2 Effects of seasonally varying predation on mosquito abundance

In Section 3.3.1 it was shown that patterns of immature abundance were only captured when density-dependent mortality was included in the larval stage (Figure 3.6). Intra- and inter-specific competition are both density-dependent processes which have been shown to affect larval mortality and development time of many mosquito species (Costanzo et al. 2005; Legros et al. 2009). However predation has often been seen to act as the main source of population regulation in *Culex* mosquitoes (Rajagopalan et al. 1976; Menon and Rajagopalan 1981; Mogi and Okazawa 1990). Due to the wide range of breeding sites utilised by *Cx. pipiens* (Vinogradova 2000), *Cx. pipiens* larvae are believed to be most at risk from a range of generalist predators (Juliano 2007). These predators will exhibit a wide range of consumptive abilities and show a range of seasonal abundance patterns, which may be independent on larval population size (Onyeka 1983). Further, it is possible that climate impacts may have differential effects on the prey and predator populations, which may cause misaligned timings of the populations' active seasons. Finally, predators have been suggested as alternatives to insecticide treatments in vector control programmes (Lord 2007; Shaalan and Canyon 2009), meaning that the implementation of the control strategy will determine seasonal variation in larval predation.

The inclusion of seasonal variation in predation was found to have a profound effect on abundance patterns in the year upon which the predation acted. Further, when predation occurred in the early part of the year, increased larval survival late in the season led to large diapausing

populations, with implications for abundance in the following season (Figure 4.12). Inclusion of seasonal variation in the number of predators per larva improved agreement with field data, when compared to the original model (Figures 4.14-4.15). These results suggest that the coincidence of predators and mosquito emergence may be an important factor in regulation of the mosquito population in a given year. However, intraspecific competition for resources may also play an important role in population regulation in the absence of predators and should be considered in future studies. It is also evident that predators are important across the whole season, with predators in the early months affecting the active population that year and predation in the later months affecting the following year. By including variable predation dynamics in the model, it would be possible to use the model to predict the efficacy of using predators in mosquito control and to assess the best methods of implementation of particular control measures.

4.5.3 Temperature impacts on seasonal abundance

Recent studies have highlighted the effects of diurnal temperature variation on mosquitoes. *Aedes aegypti* have exhibited extended immature development, lower larval survival, reduced reproductive output, increased adult mortality and decreased susceptibility to virus infection when exposed to diurnal temperatures variations, rather than constant temperatures (Lambrechts et al. 2011; Carrington et al. 2013). I observed that the updated model predicted higher abundances in each life stage when lower resolution butt 1 water temperature measurements were used as inputs (Figures 4.17). Inclusion of temporal resolution in water temperatures was observed to be more influential than including diurnal temperature variability in air temperatures (Figure 4.18). These findings are based on the assumption that temperatures experienced at all times throughout the day will have equal effects on mosquito vital rates. To my knowledge, no studies have investigated changes in immature mosquito behaviour throughout the day. However, adult mosquitoes of different species are known to be most active during specific periods of the day (Rund et al. 2016), meaning that temperatures at these times may be more influential. The finding that aquatic temperatures appear to be more influential, likely stems from the fact that the immature population is substantially larger in size than the adult population, as mid-season egg-to-adult survival is below 1%. Consequently, a small change to water temperatures affects a large proportion of the population and has substantial implications for abundance. This highlights the importance of explicitly modelling each mosquito life stage, as the immature stages are seen to be very sensitive to small changes in conditions.

Failing to account for water diurnal temperature variability may not always lead to higher abundance estimates, as it does in this case. The effect of including diurnal temperature variability will depend on the full range of temperatures experienced by the population. In habitats where water temperatures within a day regularly exceed the upper temperature threshold for immature survival one would expect accounting for diurnal temperature variability may reduce abundance predictions if it causes the population to endure damagingly high temperatures (Colinet et al. 2014). It is likely that UK mosquito populations are well adapted to current local temperature variability. However, temperatures in butt 1 were observed to exceed thermal development thresholds at some points in the year at the field site. Climate change predictions state that UK temperatures are likely to rise in the coming years (UKCIP 2010). Consequently, it is important that we understand the potential impacts of temperatures outwith the range typically experienced by UK mosquito populations at present, as potentially damaging temperatures for mosquito development may occur more frequently. Damaging temperatures would not be captured by analyses studying mean temperatures, such as in Chapter 2, meaning that inclusion of diurnal temperature variability in mosquito abundance models will be important in determining the effects of shorter periods of particularly high temperature.

The temporal resolution of input air temperatures was seen to have a negligible effect on abundance predictions (Figure 4.18). In the model, the adult stage is less sensitive to temperature fluctuations around the low-to-medium temperature range than the immature stages. Temperatures at the field site tend to be in this low-to-medium range ($10 - 20\,^{\circ}\mathrm{C}$) (Figure 4.4). However, the effects of temperatures in this range on adult activity have not been well studied, meaning the model is not sensitive to changes in this region. Further laboratory and field studies would be needed to allow for more accurate parametrisation of adult rate functions, specifically at lower thermal limits. This would inform on whether the lack of sensitivity is a consequence of model parameterisation or of mosquito biology.

The vast majority of both statistical (Wang et al. 2011; Mulatti et al. 2014; Jian et al. 2014b) and mechanistic (Shaman et al. 2006; Cailly et al. 2012; Beck-Johnson et al. 2013; Tran et al. 2013; Lončarić and Hackenberger 2013; Marini et al. 2016) vector and disease models, which incorporate environmental drivers, only consider air temperature for both immature and adult development. This can lead to erroneous results, as water temperatures are often warmer than surrounding air temperatures (Figure 4.4), leading to an increased rate of immature mosquito development. I showed that using air temperature as a proxy for water temperature in the updated model led to erroneous seasonal abundance predictions, with population extinction falsely predicted when using only air temperatures for all life stages

(Figure 4.19). Consequently, underestimation of temperatures, and thus development rates and survival, appears to be particularly problematic in temperate regions, like the UK, where temperatures are often close to the lower boundary of the mosquito thermal development range.

The ability to convert air temperatures to water temperatures is a major roadblock, with water temperatures being dependent on a wide range of variables such as water body size, wind and sun exposure, and whether the container is natural or artificial. Paaijmans and Heusinkveld (2008) have developed a model to predict diurnal water temperature dynamics in shallow tropical water pools using common weather data (air temperature, air humidity, wind speed and cloud cover). Further, recent work by Asare et al. (2016) attempts to predict water temperatures across a peri-urban area in Ghana using only minimum and maximum air temperatures, with some success. However, this work studies temperatures in three identical ditches, and *Cx. pipiens* are known to be opportunistic when ovipositing, meaning the range of sites for which temperatures must be estimated would be much larger. Developments of this type for the full range of temperate mosquito habitats should be a priority if we wish to accurately model mosquito populations.

Failing to account for the discrepancy between air and water temperatures will not always result in differences in predictions as stark as those seen here, where using air temperature as a proxy for water temperature resulted in a prediction of extinction. This work focusses on a temperate climate where the temperature is often only slightly higher than the lower temperature threshold for mosquito development. At the boundary of the mosquito thermal development thresholds, a small discrepancy between air and water temperatures can mean air temperatures act as poor predictors of immature survival. Figure 4.4 (a) shows that the mean air temperature at the field site regularly dropped below the lower thermal threshold for development of *Cx. pipiens* ($10\,^{\circ}\mathrm{C}$) in the spring (Almirón and Brewer 1996; Loetti et al. 2011). Water temperatures are consistently above this threshold and higher than ambient air temperatures, once diapause emergence has occurred. Consequently, failing to account for warmer water temperatures can have large impacts on predictions of mosquito seasonal abundance. This is particularly true in locations where temperatures fluctuate around thermal development thresholds. Models should explicitly include or estimate water temperature, alongside diurnal variability in water temperatures, to combat these issues.

4.5.4 Mosquito overwinter survival effects on pathogen persistence

Overwinter survival will have a direct impact on the probability of WNV persistence between seasons (Nelms et al. 2013). Further, winter mortality of adults will affect spring population size, which may influence population dynamics in the following season (Lord 2004). Estimates of overwinter survival of diapausing mosquitoes show substantial variability between sites and years, with published survival estimates ranging from 2% to 60% (Bailey et al. 1982; Sulaiman and Service 1983; Onyeka and Boreham 1987). However, the underlying causes of this variability are not clear. Model simulations showed that overwinter survival of adult females impacts abundance patterns throughout the following season and not only in the spring, as may be expected (Figure 4.10). Whilst overwinter survival appears to be particularly influential in determining population and pathogen dynamics, the effect of winter temperature on survival of diapausing adult females of temperate mosquito species has not received much attention. Consequently, lab and field studies investigating this should be a priority.

There are three main pathways by which WNV persistence between seasons is believed to be possible: overwinter infection in the host avian population (Calzolari et al. 2013), gonotrophic dissociation, where the ovaries of a blood-fed female remain undeveloped allowing it to successfully overwinter (Eldridge 1966), and vertical transmission from an infected parent to a diapausing offspring followed by horizontal transmission from that offspring the following season (Anderson and Main 2006) (Figure 4.21).

Eldridge (1966) showed that gonotrophic dissociation occurred in *Cx. pipiens* when individuals were reared at sufficiently low temperatures and photoperiods (< 12 hours and $< 15\,^{\circ}\mathrm{C}$ for a laboratory colony from Indiana). The findings of Eldridge (1966) imply that approximately 30% of adults emerging in the final pupal peak of the field population, observed in mid-September, may exhibit gonotrophic dissociation, given the temperatures experienced. Consequently, 30% of the adult female population may be able to facilitate pathogen persistence through gonotrophic dissociation if they were to feed on an infected individual. The exact values published by Eldridge (1966) may not be appropriate given that their experiment used a *Cx. pipiens* colony from West Lafayette, Indiana, which is located at a latitude $10\,^{\circ}$ south of the UK field site and in a different eco-climatic zone. However, the fact that gonotrophic dissociation has been shown to occur in *Cx. pipiens* suggests that it may act as a pathway by which pathogen persistence could occur in the UK.

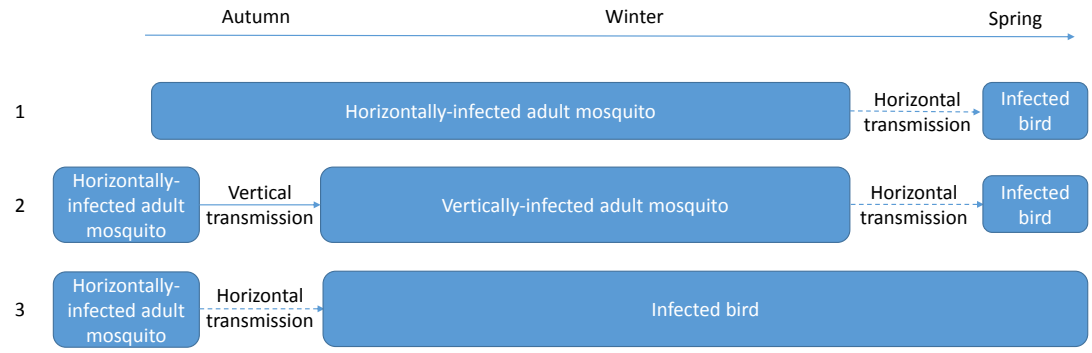

Figure 4.21: Overwinter transmission pathways flowchart: A flowchart showing the three main overwinter disease transmission pathways: overwinter survival of horizontally-infected adults through gonotrophic dissociation, survival of vertically-infected diapausing individuals and survival of infected birds.

Vertical transmission is the other mechanism by which diapausing females may act as an overwinter reservoir for WNV (Nelms et al. 2013). In Section 4.4.5 it was shown that, given sufficient larval habitat, pathogen persistence between seasons by this route may be possible, assuming large enough MFIR and pre-diapause infection prevalence. Consequently, the hypothesis that overwintering females only survive long enough to complete one gonotrophic cycle after diapause emergence becomes particularly important. The restriction to one blood meal means that pathogen persistence would require transfer from the surviving, vertically-infected female mosquitoes to the hosts to take place in this one blood-feeding instance. Alternatively, further vertical transmission would need to occur between adult females and their egg rafts in the early season. The low prevalence of vertical transmission, with estimates of the MFIR from laboratory studies in the range $0.04 - 8.1$ (Nelms et al. 2013), make this highly unlikely. The probability of two successive instances of vertical transmission would be expected to fall in the range $(1.6 \times 10^{-9} - 6.561 \times 10^{-5})$. Therefore, early-season transmission of the virus from vectors to hosts will be particularly important in determining the risks of pathogen persistence.

Post-diapause mortality of adult females has not been included in seasonal abundance models for other temperate mosquito species. It was shown that the model incorporating this added mortality was better able to capture the seasonal abundance patterns in the field data (Figure 4.11). Not only will this term affect pathogen persistence between seasons, the added mortality also has implications for our understanding of the mosquito biting season. Mortality of post-dipause females will increase variability in biting intensity in the early part of the transmission season. Biting rates will briefly increase immediately following diapause exit,

before decreasing again until emergence of the first spring generation. Without this post-diapause mortality rate the adult population would steadily increase and any drop in biting intensity caused by this high post-diapause mortality would not be captured.

Chapter 5

Impacts of current and future temperatures on UK WNV transmission

5.1 Introduction

Recent decades have seen dramatic expansions in the global distributions of a number of vector-borne diseases (Jones et al. 2008). These include outbreaks of chikungunya fever in Italy (Angelini et al. 2007), dengue fever in France (Succo et al. 2016), zika virus in south and central America (Fauci and Morens 2016), the introduction of Bluetongue virus into southern and then northern Europe (Carpenter et al. 2009) and WNV in North America and the Mediterranean basin (Reisen 2013; Sambri et al. 2013). These diseases have resulted in severe economic losses and substantial human morbidity and mortality (Wilder-Smith et al. 2017). Understanding the factors responsible for these changing distributions and predicting future spread has become an important issue in global health research (Campbell-Lendrum et al. 2015). Numerous studies have detected strong links between climatic factors and the seasonality in disease outbreaks (Altizer et al. 2006; Mirski et al. 2012). Understanding the relationship between fluctuating environmental conditions and disease outbreaks requires that knowledge of climatic effects on vectors and disease transmission processes be explicitly linked (Lord 2004).

In Europe, WNV has become endemic in areas of the Mediterranean basin (Barzon et al. 2012; Sabatino et al. 2014), with reported human cases as close to the UK as southern France

and northern Italy in 2015 and 2016 (Figure 1.2). Further, the unexpected but highly successful introduction and rapid spread of WNV in North America highlights the ability of the virus to establish itself in previously uninfected areas (Reisen 2013). Semenza et al. (2016) predict expansion of current European WNV transmission areas between now and 2050 in response to climate warming, using a correlative model linking environmental variables to presence or absence of disease within European regions. In addition, Paz et al. (2013) observed that temperatures above seasonal averages in summer acted as precursors to WNF outbreaks in humans, particularly at northerly latitudes. It is predicted that climate change will cause increases in UK temperatures in the coming years (MetOffice 2009), potentially increasing the ability of these vectors to transmit WNV if it were to be introduced. These findings, combined with the proximity of cases in Southern France and Northern Italy, have caused concern about the possibility of WNV outbreaks in the UK, particularly because the UK is home to a high abundance of effective vectors, in *Cx. pipiens* (Golding 2013), and numerous susceptible bird species migrate to the UK from Southern France, where WNV outbreaks have occurred (Paz et al. 2013; Bessell et al. 2014). In order to predict transmission of WNV under predicted climate scenarios, we must understand the underlying relationships between vector ecology, disease transmission and environmental conditions.

Correlative statistical models have shown relationships between a wide range of environmental variables and outbreaks of vector-borne disease, however these results often show regional variability. For example, studies of regional variation in WNV outbreaks in the USA have shown that, whilst warmer temperatures consistently increased human infection rates, precipitation levels could have either positive or negative effects on disease cases dependent on the local conditions (Landesman et al. 2007; Wimberly et al. 2014). Similar patterns have been found in population models of WNV vectors, with higher temperatures consistently increasing population size and biting rates, whilst rainfall effects are variable (Mulatti et al. 2014; Rosà et al. 2014). These models are valuable tools by which environmental variables influencing the vector life and disease transmission cycles can be detected. However, because climatic conditions may have opposing impacts on disease cycle and vector life parameters, models that integrate such processes to predict overall impacts on disease transmission are required.

Most epidemiological systems use a compartmental approach, such as the susceptible-infectious-recovered/removed (SIR) framework, in which the host population is categorized according to infection status as either susceptible, infectious, or recovered/removed (Kermack

and McKendrick 1927; Wearing et al. 2005). This allows calculation of the R_0 value (Equation 1.5), which gives the number of secondary infections arising from introducing an infectious individual into a population of entirely susceptible individuals (Wonham et al. 2004; Cruz-Pacheco et al. 2005; Bowman et al. 2005; Rogers and Randolph 2006). This idea can be extended for vector-borne diseases, such that the vector population is split into susceptible and infectious compartments, as shown in (Figure 5.1 (a)). A common extension within vector-borne disease models is to include an additional exposed (but not yet infectious) vector class (susceptible-exposed-infectious-recovered/removed (SEIR) models) to account for the temperature-dependent extrinsic incubation period (EIP) of the vector (Wearing et al. 2005), as in Figure 5.1 (b). For mosquito-borne disease models, the EIP is the time required for the virus to replicate within the mosquito and to reach the salivary glands (Anderson et al. 2008). Once this has happened the mosquito becomes infectious and the virus may be passed on during the taking of a blood meal. The specific calculation of the R_0 value will depend on the assumptions of a given model but an example is given by

$$R_0 = \frac{\iota \mathcal{T}_{mb} \mathcal{T}_{bm} \mathcal{B}^2 \exp(-\delta \tau_{EIP})}{\delta \mathcal{R}}, \tag{5.1}$$

where ι is the vector-host ratio, $\mathcal{T}_{mb}$ and $\mathcal{T}_{bm}$ are the vector-host and host-vector transmission coefficients, $\mathcal{B}$ and δ are the vector biting and death rates, τ_{EIP} is the duration of the EIP and $\mathcal{R}$ is the host recovery rate (Rogers and Randolph 2006).

This R_0 equation (Equation 5.1) highlights the importance of vector dynamics and seasonality on disease transmission; the vector-host ratio, ι, will fluctuate depending on environmental effects on the size of the mosquito population (Altizer et al. 2006). Further, mosquito biting rates, $mathcalB$, and death rates, δ, are known to increase with increasing temperature, whilst the duration of the EIP, τ_{EIP}, will decrease with increasing temperature (Reisen et al. 2006a; Ciota et al. 2014). However, traditionally R_0 values can only be calculated at population equilibrium, meaning that most models only capture behaviour for a specific set of environmental conditions (Wonham et al. 2004; Cruz-Pacheco et al. 2005; Bowman et al. 2005).

SEIR models are most typically expressed using a series of ODEs, where each ODE defines one compartment of the model (Wonham et al. 2004; Bowman et al. 2005; Cruz-Pacheco et al. 2005; Rubel et al. 2008; Erickson et al. 2010a; Charron et al. 2011; Bergsman et al. 2015; Robertson and Caillouet 2016). One of the fundamental assumptions of such models

is that the rate at which individuals leave each class is exponentially distributed and independent of the time already spent there. Consequently, the exposed vector population begins to become infectious immediately, contrasting with laboratory observations that there is a delay between taking an infected blood meal and becoming infectious (Reisen et al. 2006a). Hartemink et al. (2015) compared estimates of R_0 when approximating the exposed period by an exponential distribution and when assuming a fixed duration for the exposed period, and showed that assuming an exponential distribution resulted in overestimation of R_0 values.

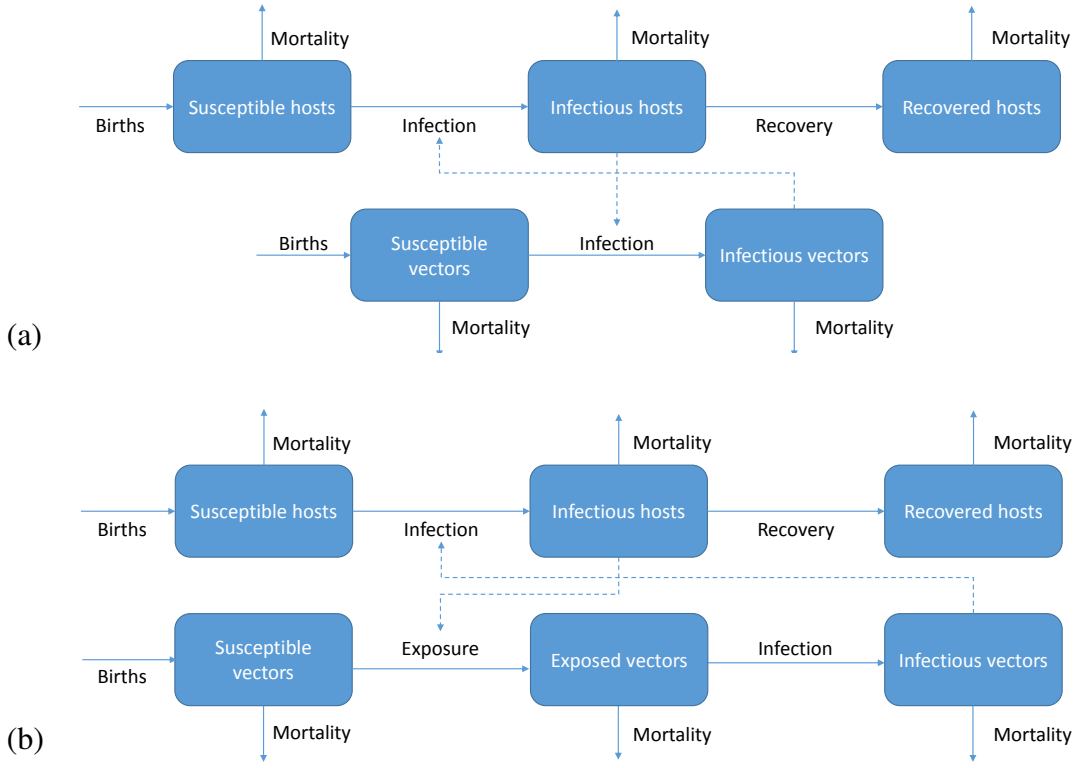

Figure 5.1: SIR and SEIR Models: Diagram (a) shows a simple SIR model for a hypothetical host and vector population. Diagram (b) shows an SEIR model, where an exposed class has been added for the vector population. Vector-host and host-vector transmission are the only pathways considered in both cases.

It is clear from Equation 5.1 and Figure 5.1, which shows diagrams of SIR and SEIR-type models, that seasonality in the vector population will affect R_0 values and disease transmission, through changes to the vector-host ratio, ι. However, historically, the majority of epidemiological models do not explicitly incorporate vector seasonality. A recent review paper by Reiner et al. (2013) found that 61% of mathematical models of mosquito-borne pathogen transmission published between 1970 and 2010, which included at least one equation of mosquito dynamics, held the mosquito population size constant. Further, only 12%

of all models explicitly modelled the aquatic stage of the mosquito population, whilst 7% of all models included density-dependence in the aquatic stage. Recently, Evans et al. (2013) argued for increased complexity in models when making predictions about real ecological systems. The authors argue that, to understand which processes have the greatest effects on model predictions, models must incorporate the full range of relevant ecological processes to allow thorough testing. Intra- and inter-species interactions and climatic effects are important determinants of mosquito phenology (Bewick 2016), as shown in Chapters 2-4. Consequently, the direct integration of mosquito population models that incorporate this range of biotic and abiotic processes, into epidemiological models, is expected to improve predictions regarding mosquito-borne disease (Smith et al. 2014). This integration is particularly important in planning and implementing control measures to guard against disease outbreaks, as these often target a particular stage of the mosquito life cycle (Lord 2007).

In line with the wider vector-borne disease research, the majority of epidemiological models for WNV adopt an SIR or SEIR framework, with each compartment most commonly described by an ODE. This is highlighted in Table 5.1, which lists dynamical mathematical WNV models developed since 2000. WNV-induced mortality in bird populations, avian recovery rates from infection and variable transmission rates between vector and host are regularly included in disease models. However, seasonality in the mosquito and bird populations remain largely neglected in disease models, which will impact R_0 predictions through assumptions made about vector-host ratios. Further, none of the dynamical WNV models include vector diapause, meaning that predictions across multiple seasons would only be valid in southerly regions where diapause incidence may be low, as in Hartley et al. (2012). Whilst half of the models shown include an exposed vector stage, only two models incorporate temperature-dependence in the EIP duration and all models assume the exposed vector stage is exponentially distributed (Table 5.1). This will influence R_0 predictions and subsequent disease transmission, as previously discussed. Use of DDEs facilitates removal of the assumption of exponentially distributed stage durations, as stage durations can be of fixed lengths or may vary with temperature. Only one model utilises DDEs to capture the vector dynamics (Fan et al. 2010), showing that inclusion of mosquito developmental delays influences both the mosquito abundance and the number of transmission peaks within a year. However, the Fan et al. (2010) DDE model does not include seasonal forcing in the vector population and ignores the EIP.

Most WNV models ignore temperature-dependence in disease transmission and mosquito life cycle processes, such as biting rates and virus incubation rates, making the assumption that these processes occur at constant rates (Lord and Day 2001; Wonham et al. 2004;

Process	1	2	3	4	5	6	7	8	9	10	11	12	13	14	Total	Prop
Seasonality, V	✓	×	✓	×	×	×	×	×	×	×	✓	×	×	×	3	✓
Seasonality, H	✓	×	×	×	×	×	×	×	×	×	×	×	×	×	1	✓
Immature dynamics, V	×	×	✓	×	×	×	×	×	×	✓	✓	✓	×	×	4	✓
Density-dependence, V	×	×	×	×	×	×	×	×	×	×	✓	✓	×	✓	3	✓
Exposed class, V	✓	✓	✓	×	×	×	✓	×	×	×	✓	✓	✓	×	7	✓
EIP temp-dependence, V	✓	×	×	-	-	-	×	-	-	-	✓	×	×	-	2	✓
EIP distribution, V	Exp	Exp	-	-	-	-	Exp	-	-	Exp	Exp	Exp	Exp	-	-	Step
Trans probabilities, VH	✓	×	✓	✓	✓	✓	✓	✓	✓	✓	✓	✓	✓	✓	13	✓
Range of competencies, H	✓	×	×	×	×	×	×	×	×	×	✓	×	✓	✓	4	✓
Biting preference, V	✓	×	×	×	×	×	×	×	×	×	×	×	✓	✓	3	×
Host-host transmission, H	×	×	×	×	×	×	✓	×	×	×	✓	×	×	✓	3	✓
WNV-induced mortality, H	✓	×	✓	✓	✓	✓	✓	✓	✓	✓	✓	✓	✓	✓	13	✓
Recovery from WNV, H	✓	✓	✓	×	✓	×	×	✓	✓	✓	✓	✓	✓	×	10	✓
Loss of immunity, H	×	×	×	-	×	-	-	×	×	×	×	×	✓	-	1	×
Vertical transmission, V	×	✓	×	×	✓	×	×	✓	✓	✓	✓	×	×	✓	7	✓
Diapause, V	×	×	×	×	×	×	×	×	×	×	×	×	×	×	0	✓
Spatial structure	×	×	×	×	×	✓	×	×	✓	×	×	×	×	×	2	×
Human compartment	×	✓	×	✓	×	×	×	×	×	×	×	✓	×	×	3	×
Model structure	ODE	Diff	ODE	ODE	ODE	ODE	ODE	Diff	PDE	DDE	ODE	ODE	ODE	ODE	-	DDE
Total	9	4	6	3	4	3	4	4	5	5	11	7	7	7	-	13

Table 5.1: Dynamical mathematical WNV models: A table showing the features which are included and excluded from a range of dynamical mathematical models of WNV transmission, where each column represents a published model. “Diff" stands for a discrete-time difference model, “Exp" stands for an exponential distribution, “Step" represents an exposed period where the stage duration is a fixed time for all individuals and “Prop" represents the model proposed in this Chapter. The proposed model is the model presented in this Chapter. 1 - Lord and Day (2001), 2 - Thomas and Urena (2001), 3 - Wonham et al. (2004), 4 - Bowman et al. (2005), 5 - Cruz-Pacheco et al. (2005), 6 - Liu et al. (2006), 7 - Hartemink et al. (2007), 8 - Jang (2007), 9 - Maidana and Yang (2009), 10 - Fan et al. (2010), 11 - Hartley et al. (2012), 12 - Pawelek et al. (2014), 13 - Bergsman et al. (2015), 14 - Marini et al. (2017).

Cruz-Pacheco et al. 2005; Durand et al. 2010; Pawelek et al. 2014; Bergsman et al. 2015). However, the compounding effects of these processes make predicting the influence of temperature on disease transmission difficult, highlighting the need for models which can explicitly incorporate temperature relationships. In this Chapter, I extend my existing *Cx. pipiens* model to explicitly incorporate temperature-dependence in a wide range of WNV transmission dynamics (Table 5.1). This model is twinned with a compartmental model for host avian dynamics. In this way, environmental conditions act as drivers of not only seasonality in the vector population, but also seasonality in disease transmission. Using this model, I intend to answer the following key epidemiological questions:

1. If WNV were to be introduced to Southern England how likely is it that an outbreak would occur under average climate conditions?
2. Which parameters are the most influential in determining WNV transmission?
3. How will predicted warming in the UK alter transmission potential of WNV?

In the next section, prior to outlining the model, I set out the key features of the ecology of the WNV system that underpin the model design and application.

5.1.1 Host and vector ecology

Temperature-induced seasonality in vector abundance, alongside the effects of temperature on pathogen replication in vectors means that patterns of WNV transmission exhibit strong seasonality in temperate regions (Altizer et al. 2006). Figure 5.2 demonstrates this effect in human WNV cases in both the USA and Europe throughout 2007 and 2010, respectively, with incidences peaking throughout August and September. This mimics observed seasonality in *Cx. pipiens* abundance in North America, which has been seen to reach maximum abundances in late summer and autumn (Madder et al. 1983b; Lampman et al. 2006; Jackson and Paulson 2006). The profound impact of environmental conditions on mosquito populations, and likely impacts on disease transmission, mean that inclusion of seasonal environmental forcing is expected to affect prediction and management of potential WNV outbreaks.

WNV is sustained through a transmission cycle between mosquitoes and birds, with humans and equines acting as dead-end hosts, which may experience morbidity and mortality (Figure 5.3). *Cx. pipiens* are primarily a maintenance vector for the virus, as they are ornithophilic, and consequently are effective at circulating the virus within the reservoir bird population (Hamer et al. 2009). However, *Cx. pipiens* will also bite mammals when they are a highly abundant food source relative to birds, meaning that they can act as a bridge vector to the

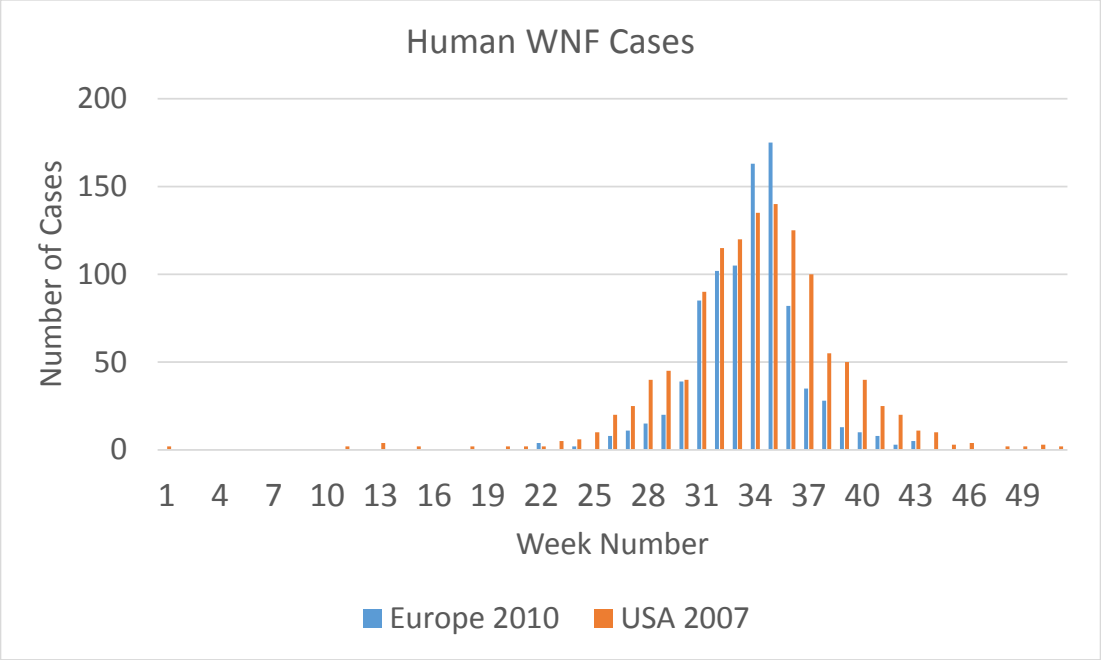

Figure 5.2: WNF weekly cases: The number of WNF neuroinvasive disease cases by week of illness onset across the entire United States in 2007 (CDC 2007) and across Europe in 2010 (Paz et al. 2013) is shown.

human population (Hamer et al. 2009). In some areas, *Cx. modestus* are also likely to act as bridge vectors as they are aggressively mammophilic. *Cx. modestus* was detected in the North Kent marshes in 2010 (Golding et al. 2012) and has been recorded more widely across South East England in recent years (Medlock et al. 2014; Vaux et al. 2015). Several other potential WNV vectors have been found within the UK (Chapman et al. 2016), however *Cx. pipiens* is widely regarded to be the main driver of WNV transmission in Europe and North America, due to its strong preference for feeding on birds (Gubler 2002; Zeller and Schuffenecker 2004; Higgs et al. 2004; Calistri et al. 2010; Reisen 2013). Given this, the seasonal abundance model for *Cx. pipiens* developed in the previous chapters forms a good basis for a WNV model within the UK. WNV infection has been shown to vary across bird species, with different species exhibiting different disease-induced death rates, viremia levels and recovery rates (which will affect the duration over which viremia remains high) (Table 1.1) (Komar et al. 2003; Pérez-Ramírez et al. 2014). Passeriformes have been observed to act as particularly competent hosts of WNV, though there is considerable variability between orders in levels of viremia (Komar et al. 2003).

Vector-host transmission, is believed to be the most common transmission pathway (Komar et al. 2003) and occurs either when an infectious mosquito bites a susceptible bird or when a susceptible mosquito bites an infected bird (Figure 5.3). When bitten by an infectious

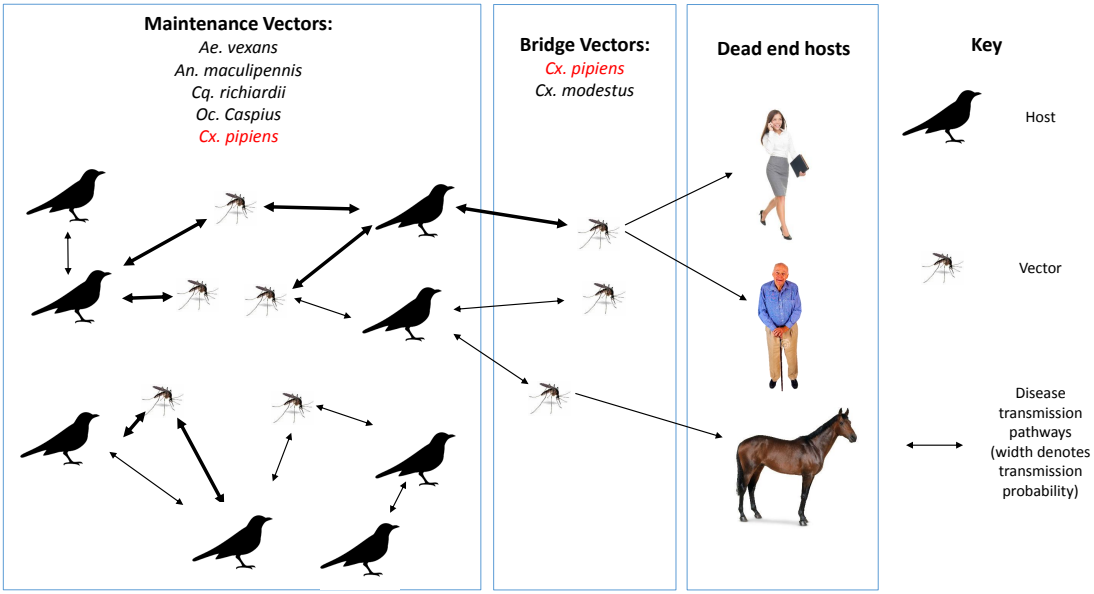

Figure 5.3: WNV transmission cycle: The diagram shows the WNV transmission cycle. *Cx. pipiens* is highlighted in red to emphasise its role as both a maintenance and bridge vector of WNV. UK mosquito species' status as either a maintenance or bridge vector is based on the classification in Chapman et al. (2016). Temperature will affect all vector-host and host-vector transmission rates through its effects on the biting rate and EIP. It will also affect mosquito seasonality through the numerous effects on mosquito vital rates discussed previously.

mosquito, a susceptible bird is assumed to become infectious immediately because the viral incubation time in birds is short, with high viremia typically detected the day after infection (Komar et al. 2003). If a susceptible mosquito bites an infected bird, however, then the mosquito will only become infectious to others once it has undergone the EIP. The impact of temperature on the WNV EIP can be large (Reisen et al. 2006a; Reisen 2013), with the duration of the EIP of WNV for *Cx. tarsalis* taking from under ten days at high temperatures ($> 25\,^{\circ}\mathrm{C}$) to over twenty days at lower temperatures ($< 20\,^{\circ}\mathrm{C}$) (Reisen et al. 2006a). Temperature will also influence disease transmission rates through its effect on the length of the gonotrophic cycle, and thus the biting rate. Increasing temperatures will decrease the gonotrophic cycle, causing the biting rate to increase (Hartley et al. 2012). Increases in the biting rate mean that mosquitoes will take more blood meals and the opportunities for the virus to be spread will increase substantially (Equation 5.1).

Birds also play a vital role as a mechanism by which the virus can be introduced to new areas, through migration of infected individuals (Dusek et al. 2009; Bessell et al. 2014). Such introduction to the UK could occur through infected birds returning from winter habitats. For successful introduction to occur, the virus must have a sufficiently mild impact on the bird's fitness to allow migration to be completed. However, the host must also maintain a

high enough viremia that host-vector transmission is possible upon arrival. The timing and location of introduction of infected birds are also expected to be important drivers of transmission potential. Arrival of the infected hosts must occur during the vector biting season, to allow horizontal transmission to occur. Further, the composition of the bird population at the arrival site will affect subsequent amplification or dilution of the virus. Bessell et al. (2014) showed that at least one infected migratory bird was expected to reach the UK in 88% of years where a WNV outbreak occurred in the Camargue (a hotspot for both migratory bird and vector activity in Southern France). Across all years during which an outbreak occurred in the Camargue, a median of 2 infected birds were expected to arrive (95% CI = $0, 6$) with a total of 2.17 days of active infection remaining. If a WNV outbreak were to occur further north in France, the risk of introduction would increase substantially (Bessell et al. 2014). Once introduction has occurred, the resident bird population could become infected and act as an overwinter reservoir (Dawson et al. 2007), or the virus may overwinter in the mosquito population (Nelms et al. 2013).

Alternative WNV transmission pathways are host-host and vector-vector transmission. Host-host transmission is thought to be possible through faecal shedding at communal roost sites (Dawson et al. 2007; Hinton et al. 2015), predation (Garmendia et al. 2000), or scavenging of infectious carcasses (Komar et al. 2003). This is believed to occur at lower rates than vector-host transmission but may still contribute to disease spread (Komar et al. 2003). Hartemink et al. (2007) found that host-host transmission had more profound impacts on calculated R_0 values than vertical transmission in vectors. In particular, host-host transmission may be an important pathway by which the virus could overwinter in resident bird populations when mosquito populations are not active (Dawson et al. 2007). Finally, vertical transmission from infected adult mosquitoes to their offspring has been shown to occur in WNV-infected *Cx. pipiens* at low rates (0.04-8.1 infected adults per 1000 eggs) (Dohm et al. 2002a; Anderson and Main 2006; Nelms et al. 2013). It is likely that vertical transmission would be dwarfed by vector-host transmission cycles during the biting season (Komar et al. 2003) but it would certainly be a key process mediating disease persistence between years if WNV were to successfully overwinter in diapausing adult mosquitoes (Anderson and Main 2006; Andreadis et al. 2010).

5.2 Methods: Mathematical framework

The extension made to the *Cx. pipiens* population model in this Chapter is that the adult stage is split into three separate stages, to explicitly model susceptible, exposed and infectious

adults, using the SEIR framework as shown in Figure 5.4. All vector life cycle functional forms are as described in the updated model in Chapter 4 (Section 4.3), with the exception of density-dependent mortality due to predation, which is assumed not to experience seasonal forcing, as discussed in Appendix C. The assumption that predator abundance remains a constant proportion of larval abundance throughout the year ensures that population size is regulated during spring under climate warming scenarios, when temperature conditions become favourable for mosquito development. In the absence of disease, the exposed and infectious adult stages will remain empty and the model framework will collapse back to that described in Chapter 4. The extended mosquito population model is linked with a bird population, which is split according to the SIR framework, such that birds are either susceptible, infectious or recovered stages. I model recovered birds, rather than removed birds, because recovered birds develop immunity and can still be bitten by mosquitoes, acting as incompetent hosts within the population. The bird population exhibits seasonality through a seasonally varying birth rate, which restricts births to occur in spring and summer. Disease transmission between the vector and host populations occurs through infectious mosquitoes feeding on susceptible birds and susceptible mosquitoes feeding on infectious birds (Figure 5.4). Disease transmission within the host population can also occur through host to host transmission and in the vector population through vertical transmission. I first describe the seasonal dynamics of the bird population (Section 5.2.1). I then give a detailed description of how the system of DDEs used to describe mosquito dynamics has been updated to include disease transmission (Section 5.2.2). Finally, I describe the disease transmission processes within the bird population (Section 5.2.3). For simplicity, I do not explicitly model the human population. Instead I use the density of infectious adult mosquitoes and the minimum infection rate (MIR), which is the number of infectious mosquitoes per 1000 adult females, to infer the relative risk of human infection.

5.2.1 Host seasonality and migration

The bird population is modelled using a system of ODEs, which describe the dynamics of susceptible, infectious and recovered birds through time. Stage-structure was not included in the bird dynamics due to the wide range of species which will be involved in WNV transmission (Komar et al. 2003). The wide range of species means that attempting to explicitly capture the dynamics of the full range of host species was deemed too complex for this study. Instead I perform an exploratory analysis, modelling a general trend of bird seasonality throughout the season. In doing so, the following assumptions about avian population dynamics were made:

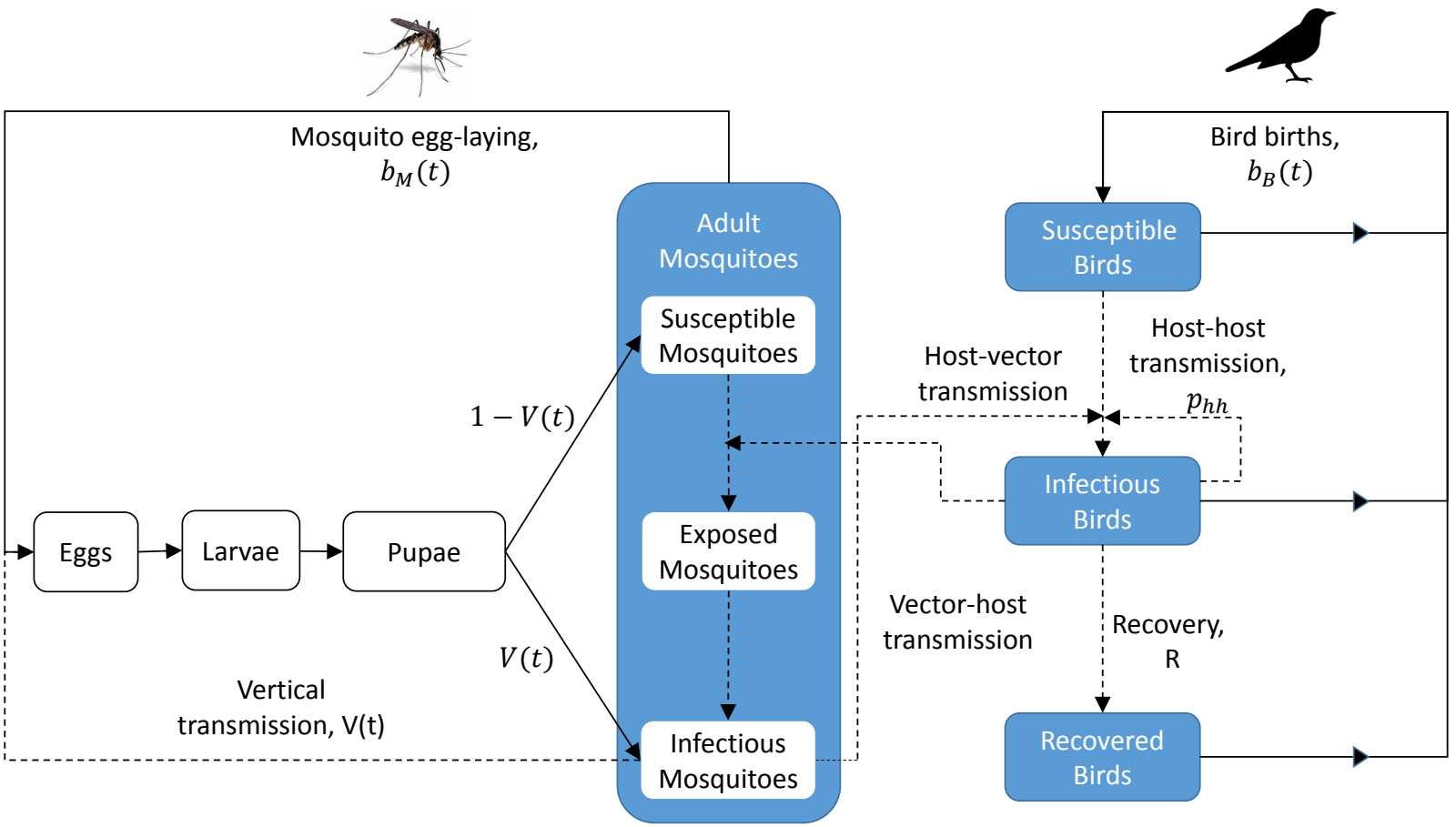

Figure 5.4: Flowchart showing the model structure and highlighting the disease-related parameters. All stages have an associated death rate, which is not displayed here for clarity. All disease transmission processes are shown by dashed lines, whilst life cycle processes are shown by solid lines.

- In temperate latitudes birds generally only breed in spring and summer (Crick et al. 1993), so births were assumed to occur seasonally during these months.
- There is evidence of slight seasonal mortality patterns in British bird populations, with mortality peaking during the breeding season (Dobson 1987). It was assumed that density-independent bird mortality occurred at a constant rate and any seasonality in mortality was due to density-dependent mortality in the breeding season (Sæther et al. 2016).
- It has been shown that survival of fledglings is strongly regulated by density-dependent competition for resources across a range of bird populations (Sæther et al. 2016). I assume that density-dependent mortality, due to competition for resources, occurs during the breeding season when the number of fledglings is high. Density-dependence was not considered to influence the birth rate as density-dependent survival has been shown to have a much greater impact on bird dynamics than fecundity, when populations are at carrying capacity in the mid-to-late summer (Sæther et al. 2016).
- Bird migration to and from the UK will influence seasonal patterns of abundance of various bird species and consequently the overall avian abundance (Newton 2007). However, attempting to explicitly model these processes would greatly increase the complexity of the model. Consequently, I make the simplifying assumption that the arrival and departure of migratory birds does not influence patterns of seasonal abundance but will act as a mechanism by which infection can be introduced.

The total bird population, in the absence of infection, $N_B(t)$, can be described by a single ODE,

$$\frac{dN_B}{dt} = b_B(t)N_B(t) - (\delta_B + h(t)N_B(t))N_B(t), \tag{5.2}$$

such that $b_B(t)$ is the avian birth rate, δ_B, is the density-independent death rate of uninfected birds and $h(t)$ is the density-dependent avian death rate. The solution of this ODE, for the parameter values described in Section 5.2.1, is shown in Figure 5.5 (b).

Avian birth and death rates

Births were assumed to occur seasonally according to a periodic Gaussian function (Figure 5.5 (a)). This functional form has been used to accurately capture seasonal birth pulses in a

range of mammal species by Peel et al. (2014), though there is no reason why, given appropriate parameterisation, the function would not be appropriate for describing bird dynamics. The function is given by

$$b_B(t) = \frac{1}{2} k_B \exp\left(-s_B \left(\cos\left(\frac{\pi t + \phi_B}{365}\right)\right)^2\right). \tag{5.3}$$

Here $k_B (= 0.15 \text{ days}^{-1})$ is a scaling factor proportional to the annual per capita birth rate, $\phi_B (= 50 \text{ days})$ gives the timing of the birth pulse, $s_B (= 10)$ controls the duration of the birth pulse and the factor of $\frac{1}{2}$ reflects that only female birds lay eggs (assuming a 1:1 sex ratio in the bird population). Figure 5.5 (a) shows the avian birth function, $b_B(t)$. Parameters were chosen to reflect the breeding season observed in UK house sparrow populations, as house sparrows are the most common UK bird species (RSPB 2017) and a competent host for WNV (Komar et al. 2003). This parameterisation gives a breeding season running from April to August, with ten eggs laid per female bird in this time (Figure 5.5 (a)), which is common for sparrow populations (RSPB 2017).

Given the assumption that there is no seasonality in density-independent death rates, a constant death rate, $\delta_B (= 6.85 \times 10^{-4} \text{ day}^{-1})$, corresponding to the house sparrow's expected lifespan of 4 years, was assumed. I assume that density-dependent mortality, $h(t)$, due to competition for resources, occurs during the breeding season (Figure 5.5 (a)) when the number of fledglings is high, such that $h(t) = \frac{b(t)}{K}$, where K is the carrying capacity of the population. In the population model, bird and mosquito abundances are assumed to be independent of one another. Consequently, the vector-to-host ratio is assumed in advance, via a carrying capacity for the bird population. The determination of the vector-host ratio is discussed in detail in Section 5.3.2. Given this parameterisation, an example of the annual bird population cycle without infection is shown in Figure 5.5 (b).

5.2.2 Vector seasonality and disease transmission dynamics

In extending the *Cx. pipiens* population model in Chapter 4 to explicitly include disease transmission processes it was necessary to make a number of assumptions regarding the effects of infection on the vector population and the biting process:

- Infection with mosquito-borne diseases, such as malaria and dengue, has been shown to alter fitness and behaviour in a range of mosquito species, primarily through survival, fecundity, host location, and probing behaviour (Maier and Seitz 1987; Maciel-de-Freitas et al. 2011). However, the effects of WNV infection on mosquito fitness

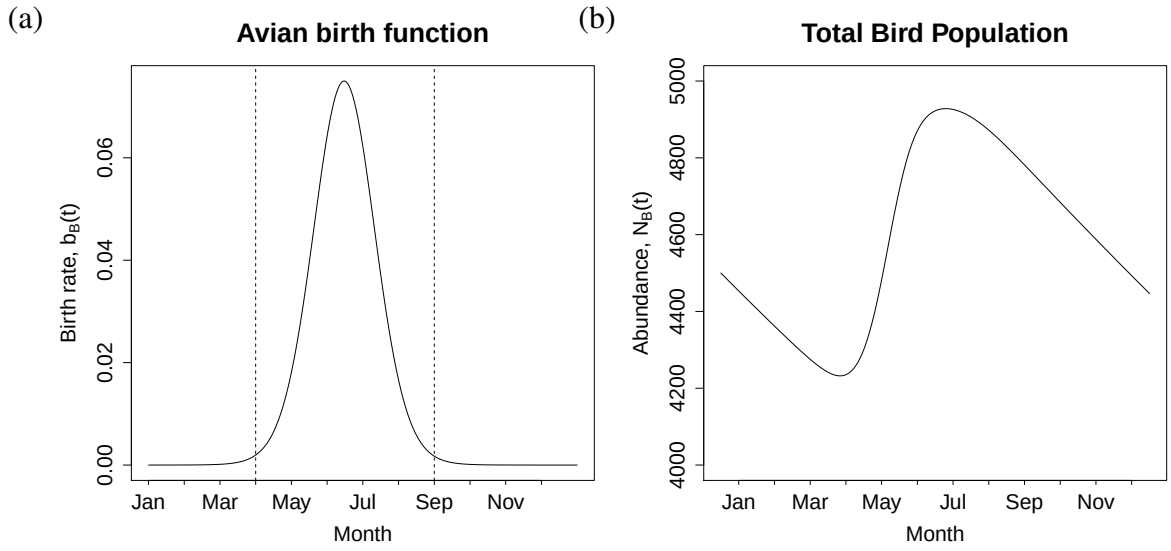

Figure 5.5: Bird dynamics: (a) shows the bird birth function, $b_B(t)$, given by Equation 5.3, with the dotted line depicting the start and end of the breeding season and (b) showns an example annual cycle of bird abundance by solving Equation 5.2.

have not been well studied (Coffey and Reisen 2016), making quantification of any such relationships problematic. Consequently, WNV infection is assumed not to influence the vital rates or behaviour of mosquitoes. This means that egg-laying rates, gonotrophic cycle length (and consequently biting rates), adult mortality, and survival and development of vertically infected immatures are unaffected by infection status.

- Infectious mosquitoes were not able to recover from WNV infection (Kilpatrick et al. 2007).
- Host-frequency-dependent transmission is assumed, meaning that the biting rate by vectors is constant across host densities, and the biting rate experienced by hosts increases with vector density. This is consistent with the majority of WNV models, as mosquitoes are expected to bite once per gonotrophic cycle regardless of host densities (Wonham et al. 2006).
- Laboratory studies have not uncovered a relationship between larval rearing temperature and WNV infection, dissemination or transmission rates in *Cx. tarsalis* (Dodson et al. 2012). Further, no evidence has been shown to suggest a relationship between ambient temperature and either host-vector or vector-host transmission probabilities, which is thought to be dependent on viremia levels in the infectious host or vector (Komar et al. 2003; Kilpatrick et al. 2007). Consequently, it is assumed that transmission probability is independent of temperature.
- Vertical transmission has been shown to occur in *Cx. pipiens* infected with WNV

(Nelms et al. 2013) and is assumed to occur from infectious mosquitoes to their offspring with probability p_{vt}.

Given these assumptions it is possible to extend the *Cx. pipiens* population abundance model from Chapter 4 to include disease transmission by splitting the adult stage into susceptible, exposed and infectious individuals. The state equations corresponding to eggs, $E(t)$, larvae, $L(t)$, pupae, $P(t)$, susceptible, $A_S(t)$, exposed, $A_E(t)$, and infectious, $A_I(t)$, adult mosquitoes are given by

$$\begin{aligned}
\frac{dE}{dt} &= R_E(t) - M_E(t) - \delta_E(T(t))E(t),\\
\frac{dL}{dt} &= R_L(t) - M_L(t) - (\delta_L(T(t)) + \delta_\pi(L(t)))L(t),\\
\frac{dP}{dt} &= R_P(t) - M_P(t) - \delta_P(T(t))P(t),\\
\frac{dA_S}{dt} &= R_{A_S}(t) - \Pi_{A_S}(t) - \delta_A(T(t))A_S(t),\\
\frac{dA_E}{dt} &= R_{A_E}(t) - M_{A_E}(t) - \delta_A(T(t))A_E(t),\\
\frac{dA_I}{dt} &= R_{A_I}(t) - \delta_A(T(t))A_I(t)
\end{aligned} \tag{5.4}$$

where $\delta_i(T(t))$ ($i = E, L, P, A$) represents the stage-specific, density-independent, temperature-driven, mortality rate, $\delta_\pi(L(t))$ represents the larval mortality rate due to external predation, $R_i(t)$ and $M_i(t)$ represent the rate of recruitment to and maturation from stage i respectively, and $\Pi_{A_S}(t)$ gives the rate of transition of susceptible to exposed vectors. Transition from susceptible to exposed adult vectors occurs instantaneously upon biting an infectious host, rather than after a defined time period, hence the distinction between transition and maturation. In the absence of disease, the exposed and infectious stages would be zero, as would transition from susceptible adults to exposed adults, $\Pi_{A_S}(t)$. Consequently, the Equation 5.4 would be unchanged from Chapter 4 (Equation 4.1). The recruitment and maturation equations for the immature stages are defined as

$$\begin{aligned}
R_E(t) &= b_A(t)(A_S(t) + A_E(t) + A_I(t)),\\
M_E(t) = R_L(t) &= R_E(t - \tau_E(t))S_E(t)\frac{g_E(T(t))}{g_E(T(t - \tau_E(t)))},\\
M_L(t) = R_P(t) &= R_L(t - \tau_L(t))S_L(t)\frac{g_L(T(t))}{g_L(T(t - \tau_L(t)))},\\
M_P(t) &= R_P(t - \tau_P(t))S_P(t)\frac{g_P(T(t))}{g_P(T(t - \tau_P(t)))}
\end{aligned} \tag{5.5}$$

with $b_A(t)$ as the egg-laying rate of adults in each adult stage at time t, $\tau_i(t)$ and $S_i(t)$ as the stage duration and survival of individuals in stage i ($i = E, L, P$) at time t respectively and $g_i(T(t))$ as the development rate of individuals in stage i at temperature $T(t)$. Given the assumption that the adult egg-laying rate is unaffected by infection status (Coffey and Reisen 2016), and the fact that both infected and uninfected individuals are grouped into the same immature classes (Figure 5.4), $R_E(t)$ can be calculated using the total number of adults across the infection classes and the egg-laying rate (Appendix B). The proportion of individuals which survive from recruitment into one immature class, to maturation to the next, is defined by the following system of DDEs (unchanged from Equation 4.3),

$$\begin{aligned}
\frac{dS_E}{dt} &= S_E(t)\left(\frac{g_E(T(t))\delta_E(T(t-\tau_E(t)))}{g_E(T(t-\tau_E(t)))} - \delta_E(T(t))\right),\\
\frac{dS_L}{dt} &= S_L(t)\Bigg[\Big(\delta_\pi(t-\tau_L(t)) + \delta_L(T(t-\tau_L(t)))\Big)\left(\frac{g_L(T(t))}{g_L(T(t-\tau_L(t)))}\right)\\
&\quad - \delta_\pi(L(t)) - \delta_L(T(t))\Bigg],\\
\frac{dS_P}{dt} &= S_P(t)\left(\frac{g_P(T(t))\delta_P(T(t-\tau_P(t)))}{g_P(T(t-\tau_P(t)))} - \delta_P(T(t))\right).
\end{aligned} \tag{5.6}$$

The rate of change of the duration of the three immature life stages is given by

$$\frac{d\tau_i(t)}{dt} = 1 - \frac{g_i(T(t))}{g_i(T(t-\tau_i(t)))}. \tag{5.7}$$

where $i = E, L, P$. Here the development rate, $g_i(T(t))$, is dependent on temperature. The development of the gonotrophic cycle is given by,

$$\frac{d\tau_G(t)}{dt} = 1 - \frac{g_G(T(t))}{g_G(T(t-\tau_G(t)))}, \tag{5.8}$$

where G denotes that we are concerned with the gonotrophic cycle.

Using the same approach as was used to define the gonotrophic cycle length, one can define an analogous delay differential equation for the duration of the extrinsic incubation period. The EIP is defined as the length of time between a mosquito contracting the virus by taking an infected blood meal and the mosquito becoming infectious itself. One can consider the growth from some "development point", d_i, when the susceptible mosquito becomes exposed by taking an infected blood meal, to some later point, d_{i+1} when the exposed mosquito

becomes infectious. By defining these development points one can then follow through the same arguments as for the durations of the immature life stages and the gonotrophic cycle to give

$$\frac{d\tau_{A_E}}{dt} = 1 - \frac{g_{A_E}(T(t))}{g_{A_E}(T(t - \tau_{A_E}(t)))}, \tag{5.9}$$

where, $g_{A_E}(T(t))$ gives the rate of progression of the EIP and $\tau_{A_E}(t)$ refers to the duration of the EIP at temperature $T(t)$ and time t respectively.

The survival of adult mosquitoes through the exposed class can be defined analogously to the survival through the egg and pupal classes, as there is no density-dependent mortality in adult stages, giving

$$\frac{dS_{A_E}}{dt} = S_{A_E}(t)\left(\frac{g_{A_E}(T(t))\delta_A(T(t - \tau_{A_E}(t)))}{g_{A_E}(T(t - \tau_{A_E}(t)))} - \delta_A(T(t))\right). \tag{5.10}$$

The recruitment, maturation and transition equations for the adult mosquito stages can now be defined. Firstly, recruits into susceptible adults are given by

$$R_{A_S}(t) = M_P(t)(1 - \mathcal{V}(t)), \tag{5.11}$$

where, $(1 - \mathcal{V}(t))$ gives the proportion of emergent adult mosquitoes which are not infected through vertical transmission from their parents, at time t. The proportion of vertically infected emergent adults at time t, $\mathcal{V}(t)$, is given by the proportion of emergent adults whose parents were infectious, multiplied by the probability of vertical transmission (Nelms et al. 2013),

$$\mathcal{V}(t) = \frac{A_I(t - \tau_I(t))}{N_V(t - \tau_I(t))} p_{vt}, \tag{5.12}$$

where p_{vt} is the probability of vertical transmission from parent to child, $N_V(t)(= A_S(t) + A_E(t) + A_I(t))$ is the total number of adults vectors across all infection states at time t and $\tau_I(t)$ is the time required for development through all immature stages,

$$\tau_I(t) = \tau_P(t) + \tau_L(t - \tau_P(t)) + \tau_E(t - \tau_P(t) - \tau_L(t - \tau_P(t))). \tag{5.13}$$

It is shown in Appendix B that modelling vertical transmission in this way is equivalent to including a new set of immature stages for vertically infected individuals, given the assumption that infection status does not affect immature development or survival, as previously stated (Coffey and Reisen 2016). Given that recruitment into the exposed vector class, $R_{A_E}(t)$, can only occur by taking a blood meal from an infectious host, and that host-frequency-dependent transmission is assumed, the rate of transition out of susceptible mosquitoes is equal to the rate of recruitment into exposed mosquitoes, such that

$$\Pi_{A_S}(t) = R_{A_E}(t) = \mathcal{B}(t)A_S(t)\frac{\mathcal{T}_{BM}I_B(t)}{N_B(t)}. \tag{5.14}$$

Here $\mathcal{B}(t)$ is the per capita mosquito biting rate at time, t, such that $\mathcal{B}(t) = \frac{1}{2\tau_G(t)}$, as adult females bite once per gonotrophic cycle. The total number of birds at time t is given by $N_B(t)$. Birds are considered to be susceptible, infectious or recovered at any given point in time, such that such that $N_B(t) = S_B(t) + I_B(t) + R_B(t)$ where $S_B(t)$, $I_B(t)$ and $R_B(t)$ are the number of susceptible, infectious birds and recovered birds, respectively. The transmission probability from infected birds to susceptible mosquitoes is given by $\mathcal{T}_{BM}$.

Maturation from the exposed vector class occurs upon completion of the EIP and is given by the recruits into the exposed stage the length of the EIP, $\tau_{A_E}(t)$, ago, multiplied by the survival of exposed adults, $S_{A_E}(t)$, and a term reflecting changes in the stage duration, as observed for the immature stages (Equation 5.5),

$$M_{A_E}(t) = R_{A_E}(t - \tau_{A_E}(t))S_{A_E}(t)\frac{g_{A_E}(T(t))}{g_{A_E}(T(t - \tau_{A_E}(t)))}. \tag{5.15}$$

Finally, recruitment into infectious adult vectors is given by

$$R_{A_I}(t) = M_{A_E}(t) + M_P(t)\mathcal{V}(t), \tag{5.16}$$

such that recruits are comprised of maturations from the exposed stage plus the number of newly emergent adults which are vertically infected from their parents.

These terms can be combined to give the following set of equations for the adult infection dynamics,

$$\begin{aligned}
\frac{dA_S}{dt} &= \overbrace{M_P(t)(1-\mathcal{V}(t))}^{\text{emergent uninfected pupae}} - \overbrace{\mathcal{B}(t)A_S(t)\frac{\mathcal{T}_{BM}I_B(t)}{N_B(t)}}^{\text{host-to-vector transmission}} - \overbrace{\delta_A(t,T(t))A_S(t)}^{\text{death}}, \\
\frac{dA_E}{dt} &= \overbrace{\mathcal{B}(t)A_S(t)\frac{\mathcal{T}_{BM}I_B(t)}{N_B(t)}}^{\text{host-to-vector transmission}} - \overbrace{R_{A_E}(t-\tau_{A_E}(t))S_{A_E}(t)\frac{g_{A_E}(t)}{g_{A_E}(t-\tau_{A_E}(t))}}^{\text{maturation of exposed mosquitoes}} - \overbrace{\delta_A(t,T(t))A_E(t)}^{\text{death}}, \\
\frac{dA_I}{dt} &= \overbrace{R_{A_E}(t-\tau_{A_E}(t))S_{A_E}(t)\frac{g_{A_E}(t)}{g_{A_E}(t-\tau_{A_E}(t))}}^{\text{maturation of exposed mosquitoes}} + \overbrace{M_P(t)\mathcal{V}(t)}^{\text{emergent infected pupae}} - \overbrace{\delta_A(t,T(t))A_I(t)}^{\text{death}}.
\end{aligned} \tag{5.17}$$

5.2.3 Host SIR model

The bird population can be split into susceptible, infectious and recovered birds, using the SIR framework first described in Kermack and McKendrick (1927). A system of ODEs is used to describe the bird population, with stage transitions which occur instantaneously upon biting, due to the short time period required for birds to develop high viremia, as previously discussed (Section 5.2.1). The host competencies of these species is unknown in many cases due to the lack of research into WNV infection in resident UK bird populations. Consequently, I model the bird population as a single species, taking values for transmission processes which correspond to average reported values across many species. Avian transmission processes are modelled subject to the following assumptions

- Bird species which act as hosts of WNV typically exhibit high viremia within a day of contracting the virus (Komar et al. 2003). No studies have investigated the spread of the virus within birds at a time scale of less than one day. Given this, and the speed with which birds have been shown to become infectious, I assume that infection of birds happens instantaneously, meaning that an exposed period was not required for the bird population. Infectious birds then recover at a constant rate, $\mathcal{R}$.
- Recovered birds have been shown to develop WNV antibodies (Gibbs et al. 2005; Gibbs et al. 2006; Nemeth et al. 2009) and therefore are assumed to be immune to WNV and will not become infectious if bitten by an infectious vector.

- McKee et al. (2015) showed that WNV antibodies decay in free-ranging birds, with an average period of 2 years. Given that I only investigate results in the year immediately following WNV introduction, any possible loss of immunity in subsequent seasons is ignored.
- Gibbs et al. (2005) showed that maternal antibodies were present for the first few weeks of rock pigeons lives. However, the short duration of these antibodies presence combined with the lack of age-structure in the modelled avian population means that I assume WNV immunity cannot be inherited within bird populations.
- Host-host transmission (Komar et al. 2003) is assumed to occur between infectious and susceptible birds.
- WNV infection is known to result in increased mortality in certain bird species (Komar et al. 2003). Consequently, a WNV-induced death rate is assumed to affect infectious birds.
- Mosquitoes are known to be more attracted to malaria-infected birds than uninfected birds (Cornet et al. 2013). However, similar studies investigating WNV infection are yet to be carried out. As such, mosquitoes are assumed to feed on each infection class of bird according to its relative abundance in the bird population, independent of infection status.
- The ability of birds to act as hosts of WNV has been shown to vary across species (Komar et al. 2003). For simplicity, I assume that all birds are equally competent hosts of WNV and conduct a sensitivity analysis on this competence level.
- In absence of data allowing quantification of any effects of WNV infection on ability to compete for resources I assume that density-dependent mortality affects all infection classes of birds equally.

Given these assumptions, the rate of change of susceptible birds at time t is given by

$$\begin{aligned}\frac{dS_B(t)}{dt} = &\overbrace{b_B(t)N_B(t)}^{\text{births}} - \overbrace{\mathcal{B}(t)\mathcal{T}_{MB}A_I(t)\frac{S_B(t)}{N_B(t)}}^{\text{vector-to-host transmission}} - \overbrace{p_{hh}\frac{I_B(t)S_B(t)}{N_B(t)}}^{\text{host-host transmission}} \\ &- \underbrace{(\delta_B - h(t)N_B(t))S_B(t)}_{\text{death}},\end{aligned} \tag{5.18}$$

where p_{hh} is the host-host transmission rate and $\mathcal{T}_{MB}$ is the transmission probability when an infected mosquito bites a susceptible bird. All births enter the susceptible stage because

of the assumption that newborns could not inherit WNV immunity from their parents. The infectious bird population is described by

$$\frac{dI_B(t)}{dt} = \overbrace{\mathcal{B}(t)\mathcal{T}_{MB}A_I(t)\frac{S_B(t)}{N_B(t)}}^{\text{vector-to-host transmission}} + \overbrace{p_{hh}\frac{I_B(t)S_B(t)}{N_B(t)}}^{\text{host-host transmission}} - \overbrace{(\delta_B + \delta_{WNV} - h(t)N_B(t))I_B(t)}^{\text{death}} - \underbrace{\mathcal{R}I_B(t)}_{\text{recovery}}, \tag{5.19}$$

where $\mathcal{R}$ gives the rate of recovery of WNV-infected birds and δ_{WNV} gives the rate of death due to WNV. Finally, the recovered bird population is modelled by

$$\frac{dR_B(t)}{dt} = \overbrace{\mathcal{R}I_B(t)}^{\text{recovery}} - \overbrace{(\delta_B - h(t)N_B(t))R_B(t)}^{\text{death}}. \tag{5.20}$$

5.3 Methods: Vector and WNV functional forms and parametrisation

5.3.1 Mosquito functional forms and parametrisation

All vector life cycle functional forms are as described in the updated model in Chapter 4 (Section 4.3), with the exception of density-dependent mortality due to predation, which is assumed not to experience seasonal forcing, as discussed in Appendix C. Only the functional form for the EIP has not been defined previously.

Extrinsic incubation period (EIP)

The EIP is the time required for the virus to replicate in the mosquito to a level where mosquitoes become infectious. This time period is strongly dependent on temperature, with higher temperatures leading to shorter EIPs (Dohm et al. 2002b; Reisen et al. 2006a). The majority of WNV models which incorporate an exposed stage in the vector population assume a fixed duration for the EIP (Table 5.1). Temperatures in the UK show fluctuations which include values both within and outwith the range for which incubation of the virus is possible (Figure 5.6). Consequently, it is likely that intra-annual temperature variation will

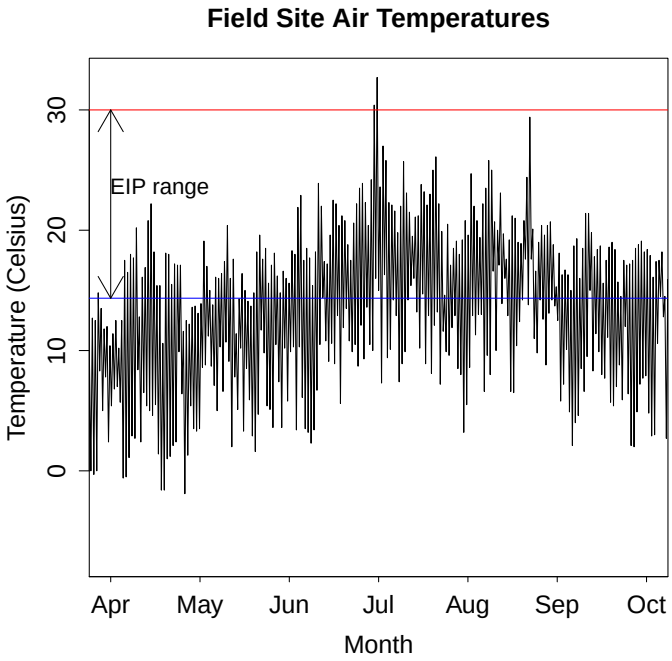

Figure 5.6: Field site air temperatures: The air temperatures at the Wallingford field site in 2015 are shown. The blue line shows the lower thermal threshold at which progression of the EIP can take place. The red line at $30\,^{\circ}\mathrm{C}$ represents the highest temperature at which the EIP duration was recorded in the laboratory experiments (Reisen et al. 2006a).

be an important determinant of transmission potential throughout the season.

Many studies compare vector competence across mosquito species by investigating the proportion of exposed mosquitoes which have become infectious after a given time (Jupp and McIntosh 1970; Jupp 1976; Turell et al. 2001; Sardelis et al. 2001; Tiawsirisup et al. 2004; Turell et al. 2005; Erickson et al. 2006), rather than intensively studying transmission for one species. Consequently, these studies typically compare competencies by examining the difference in infection prevalence across species held for a fixed time at one fixed temperature. Such studies allow for estimation of vector-host transmission probabilities at fixed temperatures but do not enable parameterisation of a temperature-EIP relationship. The relationship between temperature and WNV EIP duration has been studied relatively infrequently across a small number of mosquito species (Cornel et al. 1993; Dohm et al. 2002b; Reisen et al. 2006a). The most extensive such study, in terms of the range of temperatures examined and the sampled number of mosquitoes at each temperature, was carried out by Reisen et al. (2006a). The authors examined incubation times in *Cx. tarsalis* at $10, 14, 18, 22, 26$ and

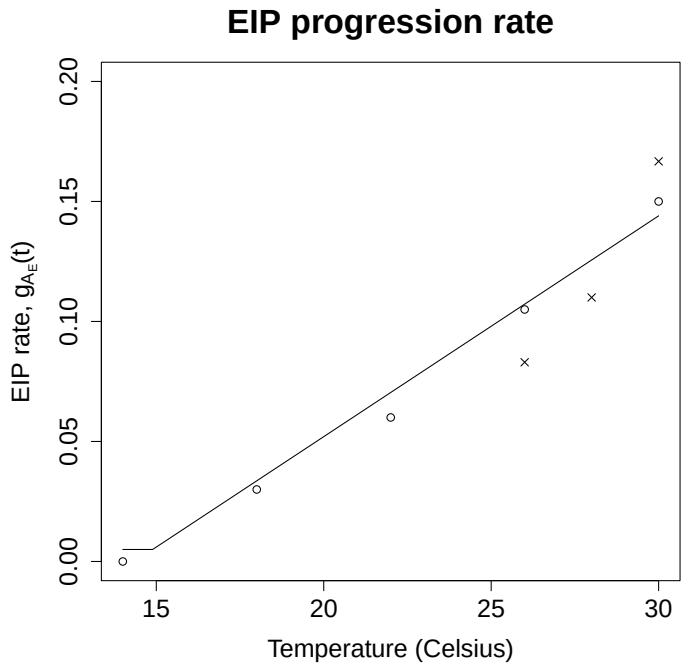

Figure 5.7: EIP rate: The EIP progression rate at a range of temperatures for *Cx. tarsalis* is shown in by circles, using data from (Reisen et al. 2006a). The crosses correspond to EIP estimates for *Cx. pipiens* (Dohm et al. 2002b; Goddard et al. 2003). The values correspond to the median EIP observed at each temperature.

$30\,^{\circ}\mathrm{C}$, finding that the rate of incubation increased linearly with temperature according to

$$g_{A_E}(T(t)) = \begin{cases} \alpha_{\mathcal{X}} T(t) - \beta_{\mathcal{X}} & : T(t) \geq 14.35\,^{\circ}\mathrm{C}, \\ 0 & : T(t) < 14.35\,^{\circ}\mathrm{C}, \end{cases} \tag{5.21}$$

where $\alpha_{\mathcal{X}}$ and $\beta_{\mathcal{X}}$ are fitted constants (Figure 5.7).

Figure 5.7 shows that the EIP calculated for *Cx. pipiens* (Dohm et al. 2002b; Goddard et al. 2003) at three temperatures gives good agreement with the *Cx. tarsalis* data. Dohm et al. (2002b) also show that *Cx. pipiens* can complete the EIP at lower temperatures of $18\,^{\circ}\mathrm{C}$ and $20\,^{\circ}\mathrm{C}$, however the authors' laboratory experiment did not track the population for sufficient time at these temperatures to provide an estimate of the EIP which was suitable for comparison with the *Cx. tarsalis* data. Since *Cx. tarsalis* shares its North American range with *Cx. pipiens*, both species have been shown to exhibit similar EIPs at similar temperatures, and there is a lack of appropriate *Cx. pipiens* data, I assume that the published temperature-EIP relationship for *Cx. tarsalis* can be used in this case.

I make a slight modification to the linear relationship in Equation 5.21, such that

$$g_{A_E}(T(t)) = \begin{cases} \alpha_{\mathcal{X}} T(t) - \beta_{\mathcal{X}} & : T(t) \geq 14.89\,^{\circ}\mathrm{C}, \\ 0.005 & : T(t) < 14.89\,^{\circ}\mathrm{C}, \end{cases} \tag{5.22}$$

thus constraining the rate of EIP progression not to drop below 0.005 to avoid dividing by zero when calculating the stage duration (Equation 5.9). The lower bound of 0.005 results in an EIP of 200 days at low temperatures, which will not affect transmission within a single season. EIP duration above $30\,^{\circ}\mathrm{C}$ has not been measured in the laboratory. Consequently, I assume a continuation of the stated linear relationship at temperatures above $30\,^{\circ}\mathrm{C}$. This is unlikely to affect results due to the rarity of temperatures exceeding this threshold in the UK (Figure 5.6) and the high mosquito adult mortality rate at temperatures above $30\,^{\circ}\mathrm{C}$ (Equation 4.10).

5.3.2 WNV transmission parameters and processes

The full set of WNV transmission parameter values used in the model, alongside the ranges observed in the literature are presented in Table 5.2. In the subsections below I present a discussion of the parameter values given in Table 5.2.

Process	Parameter	Value	Range	Source
Vector-host transmission	$\mathcal{T}_{MB}$	0.88	0.86 – 0.88	1-2
Host-vector transmission	$\mathcal{T}_{BM}$	0.4	0-0.68	3
Host-host transmission (day^{-1})	p_{hh}	0.33	-	3-4
Vertical transmission	p_{vt}	0.004	0.00004 – 0.0081	5-9
Recovery (day^{-1})	$\mathcal{R}$	0.25	0.18 – 1	3
WNV mortality (day^{-1})	δ_{WNV}	0.16	0.11 – 0.22	3
Vector-to-host ratio	ι	~ 5	0.8-8.9	3,11,15
No. of infected migrants	M_{inf}	2	0 – 50	12
Infection arrival date	t_{arr}	31st May	1st Mar - 31 May	13
EIP parameters (degrees^{-1} day^{-1})	$\alpha_{\mathcal{X}}$	0.0092	-	14
	$\beta_{\mathcal{X}}$	0.132	-	14

Table 5.2: Transmission parameters: A table showing the values taken for the various disease transmission processes, alongside the range of these parameters found in the literature. Sources: 1 - Turell et al. (2000), 2 - Turell et al. (2001), 3 - Komar et al. (2003), 4 - McLean et al. (2001), 5 - Nelms et al. (2013), 6 - Anderson and Main (2006), 7 - Anderson et al. (2008), 8 - Dohm et al. (2002a), 9 - Reisen et al. (2006b), 10 - McKee et al. (2015), 11 - Cruz-Pacheco et al. (2005), 12 - Bessell et al. (2014), 13 - BTO (2017), 14 - Reisen et al. (2006a), 15 - Durand et al. (2010).

Vector-host ratios

Vector-host ratios are often overlooked in WNV models due to difficulties in their estimation, with half of the models in Table 5.1 making no reference to the choice of vector-host ratio or choosing arbitrary values which are not grounded in field data. Other models justify their choice of vector-host ratio by referencing previous modelling studies (Maidana and Yang 2009; Marini et al. 2017), which based their values on laboratory experiments that are unlikely to be representative of field conditions (Cruz-Pacheco et al. 2005). This leads to a wide range of vector host ratios being used across WNV models, with those studies detailed in Table 5.1 using values in the range of 0.33-5000 vectors per host. However, these values are often not well supported by field observations.

Durand et al. (2010) estimated vector-host ratios at a European site and at both dry and wet sites in Africa, using observed seroprevalence data in bird populations. The authors assumed that the numbers of tested and seropositive birds arose from a binomial process, such that maximisation of the log-likelihood of this data, given estimated transmission parameters, could enable estimation of the relative sizes of both populations in the field. It was found that the estimated vector-host ratio was highest for the dry African site ($14.1, 95\%$ CI: 7.5–26.5) and lowest for the European site ($2.6, 95\%$ CI: 0.8–8.9), with the range of estimates across all sites as 0.8-26.5.

The majority of WNV models do not incorporate seasonality in the vector or host populations (Table 5.1), meaning that the vector-host ratio can be considered as static. In reality, by including the effects of seasonality on population sizes, particularly in vectors, the vector-host ratio will show intra- and inter-annual fluctuations. I choose the avian carrying capacity such that the vector-host ratio is approximately 5 at the peak in mosquito abundance, given the conditions at the Wallingford field site. Given the variation in mosquito abundance throughout the season, this means that vector-host ratio is approximately 2.5 at the start of the biting season, though this value is dependent on the parameter values chosen. These values correspond with the estimated range of vector-host ratios for the European site studied by Durand et al. (2010). I perform a sensitivity analysis on vector-host ratios from 0 to 20 to understand the effects of varying the vector-host ratio on abundance of infectious mosquitoes (Section 5.5.2).

WNV transmission pathways

Mosquito to bird transmission probability, $\mathcal{T}_{MB}$, has been shown to take values in the range 0.86-0.88 in the literature (Turell et al. 2000; Turell et al. 2001). I chose to use a baseline value of 0.88, presented in Turell et al. (2001), as the sample size in this study was over twice the sample size in Turell et al. (2000), which presented a very similar estimate of 0.86.

Komar et al. (2003) found in a laboratory study that the host competence, which gives the transmission probability from an infectious bird to a susceptible host, $\mathcal{T}_{BM}$, varied in the range 0-0.68 across 25 bird species. I choose a baseline value of 0.4 as this fits well with the observed transmission rates for many of the studied bird species.

Rates of host-host transmission may vary by bird species, however relatively few studies have quantified transmission rates (Dawson et al. 2007; Hinton et al. 2015). The baseline host-host transmission rate was taken as the reported contact transmission rate in crows (p_{hh} = 0.33) after Hartemink et al. (2007).

Vertical transmission of WNV from infected adult female mosquitoes to their offspring has been shown to occur in *Cx. pipiens* at low rates (0.04-8.1 infected adults per 1000 eggs) (Dohm et al. 2002a; Anderson and Main 2006; Reisen et al. 2006b; Anderson et al. 2008; Nelms et al. 2013). Consequently, I assume vertical transmission occurs at a low rate, given in Table 5.2.

Host WNV recovery and mortality rates

There is some evidence that more highly competent hosts of the virus may recover more slowly from infection, due to the increased viremia levels in their system (Komar et al. 2003). However, recorded mean recovery times rarely exceed 4 days for the most competent species, so I took the conservative baseline estimate that all species recovered in line with the rate observed in highly competent species.

Komar et al. (2003) observed mean time periods from infection to death ranging from 4.5 to 9 days across eight bird species following infection from WNV. I choose a baseline value corresponding to a mean longevity of 6 days after infection, as this was the most commonly observed time of death.

Arrival of WNV in the population

WNV is assumed to be introduced to the bird population through the arrival of infected migratory birds, as discussed in Bessell et al. (2014). Given the complexities of modelling migration across a wide range of bird species, I make the simplifying assumption that the arrival and departure of migratory birds does not influence patterns of seasonal abundance of the total bird population. Given this, the arrival of WNV in the model occurs as a result of a perturbation to the system, where the number of infectious birds arriving, $\mathcal{M}_{inf}$, is added to the infectious bird class, $I_B(t)$, at some time, t_{arr}. The number of infectious birds arriving, $\mathcal{M}$, is taken from the findings of Bessell et al. (2014), who simulated the arrival of WNV-infected birds in the UK following outbreaks in different regions of France. These infectious individuals are added to the system using the event finder and change function in the DDE solver code (Thompson and Shampine 2004). The range of these values is given in Table 5.2. Infectious birds are assumed to arrive between the 1st of March and the 31st of May, based on data from the British Trust for Ornithology (BTO 2017). I chose the latest anticipated arrival time of May 31st as the baseline value to ensure that infection arrival occurred after adult emergence of the first spring generation. I assume that only one introduction will occur within a given year. I carry out a detailed investigation of the effect of the infection arrival time on disease transmission.

As previously discussed in Section 5.2.3, I assume that mosquitoes bite each infection class of bird according to the relative abundance of that infection class in the population. Consequently, the total size of the bird population to which the infectious individuals are added will affect the initial prevalence of infection in the bird population and the rate of disease transmission immediately following virus introduction. In field conditions, the size of the total bird population at the introduction site will be variable, dependent on the destination of the infected birds, which will depend on the species of the infected migrants. Therefore, a sensitivity analysis investigating the effect of infection rate in the bird population, at the time of virus introduction, $\mathcal{P}_{inf}$, was conducted.

5.3.3 Proportion of infectious mosquitoes versus infectious mosquito density

Infection in the vector population is commonly presented either as the MIR or as the density of infectious mosquitoes within a given region. The density of infectious mosquitoes is the more informative measure when considering a specific region, for which one has confidence in the estimate of the total mosquito population size or density. In such cases, by considering

the density of infectious individuals, it is possible to understand the number of infectious bites which are expected to occur in a given time period and to predict the risk to humans. However, in the case where considerations are not being made about a specific region, or where information about mosquito habitat in that region is lacking, the total population size or density will not be well known. In this case, the MIR may be the more appropriate measure of infection risk to humans because it will not be influenced by uncertain estimates of population size.

The presence and volume of larval breeding sites will vary substantially both temporally and geographically across the UK. The number and size of breeding sites in a given area will substantially influence the model estimates of mosquito population size and therefore density of infectious mosquitoes. Further, changes in the population size induced by variation in breeding site availability will affect vector-host ratios. In order to estimate infectious mosquito density it would be necessary to determine and include the volume of larval habitat for the region in question. I make the simplifying assumption of a closed system, where the only breeding habitat available is provided by one water butt, as used in the fieldwork. Given a flight range of 1.25km for *Cx. pipiens* (Ciota et al. 2012; Hamer et al. 2014), this corresponds to the expected number of infectious mosquitoes per 5km^2. This allows comparisons to be drawn between simulations and the relative sizes of infectious populations to be determined. I also present results using the MIR, for comparison with observed infection rates across the *Cx. pipiens* range.

5.4 Methods: Model history and initial conditions

The inoculation and history processes remain unchanged from those used in Section 4.3.2. For historical values, $t < 0$, it was assumed that temperatures were constant and equal to the first temperature observation corresponding $t = 0$. The adult mosquito population was inoculated on the 1st of January 2015 with 5000 individuals. Simulations were run over two years, with infection introduced and results studied for the second year. This allowed effects of each temperature regime to be studied once the population had settled to a size determined by the predicted temperature conditions.

5.4.1 Aims and simulation plan

I now carry out four groups of simulations to investigate potential transmission risks of WNV in the UK under different scenarios. In all cases, I use the parameter values specified in

Tables 4.1 and 5.2 and the highest resolution water and air temperatures experienced at the CEH Wallingford field site in 2015, unless otherwise stated.

1. **WNV transmission predictions for CEH Wallingford temperature conditions:** I present the WNV transmission dynamics following an introduction of WNV (on May 31st) given temperature conditions measured at the Wallingford field site in 2015. In doing so, I explore whether or not disease transmission is thought to be possible under current UK field conditions.

2. **Sensitivity of disease transmission to WNV transmission parameters:** I investigate the sensitivity of infectious vector density to changes in disease transmission parameters by varying the parameters within their estimated ranges, as given in Table 5.2. I relate the magnitude of the changes in infectious mosquito density to the uncertainty in estimation of each parameter. The changes to infectious mosquito density are quantified by examining the changes in both the peak density of infectious mosquitoes on a given day and the average density of infectious mosquitoes per day during the biting season. This allowed me to understand if any possible predicted WNV outbreaks were strongly dependent on estimated values of particular transmission parameters. In doing this I place particular emphasis on the effect of timing of introduction of the virus on subsequent transmission.

3. **Contributions of EIP duration and biting rate to WNV transmission:** I investigate the relative contributions of the EIP duration and the biting rate to potential WNV transmission (Figure 5.11) and explore the effects of the common model assumption that these processes can be approximated using constant values. I do this by holding each of these processes constant at a commonly used value from the literature in turn and running simulations as described above. I investigate the effects of these parameters on the percentage of birds which are infectious and the MIR in vectors.

4. **Potential WNV transmission under warming scenarios:** Finally, I investigate warming scenarios to understand the predicted impacts of anticipated temperature increases on the likelihood that WNV will be established in the UK between now and the 2080s. I consider the effects of climate warming alongside the effects of varying the time of introduction of WNV.

5.5 Results

5.5.1 WNV transmission predictions for temperature conditions measured at the Wallingford field site

Figure 5.8 shows the full time series for the density of each mosquito life stage and each mosquito and avian infection class. Figure 5.8 (a)-(d) shows that mosquito seasonal abundance patterns are not substantially changed from the disease-free case (Figure C.1), as the predicted density of exposed and infectious mosquitoes is well below 1 throughout the full year (Figure 5.8 (e)-(f)). Similarly, seasonal abundance of susceptible birds (Figure 5.8 (g) shows negligible difference to the pattern of abundance in the absence of infection (Figure 5.5 (b)). Infectious birds show a small peak in abundance at the introduction time (Figure 5.8 (h)), however these infectious birds quickly recover or die, leaving low rates of infection in the bird population. I predict that an outbreak of WNV would not be possible at the Wallingford field site if WNV were to be introduced at the end of May.

5.5.2 Sensitivity analysis of WNV-related parameters

I conducted a sensitivity analysis, following WNV introduction at the end of May, to quantify the influence exerted by each of the WNV transmission parameters in Table 5.2 on infectious mosquito density. I investigated if the prediction that WNV outbreaks would not occur at the Wallingford field site would be altered by changing any of these transmission parameters within their known ranges. All simulations are run according to the procedure and using parameter values described in Sections 5.4 and 5.4.1, with only the parameter of interest varied in each case.

The infectious mosquito density was more sensitive to the probability of host-vector transmission, $\mathcal{T}_{BM}$, across the parameter range studied than the probability of vector-host transmission, $\mathcal{T}_{MB}$ (Figure 5.9 (a)-(b)). The range of values of vector-host transmission from the literature was very small (0.86-0.88 Table 5.2) but, even considering values outwith this range ($0.6-1$), increasing transmission led to small increases in infectious mosquito density. Conversely, host-vector transmission probabilities are known to be very variable (Komar et al. 2003) and increasing or decreasing values within the stated range ($0-0.68$) leads to corresponding increases or decreases in infectious mosquito density of $\pm 100\%$. It is unlikely that values as extreme as 0 or 0.68 would occur in nature because these values would correspond

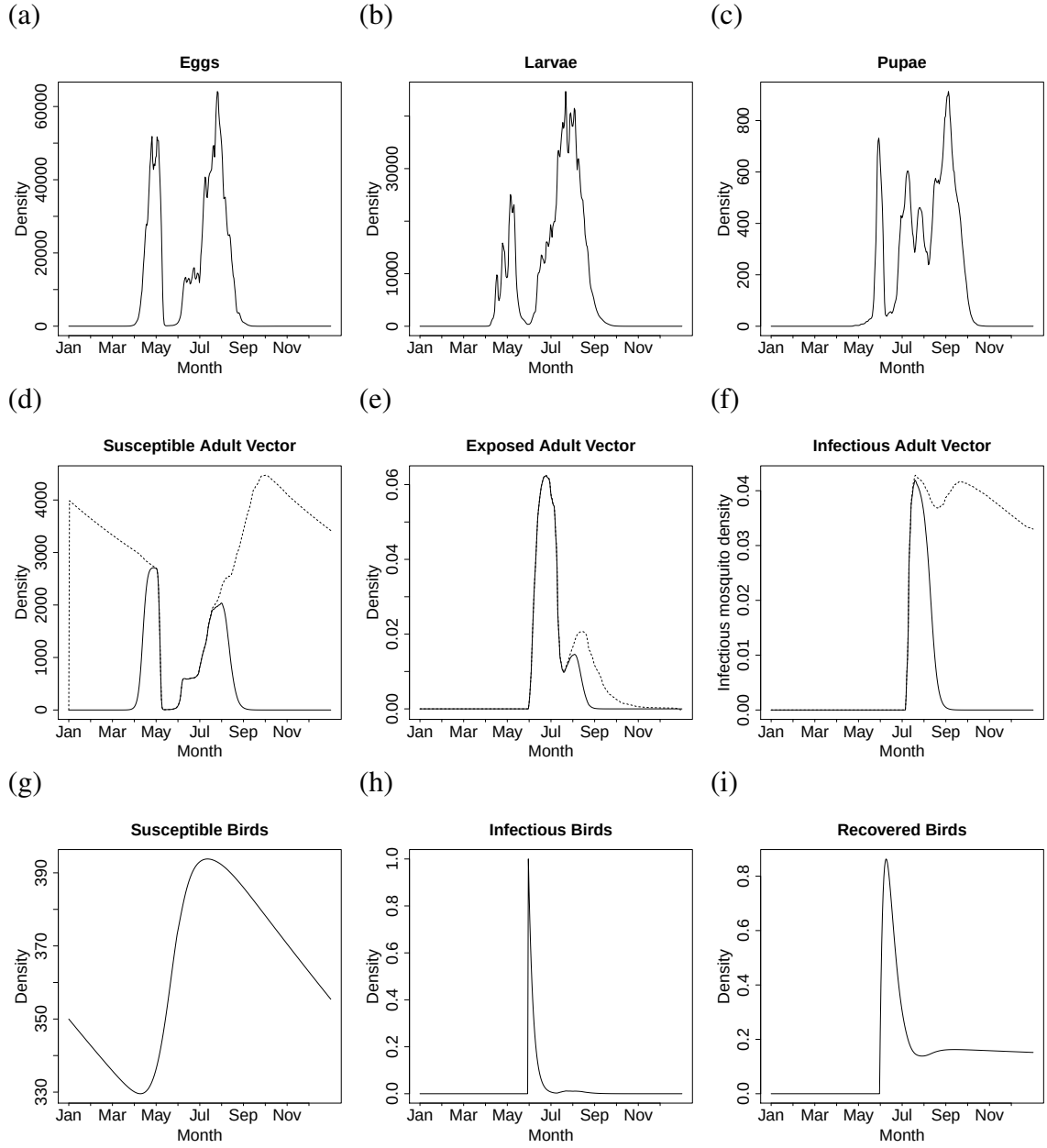

Figure 5.8: Disease predictions: The plots show time series of predicted densities of each life stage and infection class for hourly water temperatures taken from butt 4 and minimum and maximum daily air temperatures from Wallingford. As in Chapter 4, the dotted lines show all adults whilst the solid lines show only active (biting) adults. All WNV parameters are as in Table 5.2.

to populations composed entirely of incompetent or highly competent hosts, respectively. However, the average competence of field populations are likely to vary within the stated range.

Host-host transmission, p_{hh}, was shown to be a much more influential determinant of disease transmission than vertical transmission between mosquitoes (Figure 5.9 (c)-(d)), supporting

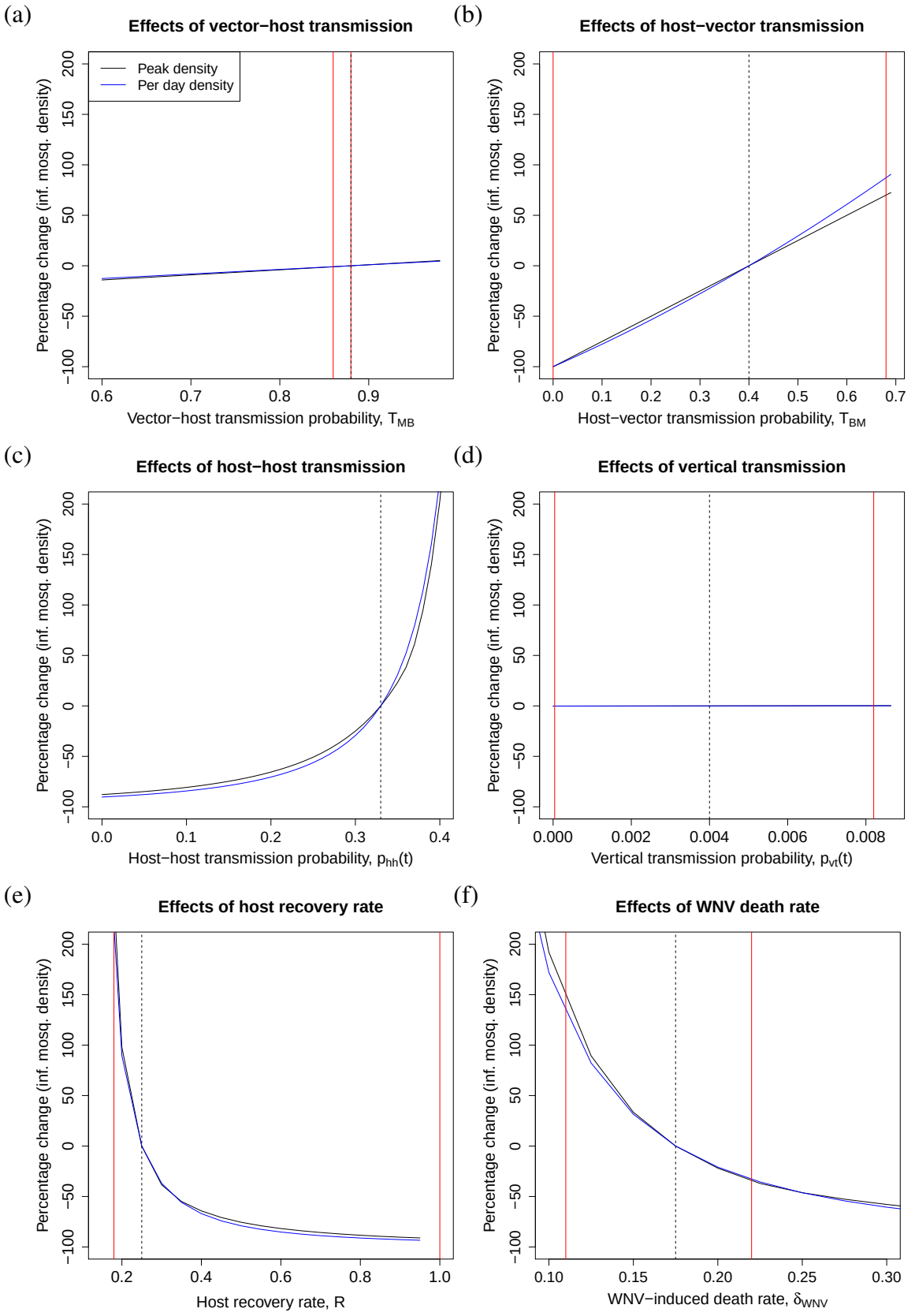

Figure 5.9: Sensitivity analysis: Sensitivity analyses are shown for the parameters in Table 5.2. The black lines show the percentage change in the maximum predicted density of infectious mosquitoes at any point in the year. The blue lines show the percentage change to the average density of infectious mosquitoes per day during the months of April to August, which correspond to the main active mosquito season (calculated as $\frac{1}{243-91}\int_{91}^{243} A_I(t)dt$). The dotted black line shows the baseline value assumed for the given parameter across the other simulations. Red lines show the range of predicted values from the literature, where a range could be determined.

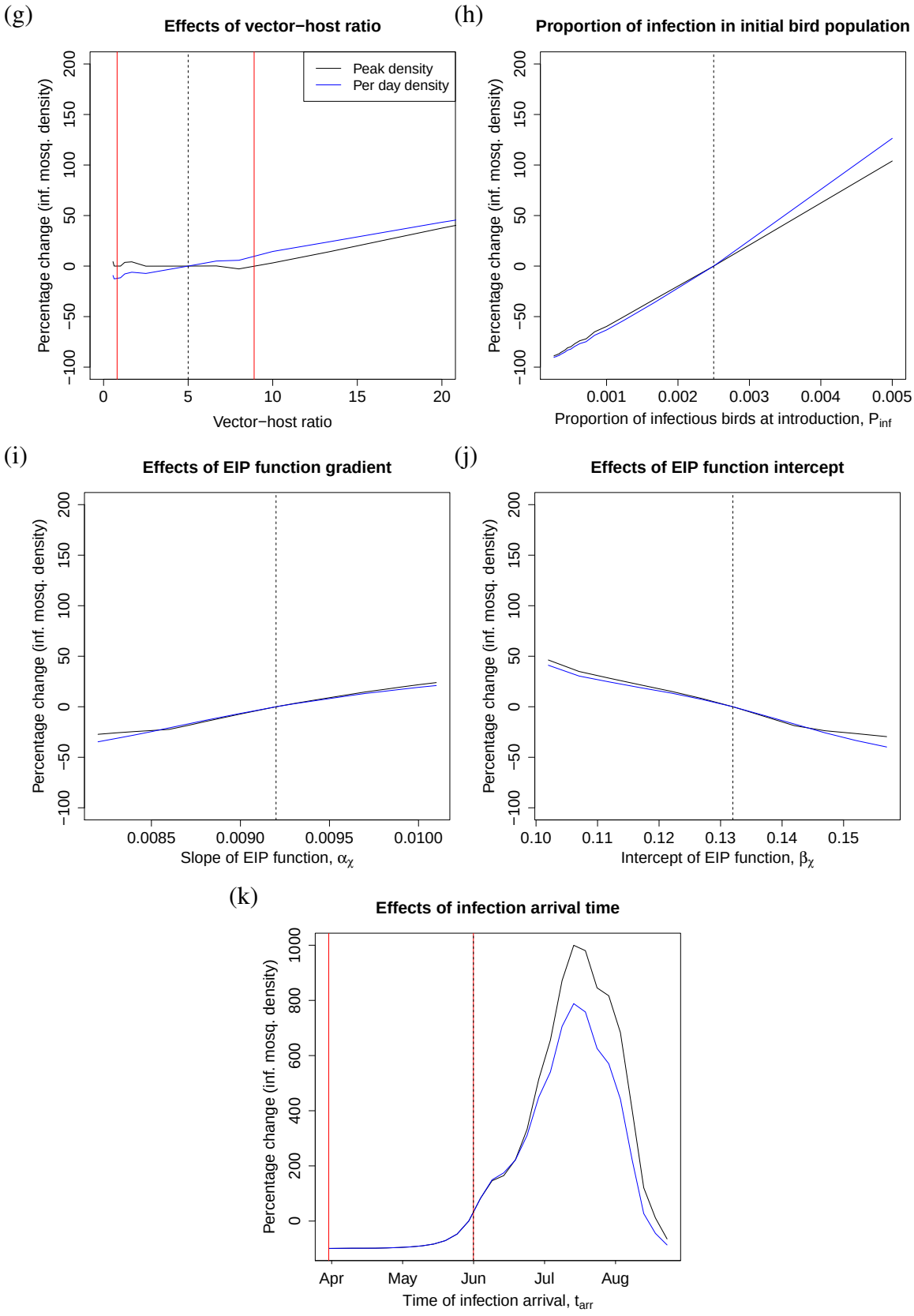

Figure 5.9: Sensitivity analysis (continued): Sensitivity analyses are shown for the parameters in Table 5.2. The black lines show the percentage change in the maximum predicted density of infectious mosquitoes at any point in the year. The blue lines show the percentage change to the average density of infectious mosquitoes per day during the months of April to August, which correspond to the main active mosquito season (calculated as $\frac{1}{243-91}\int_{91}^{243} A_I(t)dt$). The dotted black line shows the baseline value assumed for the given parameter across the other simulations. Red lines show the range of predicted values from the literature, where a range could be determined.

the findings of Hartemink et al. (2007). Vertical transmission was observed to have almost no effect on transmission within a given season, due to the very low rates observed. Host-host transmission had a very large impact on disease transmission within a season, with small increases to the baseline value inducing large increases in infectious mosquito density (Figure 5.9 (c)). However, it is likely that field host-host transmission rates will be lower than the baseline value, rather than higher, because the current value was taken from crows, which are known to be strongly affected by WNV infection (Komar et al. 2003). When considering the full range of potential hosts, host-host transmission is therefore thought likely to be lower than was observed for crows.

The host recovery rate, $\mathcal{R}$, was shown to strongly influence the density of infectious mosquitoes (Figure 5.9 (e)). Even small increases to the duration of infection in hosts led to steep increases to the density of infectious mosquitoes. Increasing the duration of infection from 4 days to 5.5 days led to an approximate 200% increase in infectious mosquito density, whilst reducing this duration to 2 days reduced infectious mosquito density by approximately 70%. The likelihood of observing an average recovery rate as low as 0.18 (giving a recovery time of 5.5 days) across the host population is very low, as this recovery rate corresponds to the lowest observed rate across 25 bird species studied by Komar et al. (2003). As such, a 200% increase in infectious mosquito density is very unlikely.

The WNV-induced death rate, δ_{WNV}, showed similar effects on infectious mosquito density to the recovery rate (Figure 5.9 (f)), as decreasing the death rate increased the duration for which infectious birds will survive to transmit the virus. Values for the WNV-induced death rate from the literature suggest that the lowest recorded death rates would approximately double infectious mosquito density, whilst the highest recorded estimates would approximately half this density.

Increasing the vector-host ratio from the baseline value was seen to approximately linearly increase both the peak and the daily infectious mosquito density after a threshold value of 10 (Figure 5.9 (g)). Reductions to the size of the peak in vector infection, upon decreasing vector-host ratio, tailed off at lower values because due to the very low rates of infection in the mosquito population. Within the range of vector-host ratios found by Durand et al. (2010) for a European site, the vector-host ratio had little effect on infectious mosquito density due to the very low rates of infection in the population.

The proportion of the bird population which is comprised of infectious individuals at the time

of introduction, $\mathcal{P}_{inf}$, which will be influenced by the number of infectious arrivals, $\mathcal{M}_{inf}$, and the size of the resident population, will have a large effect on outbreak potential (Figure 5.9 (h)). Decreasing $\mathcal{P}_{inf}$ from the baseline value of 0.25% led to an approximately linear decrease in infectious mosquito density. Doubling $\mathcal{P}_{inf}$ increased the infectious mosquito density by nearly 100%, however it seems unlikely that such high values would be observed in the field. Bessell et al. (2014) predict that, given a WNV outbreak in the Camargue, the most likely number of infectious birds to arrive is two per year. Assuming that both birds migrate to the same area, this high prevalence of infection would require that infectious migrants made up 0.5% of the total bird population at the introduction site. Given this, P_{inf} values at the lower end of the studied values appear to be more likely.

The EIP function parameters, α_χ, and β_χ, were both shown to have moderate impacts on infectious mosquito density, with changes in the chosen range leading to changes of at most $\pm 50\%$ (Figure 5.9 (i)-(j)).

Finally, Figure 5.9 (k) shows that the peak annual density of infectious mosquitoes is very sensitive to the timing of arrival of infection. Shifting the arrival time before the baseline value of the 31st of May quickly led to nearly 100% reduction in infectious mosquito densities due to the post-diapause mortality killing of the exposed mosquitoes. When infection arrived before mortality of the post-diapause adult females and the emergence of the spring generation, the virus died out very quickly (Figure 5.9 (k)). This occurred because the mosquitoes which fed on the infectious birds did not survive long enough to become infectious and were wiped out by the post-diapause mortality. Infectious mosquito population size steadily increased when introduction moved from early May to mid-July, as introduction then occurred when temperatures were warmer and vector-host ratios were higher. After mid-July, introduction led to decreasing infectious mosquito populations because the window of time during which transmission could occur before mosquitoes entered diapause was short.

With the exception of the timing of WNV introduction, the most influential parameters investigated above result in changes of within the range of -100% to $+200\%$. Given the very low predicted prevalence of infection at the field site, infectious mosquito densities above one are not expected even at the most extreme ends of these parameter ranges. Even considering the very large effects of the timing of WNV introduction (Figure 5.9 (k)), infectious mosquito densities are predicted to remain below one for introduction at any point of the year.

5.5.3 How is WNV transmission suppressed under the current observed field conditions?

The increased prevalence of infection in the mosquito population when infectious individuals are added to the model later in the year (Figure 5.9 (k)) stems from the warmer conditions at this point. The increased disease transmission when infection arrives in summer, instead of spring, implies that the higher temperatures may increase disease transmission through one or more of the following processes:

1. Increased temperature in the summer months decreases the length of the EIP (Figure 5.10 (a)), increasing the number of infectious mosquitoes.
2. Increased temperature increases the mosquito biting rate (Figure 5.10 (b)), leading to increased rates of virus transmission between mosquitoes and birds.
3. The increased vector-host ratio in summer means that infectious birds are bitten more often, increasing transmission.

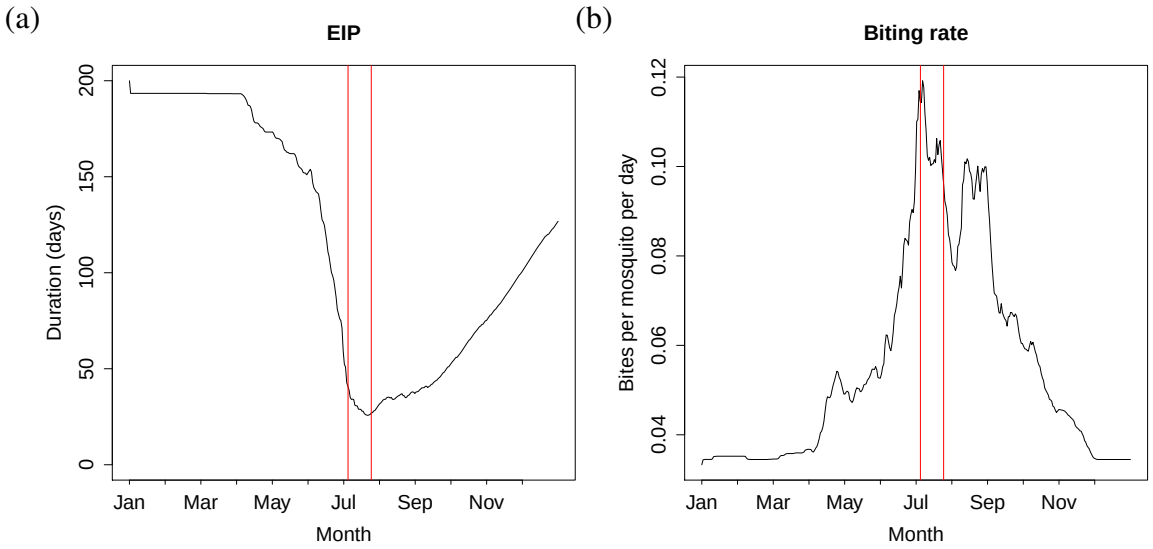

Figure 5.10: Disease transmission processes: (a) shows the estimated duration of the EIP throughout the year given the air temperatures experienced. (b) shows the predicted biting rate throughout the year given the air temperatures experienced. The red lines show the period over which virus introduction led to a predicted mosquito density greater than one.

Figure 5.10 (a) shows that the predicted duration of the EIP is very long (> 100 days) until June. This contrasts with values used in other WNV models for Europe and North America, where the duration of the EIP is generally assumed to be 1-2 weeks (Wonham et al. 2004; Durand et al. 2010; Pawelek et al. 2014; Bergsman et al. 2015). This difference in EIP duration occurs because my model allows the EIP to vary in response to temperature, where more traditional models assume a fixed EIP corresponding to average temperatures above

those observed in the UK (Wonham et al. 2004; Durand et al. 2010; Pawelek et al. 2014; Bergsman et al. 2015). Given the assumed relationship between the temperature and EIP, an EIP of 1-2 weeks would require temperatures of 22-30 °C. Similarly, my model predicts a mosquito biting rate below 0.06 before June, whereas WNV models commonly take values in the range 0.125-0.25 at all points in the year (Lord and Day 2001; Cruz-Pacheco et al. 2005; Durand et al. 2010). Based on the relationship between temperature and gonotrophic cycle length used, biting rates within this common range would require temperatures above 20 °C. The temperatures required to reach biting rates and EIP durations typically used by WNV models are common in areas of Europe and North American where WNV currently circulates, however they exceed those observed at the UK field site in spring. This causes a large mismatch between the predicted duration of the EIP in the UK when compared with models tuned to areas where WNV is currently transmitted.

I ran a number of simulations to understand the relative contributions of the EIP duration and the biting rate to WNV transmission (Figure 5.11), as described in Sections 5.4 and 5.4.1. By including the temperature dependencies of these processes in turn, I aimed to understand if the lack of disease transmission in the UK could be attributed to low temperatures causing prohibitively low biting rates or long EIPs.

Figure 5.11 (a) shows that holding the EIP constant at 10 days (Wonham et al. 2004; Pawelek et al. 2014; Bergsman et al. 2015) led to a small increase in MIR, when compared to the temperature-dependent case. Fixing the gonotrophic cycle length at 4 days (and consequently the biting rate at 0.25) (Durand et al. 2010) caused a similar increase in MIR, though this occurred later in the year due to the longer estimate of the EIP (Figure 5.11 (c)). Holding both the biting rate and EIP constant increased the MIR substantially, leading to the largest prediction from any scenario. Removing the temperature-dependence from both processes led to a substantially increased MIR, with the MIR approaching 1.5 by the end of the biting season (Figure 5.11 (e)). The profiles of infectious bird densities shown in Figures 5.11 (b), (d) and (f) parallel the mosquito MIR findings in terms of which simulations lead to more or less infection in the population. These findings demonstrate the importance of explicitly incorporating the temperature-dependence of disease transmission processes, by highlighting that the assumption of constant transmission rates results in an overestimation of transmission. Further, it can be seen that the low biting rate and long EIP brought about by the cooler spring weather would act to suppress virus transmission at the field site. The magnitude of these effects will vary throughout a season, dependent on the timing of introduction of the virus.

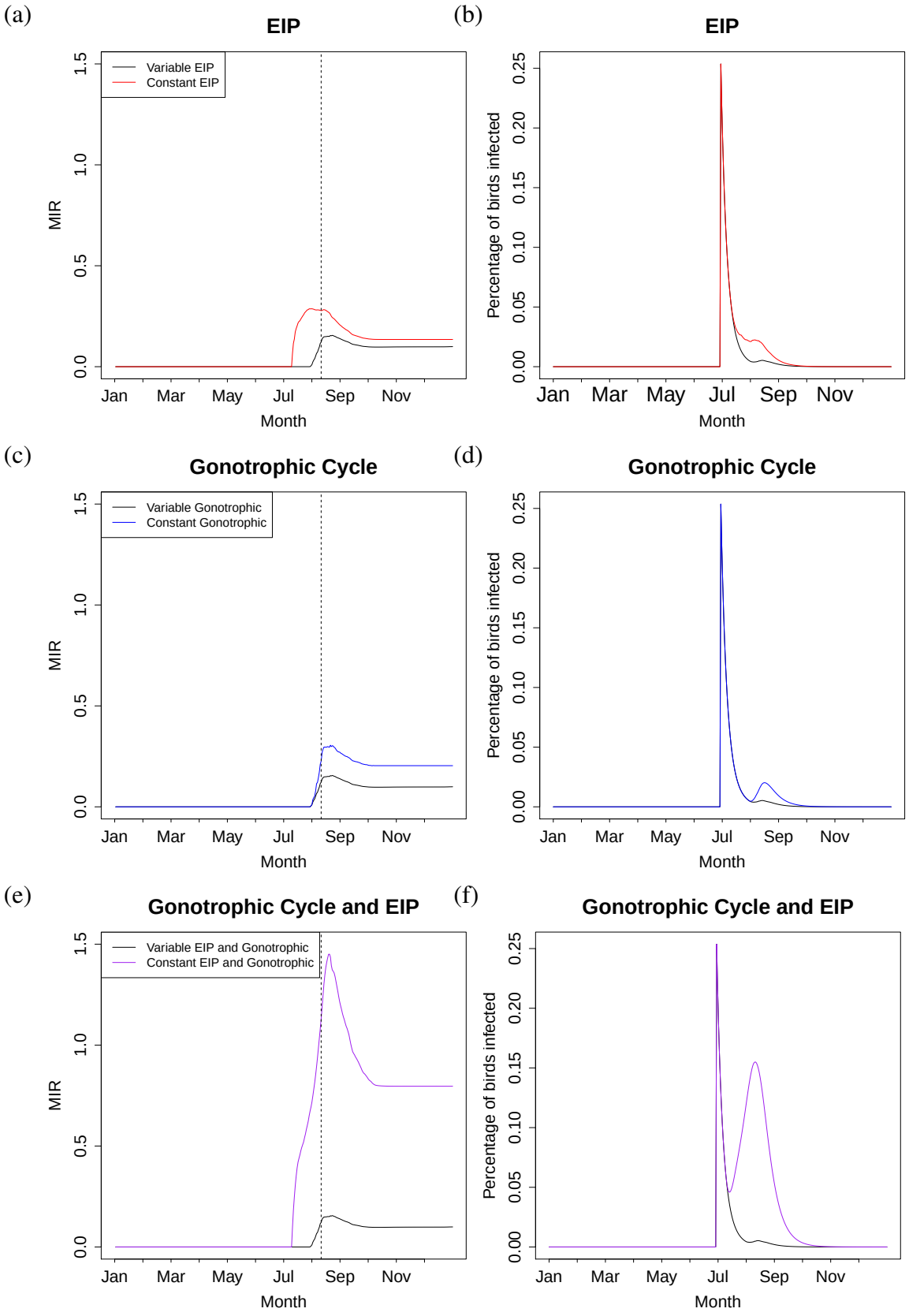

Figure 5.11: Disease transmission processes: (a) and (b) show the mosquito MIR and percentage of infected birds, respectively, assuming both constant and variable EIP duration. (c) and (d) show the mosquito MIR and percentage of infected birds, respectively, assuming both a constant gonotrophic cycle length and a variable duration. (e) and (f) show mosquito MIR and percentage of infected birds, respectively, assuming that either both the EIP and gonotrophic cycle are constant, or both processes are variable. The dashed line shows the end of the biting season. Virus introduction is assumed to occur on the first of July, as this most clearly showed the differences between model runs.

5.5.4 Implications of predicted warming scenarios on WNV transmission

UK temperatures are predicted to increase between now and 2080, with the median estimate of warming expected to be in the range of $3\,^{\circ}\mathrm{C}$ to $4.9\,^{\circ}\mathrm{C}$ increase in annual average temperature, dependent on emission of greenhouse gases (MetOffice 2009). In Chapter 2 it was shown that projected warming would increase mosquito population sizes in the UK. To understand the effects of predicted warming scenarios on WNV transmission potential, I use a sinusoidal wave, similar to that used in Chapter 2, to describe average seasonal temperature profiles and to allow UK Climate Impacts Programme (UKCIP) warming scenarios (MetOffice 2009) to be investigated. These warming scenarios predict changes to the UK climate, relative to a baseline measured from 1961-1990, under a range of different emission scenarios. With the exception of the use of the sinusoidal temperature function, all simulations are run according to the methods set out in Sections 5.4.1 and 5.4.

Methods: Temperature inputs and their effects on vector-host ratios

Before discussing the predicted mosquito densities under climate warming scenarios it is necessary to briefly return to the methods, to explain the temperature profiles used. I build upon the temperature function used in Chapter 2 (Equation 2.20) by including diurnal temperature range and estimating water temperatures using observed air temperatures and the relationship presented in Section 4.1.3. The air temperature function, including DTR, is given by

$$T_{air}(t) = \mu + \lambda \cos\left(\frac{2\pi(t-\phi)}{365}\right) - \frac{T_{DTR}}{2}\cos(2\pi t), \tag{5.23}$$

where μ(= $9.8\,^{\circ}\mathrm{C}$) is the annual mean temperature, λ(= $6.4\,^{\circ}\mathrm{C}$) is the amplitude of seasonal temperature fluctuations, ϕ(= 28.9 days) determines the timing of the annual peak temperature and T_{DTR} gives the diurnal temperature range. The diurnal temperature range was calculated as $9.4\,^{\circ}\mathrm{C}$, by calculating the average DTR across the range of temperatures observed at the field site. Values for μ, λ and ϕ where calculated from the UKCIP baseline values (MetOffice 2009). The water temperature can then be calculated from the simulated air temperature using

$$T_{water}(t) = 0.9491 T_{air}(t) + 3.9174, \tag{5.24}$$

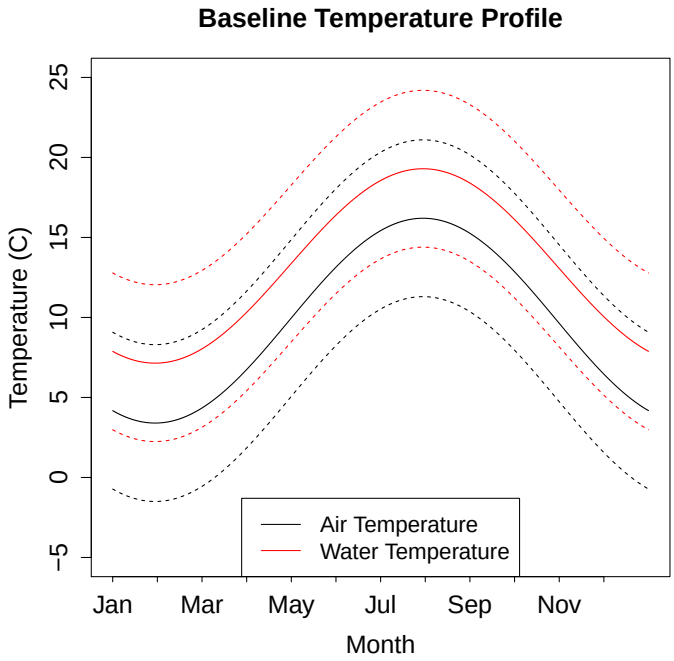

Figure 5.12: Baseline temperature profile: The baseline temperature profile (1961-1990) from the UKCIP data is shown (MetOffice 2009). The solid lines show the mean daily air and water temperatures, whilst the dotted lines show the upper and lower bounds of the daily temperatures, given the diurnal temperature range estimated.

as observed in the field experiment detailed in Chapter 3 and shown in Figure 4.2. The baseline temperature profiles for both water and air temperature are shown in Figure 5.12. Warming scenarios are then implemented by increasing the mean air temperature, μ (Equation 5.23), in line with predictions from the UK Climate Impacts Programme (MetOffice 2009).

Warming scenario effects on WNV transmission

I investigated disease transmission under various degrees of warming and allowing for introduction of the virus at a range of times throughout the year. Figure 5.13 (a) and (b) show that under the 1961-1990 baseline temperatures (Figure 5.12) WNV outbreaks are not thought to be possible regardless of the introduction time because infectious mosquito densities are below one at all points of the year. Further, when WNV introduction occurs before the end of May (the latest expected arrival time of migratory birds), the MIR remains below 0.05, which is lower than is typically observed during WNV outbreaks (Engler et al. 2013).

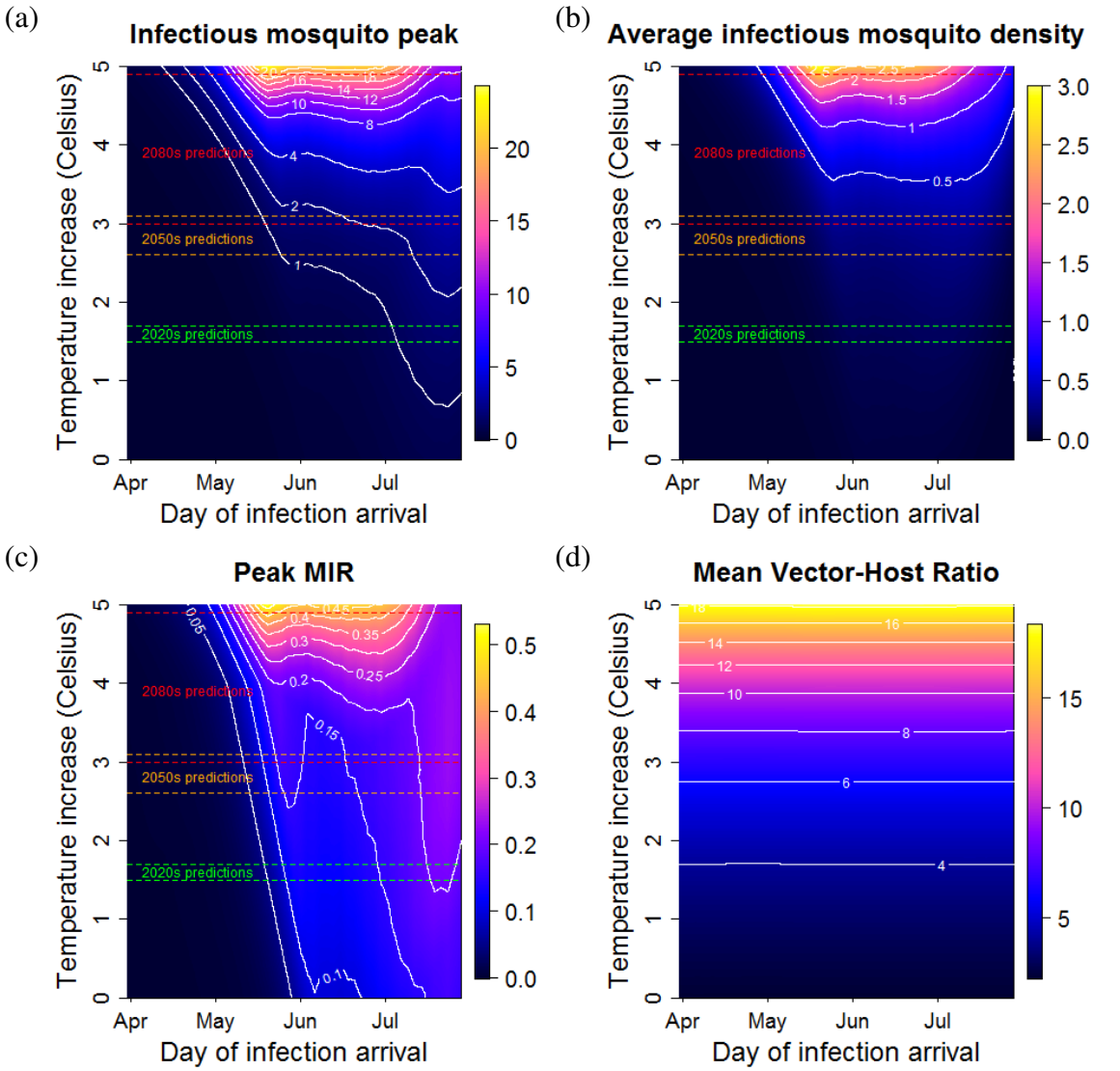

Figure 5.13: Effect of warming scenarios: (a) shows the predicted maximum density of infectious mosquitoes observed on a particular day under a range of warming and introduction scenarios. (b) shows the predicted density of infectious mosquitoes per day during the months of April to August, corresponding to the main active mosquito season, under different warming and introduction scenarios. (c) shows the predicted minimum infection rate (MIR), which is the number of infectious adults per 1000 adult females. (d) shows the mean vector-host ratio during the active mosquito season (April to September).

The UKCIP projections for 2020 under low, medium and high emission scenarios predict warming of $1.5 - 1.7\,^{\circ}\mathrm{C}$ above the baseline temperature. These temperatures give predictions of less than 1 infectious mosquito per day for virus introduction at any time of year (Figure 5.13 (b)), whilst the peak density of infectious mosquitoes only exceeds one when virus introduction occurs in July (Figure 5.13 (a)). These predictions show good agreement with those obtained under the conditions at the Wallingford field site in 2015 (Figure 5.8), for which the mean temperature at the field site in 2015 was $1.9\,^{\circ}\mathrm{C}$ higher than the baseline

mean, whilst the amplitude, λ, was unchanged and the peak, ϕ occurred 2 days later.

UKCIP projections for 2080 estimate the increase in mean summer temperatures as $3\,^{\circ}\mathrm{C}$, $3.9\,^{\circ}\mathrm{C}$ and $4.9\,^{\circ}\mathrm{C}$ under low, medium and high emission scenarios, respectively. Under the low emissions scenario, predictions of infectious mosquito density remain low even with WNV introduction at times of highest risk, with daily infectious mosquito density below 0.5 and low MIR values of approximately 0-0.2 throughout the year (Figure 5.13 (b) and (c)). The medium emission scenario predicts slightly higher infectious mosquito densities, however average infectious mosquito density is still below one and MIR values remain between 0 and 0.25 (Figure 5.13 (a) and (b)). Finally, under the high emission scenario, the average infectious mosquito density reaches 2.5 for some introduction times and the peak in infectious mosquito density approaches 20. Under this high emission scenario, MIR values reach 0.45, which is consistent with the lower range of values observed in WNV transmission areas (Engler et al. 2013).

Comparing the results given by this sinusoidal temperature approximation and the results obtained when using observed temperature values it becomes clear that intra-annual temperature fluctuations will also be influential. Figure 5.14 considers the MIR values when using the temperatures observed at the Wallingford field site, with a fixed temperature increase applied, giving a mean air temperature equal to that predicted under the 2080 high emissions scenario. This profile is compared with a sinusoidal approximation based on the observed Wallingford temperatures with an air temperature increase in line with predicted warming applied. Water temperature increases are applied according to the water-air temperature relationship in Equation 5.24. When using a sinusoidal approximation with the same annual mean, amplitude, and centred at the same time of year, the predicted peak MIR more than doubles if compared with the case using observed temperatures at the field site, regardless of warming, when infection arrives at the end of May (Figure 5.14 (a)). However, when virus introduction occurs on June 30th, the MIR values under the two methods in the absence of warming are almost identical, whilst the MIR values under warming were almost equal when infection was introduced in May (Figure 5.14).

This difference in MIR values dependent on infection introduction time highlights that the exact temperature conditions at the time of introduction may be particularly influential determinants of subsequent transmission. Consequently, periods of extreme warm temperatures are likely to be accompanied by an increased WNV risk were introduction to occur. This finding echoes the results of Chapter 2, where it was found that predictions of mosquito

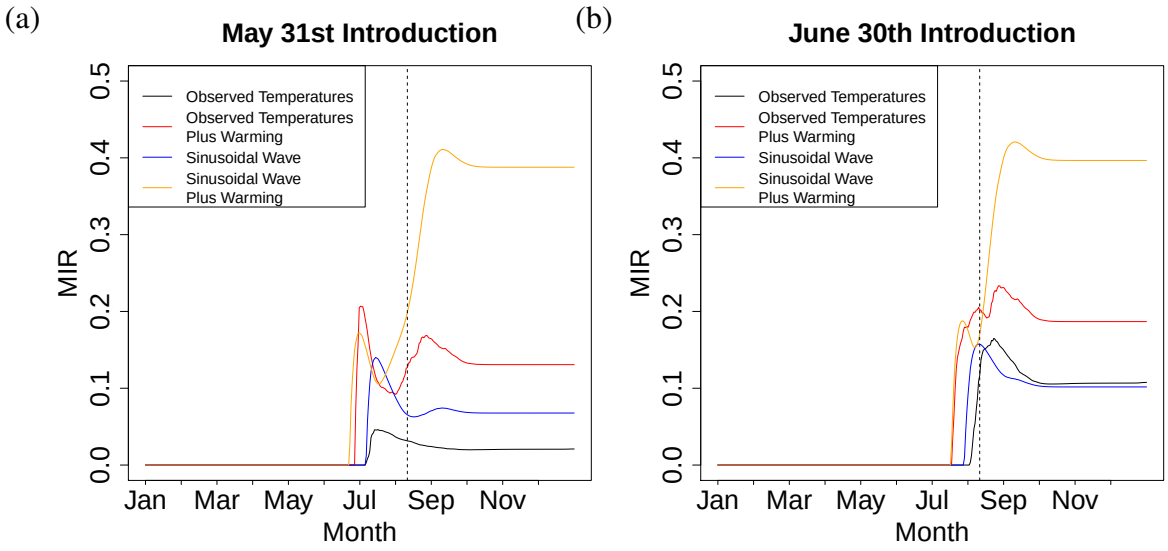

Figure 5.14: Comparison of temperature inputs: The density of infectious mosquitoes is shown under four temperature input scenarios. “Observed temperatures" - uses the hourly water and minimum/maximum daily air temperatures observed at the field site in 2015. “Observed temperatures plus warming" uses the temperatures from the observed temperatures scenario with $2\,^{\circ}\mathrm{C}$ added at all points, to give a mean temperature as predicted to occur in 2080 under the medium emissions scenario. “Sinusoidal wave" captures the annual temperature variation using a sinusoidal wave of the form shown in Equation 5.23 (μ = 11.7, λ = 6.4, ϕ = 31, T_{DTR} = 9.4) fitted to the air temperature data from the Wallingford field site in 2015. Water temperatures are then estimated according to Equation 5.24. “Sinusoidal wave plus warming" uses the sinusoidal wave described for the scenario without warming with the mean temperature, μ, increased to 13.7 to give the mean temperature predicted by 2080 under the medium emission scenario. Each scenario is run for one year under a sinusoidal temperature profile with the stated degree of warming before the described temperature profile is applied. The dashed lines show the end of the mosquito biting season. Plot (a) shows infection introduction on May 31st, whilst (b) shows infection introduction on June 30th.

population abundance often differed substantially when using observed field temperatures as opposed to sinusoidal approximations (Figure 2.11). This discrepancy occurs because, by using sinusoidal approximations we are considering an average, meaning that intra-annual, daily and diurnal temperature fluctuations around this average will affect the rates of disease transmission processes.

5.6 Discussion

I predict that current UK temperatures are too low for WNV transmission cycles to be established, as biting rates are insufficient and the virus replication time in mosquitoes is too long (Figure 5.11). Predicted increases to UK temperatures in the coming years will increase the transmission ability of WNV, with predicted MIR values by 2080 under the high emissions scenario reaching the lower range of MIR values typically observed during WNV outbreaks

in other regions (Figure 5.14). However, the probability of WNV outbreaks is likely to be dependent on the effects of climate warming on biting season duration, with increases to the duration of the mosquito biting season increasing the predicted risks of outbreaks in Autumn (Figure 5.14). Further, inter- and intra- annual temperature fluctuations around predicted seasonal averages may affect the probability and extent of WNV outbreaks, as shown by Figure 5.14. The findings that WNV outbreaks are unlikely in the UK given predicted climate warming support those of Semenza et al. (2016), who recently predicted that WNV would not reach Northern Europe by 2050.

Minimum infection rates (MIR values) have been studied across a range of WNV endemic areas in both North America (Kulasekera et al. 2001; Bernard et al. 2001; Anderson et al. 2004; Bolling et al. 2007), and Europe (Engler et al. 2013; Kemenesi et al. 2014). Such studies give valuable information on the levels of infection required in mosquito populations for spill-over to humans to be possible. Kulasekera et al. (2001), Bernard et al. (2001) and Anderson et al. (2004) studied WNV outbreaks in the Eastern USA during 2001 to 2003, finding that human cases typically occurred in areas where the *Cx. pipiens* MIRs ranged from 5-16, though one case was observed under an MIR of 0.16 (Bernard et al. 2001). In Colorado human cases were observed at MIRs of 8.7 and 1.37 in consecutive seasons, though the first outbreak was more severe. In Europe, Kemenesi et al. (2014) observed an MIR of 1.61 (95% CI: 0.7-3.1) in Serbia during 2013, during which time 300 human cases of WNV were detected. Further, national and regional Italian studies predict an MIR of 4.16 over 2008 to 2012, when numerous WNV outbreaks occurred, and human WNV cases have been observed in Spain, where the MIR has been estimated at 0.27 (Engler et al. 2013). These findings suggest that under the highest warming scenarios MIRs may reach the lower limits of the range of MIR values within which spill-over to humans has occurred in other regions (Figure 5.13 (c)). However, the most typical MIR values observed during WNV outbreaks (MIR > 1) exceed those predicted for the UK climate.

In many of the presented simulations, it can be seen that the predicted peak in infection occurs after the end of the current biting season due to the time required for exposed mosquitoes to become infectious (Figure 5.11 and 5.14). However, these simulations do not account for the likely effects of climate warming on season length, as the diapause induction time in the model occurs purely as a result of photoperiod decrease and is not sensitive to temperature. It is likely that under increased temperatures, mosquito active seasons will increase in duration (Bale and Hayward 2010), such that biting will continue later in the season. In such scenarios, mosquitoes would be likely to bite into the month of September, as is currently commonly observed in the Mediterranean basin (Rosà et al. 2014). This will have

implications for mosquito population sizes, as the active season will be longer and energetic demands of diapause will decrease, and for potential disease transmission.

Many vector-borne disease transmission models make the simplifying assumption that processes which are temperature-dependent, such as the biting rate or EIP, can be approximated by constant rates (Lord and Day 2001; Wonham et al. 2004; Cruz-Pacheco et al. 2005; Durand et al. 2010; Pawelek et al. 2014; Bergsman et al. 2015). This assumption of constant rates makes model analysis more straightforward, however in fluctuating thermal environments assuming constant rates may do a poor job of capturing disease transmission cycles. By comparing model predictions under commonly used constant values for biting rates and EIP durations, I was able to understand the effects of including or excluding temperature-dependence in disease transmission processes. Figure 5.11 shows that using constant rates led to very large increases in the mosquito MIR, when compared with temperature-dependent rates. In fact, given the observed mean air temperature of $13.6\,^{\circ}\mathrm{C}$ between April and September at the Wallingford field site one would predict that EIP completion would be impossible (Equation 5.22), whilst Figure 5.10 (a) shows that EIP completion should occur in 20-30 days during July, given observed temperatures. These findings highlight the importance of understanding and quantifying the temperature-dependence of the adult mosquito life cycle and transmission processes, which is an area which has received relatively little attention (Section 5.3.1).

In assuming that environmental conditions remain constant, most traditional WNV models also assume that the vector population size remains fixed (Table 5.1). Holding conditions constant allows these models to calculate R_0 values and assess disease risks analytically (Wonham et al. 2004; Bowman et al. 2005; Cruz-Pacheco et al. 2005). However, the fact that environmental conditions will fluctuate means that the inferences drawn may only be valid under the chosen equilibrium conditions and erroneous under field conditions. My findings highlight that the size of the vector population is highly variable throughout the season (Figure 5.8) and that increases to the vector-host ratio will approximately linearly increase the predicted peak infectious mosquito density, provided temperatures are such that virus transmission is possible (Figure 5.9 (g)). This highlights that inclusion of vector seasonality, in addition to temperature-dependence of disease transmission processes, can have a large impact on predictions of disease risk, particularly when seasonal thermal fluctuations are large.

In my analysis I do not directly explore the likelihood of WNV overwintering in UK mosquito

populations. To estimate the risks of WNV successfully overwintering in UK mosquito populations, better understanding of virus overwintering processes, such as vertical transmission and gonotrophic dissociation (Eldridge 1966; Nelms et al. 2013) would be required. Separate laboratory studies have drawn contrasting conclusions regarding the occurrence of gonotrophic dissociation (the ability of blood-fed mosquitoes to enter diapause) in *Cx. pipiens*, dependent on rearing conditions and blood meal availability (Eldridge 1966; Eldridge and Bailey 1979; Mitchell 1983; Mitchell and Briegel 1989). The occurrence of the peak in infectious mosquito density after the initiation of diapause suggests that if gonotrophic dissociation were to occur in nature, this would strongly influence potential virus persistence between seasons as horizontally infected mosquitoes may be able to survive overwinter. However, it is generally believed that instances of gonotrophic dissociation in nature will be rare (Sanburg and Larsen 1973; Washino 1977). As discussed in Chapter 4, vertical transmission rates in *Cx. pipiens* have only been studied for laboratory colonies in the USA (Eldridge 1966; Nelms et al. 2013).

Vertical transmission and possible gonotrophic dissociation could be included in the model by further splitting the adult stage, such that horizontally infected and uninfected/vertically infected adults experience different levels of mortality, as horizontally infected adults show higher diapause mortality rates than those which are not blood fed (Mitchell and Briegel 1989). Further, the possible effects of climate warming on diapause induction and termination times may influence the size of the infectious mosquito population at the beginning of winter (Figure 5.14). Bird population dynamics are also likely to affect the probability of virus persistence, as bird migration may alter infection proportions in the host population. The geographical origin of migratory birds, alongside climate change effects in the source areas of these migrants will also affect the likelihood and magnitude virus introduction to the UK. Further, birds are thought to act as potential overwinter reservoirs of WNV in some areas (Dawson et al. 2007; Hinton et al. 2015). However, given the low rates of WNV predicted in the mosquito population (Figure 5.13 (c)), and the low rates at which vertical transmission and gonotrophic dissociation occur (Eldridge 1966; Nelms et al. 2013), virus overwintering in UK populations appears to be unlikely.

Throughout this Chapter, the arrival of infected migratory birds has been considered to be the most likely pathway by which WNV may be introduced to the UK (Higgs et al. 2004; Bessell et al. 2014). Introduction by this route would be thought to be possible in the months of March to May, given the documented arrival times of migratory birds (BTO 2017). Introduction before the emergence of the first spring mosquito generation led to the virus dying

out almost immediately, whilst introduction from early May until mid July led to progressively larger infectious adult mosquito populations. Virus introduction through transport of mosquitoes is typically believed to occur through accidental shipping of eggs and larvae, as has occurred in *Aedes albopictus* (Tatem et al. 2006). However, this pathway seems unlikely for WNV, since it is adult mosquitoes which diapause. Further, ports and planes tend to be disinfected and remote from UK mosquito breeding habitat. Alternatively, it is possible that WNV could be introduced through movement of infected livestock (Tatem et al. 2006). In this case, pathogen introduction could occur at any point throughout the year. The time of introduction of the virus was found to have a profound effect on subsequent transmission potential and the likelihood of an outbreak (Figure 5.9 (k)), as has previously been observed in Scotland in the midge-borne virus Schmallenberg (Bessell et al. 2013).

The avian ecology at a WNV introduction site is believed to profoundly influence disease transmission dynamics due to the range of responses elicited to infection across bird species (Komar et al. 2003; Reisen 2013). In conducting the sensitivity analysis, it was observed that many of the avian infection parameters appeared to be highly influential determinants of disease transmission. Specifically, host-vector and host-host transmission, avian recovery and WNV-induced mortality rates, and the initial proportion of infected individuals in the avian population were all observed to influence infected mosquito population size by as much as 100% within the parameter range considered (Figure 5.9). Consequently, future model extensions should attempt to address this variability by including the range of avian host competencies.

A small proportion of existing WNV models attempt to incorporate a range of host competencies by splitting the host population into $2-3$ different competency classes (Table 5.1). Marini et al. (2017) found that inter-specific competition between hosts, alongside vector feeding preferences for particular host species, can strongly influence pathogen invasion, the probability of an epidemic, and subsequent transmission rates. Exploratory analyses, such as that presented by Marini et al. (2017) are valuable in highlighting the potential effects of host ecology on WNV transmission. However, to draw inferences about disease risk in particular regions a great deal of information on local ecology is required.

In my model I make a number of simplifying assumptions about the host population, which may affect WNV outbreak potential and transmission cycles and should be investigated in future model extensions:

- All birds are assumed to have equal host competencies and to respond in the same

manner to WNV infection, when in reality hosts show a wide variety of responses (Komar et al. 2003). Splitting the host population into competency classes, as in previous studies (Hartley et al. 2012; Bergsman et al. 2015) would improve understanding of the effects of local avian ecology on WNV transmission cycles. To determine risks for specific regions of the UK it would be necessary to understand the relative abundances of the bird species in those regions, as well as their host competencies for WNV. No studies investigating WNV infection across UK species have been carried out, so current data will only be available for species present in other WNV endemic areas (Komar et al. 2003; Pérez-Ramírez et al. 2014).

- Density-dependent avian mortality was assumed to affect all birds equally. However, some species are adversely affected by WNV infection and show reduced fitness (Komar et al. 2003), meaning that density-dependent mortality may be increased in infectious hosts, as they may be less able to compete for resources. However, experimental studies allowing quantification of this effect have not yet been carried out, causing problems in parameterisation of mathematical models.
- The effects of migration on seasonal patterns of avian population abundance were excluded from my model. Given the large number of migratory bird species (BTO 2017) migration would be very difficult to incorporate on a large scale. However, more localised analyses could use estimates of migration times alongside estimates of relative sizes of the migratory and resident bird populations to understand migration effects on WNV transmission. This would also improve estimates of the proportion of hosts which are infectious at the time of WNV introduction, which was shown to be influential in determining transmission (Figure 5.9 (h)).

In response to dispersal of bird populations and seasonal decline in bird abundances, *Cx. pipiens* has been shown to exhibit a feeding switch from its preferred avian hosts to humans in the late summer and early autumn (Kilpatrick et al. 2006). Vector-borne disease models and WNV models which look directly at control measures also often attempt to relate disease risk more directly to humans by including a human compartment into SIR frameworks (Bowman et al. 2005; Pawelek et al. 2014). By incorporating a human compartment in this way, it would be possible to investigate the effects of the host switch from birds to humans late in the year on potential human WNV cases. A human compartment would also provide a more direct measure of disease risk than using infectious mosquito density as a proxy. However, this extension faces difficulties similar to those faced when attempting to capture the avian ecology. In particular, including humans requires that human landing rates, which will be dependent on vector-host-human ratios, are accurately estimated. Like vector-host

ratios, estimates of landing rates will be subject to substantial uncertainty and geographic variability.

In summary, the model predicts that a WNV outbreak is currently unlikely given temperatures in the UK. Considering predicted UK climate warming scenarios leads to increases in predicted densities of infectious mosquitoes, with MIR values reaching 0.45 following introduction under temperatures predicted by the 2080s high emission scenario. However, values are not predicted to reach levels most typically observed during WNV outbreaks elsewhere in Europe and North America (Engler et al. 2013). Traditional methods of assuming constant viral incubation times, mosquito biting rates and population sizes, based on existing WNV transmission regions, will lead to vast overestimates of outbreak probability or spill-over into human populations. Assuming constant temperatures based on UK averages is expected to result in underestimation of the risks of future disease outbreaks. Further model development, explicitly incorporating avian ecology and the range of host competencies across bird species is required to improve predictions of disease transmission following virus introduction.

Chapter 6

Discussion

The following general discussion recapitulates the content and principal findings of the thesis, discusses some relevant issues and draws overall conclusions.

6.1 Recapitulation

Chapter 2 developed a variable-delay DDE model to estimate seasonal abundance of each life stage of *Cx. pipiens*, given temperature and photoperiod conditions experienced. The model uses data from published laboratory and field experiments to parameterise relationships between temperature and mosquito vital rates. This relaxes the common assumption of fixed mosquito generation times and immature survival by allowing development rates and mortality to fluctuate in response to changes in thermal conditions. Predictions were then made about the response of mosquito populations to a range of different seasonal temperature profiles, highlighting that the timing and intensity of warm periods can be more influential in shaping abundance patterns than average temperatures.

There is a dearth of studies which monitor the various life stages of *Cx. pipiens* in the field, which means that model predictions are often not compared to field data, potentially leading to spurious conclusions. Chapter 3 presents an extensive field study to collect a high temporal resolution seasonal abundance dataset of each life stage of *Cx. pipiens*. This dataset was used to validate the model-estimated development rates of immature mosquito life stages and to assess the relative contributions of density-dependent and density-independent mortality to larval survival. The collected field data was then compared with empirical phenology data

from across the *Cx. pipiens* range in an attempt to identify geographical patterns in phenology.

Chapter 4 challenged assumptions of the DDE model from Chapter 2 in light of the seasonal abundance data collected in Chapter 3, leading to reparameterisation of the diapause process and inclusion of mortality in post-diapause adults. The implications of assuming air temperatures to be equal to water temperatures in mosquito models were investigated, revealing that, for the field conditions measured, this assumption led to erroneous predictions of population extinction, as water temperatures were typically higher than air temperatures. Further, inclusion of diurnal temperature range in input data substantially reduced abundance estimates across all mosquito life stages indicating that simple approximations of seasonal average conditions commonly used in models are likely to substantially over-estimate UK mosquito abundance and vector host ratios.

Chapter 5 extended the DDE model from Chapter 4 to explicitly model WNV transmission cycles between mosquito vectors and avian hosts. The disease model predicts that the current climate in the South of England is too cold to permit WNV outbreaks. Predicted warming in the UK in coming decades will increase the transmission potential of WNV, with predicted average temperatures under a high emissions scenario leading to MIR values at the lower end of those observed in other WNV transmission regions.

6.2 Main findings

I will now discuss the findings of the thesis with respect to the aims set out at the beginning of Chapter 1. The first stated aim of the thesis was:

> To develop and validate an environmentally driven seasonal abundance model for *Cx. pipiens*, a temperate mosquito vector, which accounts for changing environmental conditions by explicitly incorporating variation in developmental delays of each life stage.

Many vector-borne disease models make simplifying assumptions about vector seasonality (Reiner et al. 2013), as such assumptions make models more tractable for mathematical analysis. However, this stands in contrast to a large body of literature detailing how environmental conditions, in particular temperature, affect mosquito vital rates (Couret et al. 2014; Ciota et al. 2014) and consequently vector and disease seasonality (Lord 2004; Altizer et al. 2006; Cruz-Pacheco et al. 2009). By using a DDE framework with variable delays,

I was able to explicitly include the effects of temperature on development and survival of each immature stage of the *Cx. pipiens* life cycle, thus allowing the effects of fluctuating temperatures on mosquito generation times and abundance patterns to be explored. In doing so, I found that intra- and inter-annual temperature fluctuations had large impacts on patterns of seasonal abundance. Direct incorporation of temperature effects also allowed me to study the impact of climate warming scenarios, with increases to mean temperatures or amplitude of seasonal temperature fluctuations both predicted to increase mosquito population sizes in the UK.

I chose to parameterise my DDE model using data from *Cx. pipiens*, as it is believed to be the primary vector of WNV across Europe and North America (Gubler 2002; Calistri et al. 2010; Reisen 2013). Whilst laboratory studies examining the relationship between temperature and *Cx. pipiens* vital rates are relatively common, high temporal resolution (sub-weekly) field collected seasonal abundance datasets are rare and are not typically publically available (Chapter 3, Table 3.5). In analysing a 9-year daily time series of *Aedes vexans* and *Culiseta melanura* in North Carolina, it was recently highlighted by Jian et al. (2014a) that observations of adult mosquito populations should be based on a sub-weekly sampling frequency to separate the effects of a varying mosquito activity from actual changes in the abundance of the underlying population. I made multiple collections of each *Cx. pipiens* life stage each week throughout 2015 to enable model validation and to improve understanding of environmental effects on species phenology at short time scales. This furthered our knowledge of season start and end dates for UK *Cx. pipiens*, allowed model-predicted development and mortality rates to be validated against field data and enabled the effects of diurnal temperature variation and temperature differences between micro-habitats to be studied.

The second aim stated at the outset of this thesis was:

> To use this model to predict the possible risks of West Nile virus (WNV) introduction and subsequent transmission within the UK.

WNV outbreaks have occurred in recent years in various parts of the Mediterranean basin (Engler et al. 2013; Sabatino et al. 2014), whilst WNV has become endemic in the USA since introduction in 1999 (Reisen 2013). This has prompted concern that WNV outbreaks may occur in the UK if the virus were to be introduced. Previous studies discussing risks of WNV introduction to, or transmission within, the UK have focussed primarily on the likelihood of virus introduction (Bessell et al. 2014) or presence of potential WNV vectors within the UK (Higgs et al. 2004; Golding et al. 2012; Vaux et al. 2015; Chapman et al. 2016). These studies found that known WNV vectors were present across many parts of the UK and that

WNV introduction through avian migration was possible, albeit at low levels (Bessell et al. 2014). However, no studies have modelled hypothetical transmission of WNV under the UK climate, to understand the risks of outbreaks occurring following virus introduction. The extent of seasonal temperature fluctuations in the UK, alongside the fact that temperatures are too low for incubation of the virus in mosquitoes for most of the year (Reisen et al. 2006a), means that any disease model would need to explicitly incorporate temperature-dependence of virus transmission processes.

Having extended the temperature-dependent seasonal abundance model to explicitly incorporate disease transmission, I predict that WNV outbreaks will not be possible under current UK temperature conditions. Average temperatures predicted for the South of England by the 2080s, under a high emissions scenario, result in MIR values consistent with the lowest values observed in other WNV transmission regions (Engler et al. 2013). The likelihood of disease transmission was most dependent on the timing of virus introduction, with introduction in the summer leading to the highest risk of transmission due to relatively high vector host ratios and biting rates and low EIPs. Host-host transmission, host recovery rate and WNV-induced death rates in hosts were all also observed to be particularly influential drivers of disease transmission. Consequently, improving understanding of the effects of WNV infection in UK bird species remains an important area of further research if predictions regarding potential transmission in the UK are to be improved.

6.3 Future mathematical model developments

Estimating transmission of vector-borne diseases is made particularly challenging by the wide range of processes affecting host, vector and pathogen dynamics, many of which will be climate-dependent (Tabachnick 2010). This complexity means that simplifying assumptions typically have to be made about some processes. Here, I identify three key simplifying assumptions made during this thesis and discuss future research directions which could address these simplifications.

6.3.1 Effects of hydrology on mosquito seasonal abundance

The availability of immature breeding sites is an important determinant of development rates, larval survival, adult fitness, vector population size and vector competence, as previously discussed (Higgs et al. 2005; Alto et al. 2008; Reiskind and Lounibos 2009; Loetti et al. 2011;

Couret et al. 2014). This importance of the larval stage is reflected in the emphasis of larval source management as a mosquito control measure (Gu et al. 2006; Fillinger et al. 2008; Smith et al. 2013). However, the effects of larval habitat size are more difficult to account for in mathematical models than those of temperature, due to the relative lack of available data on breeding site presence and size, and direct human influences on local ecology through irrigation and water storage (Shaman et al. 2010). This difficulty is compounded when studying a mosquito species, like *Cx. pipiens*, which exhibits opportunistic egg-laying behaviour by utilising a very wide range of natural and man-made breeding sites (Vinogradova 2000). UK climate predictions state that summer precipitation is expected to decrease in coming years (Osborn and Hulme 2002; Beniston et al. 2007; Murphy et al. 2010). However, using only environmental variables, such as precipitation, to estimate breeding site availability fails to account for the full range of *Cx. pipiens* breeding sites (Vinogradova 2000; Townroe and Callaghan 2014). Finally, whilst periods of low rainfall may decrease vector-host ratios, droughts have been shown to bring vectors and hosts into close contact at breeding sites, leading to amplification of vector-borne diseases in some instances (Shaman et al. 2005, 2010).

When considering the effects of hydrology on patterns of mosquito abundance, future model extensions should include density-dependent mortality due to competition in the larval stage. Larval mortality of various mosquito species, including *Cx. pipiens* has been shown to increase under increasing larval densities in laboratory and semi-field conditions (Madder et al. 1983b; Legros et al. 2009; Alto et al. 2012; Couret et al. 2014). Though less well-studied, inter-specific competition for resources has also been shown to affect larval population sizes in *Cx. pipiens* (Duquesne et al. 2011). Similarly, the larvae of many mosquito species, including *Cx. pipiens*, have been shown to suffer substantial mortality through inter-specific predation both under laboratory and field conditions (Mogi and Okazawa 1990; Marti et al. 2006; Quiroz-martinez and Rodriguez-Castro 2007; Fischer et al. 2012, 2013). However, parameterisation of these different density-dependent mortality sources is very difficult. Mortality due to intra-specific competition for nutrients between larvae will be strongly dependent on the amount of nutrients available in the breeding habitat, which will vary across all habitats, with particular variation between natural and man-made habitats (Alto et al. 2012; Vinogradova 2000). Similarly, mortality due to predation will depend on the number and species of predators in each breeding site, which will be changeable across the range of breeding habitats (Medlock and Snow 2008). No studies currently investigate the interaction between predation and competition to understand the relative contributions of these two processes to total larval mortality.

In Chapter 5 and Appendix C, it was observed that, given sufficiently high temperatures, seasonal predation was insufficient to regulate mosquito population size, if predator numbers were low during any part of the active mosquito season. This led to rapidly increasing vector abundance under warming scenarios, causing unrealistically high vector-host ratios and large predicted MIR values (Figure C.3). To resolve this issue, I reverted to the original model formulation in Chapter 2, such that the strength of predation was assumed to remain constant throughout the season. This resulted in slight decreases to the correlation values between the egg, larval and adult model predictions and the field data (Appendix C), however MIR values remained in line with those calculated for field sites (Figure 5.13). In reality, when predator numbers are low and temperatures are adequate for development, it is likely that density-dependent competition for resources between larvae would regulate the population size. Consequently, in the model where predator numbers vary seasonally, larval competition would be required to prevent unrealistically high larval densities, unless temperatures are cold enough to regulate the larval population. Further, incorporating variable breeding habitat volume and availability is also likely to affect the strength of competition. Increasing the size and number of breeding sites is likely to decrease mortality due to predation, as predators will spend more time searching for prey and rainfall may produce temporary, predator-free habitats. Similarly, increasing larval habitat is likely to decrease competition, though the extent of any change to mortality may depend on whether or not it is accompanied by an equivalent change in nutritional content at the breeding site i.e. diluting the existing food source in a larger pool of water may not reduce the mortality due to competition. As it appears likely that both predation and competition will be important pathways by which mosquito populations are regulated under changing climate, future models should attempt to incorporate both processes. Such efforts would be aided by further laboratory and field studies investigating the contributions of both processes to total larval mortality.

Valdez et al. (2017) recently developed a model to predict the effects of precipitation on *Culex* mosquito population dynamics, which begins to address some of these issues. In particular, the authors investigate the effects of the number of rainy days and the mean monthly precipitation on the maximum yearly abundance of *Cx. quinquefasciatus*. In the model presented, population dynamics of the mosquito are affected through the dependence of the egg-laying rate on the amount of habitat available. Visually, the model appears to capture the pattern of seasonality in adult female catch data from Cordoba, Spain, though no quantitative goodness of fit measure is given. The authors assume that immature development and death rates take constant values over the season, however the model formulation presented is such that the predicted amount of habitat could be used to estimate density-dependent mortality and development rates. Coupling a rainfall model such as this, with the mosquito abundance

and disease model presented in this thesis, would allow for the combined effects of precipitation, temperature and photoperiod on mosquito abundance, and consequently disease transmission, to be studied.

The complexity of both natural and human influences on mosquito breeding sites means that, whilst exploratory analyses can be carried out to investigate effects of changing rainfall patterns on abundance and disease patterns, the results will still be subject to caveats regarding human behaviours. Humans will influence local hydrology by artificially creating larval habitat through water storage and irrigation (Townroe and Callaghan 2014; Carrieri et al. 2014). Further, hydrology will affect how people use the landscape and consequently their exposure to infected mosquitoes, as has been observed in Southern France (Ponçon et al. 2007a; Linard et al. 2009). Consequently, when looking to make more detailed predictions about a specific site or region, the mosquito abundance and disease transmission model should be coupled with a hydrological model for that region (Bomblies et al. 2008; Soti et al. 2012; Montosi et al. 2012). Such an extension could be applied to this model for a particular area of the UK, given appropriate hydrological data, by simply using the volume of habitat specified by the hydrological model.

6.3.2 Modelling of adult life cycle processes

In Chapter 4, I showed that the model predicted a longer period of high egg-laying activity than was shown in the data (Figure 4.9) and I hypothesised that this was due to the assumption of a constant egg-laying rate. To address this, the adult stage could be split into multiple stages corresponding firstly to adults taking a blood meal and developing eggs, and secondly to adults ovipositing. The time required to develop eggs is known to be temperature-dependent (Reisen et al. 2006a; Lardeux et al. 2008), meaning egg development could be assigned a variable delay, similar to the immature stages. However, the incorporation of this delay becomes an issue when the model is extended to include disease transmission. When including disease, adults must progress through both the time delay associated with locating a blood meal and developing eggs, and the time delay corresponding to the EIP. The process of tracking both of these processes at once can be thought of like using two countdown timers with a shared reset trigger. Once one of these stages has been completed, the individual moves to another life stage, resetting both timers. The act of resetting both timers means that the time required to finish the incomplete stage is now unknown. Consequently, either the EIP or ovarian development, but not both, can be explicitly modelled at one point in time, using current methodology. I could not find a satisfactory solution to this problem during the course of the thesis, however this would be an interesting topic for future research.

6.3.3 Avian ecology

Avian ecology and community composition is known to have profound impacts on WNV transmission cycles (Jourdain et al. 2007; Reisen 2013) due to the wide range of responses different species exhibit to WNV infection (Komar et al. 2003). Different bird species develop different levels of viremia in their systems, affecting WNV-induced mortality rates, recovery rates and transmission probabilities, as discussed in Chapter 5. Further, the particular strain of WNV can have a large impact on the response of hosts to infection (Reisen 2013). It has been observed that the strain of WNV introduced in the New World in 1999 (NY99) has had much more severe effects on avian populations than WNV outbreaks in the Mediterranean basin over the last 20 years (Reisen 2013). Further, recovered birds are known to develop WNV antibodies in response to infection, meaning that transmission is likely to be repressed in areas where outbreaks have recently occurred (McKee et al. 2015).

The model presented in Chapter 5 assumes that all birds are equally susceptible to WNV and exhibit the same response upon infection. A first step to relaxing these assumptions would be to split the host population into multiple classes according to their host competence, in a manner similar to Hartley et al. (2012), such that the effects of avian ecology could be better explored. In addition to this extension to the model, further experimental work investigating the host competence of a range of UK bird species, which remain poorly studied (Komar et al. 2003), would aid in parameterising such models. With this information, the model could be tuned to predicted likely WNV introduction sites, such as those presented by Bessell et al. (2014), to improve predictions of transmission risk at these locations.

6.4 Application of the DDE model to predict disease transmission outwith the UK

The parameterisation of mosquito vital rates was carried out using data from field and laboratory experiments from across Europe and North America, with only estimates of the diapause initiation and termination timings coming specifically from UK data. To extend the model and predict WNV transmission across more of Europe would therefore be possible, provided that information regarding geographical variation in diapause timings and hydrology could be determined. Potential methods allowing the effects of precipitation on *Cx. pipiens* abundance to be incorporated were discussed in Section 6.3.1. In Chapter 3, I discussed the shortcomings of existing datasets with regards to our ability to determine any possible geographical patterns in *Cx. pipiens* diapause timings. With improved information on the

combined effects of temperature and photoperiod on *Cx. pipiens* season start and end dates, it would be possible to apply and validate the mosquito model over a much larger geographical range. This could then be used to develop hypotheses or make predictions about potential WNV transmission, dependent on knowledge about avian community structure and ecology.

Such an extension would require that potential geographic variability in a range of climate variables be well understood. To capture the hydrology over such a broad area, perhaps the most appropriate starting point would be to use a model which uses precipitation to estimate larval habitat volume, such as the model by Valdez et al. (2017) previously discussed. Such a model has the advantage of being able to incorporate predicted future changes to rainfall levels in a relatively straightforward manner. However, this approach would not be able to account for human impacts on local hydrology through irrigation or other artificial wetting processes. Capturing human impacts would be best achieved by using a more detailed hydrological model, relying on remote sensing of hydrological data from the study location, as has been done to map *Anopheles hyrcanus* populations in Southern France (Tran et al. 2008).

Geographic variability in temperature will also drive patterns of mosquito seasonal abundance and disease transmission. Clearly temperatures will vary across Europe, not only in terms of average temperature but in terms of the seasonal temperature profile experienced (Stainforth et al. 2013). In Chapter 2, it was shown that the timing and duration of periods of high or low temperature could be important determinants of mosquito abundance. Land use can also have potentially important effects on temperature, with the urban heat island effect (causing increased temperatures in urban areas) having been observed to increase temperatures in US cities by an average of $4.3\,^{\circ}\mathrm{C}$ in summer months, though this effect is reduced in winter (Imhoff et al. 2010). This urban heat island effect has been associated with increased *Cx. pipiens* populations in urban, as opposed to rural, locations in the UK (Townroe and Callaghan 2014). Moreover, diurnal temperature range will vary across space, (Lauritsen and Rogers 2012), and in response to land cover (Scheitlin and Dixon 2010). Finally, in Chapter 4 it was shown that, as observed across many insect species, using temperature data which is reflective of the micro-habitat used by different life stages is important in determining accurate predictions (Bryant and Shreeve 2002). This variability in environmental conditions across Europe is expected to influence mosquito seasonality and consequently potential disease transmission, as highlighted in this thesis.

It would also be possible to extend the seasonal abundance model, both within the UK and

potentially across Europe, to assess the potential transmission risks of other diseases transmitted by *Cx. pipiens*. *Cx. pipiens* has been shown to act as a competent vector for other virus including Usutu virus (USUV) (Fros et al. 2015), Rift Valley fever virus (Amraoui et al. 2012) and St. Louis encephalitis (Reisen et al. 2005). In particular, Fros et al. (2015) recently showed that North-western *Cx. pipiens* were more competent vectors of USUV than WNV at high temperatures of $28\,^{\circ}\mathrm{C}$, whilst there was no significant difference between vector competency for the two viruses at lower temperatures. To extend the model to assess USUV risks would not require any changes to be made to the underlying seasonal abundance model, since *Cx. pipiens* is the vector in both cases. Further, USUV also circulates within avian hosts. Consequently, adaptation to model USUV would rely solely on the availability of appropriate data to parameterise disease transmission processes, such as vector viral incubation times, transmission probabilities between vector and host, host-host transmission probability etc.

The DDE model framework presented here could also be adapted to model another mosquito species by reparameterising the vital rate functions and transmission processes, provided sufficient data was available. At present, DDEs with variable delays are very sparsely used within the vector-borne disease modelling community due to the relative complexity of DDEs as a modelling tool, when compared with other methods, and the requirement for empirical data to parameterise mosquito vital rates. To my knowledge, the only other mosquito model utilising a variable DDE framework is that developed for *Anopheles* by Beck-Johnson et al. (2013). However, as shown in this thesis, DDEs can be a valuable tool by which the population dynamics of insects species with multiple life stages in fluctuating thermal environments can be captured. A logical extension of the presented *Cx. pipiens*-WNV model would be to attempt to capture and include the seasonal dynamics of *Cx. modestus*, which has been implicated as a likely WNV bridge vector due to its preference for feeding on mammals (Ponçon et al. 2007a; Balenghien et al. 2008), and has recently been recorded in areas of South-east England (Golding et al. 2012; Medlock et al. 2014). However, empirical data for *Cx. modestus* remains scarce, so further laboratory and field studies investigating *Cx. modestus* vital rates and diapause behaviours would be required. Nonetheless, it is hoped that this model could be used as a template which could be adapted such that other modellers or ecologists may be able to take advantage of the features afforded by the DDE framework.

6.5 Summary

In this thesis I have used empirical data on *Cx. pipiens* vital rates and vectorial capacity to develop a novel mathematical model of WNV transmission that explicitly incorporates environmental effects on vector and disease seasonal dynamics. Vital rates and patterns of seasonal abundance predicted by the model were validated against a high temporal resolution dataset tracking each *Cx. pipiens* life stage. Under current UK climate projections, I predict that UK mosquito population sizes will steadily increase, though inter- and intra-annual variability will have profound effects on mosquito population sizes within a given year. Current temperatures remain too low for WNV outbreaks following a potential introduction to be likely. However, predicted average temperatures by 2080 under a high emissions scenario are expected to facilitate MIR values coinciding with the lowest recorded values observed during WNV outbreaks in other regions.

Appendix A

Determination of initial history with varying conditions

Here I present a discussion of the implications of assuming a constant environment for $t \leq 0$ when determining initial conditions and historical values. First I present the case where it is assumed that the environment is constant, before going on to present the variable case.

A.1 Constant case

Recall from Chapter 1 that the survival through an arbitrary stage i to be given by

$$S_i(t) = \exp\left(-\int_{t-\tau_i(t)}^{t} \delta_i(t')dt'\right), \tag{A.1}$$

which can be differentiated to give

$$\frac{dS_i(t)}{dt} = S_i(t)\left(\frac{g_i(t)\delta_i(t-\tau_i(t))}{g_i(t-\tau_i(t))} - \delta_i(t)\right). \tag{A.2}$$

An expression for the stage duration, $\tau_i(t)$, can be determined by considering the time required to transition from development point m_i to point m_{i+1}

$$m_{i+1} - m_i = \int_{t-\tau_i(t)}^{t} g_i(t')dt', \tag{A.3}$$

which can be differentiated to give

$$\frac{d\tau_i(t)}{dt} = 1 - \frac{g_i(t)}{g_i(t - \tau_i(t))}. \tag{A.4}$$

This gives an equation which defines the lags $\tau_i(t)$ for which we can compute $\tau_i(t)$ at all times $t > 0$ if we know the value, $\tau_i(0) = \tau_{i0}$, of the lag at time $t = 0$. This is relatively straightforward in the case where we assume constant conditions for $t \leq 0$, as $g_i(t)$ can be written as the constant, g_i, giving

$$m_{i+1} - m_i = \int_{t-\tau_{i0}}^{t} g_i dt' = g_{i0}\tau_{i0}. \tag{A.5}$$

Using the fact that g_i is expressed as the fraction of stage i completed, gives that

$$\tau_{i0} = \frac{1}{g_{i0}}, \tag{A.6}$$

where g_{i0} is the development rate of individuals in stage i at time $t = 0$. Similarly, by assuming constant temperatures for $t \leq 0$, $\delta_i(t)$ becomes δ_i and an initial condition for the survival equation can be determined, such that

$$S_{i0} = \exp\left(-\int_{t-\tau_{i0}}^{t} \delta_i dt'\right) = \exp(-\delta_{i0}\tau_{i0}). \tag{A.7}$$

A.2 Linearly changing conditions

Now consider the case where conditions are not constant for $t \leq 0$. In this case $g_i(t)$ and $\delta_i(t)$ cannot be simplified to constants for $t \leq 0$. Examining Equation A.2 reveals that solutions to the survival equation may be possible through separation of variables, given a solution for

$\tau_i(t)$. To find a solution for τ_{i0}, consider a the case where the temperature function for $t \leq 0$ can be approximated by a linear function, such that $T(t) = ct + d$. The development rate function will be a power function, as in the *Cx. pipiens* model used. Substituting this into Equation A.3 and solving gives

$$\begin{aligned} m_{i+1} - m_i &= \int_{t-\tau_i(t)}^{t} \alpha(ct' + d)^{\beta} dt' \\ &= \left[\frac{\alpha(ct' + d)^{\beta+1}}{c(\beta+1)} \right]_{t-\tau_i(t)}^{t} \\ 1 &= \frac{\alpha(ct + d)^{\beta+1}}{c(\beta+1)} - \frac{\alpha(c(t - \tau_i(t) + d)^{\beta+1}}{c(\beta+1)}. \end{aligned} \tag{A.8}$$

Setting $t = 0$ and rearranging gives

$$\tau_{i0} = \frac{d}{c} - \frac{1}{c}\left(d^{\beta+1} - \frac{c(\beta+1)}{\alpha} \right)^{\frac{1}{\beta+1}}. \tag{A.9}$$

To calculate an initial survival value, S_{i0}, use the death rate function from the *Cx. pipiens* model. Density-dependence will not be a factor here as $L(t) = 0$ for $t \leq 0$. Therefore, survival can be calculated as

$$S_i(t) = \exp\left(- \int_{t-\tau_i(t)}^{t} \nu_{0i} \exp\left(\left(\frac{ct' + d - \nu_{1i}}{\nu_{2i}} \right)^2 \right) dt' \right), \tag{A.10}$$

$$= \left[\exp\left(-\frac{\nu_{0i}\nu_{2i}\sqrt{\pi}}{2c} \operatorname{erfi}\left(\frac{ct' + d - \nu_{1i}}{\nu_{2i}} \right) \right) \right]_{t-\tau_i(t)}^{t}, \tag{A.11}$$

$$S_i(t) = \exp\left(-\frac{\nu_{0i}\nu_{2i}\sqrt{\pi}}{2c} \left[\operatorname{erfi}\left(\frac{c(t - \tau_i(t)) + d - \nu_{1i}}{\nu_{2i}} \right) - \operatorname{erfi}\left(\frac{ct + d - \nu_{1i}}{\nu_{2i}} \right) \right] \right). \tag{A.12}$$

Setting $t = 0$, $S_i(0) = S_{i0}$ can be written as

$$S_{i0} = \exp\left(-\frac{\nu_{0i}\nu_{2i}\sqrt{\pi}}{2c} \left[\operatorname{erfi}\left(\frac{-c\tau_{i0} + d - \nu_{1i}}{\nu_{2i}} \right) - \operatorname{erfi}\left(\frac{d - \nu_{1i}}{\nu_{2i}} \right) \right] \right). \tag{A.13}$$

into which one can substitute the value of τ_{i0} to calculate survival. So, for the case where temperature is allowed to vary linearly for $t \leq 0$ one can find initial values.

A.3 Is the linear approximation an improvement over the constant case

In Chapter 2, simulations are run using a modified cosine curve (Section 2.2.3) to determine the effects of different seasonal temperature profiles on *Cx. pipiens* abundance. To determine the effect of assuming constant historical temperature conditions, the temperature function, which is sinusoidal for $t > 0$, was approximated by a linear function for $t \leq 0$, such that $T(t) = ct + d$, and matched at $t = 0$. Further simulations were run under the assumption of constant temperatures for $t \leq 0$ and the results were compared to determine if there was an appreciable difference in outcome of the two methods (Figure A.1).

It is clear from Figure A.1 that the DDE solutions quickly converge to the same values in both cases. Simulations estimating the effects of different sinusoidal temperature curves on seasonal abundance are reported after a “burn-in" period of 18 months. Given this, one can have confidence that the assumption of constant temperatures for $t \leq 0$ does not substantially affect results when compared to the scenario where the temperature for $t \leq 0$ is given by the sinusoidal wave.

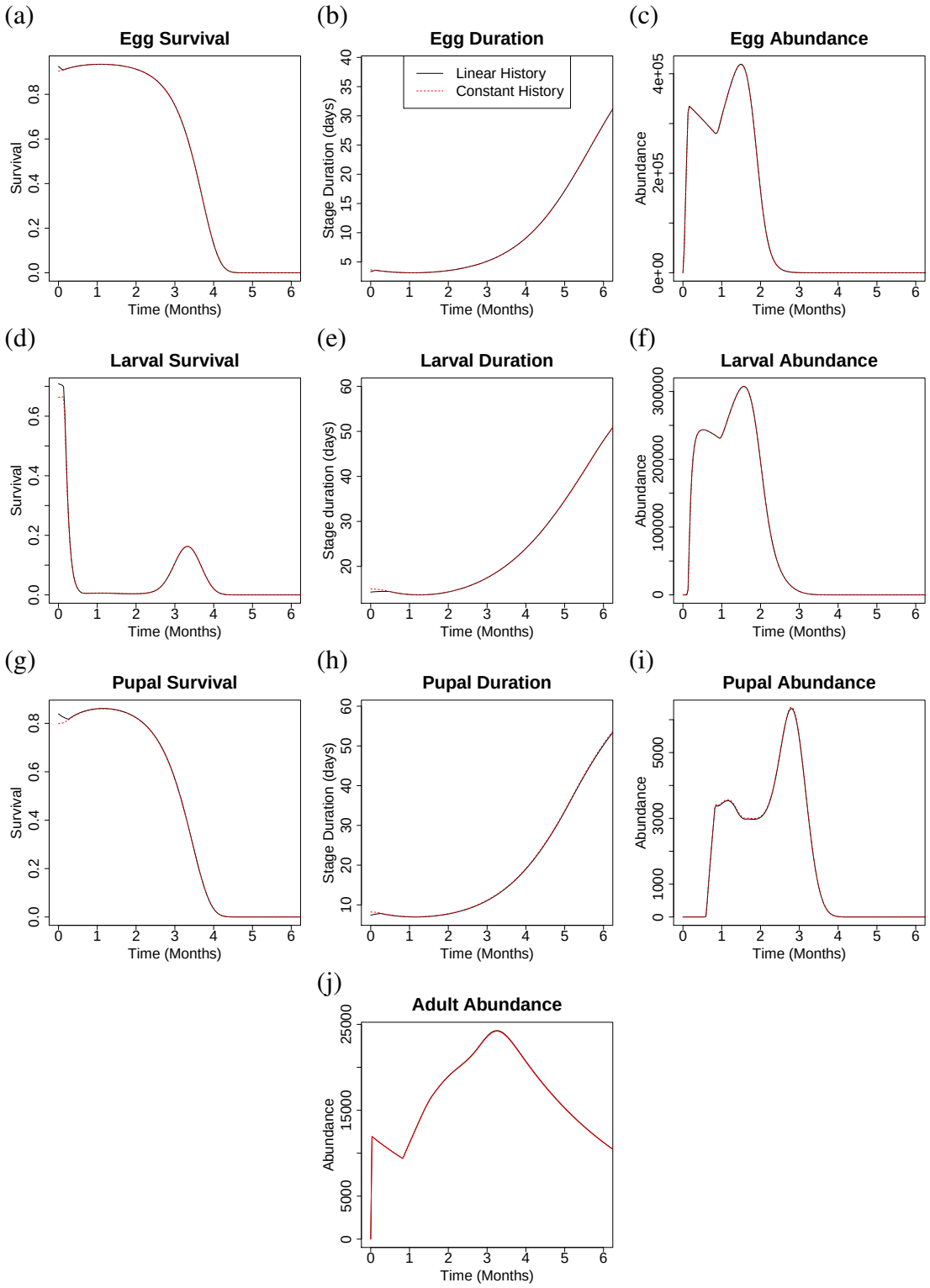

Figure A.1: Comparison between linear and constant histories: Simulations showing the comparison between estimated survival, stage duration and abundance. The solid black line shows the results using linear development and death rate functions, whilst the dotted red line shows results under constant temperatures, for $t \leq 0$.

Appendix B

Vertical transmission: infection in immature stages

Given that infection status is not thought to influence immature vital rates, the disease model in Chapter 5 was formulated such that immature individuals were not split by infection status. As such the mosquito dynamics resembled Figure B.1 (a) rather than Figure B.1 (b), where there are separate immature stages dependent on infection status.

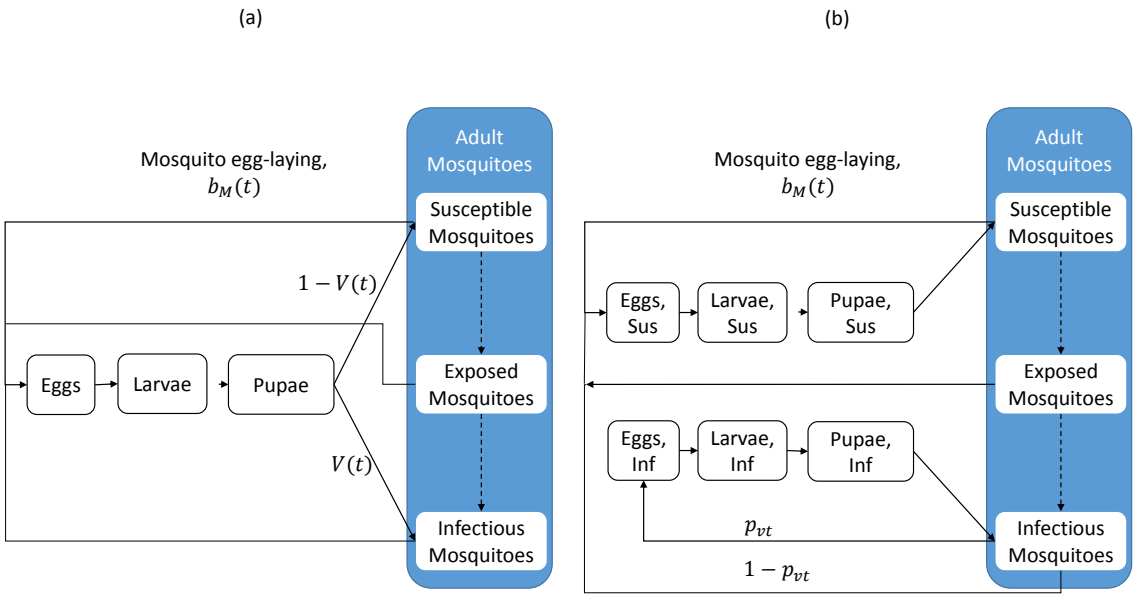

Figure B.1: Vertical transmission modelling pathways: The two possible methods by which to model vertical transmission are shown. (a) is the technique used in Chapter 5, and (b) is the alternative formulation.

It is possible to show that, given the assumption that infection status does not affect development or survival of immature mosquitoes, the two methods are equivalent. The assumption that infection status does not influence development or mortality means that all growth rates, $g_i(T(t))$, stage durations, $\tau_i(t)$, and survival terms, $S_i(t)$, for $i = E, L, P$ can be used for both infectious and uninfectious stages. Consider recruitment into infected adults, given as maturation from the exposed class, plus a proportion, $\mathcal{V}(t)$, of emergent pupae (Equation 5.16 in the main text),

$$R_{A_I}(t) = M_{A_E}(t) + M_P(t)\mathcal{V}(t). \tag{B.1}$$

Using the definition of $\mathcal{V}(t)$, given in Equation 5.12, the recruitment into the infectious adult stage can be written as

$$\begin{aligned} R_{A_I}(t) &= M_P(t)\mathcal{V}(t) + M_{A_E}(t) \\ &= \frac{M_P(t)A_I(t-\tau_I(t))p_{vt}}{N_V(t-\tau_I(t))} + M_{A_E}(t). \end{aligned} \tag{B.2}$$

Now using the definition for $M_P(t)$ it can be shown that

$$\begin{aligned} R_{A_I}(t) =& \left(b_A(t-\tau_I(t))N_V(t-\tau_I(t))S_I(t)g_I(T(t))\right)\left(\frac{A_I(t-\tau_I(t))p_{vt}}{N_V(t-\tau_I(t))}\right) + M_{A_E}(t) \\ =& b_A(t-\tau_I(t))A_I(t-\tau_I(t))p_{vt}S_I(t)g_I(T(t)) + M_{A_E}(t) \\ =& M_{P_I}(t) + M_{A_E}(t) \end{aligned} \tag{B.3}$$

where M_{P_I} is the maturation rate out of infected pupae in the split model (Figure B.1 (b)) and $g_I(T(t))$ is given by,

$$\begin{aligned} g_I(T(t)) =& \frac{g_P(T(t))}{g_P(T(t-\tau_P(t)))}\frac{g_L(T(t-\tau_P(t)))}{g_L(T(t-\tau_P(t)-\tau_L(t-\tau_P(t))))} \\ & \frac{g_E(T(t-\tau_P(t)-\tau_L(t-\tau_P(t))))}{g_E(T(t-\tau_P(t)-\tau_L(t-\tau_P(t))-\tau_E(t-\tau_P(t)-\tau_L(t-\tau_P(t)))))}, \end{aligned} \tag{B.4}$$

for brevity. Consequently, the rate of recruitment into the infectious adult class is equivalent in both methods, as the rate of maturation from the infectious pupal class in the split model equals the proportion of maturation assigned to the infectious class in the combined model. Similarly, it can be shown, using the result from above, that the rate of recruitment into the

susceptible adult class is the same in both models. Starting from the rate of recruitment into the susceptible adult class in the main text (Equation 5.11),

$$R_{A_S}(t) = M_P(t)(1 - \mathcal{V}(t)), \tag{B.5}$$

it can be shown that

$$\begin{aligned} R_{A_S}(t) &= M_P(t)(1 - \mathcal{V}(t)) \\ &= M_P(t) - M_P(t)\mathcal{V}(t) \\ &= M_P(t) - M_{P_I}(t) \\ &= M_{P_S}(t). \end{aligned} \tag{B.6}$$

This shows that recruitment into susceptible adults is given by maturation from susceptible pupae in the split model and an equivalent proportion of the total pupal population in the combined model.

Appendix C

Seasonally forced predation under warming scenarios

In Chapter 4, seasonal forcing in the predator population was added to the model to account for observations at the field site that predator numbers increased throughout the season. Simulations were run to understand the effects of this seasonal variation in the relative numbers of predators to prey (Figures 4.12-4.15). Figure C.1 shows that inclusion of seasonal variation in the ratio of predators to larvae improved the ability of the model to capture the observed relative peak sizes in the egg, larval and adult stages, though in the pupal stage the constant predation case performs better. This is reflected in the Pearson's correlation values between model predictions and data, with correlation changes of $+0.07$ for eggs, $+0.06$ for larvae, -0.07 for pupae, and $+0.17$ for adults, when including seasonality in predation.

Whilst investigating warming scenarios in Chapter 5, it was observed that the inclusion of seasonal variation in predator numbers led to unexpectedly large increases in mosquito abundance in the early part of the year, when predator numbers were low. Under predicted UKCIP warming scenarios, higher temperatures create favourable mosquito development conditions early in the year. These favourable conditions, coupled with relatively low rates of density-dependent mortality through predation, mean that larval survival is high early and population sizes are not regulated in the early part of the season. Figure C.2 shows that, under the warming scenario, larval survival in the months of April and May increases substantially. Whilst increased temperatures are likely to decrease temperature-dependent larval mortality, these effects can be expected to be mitigated, to some extent, by increased density-dependent mortality. However, the relative lack of predators early in the season when seasonal forcing is included means that, under warming scenarios, the mosquito abundance increases rapidly leading to unrealistically high larval densities in the early part of the year and excessively

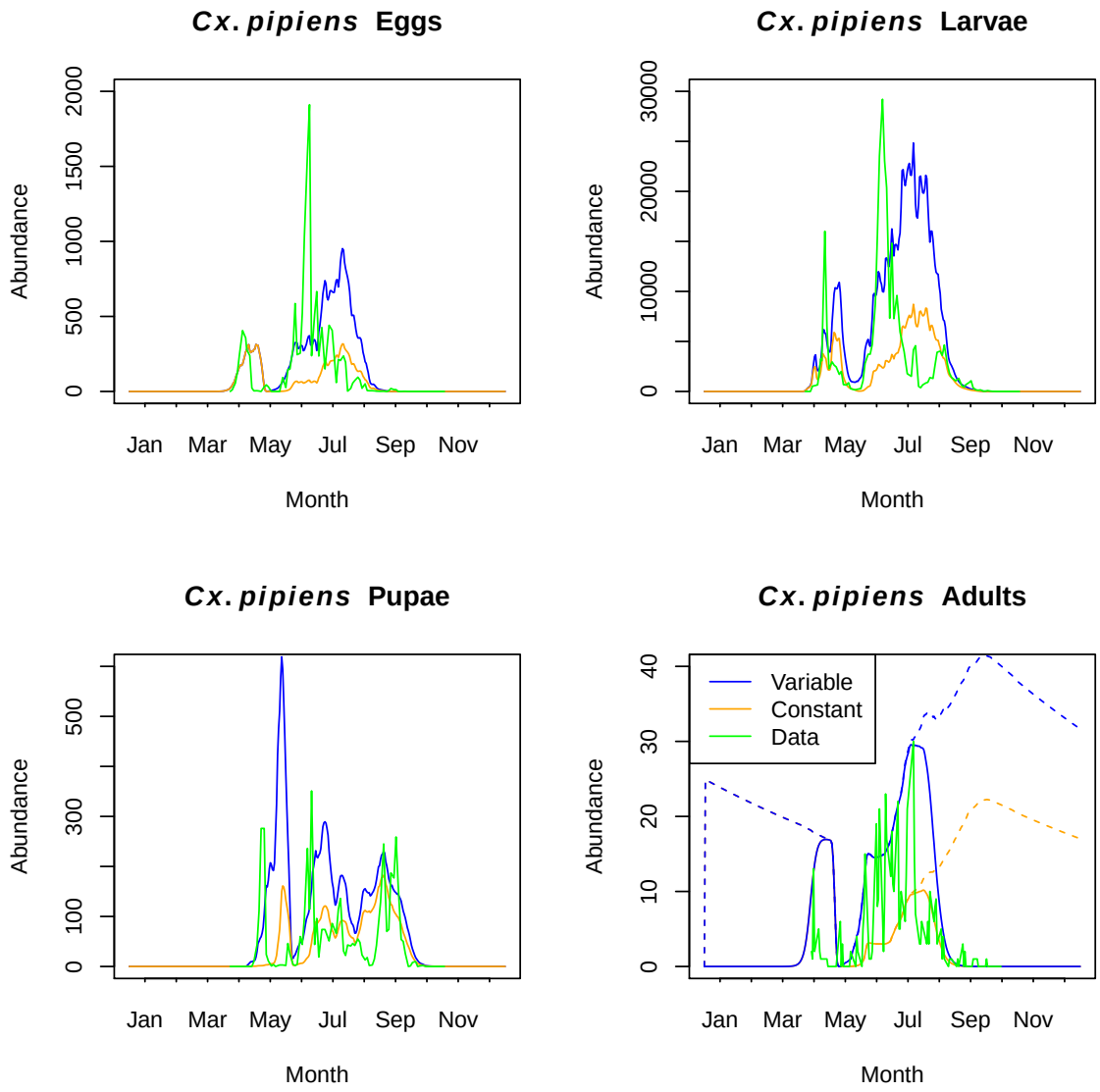

Figure C.1: Abundances under constant and variable predation: A comparison of the abundances of each life stage compared to the field data assuming both constant and variable predation, given the temperature conditions at the Wallingford field site.

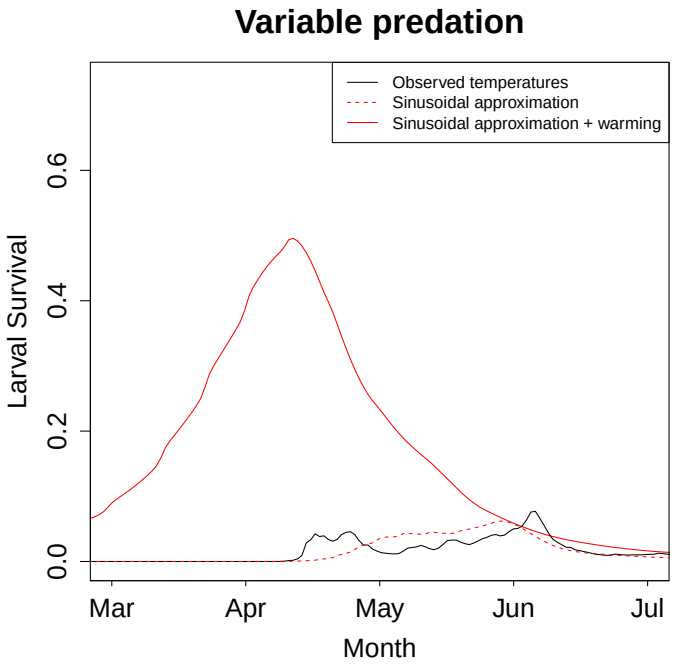

Figure C.2: Larval survival under different temperature regimes: The figure shows the larval survival during spring under three different temperature regimes when seasonal forcing is applied to the predator population. The black line represents the estimated larval survival under the observed temperature conditions in butt 4 at the Wallingford field site. The dashed red line shows the estimated larval survival when approximating those observed temperatures by a sinusoidal wave of the form described in Section 5.5.4. The solid red line shows larval survival using a sinusoidal wave fitted to the same data, with a $5\,^{\circ}\mathrm{C}$ temperature increase applied.

high vector-host ratios (Figure C.3 (d)). These high vector host ratios led to very high estimates of disease transmission (Figure C.3 (a)-(c)).

To resolve this issue it was assumed that the number of predators would remain directly proportional to the number of larvae throughout the year, as in Chapter 2. This assumption ensures that density-dependent mortality acts all year round to regulate mosquito population sizes. Figure C.4 shows that by assuming predator numbers remain directly proportional to larval numbers throughout the year, estimates of larval survival from mid-April onwards, when the mosquito active season begins, are reduced and fall more directly in line with current observations. These findings are reflected in Figure C.5, which shows that assuming seasonal variation in predation, in conjunction with a warming scenario, results in a more than hundredfold increase in abundance of each life stage when compared with the constant predation case. By comparison, in the absence of warming, estimates under seasonally varying predation exceed those under constant predation by a factor of 2-3. A discussion of alternative methods by which to incorporate seasonal predation and increased temperatures

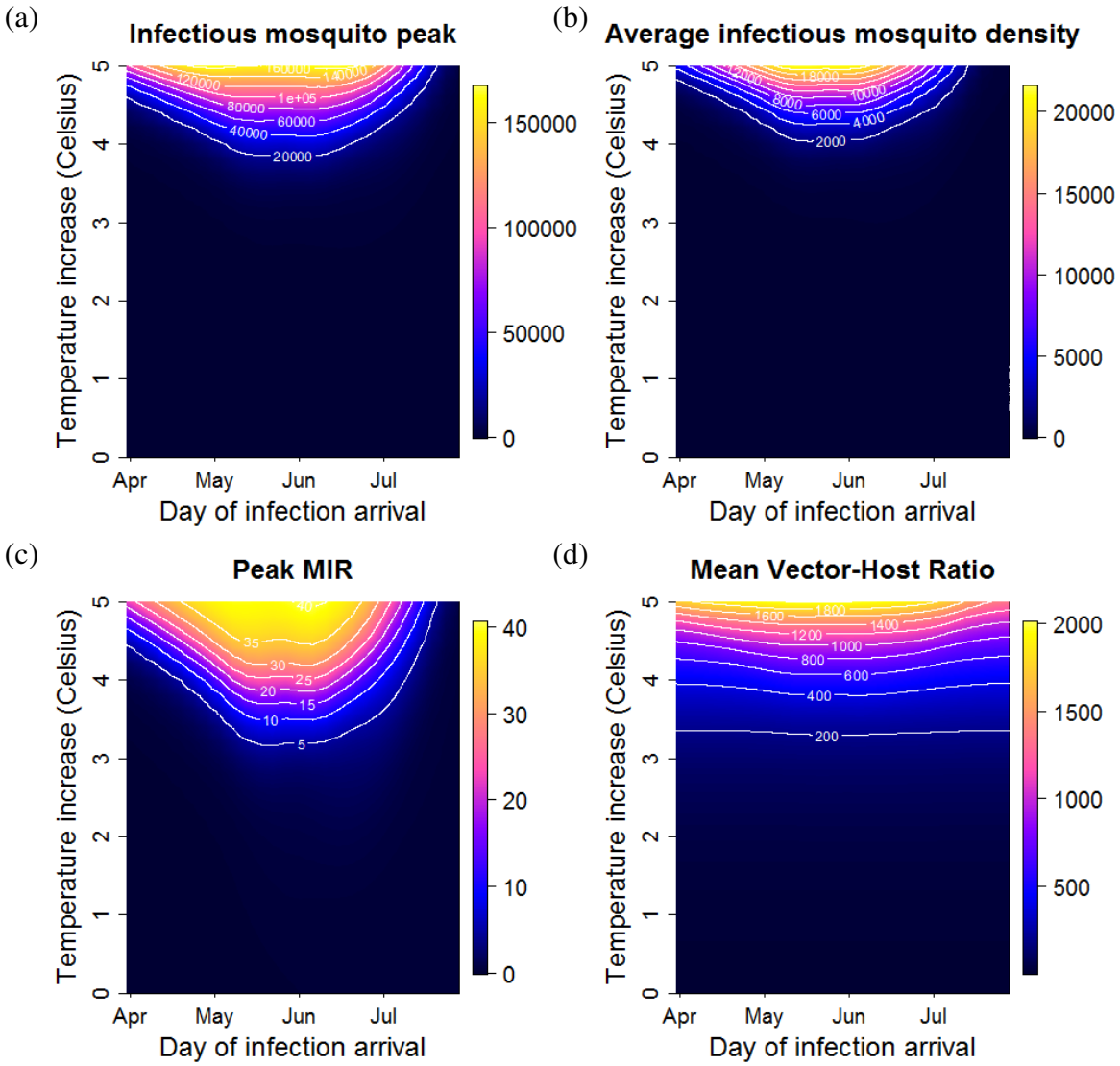

Figure C.3: Effect of warming scenarios: (a) shows the predicted maximum density of infectious mosquitoes observed on a particular day under a range of warming and introduction scenarios. (b) shows the predicted density of infectious mosquitoes per day during the months of April to August, corresponding to the main active mosquito season, under different warming and introduction scenarios. (c) shows the predicted minimum infection rate (MIR), which is the number of infectious adults per 1000 adult females. (d) shows the mean vector-host ratio during the active mosquito season (April to August).

is presented in Section 6.3.1.

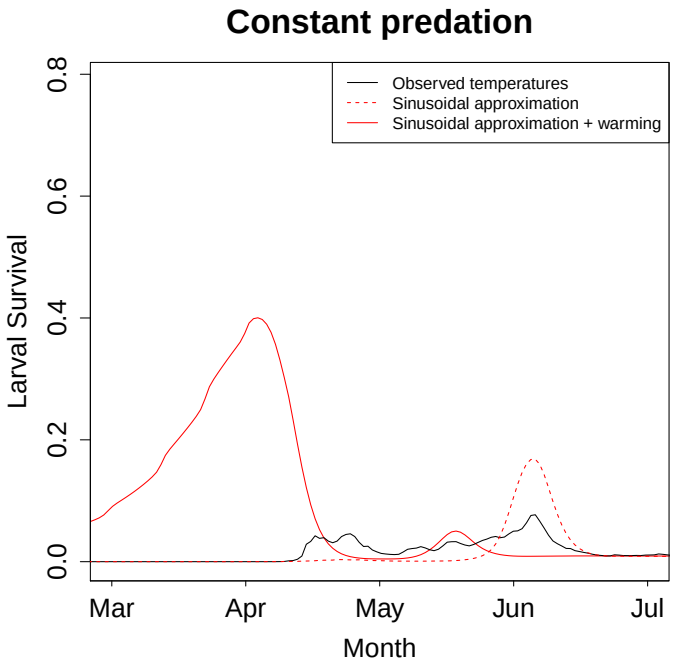

Figure C.4: Larval survival under different temperature regimes: The figure shows the larval survival during spring under three different temperature regimes in the absence of seasonal forcing of predator populations. The black line represents the estimated larval survival under the observed temperature conditions in butt 4 at the Wallingford field site. The dashed red line shows the estimated larval survival when approximating those observed temperatures by a sinusoidal wave of the form described in Section 5.5.4. The solid red line shows larval survival using a sinusoidal wave fitted to the same data, with a $5\,^{\circ}\mathrm{C}$ temperature increase applied.

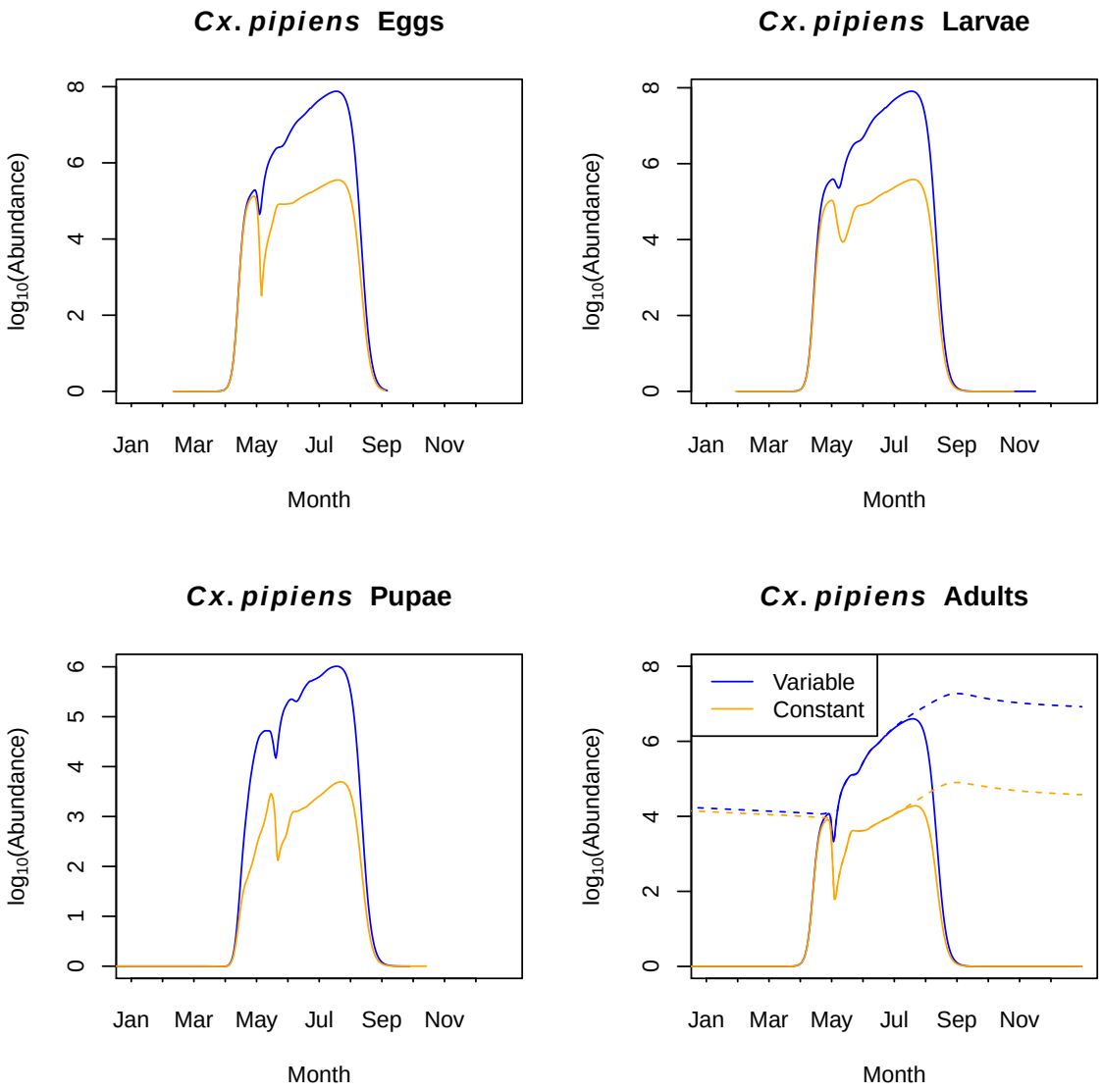

Figure C.5: Abundances under constant and variable predation with warming: A comparison of the log abundances of each life stage compared to the field data assuming both constant and variable predation, given $5\,^{\circ}\mathrm{C}$ warming above UKCIP baseline levels. Log abundances are presented due to the large difference in population size between the constant and variable predation cases.

Appendix D

Fortran Code

D.1 Chapter 2 DDE Code

```
MODULE define_DDEs

  IMPLICIT NONE

  !Set number of equations, delays and event functions
  INTEGER, PARAMETER :: NEQN=13,NLAGS=6,NEF=6
  !Set egg raft size, temperature variables and predation
     parameters
  DOUBLE PRECISION :: MAXEGG
  DOUBLE PRECISION :: M,PHASE,POWER,A,PI=3.1415927D0
  DOUBLE PRECISION :: B1,B2

CONTAINS

  SUBROUTINE DDES(T,Y,Z,DY)

    DOUBLE PRECISION :: T
    DOUBLE PRECISION, DIMENSION(NEQN) :: Y,DY
    DOUBLE PRECISION, DIMENSION(NEQN,NLAGS) :: Z
    INTENT(IN)  :: T,Y,Z
    INTENT(OUT) :: DY

    ! Define local variables
```

```
DOUBLE PRECISION :: TEMPnow, TEMPE, TEMPL, TEMPP, TEMPEL,
    TEMPLP, TEMPELP
DOUBLE PRECISION :: BIRTHnow, BIRTHE, BIRTHEL, BIRTHELP
DOUBLE PRECISION :: EGGMATnow, EGGMATE, EGGMATL, EGGMATEL,
    EGGMATLP, EGGMATELP
DOUBLE PRECISION :: LARMATnow, LARMATL, LARMATP, LARMATLP
DOUBLE PRECISION :: PPnow, PPE, PPEL, PPELP
DOUBLE PRECISION :: REt, RLt, RPt, RAt, MEt, MLt, MPt, DEt, DLt,
    DPt, DAt
DOUBLE PRECISION :: dEdt, dLdt, dPdt, dAdt, dSEdt, dSLdt, dSPdt
    , dDEdt, dDLdt, dDELdt, dDPdt, dDLPdt, dDELPdt
DOUBLE PRECISION :: E, LAR, PUP, ADU, SE, SL, SP, DE, DL, DP, DLP,
    DELP
DOUBLE PRECISION :: INOC
DOUBLE PRECISION :: DEATHeggnow, DEATHeggE, DEATHlarnow,
    DEATHlarL, DEATHpupnow, DEATHpupP, DEATHadunow
DOUBLE PRECISION :: PUPMATnow, PUPMATP, GONOTROPHICnow,
    GONOTROPHICE, GONOTROPHICEL, GONOTROPHICELP
DOUBLE PRECISION :: DIAPAUSEnow, DIAPAUSEE, DIAPAUSEEL,
    DIAPAUSEELP

! Set inoculation
INOC = INOCCULATE(T)

! Set solution values
E = Y(1)
LAR = Y(2)
PUP = Y(3)
ADU = Y(4)
SE = Y(5)
SL = Y(6)
SP = Y(7)
DE = Y(8)
DL = Y(9)
DP = Y(10)
DLP = Y(12)
DELP = Y(13)
```

```
! Set temperature values at important time points
TEMPnow = TEMP(T)
TEMPE = TEMP(T-DE)
TEMPL = TEMP(T-DL)
TEMPP = TEMP(T-DP)
TEMPEL = TEMP(T-DL-Z(8,4))
TEMPELP = TEMP(T-DP-Z(9,6)-Z(8,5))
TEMPLP = TEMP(T-DP-Z(9,6))

! Set photoperiod values at important time points
PPnow = DAYLIGHT(T)
PPE = DAYLIGHT(T-DE)
PPEL = DAYLIGHT(T-DL-Z(8,4))
PPELP = DAYLIGHT(T-DP-Z(9,6)-Z(8,5))

! Set gonotrophic cycle values values at important time
   points
GONOTROPHICnow = GONOTROPHIC(TEMPnow)
GONOTROPHICE = GONOTROPHIC(TEMPE)
GONOTROPHICEL = GONOTROPHIC(TEMPEL)
GONOTROPHICELP = GONOTROPHIC(TEMPELP)

! Set diapause and birth rate values at important time
   points
IF (DAYLIGHT(T) > DAYLIGHT(T-1)) THEN
  DIAPAUSEnow = DIAPAUSE_SPRING(PPnow)
  DIAPAUSEE = DIAPAUSE_SPRING(PPE)
  DIAPAUSEEL = DIAPAUSE_SPRING(PPEL)
  DIAPAUSEELP = DIAPAUSE_SPRING(PPELP)
  BIRTHnow = BIRTH(DIAPAUSEnow,GONOTROPHICnow,Adu,T)
  BIRTHE = BIRTH(DIAPAUSEE,GONOTROPHICE,Adu,T)
  BIRTHEL = BIRTH(DIAPAUSEEL,GONOTROPHICEL,Adu,T)
  BIRTHELP = BIRTH(DIAPAUSEELP,GONOTROPHICELP,Adu,T)
ELSE
  DIAPAUSEnow = DIAPAUSE_AUTUMN(PPnow)
  DIAPAUSEE = DIAPAUSE_AUTUMN(PPE)
```

```
      DIAPAUSEEL = DIAPAUSE_AUTUMN(PPEL)
      DIAPAUSEELP = DIAPAUSE_AUTUMN(PPELP)
      BIRTHnow = BIRTH(DIAPAUSEnow,GONOTROPHICnow,Adu,T)
      BIRTHE = BIRTH(DIAPAUSEE,GONOTROPHICE,Adu,T)
      BIRTHEL = BIRTH(DIAPAUSEEL,GONOTROPHICEL,Adu,T)
      BIRTHELP = BIRTH(DIAPAUSEELP,GONOTROPHICELP,Adu,T)
    END IF

    ! Set death rates at important time points
    DEATHeggnow = DEATHegg(TEMPnow)
    DEATHeggE = DEATHegg(TEMPE)
    DEATHlarnow = DEATHlar(TEMPnow)
    DEATHlarL = DEATHlar(TEMPL)
    DEATHpupnow = DEATHpup(TEMPnow)
    DEATHpupP = DEATHpup(TEMPP)
    DEATHadunow = DEATHadu(TEMPnow)

    ! Set development rates at important time points
    LARMATnow = LARMATURATION(TEMPnow)
    LARMATL = LARMATURATION(TEMPL)
    LARMATP = LARMATURATION(TEMPP)
    LARMATLP = LARMATURATION(TEMPLP)

    EGGMATnow = EGGMATURATION(TEMPnow)
    EGGMATE = EGGMATURATION(TEMPE)
    EGGMATL = EGGMATURATION(TEMPL)
    EGGMATEL = EGGMATURATION(TEMPEL)
    EGGMATLP = EGGMATURATION(TEMPLP)
    EGGMATELP = EGGMATURATION(TEMPELP)

    PUPMATnow = PUPMATURATION(TEMPnow)
    PUPMATP = PUPMATURATION(TEMPP)

    ! Define stage duration equations
    dDEdt = 1D0 - EGGMATnow/EGGMATE
    dDLdt = 1D0 - LARMATnow/LARMATL
    dDPdt = 1D0 - PUPMATnow/PUPMATP
```

```
dDELdt = (1D0 - dDLdt) * (1D0 - EGGMATL/EGGMATEL)
dDLPdt = (1D0 - dDPdt) * (1D0 - LARMATP/LARMATLP)
dDELPdt = (1D0 - dDPdt - dDLPdt) * (1D0 - EGGMATLP/
   EGGMATELP)

! Define recruiment rates
REt = BIRTHnow * ADU
RLt = BIRTHE * Z(4,1) * SE * EGGMATnow/EGGMATE
RPt = BIRTHEL * Z(4,2) * Z(5,4) * SL * LARMATnow/LARMATL
   * (1D0 - dDELdt)
RAt = BIRTHELP * Z(4,3) * Z(5,5) * Z(6,6) * SP *
   PUPMATnow/PUPMATP * (1D0 - dDLPdt) * (1D0 - dDELPdt) +
    INOC

! Define maturation rates
MEt = RLt
MLt = RPt
MPt = BIRTHELP * Z(4,3) * Z(5,5) * Z(6,6) * SP *
   PUPMATnow/PUPMATP * (1D0 - dDLPdt) * (1D0 - dDELPdt)

! Define death rates
DEt = DEATHeggnow * E
DLt = (B1*LAR/(B2+LAR) + DEATHlarnow) * LAR
DPt = DEATHpupnow * PUP
DAt = DEATHadunow * ADU

! Build DDEs
dEdt = REt - MEt - DEt
dLdt = RLt - MLt - DLt
dPdt = RPt - MPt - DPt
dAdt = RAt - DAt

dSEdt = SE * ((EGGMATnow * DEATHeggE / EGGMATE) -
   DEATHeggnow)
dSLdt = SL * (((B1*Z(2,4) / (B2+Z(2,4))) + DEATHlarL) *
   (1-dDLdt) - (B1*LAR / (B2+LAR)) - DEATHlarnow)
```

```
    dSPdt = SP * ((PUPMATnow * DEATHpupP / PUPMATP) -
       DEATHpupnow)

    ! Derivatives for the integrator:
    DY = (/ dEdt, dLdt, dPdt, dAdt, dSEdt, dSLdt, dSPdt,
       dDEdt, dDLdt, dDPdt, dDELdt, dDLPdt, dDELPdt /)


    RETURN
    END SUBROUTINE DDES

  SUBROUTINE BETA(T,Y,BVAL)

    DOUBLE PRECISION :: T
    DOUBLE PRECISION, DIMENSION(NEQN) :: Y
    DOUBLE PRECISION, DIMENSION(NLAGS) :: BVAL
    INTENT(IN)  :: T,Y
    INTENT(OUT) :: BVAL

    ! Set time delays
    !T - Eggdelay(T)
    BVAL(1) = T-Y(8)
    !T - Lardelay(T) - Eggdelay(T-Lardelay(T))
    BVAL(2) = T-Y(9)-Y(11)
    !T - Pupdelay(T) - Lardelay(T-Pupdelay(T)) - Eggdelay(T-
       Pupdelay(T)-Lardelay(T-Pupdelay(T)))
    BVAL(3) = T-Y(10)-Y(12)-Y(13)
    !T - Lardelay(T)
    BVAL(4) = T-Y(9)
    !T - Pupdelay(T) - Lardelay(T-Pupdelay(T))
    BVAL(5) = T-Y(10)-Y(12)
    !T - Pupdelay(T)
    BVAL(6) = T-Y(10)

    RETURN
  END SUBROUTINE BETA
```

```
SUBROUTINE HISTORY(T,Y)
  DOUBLE PRECISION :: T,TEMPhist,TEMPhistL,TEMPhistP,
     TEMPhistLP
  DOUBLE PRECISION, DIMENSION(2*NEQN) :: Y
  INTENT(IN)  :: T
  INTENT(OUT) :: Y

  !Set historical values for each equation
  TEMPhist = TEMP(T)

  Y(1) = 0D0
  Y(2) = 0D0
  Y(3) = 0D0
  Y(4) = 0D0

  Y(8) = 1D0/EGGMATURATION(TEMPhist)
  Y(9) = 1D0/LARMATURATION(TEMPhist)
  Y(10) = 1D0/PUPMATURATION(TEMPhist)

  Y(5) = EXP(-DEATHegg(TEMPhist)*(1D0/EGGMATURATION(
     TEMPhist)))
  Y(6) = EXP(-DEATHlar(TEMPhist)*(1D0/LARMATURATION(
     TEMPhist)))
  Y(7) = EXP(-DEATHpup(TEMPhist)*(1D0/PUPMATURATION(
     TEMPhist)))

  TEMPhistL = TEMP(T-Y(9))
  TEMPhistP = TEMP(T-Y(10))

  Y(11) = 1D0/EGGMATURATION(TEMPhistL)
  Y(12) = 1D0/LARMATURATION(TEMPhistP)

  TEMPhistLP = TEMP(T-Y(10)-Y(12))

  Y(13) = 1D0/EGGMATURATION(TEMPhistLP)

  RETURN
```

```
END SUBROUTINE HISTORY

SUBROUTINE EF(T,Y,DY,Z,G)

  DOUBLE PRECISION :: T
  DOUBLE PRECISION, DIMENSION(NEQN) :: Y,DY
  DOUBLE PRECISION, DIMENSION(NEQN,NLAGS) :: Z
  DOUBLE PRECISION, DIMENSION(NEF) :: G
  INTENT(IN) :: T,Y,DY,Z
  INTENT(OUT) :: G

  ! Event functions to locate peaks, troughs etc.
  G(1) = DY(4)
  G(2) = 14D0 - DAYLIGHT(T)
  G(3) = 13D0 - DAYLIGHT(T)
  G(4) = 10D0 - TEMP(T)
  G(5) = 10D0 - TEMP(T)
  G(6) = DY(6)

  RETURN
END SUBROUTINE EF

DOUBLE PRECISION FUNCTION INOCCULATE(T)

  DOUBLE PRECISION :: T

  ! Inoculate the system
  IF (T < 1D0 .AND. T > 0D0) THEN
     INOCCULATE = 12000D0
  ELSE
     INOCCULATE = 0D0
  END IF

  RETURN
END FUNCTION

DOUBLE PRECISION FUNCTION TEMP(T)
```

```
    DOUBLE PRECISION :: T

    ! Define temperature functions
    TEMP = (M-A) + A * 2 * (0.5D0 * (1D0 + COS(2D0 * Pi * (T-
       PHASE) / 365D0)))**POWER
    IF (T<0D0) THEN
      TEMP = (M-A) + A * 2 * (0.5D0 * (1D0 + COS(2D0 * Pi *
         (0D0-PHASE) / 365D0)))**POWER
    END IF

    RETURN
  END FUNCTION

  DOUBLE PRECISION FUNCTION DAYLIGHT(T)

    DOUBLE PRECISION :: T,EPS,NUM,DEN
    REAL, PARAMETER :: Pi = 3.1415927D0, L = 51D0

    ! Define photoperiod values
    EPS = ASIN(0.39795D0 * COS(0.2163108D0 + 2 * ATAN
       (0.9671396D0 * TAN(0.00860D0 * (T-3.5D0)))))
    NUM = SIN(0.8333D0*Pi/180D0) + (SIN(L*Pi/180D0) * SIN(EPS
       ))
    DEN = COS(L*Pi/180D0) * COS(EPS)
    DAYLIGHT = 24D0 - (24D0/Pi) * ACOS(NUM / DEN)

    RETURN
  END FUNCTION

  DOUBLE PRECISION FUNCTION DIAPAUSE_SPRING(PP)

    DOUBLE PRECISION :: PP

    ! Set spring diapause threshold
    DIAPAUSE_SPRING = 1D0 / (1D0 + EXP(5D0*(14D0-PP)))
```

```
    RETURN
  END FUNCTION

  DOUBLE PRECISION FUNCTION DIAPAUSE_AUTUMN(PP)

    DOUBLE PRECISION :: PP

    !Set autumn diapause threshold
    DIAPAUSE_AUTUMN = 1D0 / (1D0 + EXP(5D0*(13D0-PP)))

    RETURN
  END FUNCTION

  DOUBLE PRECISION FUNCTION BIRTH(DIAPAUSE,GONOTROPHICtime,
     Adu,T)

    DOUBLE PRECISION :: GONOTROPHICtime,EGGRAFT,Adu,T,
        DIAPAUSE

    ! Set birth rate
    EGGRAFT = DIAPAUSE*MAXEGG*0.5D0
    BIRTH = EGGRAFT/GONOTROPHICtime

    RETURN
  END FUNCTION

  DOUBLE PRECISION FUNCTION GONOTROPHIC(TEMP)

    DOUBLE PRECISION :: TEMP,GONOTROPHICRATE
    DOUBLE PRECISION :: KG=0.2024D0,QG=74.48D0,BG=0.2456D0

    ! Calculate gonotrophic cycle length
    IF (TEMP < 0D0) THEN
      GONOTROPHICRATE = 0.0333D0
    ELSE
          GONOTROPHICRATE = KG / (1+QG*EXP(-BG*TEMP))
    END IF
```

```
        IF(GONOTROPHICRATE < 0.0333D0) THEN
      GONOTROPHICRATE = 0.0333D0
    END IF
    GONOTROPHIC = 1/GONOTROPHICRATE

    RETURN
  END FUNCTION

  DOUBLE PRECISION FUNCTION DEATHegg(TEMP)

    DOUBLE PRECISION :: TEMP
    DOUBLE PRECISION :: U3=0.0157D0,U4=20.5D0,U5=7D0

    ! Calculate egg death rate
    DEATHegg = U3 * EXP(((TEMP-U4)/U5)**2)
    IF (DEATHegg > 1D0) THEN
      DEATHegg = 1D0
    END IF

    RETURN
  END FUNCTION

  DOUBLE PRECISION FUNCTION DEATHlar(TEMP)

    DOUBLE PRECISION :: TEMP
    DOUBLE PRECISION :: U3=0.0157D0,U4=20.5D0,U5=7D0

    ! Calculate larval death rate
    DEATHlar = U3 * EXP(((TEMP-U4)/U5)**2)
    IF (DEATHlar > 1D0) THEN
      DEATHlar = 1D0
    END IF

    RETURN
  END FUNCTION

  DOUBLE PRECISION FUNCTION DEATHpup(TEMP)
```

```
    DOUBLE PRECISION :: TEMP
    DOUBLE PRECISION :: U3=0.0157D0,U4=20.5D0,U5=7D0

    ! Calculate pupal death rate
    DEATHpup = U3 * EXP(((TEMP-U4)/U5)**2)
    IF (DEATHpup > 1D0) THEN
      DEATHpup = 1D0
    END IF

    RETURN
  END FUNCTION


  DOUBLE PRECISION FUNCTION DEATHadu(TEMP)

    DOUBLE PRECISION :: TEMP
    DOUBLE PRECISION :: ALPHA=2.166D-8,BETA=4.483D0

    ! Calculate adult death rate
    DEATHadu = ALPHA*(TEMP**BETA)
    IF (DEATHadu < 0.01D0) THEN
      DEATHadu = 0.01D0
    END IF

    RETURN
  END FUNCTION

  DOUBLE PRECISION FUNCTION EGGMATURATION(TEMP)

    DOUBLE PRECISION :: TEMP
    DOUBLE PRECISION :: ALPHA=0.0022D0,BETA=1.77D0

    ! Calculate egg development rate
    IF (TEMP < 0D0) THEN
        EGGMATURATION = 0.016667D0
    ELSE
```

```
        EGGMATURATION = ALPHA*(TEMP**BETA)
    END IF
    IF (EGGMATURATION < 0.016667D0) THEN
        EGGMATURATION = 0.016667D0
    END IF

    RETURN

  END FUNCTION

  DOUBLE PRECISION FUNCTION LARMATURATION(TEMP)

    DOUBLE PRECISION :: TEMP
    DOUBLE PRECISION :: ALPHA=0.00315D0,BETA=1.12D0

    ! Calculate larval development rate
    IF (TEMP < 0D0) THEN
        LARMATURATION = 0.016667D0
    ELSE
        LARMATURATION = ALPHA*(TEMP**BETA)
    END IF
    IF (LARMATURATION < 0.016667D0) THEN
        LARMATURATION = 0.016667D0
    END IF

    RETURN
  END FUNCTION

  DOUBLE PRECISION FUNCTION PUPMATURATION(TEMP)

    DOUBLE PRECISION :: TEMP
    DOUBLE PRECISION :: ALPHA=0.0007109D0,BETA=1.8865648D0

    ! Calculate pupal development rate
    IF (TEMP < 0D0) THEN
        PUPMATURATION = 0.016667D0
    ELSE
```

```
        PUPMATURATION = ALPHA*(TEMP**BETA)
    END IF
    IF (PUPMATURATION < 0.016667D0) THEN
        PUPMATURATION = 0.016667D0
    END IF

    RETURN
  END FUNCTION

END MODULE define_DDEs

!*****************************************************************


PROGRAM chapter2model

  USE define_DDEs
  USE DDE_SOLVER_M

  IMPLICIT NONE

  INTEGER :: I,J ! Local variables

  INTEGER, DIMENSION(3) :: NVAR = (/NEQN,NLAGS,NEF/)

  ! Set length of solution and output points
  INTEGER, PARAMETER :: NOUT=913D0
  DOUBLE PRECISION, PARAMETER :: T0=0D0,TFINAL=912D0
  DOUBLE PRECISION, DIMENSION(NOUT) :: TSPAN= &
  (/ (T0+(I-1)*((TFINAL - T0)/(NOUT-1)), I=1,NOUT) /)

  TYPE(DDE_SOL) :: SOL
  TYPE(DDE_OPTS) :: OPTS

  DOUBLE PRECISION :: MAXDELAY = 200D0
  CHARACTER (len=90) :: filename
```

```
  ! Options for the DDE solver
  OPTS = DDE_SET(RE=1D-11,AE=1D-20,MAX_STEPS=1000000000,
     MAX_DELAY=MAXDELAY,TRIM_FREQUENCY=10000,DIRECTION=(/
     0,-1,1,-1,1,0 /))

  ! Run the DDE solver
  SOL = DDE_SOLVER(NVAR,DDES,BETA,HISTORY,TSPAN,EVENT_FCN=EF,
     OPTIONS=OPTS)

  ! Was the solver successful?
  IF (SOL%FLAG == 0) THEN
    ! Output solutions
    WRITE(filename, '( "filename.dat" )' )
    OPEN(unit=11,file=filename)
    DO I = 1,SOL%NPTS
        WRITE(UNIT=11,FMT='(16E14.5E3)') SOL%T(I),(SOL%Y(I,J)
           ,J=1,NEQN)
    END DO
    CLOSE(11)
  ELSE
    PRINT *,' Abnormal return from DDE_SOLVER with FLAG = ',&
    SOL%FLAG
  END IF

  STOP
END PROGRAM chapter2model
```

D.2 Chapter 4 DDE Code

```
MODULE define_DDEs

  IMPLICIT NONE

  ! Set number of equations, delays and event functions
  INTEGER, PARAMETER :: NEQN=14,NLAGS=6,NEF=3
  ! Set length of temperature datasets
  INTEGER, PARAMETER :: TEMPNwater = 17520, TEMPNair = 1460
```

```
  INTEGER :: K
  DOUBLE PRECISION :: PI=3.1415927D0
  ! Set predation parameters and egg raft size
  DOUBLE PRECISION :: densa,densr,densh,UPS,SHP,MAXEGG
  ! Set time points for temperature values
  double precision, DIMENSION(TEMPNwater) :: Xtempwater= (/ (
     K/24D0, K=1,TEMPNwater) /)
  double precision, DIMENSION(TEMPNair) :: Xtempair= (/ (K/2
     D0, K=1,TEMPNair) /)

CONTAINS

  SUBROUTINE DDES(T,Y,Z,DY)

    ! Set variables for DDE solver
    DOUBLE PRECISION :: T
    DOUBLE PRECISION, DIMENSION(NEQN) :: Y,DY
    DOUBLE PRECISION, DIMENSION(NEQN,NLAGS) :: Z
    INTENT(IN)  :: T,Y,Z
    INTENT(OUT) :: DY
    INTEGER :: K,L
    ! Set values used in extracting temperature data and
       interpolating between values
    DOUBLE PRECISION :: ytempp1 = 1D0, ytemppn = 1D0
    DOUBLE PRECISION, DIMENSION(TEMPNwater) :: watertemp,
       watertemp2
    DOUBLE PRECISION, DIMENSION(TEMPNair) :: airtemp,
       airtemp2

    ! Define variable names
    DOUBLE PRECISION :: TEMPnowair,TEMPGCair
    DOUBLE PRECISION :: TEMPnowwater,TEMPEwater,TEMPLwater,
       TEMPPwater,TEMPELwater,TEMPLPwater,TEMPELPwater
    DOUBLE PRECISION :: BIRTHnow,BIRTHE,BIRTHEL,BIRTHELP
    DOUBLE PRECISION :: EGGMATnow,EGGMATE,EGGMATL,EGGMATEL,
       EGGMATLP,EGGMATELP
    DOUBLE PRECISION :: LARMATnow,LARMATL,LARMATP,LARMATLP
```

```
DOUBLE PRECISION :: REt, RLt, RPt, RAt, MEt, MLt, MPt, DEt, DLt,
    DPt, DAt
DOUBLE PRECISION :: dEdt, dLdt, dPdt, dAdt, dSEdt, dSLdt, dSPdt
    , dDEdt, dDLdt, dDELdt, dDPdt, dDLPdt, dDELPdt, dGCdt
DOUBLE PRECISION :: E, LAR, PUP, ADU, SE, SL, SP, DE, DL, DP, GC
DOUBLE PRECISION :: INOC
DOUBLE PRECISION :: DEATHeggnow, DEATHeggE, DEATHlarnow,
    DEATHlarL, DEATHpupnow, DEATHpupP, DEATHadunow
DOUBLE PRECISION :: PUPMATnow, PUPMATP
DOUBLE PRECISION :: DIAPAUSEE, DIAPAUSEEL, DIAPAUSEELP,
    DIAPAUSEnow
DOUBLE PRECISION :: PPnow, PPE, PPEL, PPELP
DOUBLE PRECISION :: GCnow, GCC

! Read in temperature data
OPEN (UNIT=7, FILE="Butt4hourlytemps-winterstart-twoyears
    .csv", STATUS="OLD", ACTION="READ")
READ(7,*)
DO K = 1, TEMPNwater
  READ (7,*) watertemp(K)
END DO
CLOSE(7)

OPEN (UNIT=7, FILE="Airminmaxmetsite-winterstart-twoyears
    .csv", STATUS="OLD", ACTION="READ")
READ(7,*)
DO L = 1, TEMPNair
  READ (7,*) airtemp(L)
END DO
CLOSE(7)

! Interpolate between temperature values using spline
CALL cubic_spline_air(xtempair, airtemp, TEMPnair,
    ytempp1, ytemppn, airtemp2)
CALL cubic_spline_water(xtempwater, watertemp, TEMPnwater
    , ytempp1, ytemppn, watertemp2)
```

```
! Give names to responses of system of equations
E = Y(1)
LAR = Y(2)
PUP = Y(3)
ADU = Y(4)
SE = Y(5)
SL = Y(6)
SP = Y(7)
DE = Y(8)
DL = Y(9)
DP = Y(10)
GC = Y(14)

! Extract temperature values at various time points
TEMPnowwater = splint(xtempwater,watertemp,watertemp2,
   TEMPnwater,T)
TEMPnowair = splint(xtempair,airtemp,airtemp2,TEMPnair,T)
TEMPEwater = splint(xtempwater,watertemp,watertemp2,
   TEMPnwater,T-DE)
TEMPLwater = splint(xtempwater,watertemp,watertemp2,
   TEMPnwater,T-DL)
TEMPPwater = splint(xtempwater,watertemp,watertemp2,
   TEMPnwater,T-DP)
TEMPELwater = splint(xtempwater,watertemp,watertemp2,
   TEMPnwater,T-DL-Z(8,4))
TEMPELPwater = splint(xtempwater,watertemp,watertemp2,
   TEMPnwater,T-DP-Z(9,6)-Z(8,5))
TEMPLPwater = splint(xtempwater,watertemp,watertemp2,
   TEMPnwater,T-DP-Z(9,6))
TEMPGCair = splint(xtempair,airtemp,airtemp2,TEMPnair,T-
   GC)

! Define temperature values for time points before T=0
IF ((T-DE) .LE. 0) THEN
  TEMPEwater = 5D0
END IF
IF ((T-DL) .LE. 0) THEN
```

```
      TEMPLwater = 5D0
    END IF
    IF ((T-DP) .LE. 0) THEN
      TEMPPwater = 5D0
    END IF
    IF ((T-DL-Z(8,4)) .LE. 0) THEN
      TEMPELwater = 5D0
    END IF
    IF ((T-DP-Z(9,6)-Z(8,5)) .LE. 0) THEN
      TEMPELPwater = 5D0
    END IF
    IF ((T-DP-Z(9,6)) .LE. 0) THEN
      TEMPLPwater = 5D0
    END IF
    IF ((T-GC) .LE. 0) THEN
      TEMPGCair = 5D0
    END IF

    ! Calculate photoperiod values for a range of time points
    PPnow = DAYLIGHT(T)
    PPE = DAYLIGHT(T-DE)
    PPEL = DAYLIGHT(T-DL-Z(8,4))
    PPELP = DAYLIGHT(T-DP-Z(9,6)-Z(8,5))

    ! Calculate gonotrophic cycle length for various time
       points
    GCnow = GONOTROPHIC(TEMPnowair)
    GCC = GONOTROPHIC(TEMPGCair)

    ! Calculate diapause percentage for given photoperiod
       values.
    ! Use these diapause percentages to caluclate birth rates
       .
    ! Do this for both spring and autumn diapause thresholds.
    IF (DAYLIGHT(T) > DAYLIGHT(T-1)) THEN
      DIAPAUSEnow = DIAPAUSE_SPRING(PPnow)
      DIAPAUSEE = DIAPAUSE_SPRING(PPE)
```

```
      DIAPAUSEEL = DIAPAUSE_SPRING(PPEL)
      DIAPAUSEELP = DIAPAUSE_SPRING(PPELP)
      BIRTHnow = BIRTH(DIAPAUSEnow,GC)
      BIRTHE = BIRTH(DIAPAUSEE,Z(14,1))
      BIRTHEL = BIRTH(DIAPAUSEEL,Z(14,2))
      BIRTHELP = BIRTH(DIAPAUSEELP,Z(14,3))
    ELSE
      DIAPAUSEnow = DIAPAUSE_AUTUMN(PPnow)
      DIAPAUSEE = DIAPAUSE_AUTUMN(PPE)
      DIAPAUSEEL = DIAPAUSE_AUTUMN(PPEL)
      DIAPAUSEELP = DIAPAUSE_AUTUMN(PPELP)
      BIRTHnow = BIRTH(DIAPAUSEnow,GC)
      BIRTHE = BIRTH(DIAPAUSEE,Z(14,1))
      BIRTHEL = BIRTH(DIAPAUSEEL,Z(14,2))
      BIRTHELP = BIRTH(DIAPAUSEELP,Z(14,3))
    END IF

    ! Calculate death rates for each life stage
    DEATHeggnow = DEATHegg(TEMPnowwater)
    DEATHeggE = DEATHegg(TEMPEwater)

    DEATHlarnow = DEATHlar(TEMPnowwater)
    DEATHlarL = DEATHlar(TEMPLwater)

    DEATHpupnow = DEATHpup(TEMPnowwater)
    DEATHpupP = DEATHpup(TEMPPwater)

    DEATHadunow = DEATHadu(TEMPnowair,GC,T)

    ! Calculate development rates for the immature stages
    LARMATnow = LARMATURATION(TEMPnowwater)
    LARMATL = LARMATURATION(TEMPLwater)
    LARMATP = LARMATURATION(TEMPPwater)
    LARMATLP = LARMATURATION(TEMPLPwater)

    EGGMATnow = EGGMATURATION(TEMPnowwater)
    EGGMATE = EGGMATURATION(TEMPEwater)
```

```
EGGMATL = EGGMATURATION(TEMPLwater)
EGGMATEL = EGGMATURATION(TEMPELwater)
EGGMATLP = EGGMATURATION(TEMPLPwater)
EGGMATELP = EGGMATURATION(TEMPELPwater)

PUPMATnow = PUPMATURATION(TEMPnowwater)
PUPMATP = PUPMATURATION(TEMPPwater)

! Innoculate the system with a given number of adults.
INOC = INOCCULATE(T)

! Delay differential equations for immature stage
   durations
dDEdt = 1D0 - EGGMATnow/EGGMATE
dDLdt = 1D0 - LARMATnow/LARMATL
dDPdt = 1D0 - PUPMATnow/PUPMATP

! Delay differential equation for gonotrophic cycle
   duration
dGCdt = 1D0 - GCnow/GCC

! Delay differential equations for stage durations
   referenced back through previous stages
dDELdt = (1D0 - dDLdt) * (1D0 - EGGMATL/EGGMATEL)
dDLPdt = (1D0 - dDPdt) * (1D0 - LARMATP/LARMATLP)
dDELPdt = (1D0 - dDPdt - dDLPdt) * (1D0 - EGGMATLP/
   EGGMATELP)

! Recruitment equations for each stage
REt = BIRTHnow * ADU
RLt = BIRTHE * Z(4,1) * SE * EGGMATnow/EGGMATE
RPt = BIRTHEL * Z(4,2) * Z(5,4) * SL * LARMATnow/LARMATL
   * EGGMATL/EGGMATEL
RAt = BIRTHELP * Z(4,3) * Z(5,5) * Z(6,6) * SP *
   PUPMATnow/PUPMATP * LARMATP/LARMATLP * EGGMATLP/
   EGGMATELP + INOC
```

```
! Maturation equations for each stage
MEt = RLt
MLt = RPt
MPt = BIRTHELP * Z(4,3) * Z(5,5) * Z(6,6) * SP *
   PUPMATnow/PUPMATP * LARMATP/LARMATLP * EGGMATLP/
   EGGMATELP

! Death equations for each stage
DEt = DEATHeggnow * E
DLt = (densa*densr*(((1D0+COS(2D0*PI*(T-182.5D0-UPS)/365
   D0))/2D0)**SHP)*LAR/(20D0+densh*LAR)+DEATHlarnow)*LAR
DPt = DEATHpupnow * PUP
DAt = DEATHadunow * ADU

! Balance equations for each life stage
dEdt = REt - MEt - DEt
dLdt = RLt - MLt - DLt
dPdt = RPt - MPt - DPt
dAdt = RAt - DAt

! Survival equations for the immature stages
dSEdt = SE * ((EGGMATnow * DEATHeggE / EGGMATE) -
   DEATHeggnow)
dSLdt =SL*(((densa*densr*(((1D0+COS(2D0*PI*(T-DL-182.5D0-
   UPS)/365D0))/2D0)**SHP)*Z(2,4)/(20D0+densh*Z(2,4)))+
   DEATHlarL) * (1-dDLdt) - (densa*densr*(((1D0+COS(2D0*
   PI*(T-182.5D0-UPS)/365D0))/2D0)**SHP)*LAR / (20D0+
   densh*LAR)) - DEATHlarnow)
dSPdt = SP * ((PUPMATnow * DEATHpupP / PUPMATP) -
   DEATHpupnow)

! Derivatives for the integrator:
DY = (/ dEdt, dLdt, dPdt, dAdt, dSEdt, dSLdt, dSPdt,
   dDEdt, dDLdt, dDPdt, dDELdt, dDLPdt, dDELPdt, dGCdt /)

  RETURN
END SUBROUTINE DDES
```

```
SUBROUTINE BETA(T,Y,BVAL)

  DOUBLE PRECISION :: T
  DOUBLE PRECISION, DIMENSION(NEQN) :: Y
  DOUBLE PRECISION, DIMENSION(NLAGS) :: BVAL
  INTENT(IN)  :: T,Y
  INTENT(OUT) :: BVAL

  ! Set the delay values
  ! T - Eggdelay(T)
  BVAL(1) = T-Y(8)
  ! T - Lardelay(T) - Eggdelay(T-Lardelay(T))
  BVAL(2) = T-Y(9)-Y(11)
  !T - Pupdelay(T) - Lardelay(T-Pupdelay(T)) - Eggdelay(T-
     Pupdelay(T)-Lardelay(T-Pupdelay(T)))
  BVAL(3) = T-Y(10)-Y(12)-Y(13)
  !T - Lardelay(T)
  BVAL(4) = T-Y(9)
  !T - Pupdelay(T) - Lardelay(T-Pupdelay(T))
  BVAL(5) = T-Y(10)-Y(12)
  !T - Pupdelay(T)
  BVAL(6) = T-Y(10)

  RETURN
END SUBROUTINE BETA

SUBROUTINE HISTORY(T,Y)
  DOUBLE PRECISION :: T,TEMPhist
  DOUBLE PRECISION, DIMENSION(2*NEQN) :: Y
  INTENT(IN)  :: T
  INTENT(OUT) :: Y

  ! Set the temperatures for T < 0
  TEMPhist = 5D0

  ! Set historical values for all stages to be zero
```

```
      Y(1) = 0D0
      Y(2) = 0D0
      Y(3) = 0D0
      Y(4) = 0D0

      ! Calculate historical survival rates based on
         temperature
      Y(5) = EXP(-DEATHegg(TEMPhist)*(1D0/EGGMATURATION(
         TEMPhist)))
      Y(6) = EXP(-DEATHlar(TEMPhist)*(1D0/LARMATURATION(
         TEMPhist)))
      Y(7) = EXP(-DEATHpup(TEMPhist)*(1D0/PUPMATURATION(
         TEMPhist)))

      ! Calculate historical development rates based on
         temperature
      Y(8) = 1D0/EGGMATURATION(TEMPhist)
      Y(9) = 1D0/LARMATURATION(TEMPhist)
      Y(10) = 1D0/PUPMATURATION(TEMPhist)
      Y(11) = 1D0/EGGMATURATION(TEMPhist)
      Y(12) = 1D0/LARMATURATION(TEMPhist)
      Y(13) = 1D0/EGGMATURATION(TEMPhist)
      Y(14) = 1D0/GONOTROPHIC(TEMPhist)


      RETURN
    END SUBROUTINE HISTORY

    SUBROUTINE cubic_spline_air(x,airtemp,n,airtempp1,airtemppn
       ,airtemp2)
      INTEGER n,NMAX
      double precision airtempp1,airtemppn,x(n),airtemp(n),
         airtemp2(n)
      PARAMETER (NMAX=1460)

      !Code taken from NUMERICAL RECIPES IN FORTRAN 77: THE ART
          OF SCIENTIFIC COMPUTING (ISBN 0-521-43064-X)
```

```
!Given arrays x(1:n) and y(1:n) containing a tabulated
   function, i.e., yi = f(xi), with
!x1 < x2 < ::: < xN, and given values yp1 and ypn for the
    first derivative of the interpolating
!function at points 1 and n, respectively, this routine
   returns an array y2(1:n) of
!length n which contains the second derivatives of the
   interpolating function at the tabulated
!points xi. If yp1 and/or ypn are equal to 1 / 1030 or
   larger, the routine is signaled to set
!the corresponding boundary condition for a natural
   spline, with zero second derivative on
!that boundary.

!Parameter: NMAX is the largest anticipated value of n.
INTEGER i,k
DOUBLE PRECISION p,qn,sig,un,u(NMAX)
IF (airtempp1.GT..99E30) THEN
  airtemp2(1)=0. !\natural"
  u(1)=0.
ELSE !or else to have a specified first derivative.
  airtemp2(1)=-0.5
  u(1)=(3./(x(2)-x(1)))*((airtemp(2)-airtemp(1))/(x(2)-x
     (1))-airtempp1)
END IF
DO i=2,n-1
  !This is the decomposition loop of the tridiagonal
  !algorithm. y2 and u are used for temporary
  !storage of the decomposed factors.
  sig=(x(i)-x(i-1))/(x(i+1)-x(i-1))
  p=sig*airtemp2(i-1)+2.
  airtemp2(i)=(sig-1.)/p
  u(i)=(6.*((airtemp(i+1)-airtemp(i))/(x(i+1)-x(i))-(
     airtemp(i)-airtemp(i-1)) / (x(i)-x(i-1)))/(x(i+1)-x(
     i-1))-sig*u(i-1))/p
END DO
IF (airtemppn.gt..99e30) THEN
```

```
      qn=0. !\natural"
      un=0.
    ELSE
      qn=0.5
      un=(3./(x(n)-x(n-1)))*(airtemppn-(airtemp(n)-airtemp(n
          -1))/(x(n)-x(n-1)))
    ENDIF
    airtemp2(n)=(un-qn*u(n-1))/(qn*airtemp2(n-1)+1.)
    DO k=n-1,1,-1
      airtemp2(k)=airtemp2(k)*airtemp2(k+1)+u(k)
    END DO

    RETURN
  END SUBROUTINE

  SUBROUTINE cubic_spline_water(x,watertemp,n,watertempp1,
     watertemppn,watertemp2)

    INTEGER :: n,NMAX
    DOUBLE PRECISION :: watertempp1,watertemppn,x(n),
       watertemp(n),watertemp2(n)
    PARAMETER (NMAX=131400)

      !Code taken from NUMERICAL RECIPES IN FORTRAN 77: THE
         ART OF SCIENTIFIC COMPUTING (ISBN 0-521-43064-X)
      !Given arrays x(1:n) and y(1:n) containing a tabulated
         function, i.e., yi = f(xi), with
      !x1 < x2 < ::: < xN, and given values yp1 and ypn for
         the first derivative of the interpolating
      !function at points 1 and n, respectively, this routine
          returns an array y2(1:n) of
      !length n which contains the second derivatives of the
         interpolating function at the tabulated
      !points xi. If yp1 and/or ypn are equal to 1 / 1030 or
         larger, the routine is signaled to set
      !the corresponding boundary condition for a natural
         spline, with zero second derivative on
```

```
      !that boundary.

      !Parameter: NMAX is the largest anticipated value of n.
      INTEGER :: i,k
      DOUBLE PRECISION :: p,qn,sig,un,u(NMAX)
      IF (watertempp1.gt..99e30) THEN
        watertemp2(1)=0. !\natural"
        u(1)=0.
      ELSE !or else to have a specified first derivative.
        watertemp2(1)=-0.5
        u(1)=(3./(x(2)-x(1)))*((watertemp(2)-watertemp(1))/(x
            (2)-x(1))-watertempp1)
      END IF
      DO i=2,n-1
        sig=(x(i)-x(i-1))/(x(i+1)-x(i-1))
        p=sig*watertemp2(i-1)+2.
        watertemp2(i)=(sig-1.)/p
        u(i)=(6.*((watertemp(i+1)-watertemp(i))/(x(i+1)-x(i))
            -(watertemp(i)-watertemp(i-1))/(x(i)-x(i-1)))/(x(i
            +1)-x(i-1))-sig*u(i-1))/p
      END DO
      IF (watertemppn.gt..99e30) THEN
        qn=0. !\natural"
        un=0.
      ELSE !or else to have a specified first derivative.
        qn=0.5
        un=(3./(x(n)-x(n-1)))*(watertemppn-(watertemp(n)-
            watertemp(n-1))/(x(n)-x(n-1)))
      END IF
        watertemp2(n)=(un-qn*u(n-1))/(qn*watertemp2(n-1)+1.)
      DO k=n-1,1,-1 !This is the backsubstitution loop of the
          tridiagonal algorithm.
        watertemp2(k)=watertemp2(k)*watertemp2(k+1)+u(k)
      END DO

    RETURN
  END SUBROUTINE
```

```
DOUBLE PRECISION FUNCTION SPLINT(xa,ytempa,ytemp2a,tempn,x
    )

 INTEGER tempn
 DOUBLE PRECISION xa(tempn),ytemp2a(tempn),ytempa(tempn)
 DOUBLE PRECISION x
 !Given the arrays xa(1:n) and ya(1:n) of length n, which
    tabulate a function (with the
 !xai 's in order), and given the array y2a(1:n), which is
     the output from spline above,
 !and given a value of x, this routine returns a cubic-
    spline interpolated value y.
 INTEGER k,khi,klo
 DOUBLE PRECISION a1,b,h1

 !We will find the right place in the table by means of
    bisection.
 !This is optimal if sequential calls to this routine are
    at random
 !values of x. If sequential calls are in order, and
    closely
 !spaced, one would do better to store previous values of
 !klo and khi and test if they remain appropriate on the
 !next call.

 klo=1
 khi=tempn
 DO
   IF (khi-klo.le.1) EXIT
   k=(khi+klo)/2
   IF(xa(k).gt.x) then
     khi=k
   ELSE
     klo=k
   END IF
 END DO
```

```
    h1=xa(khi)-xa(klo)
    IF (h1.eq.0) PAUSE 'bad xa input in splint'
    a1=(xa(khi)-x)/h1
    b=(x-xa(klo))/h1
    IF (x .le. 0) then
      splint=0.1d0
    ELSE
      splint=a1*ytempa(klo)+b*ytempa(khi)+ ((a1**3-a1)*
        ytemp2a(klo)+(b**3-b)*ytemp2a(khi))*(h1**2)/6.
    END IF

    RETURN
  END FUNCTION


  DOUBLE PRECISION FUNCTION INOCCULATE(T)

    DOUBLE PRECISION :: T

    ! Set inoculation value
    IF (T < 1D0 .AND. T > 0D0) THEN
       INOCCULATE = 5000D0
    ELSE
       INOCCULATE = 0D0
    END IF

    RETURN
  END FUNCTION

  DOUBLE PRECISION FUNCTION DAYLIGHT(T)

    DOUBLE PRECISION :: T,EPS,NUM,DEN
    REAL, PARAMETER :: Pi = 3.1415927D0, L = 51.6D0

    ! Calculate photoperiod for time, T
```

```
    EPS = ASIN(0.39795D0 * COS(0.2163108D0 + 2 * ATAN
       (0.9671396D0 * TAN(0.00860D0 * (T-185.5D0)))))
    NUM = SIN(0.8333D0*Pi/180D0) + (SIN(L*Pi/180D0) * SIN(EPS
       ))
    DEN = COS(L*Pi/180D0) * COS(EPS)
    DAYLIGHT = 24D0 - (24D0/Pi) * ACOS(NUM / DEN)

    RETURN
  END FUNCTION

  DOUBLE PRECISION FUNCTION DIAPAUSE_SPRING(PP)

    DOUBLE PRECISION :: PP

    ! Set spring diapause threshold
    DIAPAUSE_SPRING = 1D0 / (1D0 + EXP(5D0*(13.7D0-PP)))

    RETURN
  END FUNCTION

  DOUBLE PRECISION FUNCTION DIAPAUSE_AUTUMN(PP)

    DOUBLE PRECISION :: PP

    !Set autumn diapause threshold
    DIAPAUSE_AUTUMN = 1D0 / (1D0 + EXP(3.5D0*(15D0-PP)))

    RETURN
  END FUNCTION

  DOUBLE PRECISION FUNCTION BIRTH(DIAPAUSE,GONOTROPHICtime)

  DOUBLE PRECISION :: GONOTROPHICtime,EGGRAFT,DIAPAUSE

    !Set birth rate
    EGGRAFT = DIAPAUSE*MAXEGG*0.5D0
    BIRTH = EGGRAFT/GONOTROPHICtime
```

```
    RETURN
  END FUNCTION

  DOUBLE PRECISION FUNCTION GONOTROPHIC(TEMP)

    DOUBLE PRECISION :: TEMP
    DOUBLE PRECISION :: KG=0.2024D0,QG=74.48D0,BG=0.2456D0

    !Set gonotrophic cycle rate
    IF (TEMP < 0D0) THEN
      GONOTROPHIC = 0.0333D0
    ELSE
      GONOTROPHIC = KG / (1+QG*EXP(-BG*TEMP))
    END IF
    IF(GONOTROPHIC < 0.0333D0) THEN
      GONOTROPHIC = 0.0333D0
    END IF

    RETURN
  END FUNCTION

  DOUBLE PRECISION FUNCTION DEATHegg(TEMP)

    DOUBLE PRECISION :: TEMP
    DOUBLE PRECISION :: U3=0.0157D0,U4=20.5D0,U5=7D0

    ! Set death rate of eggs
    DEATHegg = U3 * EXP(((TEMP-U4)/U5)**2)
    IF (DEATHegg > 1D0) THEN
      DEATHegg = 1D0
    END IF

    RETURN
  END FUNCTION

  DOUBLE PRECISION FUNCTION DEATHlar(TEMP)
```

```
    DOUBLE PRECISION :: TEMP
    DOUBLE PRECISION :: U3=0.0157D0,U4=20.5D0,U5=7D0

    ! Set death rate of larvae
    DEATHlar = U3 * EXP(((TEMP-U4)/U5)**2)
    IF (DEATHlar > 1D0) THEN
      DEATHlar = 1D0
    END IF

    RETURN
  END FUNCTION

  DOUBLE PRECISION FUNCTION DEATHpup(TEMP)

    DOUBLE PRECISION :: TEMP
    DOUBLE PRECISION :: U3=0.0157D0,U4=20.5D0,U5=7D0

    ! Set death rate of pupae
    DEATHpup = U3 * EXP(((TEMP-U4)/U5)**2)
    IF (DEATHpup > 1D0) THEN
      DEATHpup = 1D0
    END IF

    RETURN
  END FUNCTION

  DOUBLE PRECISION FUNCTION DEATHadu(TEMP,GONOTROPHICtime,T)

    DOUBLE PRECISION :: TEMP,GONOTROPHICtime,T
    DOUBLE PRECISION :: ALPHA=2.166D-8,BETA=4.483D0,PI
       =3.1415927D0,MULTIPLIER=8D0,SIGMASQ=4D0

    !Set adult death rate
    IF (TEMP < 0D0) THEN
      DEATHadu = 0.003D0
    ELSE
```

```
      DEATHadu = ALPHA*(TEMP**BETA)
    END IF
    IF (DEATHadu < 0.003D0) THEN
      DEATHadu = 0.003D0
    END IF
    DEATHadu = DEATHadu + (MULTIPLIER/SQRT(SIGMASQ*2D0*PI))*
       EXP((-1D0/(SIGMASQ*2D0)) * (MOD(T,365D0)-
       GONOTROPHICtime-109D0)**2)

    RETURN
  END FUNCTION

  DOUBLE PRECISION FUNCTION EGGMATURATION(TEMP)

    DOUBLE PRECISION :: TEMP
    DOUBLE PRECISION :: ALPHA=0.0022D0,BETA=1.77D0

    ! Set egg development rate
    IF (TEMP < 0D0) THEN
      EGGMATURATION = 0.016667D0
    ELSE
      EGGMATURATION = ALPHA*(TEMP**BETA)
    END IF
    IF (EGGMATURATION < 0.016667D0) THEN
      EGGMATURATION = 0.016667D0
    END IF

    RETURN
  END FUNCTION

  DOUBLE PRECISION FUNCTION LARMATURATION(TEMP)

    DOUBLE PRECISION :: TEMP
    DOUBLE PRECISION :: ALPHA=0.00315D0,BETA=1.12D0

    ! Set larval development rate
    IF (TEMP < 0D0) THEN
```

```
      LARMATURATION = 0.016667D0
    ELSE
      LARMATURATION = ALPHA*(TEMP**BETA)
    END IF
    IF (LARMATURATION < 0.016667D0) THEN
      LARMATURATION = 0.016667D0
    END IF

    RETURN
  END FUNCTION

  DOUBLE PRECISION FUNCTION PUPMATURATION(TEMP)

    DOUBLE PRECISION :: TEMP
    DOUBLE PRECISION :: ALPHA=0.0007109D0,BETA=1.8865648D0

    ! Set pupal development rate
    IF (TEMP < 0D0) THEN
      PUPMATURATION = 0.016667D0
    ELSE
      PUPMATURATION = ALPHA*(TEMP**BETA)
    END IF
    IF (PUPMATURATION < 0.016667D0) THEN
      PUPMATURATION = 0.016667D0
    END IF

    RETURN
  END FUNCTION

END MODULE define_DDEs

!*****************************************************************

PROGRAM chapter_4_model

  USE define_DDEs
```

```
USE DDE_SOLVER_M

IMPLICIT NONE

INTEGER :: I,J ! Local variables

INTEGER, DIMENSION(3) :: NVAR = (/NEQN,NLAGS,NEF/)

! Set length of solution and output points
INTEGER, PARAMETER :: NOUT=551D0
DOUBLE PRECISION, PARAMETER :: T0=0D0,TFINAL=550D0
DOUBLE PRECISION, DIMENSION(NOUT) :: TSPAN= &
(/ (T0+(I-1)*((TFINAL - T0)/(NOUT-1)), I=1,NOUT) /)

TYPE(DDE_SOL) :: SOL
TYPE(DDE_OPTS) :: OPTS

! Set length of maximum delay
DOUBLE PRECISION :: MAXDELAY = 200D0
CHARACTER (len=90) :: filename

! Set options for DDE solver
OPTS = DDE_SET(RE=1D-5,AE=1D-5,MAX_STEPS=100000000,
   MAX_DELAY=MAXDELAY,TRIM_FREQUENCY=10000)

! Call DDE solver code
SOL = DDE_SOLVER(NVAR,DDES,BETA,HISTORY,TSPAN,OPTIONS=OPTS)

! Was the solver successful?
IF (SOL%FLAG == 0) THEN
   ! Output solution values
   WRITE(filename, '( "filename.dat" )' )
   OPEN(unit=11,file=filename)
   DO I = 1,SOL%NPTS
      WRITE(UNIT=11,FMT='(16E14.5E3)') SOL%T(I),(SOL%Y(I,J),
         J=1,NEQN)
   END DO
```

```
      CLOSE(11)
   ELSE
      PRINT *,' Abnormal return from DDE_SOLVER with FLAG =
         ',&
      SOL%FLAG
   END IF

   STOP
END PROGRAM chapter_4_model
```

D.3 Chapter 5 DDE Code

```
MODULE define_DDEs

   IMPLICIT NONE

   ! Set number of equations, delays and event functions
   INTEGER, PARAMETER :: NEQN=21,NLAGS=7,NEF=1
   INTEGER :: K
   DOUBLE PRECISION :: PI=3.1415927D0
   ! Set parameter values for predation and egg raft size
   DOUBLE PRECISION :: densa,densr,densh,UPS,SHP,VOL,MAXEGG
   ! Set WNV transmission parameters
   DOUBLE PRECISION :: DEATHbird=0.000685D0,DEATHbirdWNV=0.167
      D0
   DOUBLE PRECISION :: RECOVERY=0.25D0,PHH=0.33D0,VERTICAL
      =0.004D0
   DOUBLE PRECISION :: tranMB=0.88D0,tranBM=0.4D0,CAR=400D0,
      INOCB=2D0
   DOUBLE PRECISION :: M=9.8D0,A=6.4D0,PHASE=28.9D0,DTR=9.4D0,
      WARM=0D0,INOCT=151D0

CONTAINS

   SUBROUTINE DDES(T,Y,Z,DY)

      ! Parameters for DDE solver
```

```
DOUBLE PRECISION :: T
DOUBLE PRECISION, DIMENSION(NEQN) :: Y,DY
DOUBLE PRECISION, DIMENSION(NEQN,NLAGS) :: Z
INTENT(IN) :: T,Y,Z
INTENT(OUT) :: DY

! Define variable names
DOUBLE PRECISION :: TEMPnowair, TEMPGCair, TEMPEIPair,
    TEMPEair, TEMPLair, TEMPPair, TEMPELair, TEMPLPair,
    TEMPELPair
DOUBLE PRECISION :: TEMPnowwater, TEMPEwater, TEMPLwater,
    TEMPPwater, TEMPELwater, TEMPLPwater, TEMPELPwater
DOUBLE PRECISION :: BIRTHnow, BIRTHE, BIRTHEL, BIRTHELP,
    BIRTHbird
DOUBLE PRECISION :: EGGMATnow,EGGMATE,EGGMATL,EGGMATEL,
    EGGMATLP,EGGMATELP
DOUBLE PRECISION :: LARMATnow,LARMATL,LARMATP,LARMATLP
DOUBLE PRECISION :: REt, RLt, RPt, RSAt, REAt, RIAt, MEt, MLt,
    MPt, MSAt, MEAt, DEt, DLt, DPt, DSAt, DEAt, DIAt
DOUBLE PRECISION :: dEdt, dLdt, dPdt, dSAdt, dEAdt, dIAdt,
    dSEdt, dSLdt, dSPdt, dDEdt, dDLdt, dDELdt, dDPdt, dDLPdt,
    dDELPdt, dGCdt
DOUBLE PRECISION :: dSBdt, dIBdt, dRBdt, dEIPdt, dSEAdt
DOUBLE PRECISION :: E,LAR,PUP,SA,EA,IA,SE,SL,SP,DE,DL,DP,
    GC,EIP,SEA,NB,SB,IB,RB,NBEIP
DOUBLE PRECISION :: INOCM,BITINGnow,BITINGEIP
DOUBLE PRECISION :: DEATHeggnow,DEATHeggE,DEATHlarnow,
    DEATHlarL,DEATHpupnow,DEATHpupP,DEATHadunow,
    DEATHaduEIP
DOUBLE PRECISION :: PUPMATnow,PUPMATP
DOUBLE PRECISION :: DIAPAUSEE,DIAPAUSEEL,DIAPAUSEELP,
    DIAPAUSEnow,DIAPAUSEEIP
DOUBLE PRECISION :: PPnow,PPE,PPEL,PPELP,PPEIP
DOUBLE PRECISION :: GCnow,GCC,EIPnow,EIPdelay

! Give names to responses of system of equations
E = Y(1)
```

```
LAR = Y(2)
PUP = Y(3)
SA = Y(4)
EA = Y(5)
IA = Y(6)
SE = Y(7)
SL = Y(8)
SP = Y(9)
SEA = Y(10)
DE = Y(11)
DL = Y(12)
DP = Y(13)
GC = Y(17)
EIP = Y(18)
SB = Y(19)
IB = Y(20)
RB = Y(21)
NB = (SB+IB+RB)
NBEIP = Z(19,7)+Z(20,7)+Z(21,7)

! Extract temperature values at various time points
TEMPnowair = TEMPAIR(T)
TEMPnowwater = TEMPWATER(T,TEMPnowair)

TEMPEair = TEMPAIR(T-DE)
TEMPEwater = TEMPWATER(T-DE,TEMPEair)

TEMPLair = TEMPAIR(T-DL)
TEMPLwater = TEMPWATER(T-DL,TEMPLair)

TEMPPair = TEMPAIR(T-DP)
TEMPPwater = TEMPWATER(T-DP,TEMPPair)

TEMPELair = TEMPAIR(T-DL-Z(11,4))
TEMPELwater = TEMPWATER(T-DL-Z(11,4),TEMPELair)

TEMPELPair = TEMPAIR(T-DP-Z(12,6)-Z(11,5))
```

```
TEMPELPwater = TEMPWATER(T-DP-Z(12,6)-Z(11,5),TEMPELPair)

TEMPLPair = TEMPAIR(T-DP-Z(12,6))
TEMPLPwater = TEMPWATER(T-DP-Z(12,6),TEMPLPair)

TEMPGCair = TEMPAIR(T-GC)
TEMPEIPair = TEMPAIR(T-EIP)

! Calculate photoperiod values for a range of time points
PPnow = DAYLIGHT(T)
PPE = DAYLIGHT(T-DE)
PPEL = DAYLIGHT(T-DL-Z(11,4))
PPELP = DAYLIGHT(T-DP-Z(12,6)-Z(11,5))
PPEIP = DAYLIGHT(T-EIP)

! Calculate gonotrophic cycle length for various time
   points
GCnow = GONOTROPHIC(TEMPnowair)
GCC = GONOTROPHIC(TEMPGCair)

EIPnow = EXTRINSIC_INCUBATION(TEMPnowair)
EIPdelay = EXTRINSIC_INCUBATION(TEMPEIPair)

! Calculate diapause percentage for given photoperiod
   values.
! Use these diapause percentages to caluclate birth rates
   .
! Do this for both spring and autumn diapause thresholds.
IF (DAYLIGHT(T) > DAYLIGHT(T-1)) THEN
  DIAPAUSEnow = DIAPAUSE_SPRING(PPnow)
  DIAPAUSEE = DIAPAUSE_SPRING(PPE)
  DIAPAUSEEL = DIAPAUSE_SPRING(PPEL)
  DIAPAUSEELP = DIAPAUSE_SPRING(PPELP)
  DIAPAUSEEIP = DIAPAUSE_SPRING(PPEIP)
  BIRTHnow = BIRTH(DIAPAUSEnow,GC)
  BIRTHE = BIRTH(DIAPAUSEE,Z(17,1))
  BIRTHEL = BIRTH(DIAPAUSEEL,Z(17,2))
```

```
    BIRTHELP = BIRTH(DIAPAUSEELP,Z(17,3))
  ELSE
    DIAPAUSEnow = DIAPAUSE_AUTUMN(PPnow)
    DIAPAUSEE = DIAPAUSE_AUTUMN(PPE)
    DIAPAUSEEL = DIAPAUSE_AUTUMN(PPEL)
    DIAPAUSEELP = DIAPAUSE_AUTUMN(PPELP)
    DIAPAUSEEIP = DIAPAUSE_AUTUMN(PPEIP)
    BIRTHnow = BIRTH(DIAPAUSEnow,GC)
    BIRTHE = BIRTH(DIAPAUSEE,Z(17,1))
    BIRTHEL = BIRTH(DIAPAUSEEL,Z(17,2))
    BIRTHELP = BIRTH(DIAPAUSEELP,Z(17,3))
  END IF

  ! Calculate death rates for each life stage
  DEATHeggnow = DEATHegg(TEMPnowwater)
  DEATHeggE = DEATHegg(TEMPEwater)

  DEATHlarnow = DEATHlar(TEMPnowwater)
  DEATHlarL = DEATHlar(TEMPLwater)

  DEATHpupnow = DEATHpup(TEMPnowwater)
  DEATHpupP = DEATHpup(TEMPPwater)

  DEATHadunow = DEATHadu(TEMPnowair,GC,T)
  DEATHaduEIP = DEATHadu(TEMPEIPair,Z(17,7),T-EIP)

  BIRTHbird = BIRD_BIRTH_FUNC(T)

  ! Calculate development rates for the immature stages
  LARMATnow = LARMATURATION(TEMPnowwater)
  LARMATL = LARMATURATION(TEMPLwater)
  LARMATP = LARMATURATION(TEMPPwater)
  LARMATLP = LARMATURATION(TEMPLPwater)

  EGGMATnow = EGGMATURATION(TEMPnowwater)
  EGGMATE = EGGMATURATION(TEMPEwater)
  EGGMATL = EGGMATURATION(TEMPLwater)
```

```
EGGMATEL = EGGMATURATION(TEMPELwater)
EGGMATLP = EGGMATURATION(TEMPLPwater)
EGGMATELP = EGGMATURATION(TEMPELPwater)

PUPMATnow = PUPMATURATION(TEMPnowwater)
PUPMATP = PUPMATURATION(TEMPPwater)

BITINGnow = 0.5D0*DIAPAUSEnow*GONOTROPHIC(TEMPnowair)
BITINGEIP = 0.5D0*DIAPAUSEEIP*GONOTROPHIC(TEMPEIPair)

! Innoculate the system with a given number of adults.
INOCM = INOCCULATEM(T)

! Delay differential equations for immature stage
   durations
dDEdt = 1D0 - EGGMATnow/EGGMATE
dDLdt = 1D0 - LARMATnow/LARMATL
dDPdt = 1D0 - PUPMATnow/PUPMATP

! Delay differential equation for gonotrophic cycle
   duration
dGCdt = 1D0 - GCnow/GCC
dEIPdt = 1D0 - EIPnow/EIPdelay

! Delay differential equations for stage durations
   referenced back through previous stages
dDELdt = (1D0 - dDLdt) * (1D0 - EGGMATL/EGGMATEL)
dDLPdt = (1D0 - dDPdt) * (1D0 - LARMATP/LARMATLP)
dDELPdt = (1D0 - dDPdt - dDLPdt) * (1D0 - EGGMATLP/
   EGGMATELP)

! Recruitment equations for each stage
REt = BIRTHnow * (SA + EA + IA)
RLt = BIRTHE * (Z(4,1) +Z(5,1) +Z(6,1)) * SE * EGGMATnow/
   EGGMATE
RPt = BIRTHEL * (Z(4,2) +Z(5,2) +Z(6,2)) * Z(7,4) * SL *
   LARMATnow/LARMATL * EGGMATL/EGGMATEL
```

```
RSAt = BIRTHELP * (Z(4,3) +Z(5,3) +Z(6,3) * (1D0-VERTICAL
    )) * Z(7,5) * Z(8,6) * SP * PUPMATnow/PUPMATP *
    LARMATP/LARMATLP * EGGMATLP/EGGMATELP + INOCM

REAt = BITINGnow * SA * (tranBM * IB) / NB

RIAt = BITINGEIP * Z(4,7) * SEA * EIPnow/EIPdelay * (
    tranBM * Z(20,7)) / NBEIP + BIRTHELP * Z(6,3) *
    VERTICAL * Z(7,5) * Z(8,6) * SP * PUPMATnow/PUPMATP *
    LARMATP/LARMATLP * EGGMATLP/EGGMATELP

! Maturation equations for each stage
MEt = RLt
MLt = RPt
MPt = BIRTHELP * Z(4,3) * Z(7,5) * Z(8,6) * SP *
    PUPMATnow/PUPMATP * LARMATP/LARMATLP * EGGMATLP/
    EGGMATELP
MSAt = REAt
MEAt = BITINGEIP * Z(4,7) * SEA * EIPnow/EIPdelay * (
    tranBM * Z(20,7)) / NBEIP

! Death equations for each stage
DEt = DEATHeggnow * E
DLt = (densa*densr*(((1D0+COS(2D0*PI*(T-182.5D0-UPS)/365
    D0))/2D0)**SHP)*LAR/(VOL+densh*LAR)+DEATHlarnow)*LAR
DPt = DEATHpupnow * PUP
DSAt = DEATHadunow * SA
DEAt = DEATHadunow * EA
DIAt = DEATHadunow * IA

! Balance equations for each life stage
dEdt = REt - MEt - DEt
dLdt = RLt - MLt - DLt
dPdt = RPt - MPt - DPt

dSAdt = RSAt - MSAt - DSAt
```

```
      dEAdt = REAt - MEAt - DEAt
      dIAdt = RIAt - DIAt

      dSBdt = BIRTHbird * NB - BITINGnow * tranMB * IA * SB /
     NB - PHH * IB * SB / NB - (DEATHbird + BIRTHbird*NB/
     CAR) * SB

      dIBdt = BITINGnow*tranMB*IA*SB/NB + PHH*IB*SB/NB - (
     DEATHbird+DEATHbirdWNV+BIRTHbird*NB/CAR)*IB - RECOVERY
     *IB

      dRBdt = RECOVERY * IB - (DEATHbird + BIRTHbird*NB/CAR) *
     RB

      ! Survival equations for the immature stages
      dSEdt = SE * ((EGGMATnow * DEATHeggE / EGGMATE) -
     DEATHeggnow)
      dSLdt =SL*(((densa*densr*(((1D0+COS(2D0*PI*(T-DL-182.5D0-
     UPS)/365D0))/2D0)**SHP)*Z(2,4)/(VOL+densh*Z(2,4)))+
     DEATHlarL) * (1-dDLdt) - (densa*densr*(((1D0+COS(2D0*
     PI*(T-182.5D0-UPS)/365D0))/2D0)**SHP)*LAR / (VOL+densh
     *LAR)) - DEATHlarnow)
      dSPdt = SP * ((PUPMATnow * DEATHpupP / PUPMATP) -
     DEATHpupnow)
      dSEAdt = SEA * ((EIPnow * DEATHaduEIP / EIPdelay) -
     DEATHadunow)

      ! Derivatives for the integrator:
      DY = (/ dEdt, dLdt, dPdt, dSAdt, dEAdt, dIAdt, dSEdt,
     dSLdt, dSPdt, dSEAdt, dDEdt, dDLdt, dDPdt, dDELdt,
     dDLPdt, dDELPdt, dGCdt, dEIPdt, dSBdt, dIBdt, dRBdt /)

      RETURN
    END SUBROUTINE DDES

    SUBROUTINE BETA(T,Y,BVAL)
```

```
    DOUBLE PRECISION :: T
    DOUBLE PRECISION, DIMENSION(NEQN) :: Y
    DOUBLE PRECISION, DIMENSION(NLAGS) :: BVAL
    INTENT(IN)  :: T,Y
    INTENT(OUT) :: BVAL

    ! Set the delay values
    ! T - Eggdelay(T)
    BVAL(1) = T-Y(11)
    ! T - Lardelay(T) - Eggdelay(T-Lardelay(T))
    BVAL(2) = T-Y(12)-Y(14)
    !T - Pupdelay(T) - Lardelay(T-Pupdelay(T)) - Eggdelay(T-
       Pupdelay(T)-Lardelay(T-Pupdelay(T)))
    BVAL(3) = T-Y(13)-Y(15)-Y(16)
    !T - Lardelay(T)
    BVAL(4) = T-Y(12)
    !T - Pupdelay(T) - Lardelay(T-Pupdelay(T))
    BVAL(5) = T-Y(13)-Y(15)
    !T - Pupdelay(T)
    BVAL(6) = T-Y(13)
    !T - EIPdelay(T)
    BVAL(7) = T-Y(18)

    RETURN
  END SUBROUTINE BETA

  SUBROUTINE HISTORY(T,Y)
    DOUBLE PRECISION :: T,TEMPhist,TEMPhistair
    DOUBLE PRECISION, DIMENSION(2*NEQN) :: Y
    INTENT(IN)  :: T
    INTENT(OUT) :: Y

    ! Set the temperatures for T < 0
    TEMPhistair = TEMPAIR(T)
    TEMPhist = TEMPWATER(T,TEMPhistair)

    ! Set historical values for all stages to be zero
```

```
Y(1) = 0D0
Y(2) = 0D0
Y(3) = 0D0
Y(4) = 0D0
Y(5) = 0D0
Y(6) = 0D0

! Calculate historical survival rates based on
   temperature
Y(7) = EXP(-DEATHegg(TEMPhist)*(1D0/EGGMATURATION(
   TEMPhist)))
Y(8) = EXP(-DEATHlar(TEMPhist)*(1D0/LARMATURATION(
   TEMPhist)))
Y(9) = EXP(-DEATHpup(TEMPhist)*(1D0/PUPMATURATION(
   TEMPhist)))

! Calculate historical development rates based on
   temperature
Y(11) = 1D0/EGGMATURATION(TEMPhist)
Y(12) = 1D0/LARMATURATION(TEMPhist)
Y(13) = 1D0/PUPMATURATION(TEMPhist)
Y(14) = 1D0/EGGMATURATION(TEMPhist)
Y(15) = 1D0/LARMATURATION(TEMPhist)
Y(16) = 1D0/EGGMATURATION(TEMPhist)
Y(17) = 1D0/GONOTROPHIC(TEMPhistair)

Y(10) = EXP(-DEATHadu(TEMPhistair,Y(17),T)*(1D0/
   EXTRINSIC_INCUBATION(TEMPhistair)))

! Set historical EIP
Y(18) = 1D0/EXTRINSIC_INCUBATION(TEMPhistair)

! Set historical values for birds to zero
Y(19) = 0.875D0*CAR
Y(20) = 0D0
Y(21) = 0D0
```

```
    RETURN
END SUBROUTINE HISTORY


SUBROUTINE EF(T,Y,DY,Z,G)

    DOUBLE PRECISION :: T
    DOUBLE PRECISION, DIMENSION(NEQN) :: Y,DY
    DOUBLE PRECISION, DIMENSION(NEQN,NLAGS) :: Z
    DOUBLE PRECISION, DIMENSION(NEF) :: G
    INTENT(IN) :: T,Y,DY,Z
    INTENT(OUT) :: G

    ! Set events as turning points in adult time series and
       diapause entry/exit
    G(1) = T-INOCT

    RETURN
END SUBROUTINE EF

SUBROUTINE CHNG(NEVENT,TEVENT,YEVENT,DYEVENT,HINIT,
   DIRECTION,ISTERMINAL,QUIT)
! Function to change a flag so that the DDE model will
! be evaluated in subroutine DDES instead of the ODE model.

    INTEGER :: NEVENT
    INTEGER, DIMENSION(NEF) :: DIRECTION
    DOUBLE PRECISION :: TEVENT,HINIT
    DOUBLE PRECISION, DIMENSION(NEQN) :: YEVENT,DYEVENT
    LOGICAL :: QUIT
    LOGICAL, DIMENSION(NEF) :: ISTERMINAL
    INTENT(IN) :: NEVENT,TEVENT
    INTENT(INOUT) :: YEVENT,DYEVENT,HINIT,DIRECTION,
       ISTERMINAL,QUIT

    YEVENT(20) = 0.0025D0*CAR
```

```
    RETURN
  END SUBROUTINE CHNG

  DOUBLE PRECISION FUNCTION TEMPAIR(T)

    DOUBLE PRECISION :: T

    ! Calculate air temperature for time, T
    TEMPAIR = M + A * COS(2D0 * Pi * (T-PHASE-182.5) / 365D0)
        - DTR/2 * COS(2D0* Pi * T) + WARM
    IF (T<0D0) THEN
      TEMPAIR = M + A * COS(2D0 * Pi * (0D0-PHASE-182.5) /
          365D0) - DTR/2 * COS(2D0* Pi * 0D0) + WARM
    END IF

    RETURN
  END FUNCTION

  DOUBLE PRECISION FUNCTION TEMPWATER(T,AIRTEMP)

    DOUBLE PRECISION :: T,AIRTEMP

    ! Calculate water temperature for time, T
    TEMPWATER = 0.9505D0*AIRTEMP + 3.8887D0

    RETURN
  END FUNCTION

  DOUBLE PRECISION FUNCTION INOCCULATEM(T)

    DOUBLE PRECISION :: T

    ! Set inoculation value
    IF (T < 1D0 .AND. T > 0D0) THEN
      INOCCULATEM = 5000D0
    ELSE
      INOCCULATEM = 0D0
```

```
    END IF

    RETURN
  END FUNCTION

  DOUBLE PRECISION FUNCTION DAYLIGHT(T)

    DOUBLE PRECISION :: T,EPS,NUM,DEN
    REAL, PARAMETER :: Pi = 3.1415927D0, L = 51D0

    ! Calculate photperiod value
    EPS = ASIN(0.39795D0 * COS(0.2163108D0 + 2 * ATAN
       (0.9671396D0 * TAN(0.00860D0 * (T-185.5D0)))))
    NUM = SIN(0.8333D0*Pi/180D0) + (SIN(L*Pi/180D0) * SIN(EPS
       ))
    DEN = COS(L*Pi/180D0) * COS(EPS)
    DAYLIGHT = 24D0 - (24D0/Pi) * ACOS(NUM / DEN)

    RETURN
  END FUNCTION

  DOUBLE PRECISION FUNCTION DIAPAUSE_SPRING(PP)

    DOUBLE PRECISION :: PP

    ! Set spring photoperiod threshold
    DIAPAUSE_SPRING = 1D0 / (1D0 + EXP(5D0*(13.7D0-PP)))

    RETURN
  END FUNCTION

  DOUBLE PRECISION FUNCTION DIAPAUSE_AUTUMN(PP)

    DOUBLE PRECISION :: PP

    ! Set autumn photoperiod threshold
    DIAPAUSE_AUTUMN = 1D0 / (1D0 + EXP(3.5D0*(15D0-PP)))
```

```
    RETURN
END FUNCTION

DOUBLE PRECISION FUNCTION BIRTH(DIAPAUSE,GONOTROPHICtime)

    DOUBLE PRECISION :: GONOTROPHICtime,EGGRAFT,DIAPAUSE

    ! Set birth rate for mosquitoes
    EGGRAFT = DIAPAUSE*MAXEGG*0.5D0
    BIRTH = EGGRAFT/GONOTROPHICtime

    RETURN
END FUNCTION

DOUBLE PRECISION FUNCTION BIRD_BIRTH_FUNC(T)

    DOUBLE PRECISION :: T
    DOUBLE PRECISION :: K_BIRD=0.15D0,PHI_BIRD=50D0,S_BIRD=10
        D0

    ! Set birth rate for birds
    BIRD_BIRTH_FUNC = 0.5D0 * K_BIRD * EXP(-S_BIRD * (COS((PI
        *T+PHI_BIRD)/365D0))**2)

    RETURN
END FUNCTION

DOUBLE PRECISION FUNCTION GONOTROPHIC(TEMP)

    DOUBLE PRECISION :: TEMP
    DOUBLE PRECISION :: KG=0.2024D0,QG=74.48D0,BG=0.2456D0

    ! Set gonotrophic cycle rate
    IF (TEMP < 0D0) THEN
      GONOTROPHIC = 0.0333D0
    ELSE
```

```
      GONOTROPHIC = KG / (1+QG*EXP(-BG*TEMP))
    END IF
    IF(GONOTROPHIC < 0.0333D0) THEN
      GONOTROPHIC = 0.0333D0
    END IF

    RETURN
  END FUNCTION

  DOUBLE PRECISION FUNCTION EXTRINSIC_INCUBATION(TEMP)

    DOUBLE PRECISION :: TEMP

    ! Set EIP development rate
    EXTRINSIC_INCUBATION = 0.0092D0 * TEMP - 0.132D0
    IF (EXTRINSIC_INCUBATION .LE. 0.005D0) THEN
      EXTRINSIC_INCUBATION = 0.005D0
    END IF

    RETURN
  END FUNCTION

  DOUBLE PRECISION FUNCTION DEATHegg(TEMP)

    DOUBLE PRECISION :: TEMP
    DOUBLE PRECISION :: U3=0.0157D0,U4=20.5D0,U5=7D0

    ! Calculate egg death rate
    DEATHegg = U3 * EXP(((TEMP-U4)/U5)**2)
    IF (DEATHegg > 1D0) THEN
      DEATHegg = 1D0
    END IF

    RETURN
  END FUNCTION

  DOUBLE PRECISION FUNCTION DEATHlar(TEMP)
```

```
    DOUBLE PRECISION :: TEMP
    DOUBLE PRECISION :: U3=0.0157D0,U4=20.5D0,U5=7D0

    ! Calculate larval death rate
    DEATHlar = U3 * EXP(((TEMP-U4)/U5)**2)
    IF (DEATHlar > 1D0) THEN
      DEATHlar = 1D0
    END IF

    RETURN
  END FUNCTION

  DOUBLE PRECISION FUNCTION DEATHpup(TEMP)

    DOUBLE PRECISION :: TEMP
    DOUBLE PRECISION :: U3=0.0157D0,U4=20.5D0,U5=7D0

    ! Calculate pupal death rate
    DEATHpup = U3 * EXP(((TEMP-U4)/U5)**2)
    IF (DEATHpup > 1D0) THEN
      DEATHpup = 1D0
    END IF

    RETURN
  END FUNCTION

  DOUBLE PRECISION FUNCTION DEATHadu(TEMP,GONOTROPHICtime,T)

    DOUBLE PRECISION :: TEMP,GONOTROPHICtime,T
    DOUBLE PRECISION :: ALPHA=2.166D-8,BETA=4.483D0,PI
       =3.1415927D0,MULTIPLIER=8D0,SIGMASQ=4D0

    ! Calculate adult death rate
    IF (TEMP < 0D0) THEN
      DEATHadu = 0.003D0
    ELSE
```

```
      DEATHadu = ALPHA*(TEMP**BETA)
    END IF
    IF (DEATHadu < 0.003D0) THEN
      DEATHadu = 0.003D0
    END IF
    DEATHadu = DEATHadu + (MULTIPLIER/SQRT(SIGMASQ*2D0*PI))*
       EXP((-1D0/(SIGMASQ*2D0)) * (MOD(T,365D0)-
       GONOTROPHICtime-109D0)**2)

    RETURN
  END FUNCTION

  DOUBLE PRECISION FUNCTION EGGMATURATION(TEMP)

    DOUBLE PRECISION :: TEMP
    DOUBLE PRECISION :: ALPHA=0.0022D0,BETA=1.77D0

    ! Calculate egg development rate
    IF (TEMP < 0D0) THEN
      EGGMATURATION = 0.016667D0
    ELSE
      EGGMATURATION = ALPHA*(TEMP**BETA)
    END IF
    IF (EGGMATURATION < 0.016667D0) THEN
      EGGMATURATION = 0.016667D0
    END IF

    RETURN
  END FUNCTION

  DOUBLE PRECISION FUNCTION LARMATURATION(TEMP)

    DOUBLE PRECISION :: TEMP
    DOUBLE PRECISION :: ALPHA=0.00315D0,BETA=1.12D0

    ! Calculate larval development rate
    IF (TEMP < 0D0) THEN
```

```
      LARMATURATION = 0.016667D0
    ELSE
      LARMATURATION = ALPHA*(TEMP**BETA)
    END IF
    IF (LARMATURATION < 0.016667D0) THEN
      LARMATURATION = 0.016667D0
    END IF

    RETURN
  END FUNCTION

  DOUBLE PRECISION FUNCTION PUPMATURATION(TEMP)

    DOUBLE PRECISION :: TEMP
    DOUBLE PRECISION :: ALPHA=0.0007109D0,BETA=1.8865648D0

    ! Calculate pupal maturation rate
    IF (TEMP < 0D0) THEN
      PUPMATURATION = 0.016667D0
    ELSE
      PUPMATURATION = ALPHA*(TEMP**BETA)
    END IF
    IF (PUPMATURATION < 0.016667D0) THEN
      PUPMATURATION = 0.016667D0
    END IF

    RETURN
  END FUNCTION

END MODULE define_DDEs

!*****************************************************************************


PROGRAM chapter_5_model

  USE define_DDEs
```

```
USE DDE_SOLVER_M

IMPLICIT NONE

INTEGER :: I,J ! Local variables

INTEGER, DIMENSION(3) :: NVAR = (/NEQN,NLAGS,NEF/)

! Set length of solution and output points
INTEGER, PARAMETER :: NOUT=366D0
DOUBLE PRECISION, PARAMETER :: T0=0D0,TFINAL=365D0
DOUBLE PRECISION, DIMENSION(NOUT) :: TSPAN= (/ (T0+(I-1)*((
    TFINAL - T0)/(NOUT-1)), I=1,NOUT) /)

TYPE(DDE_SOL) :: SOL
TYPE(DDE_OPTS) :: OPTS

! Set length of maximum delay
DOUBLE PRECISION :: MAXDELAY = 200D0

! Set options for DDE solver
OPTS = DDE_SET(RE=1D-5,AE=1D-5,MAX_STEPS=100000000,
    MAX_DELAY=MAXDELAY,TRIM_FREQUENCY=10000)

! Run DDE solver code
SOL = DDE_SOLVER(NVAR,DDES,BETA,HISTORY,TSPAN,EVENT_FCN=EF,
    CHANGE_FCN=CHNG,OPTIONS=OPTS)

! Was the solver successful?
IF (SOL%FLAG == 0) THEN
  ! Output results
  OPEN(UNIT=10, FILE='filename.dat')
  DO I = 1,SOL%NPTS
    WRITE(UNIT=10,FMT='(28E14.5E3)') INOCT, WARM, SOL%T(I)
        ,(SOL%Y(I,J),J=1,NEQN)
  END DO
  CLOSE(10)
```

```
    ELSE
      PRINT *,' Abnormal return from DDE_SOLVER with FLAG = ',&
      SOL%FLAG
    END IF

    STOP
END PROGRAM chapter_5_model
```

Bibliography

Agnew, P., C. Haussy, and Y. Michalakis. 2000. “Effects of density and larval competition on selected life history traits of *Culex pipiens quinquefasciatus* (Diptera : Culicidae)”. *Journal of Medical Entomology* 37 (5): 732–735.

Ahumada, J. A., D. Lapointe, and M. D. Samuel. 2004. “Modeling the population dynamics of *Culex quinquefasciatus* (Diptera: Culicidae), along an elevational gradient in Hawaii.” *Journal of medical entomology* 41, no. 6 (): 1157–70. ISSN: 0022-2585.

Akaike, H. 1973. “Information theory as an extension of the maximum likelihood principle”. In *Second international symposium on information theory*, ed. by B. N. Petrov and F Csaki, 267–281. Budapest.

Aldemir, Adnan, et al. 2009. “Species composition and seasonal dynamics of mosquito larvae (Diptera: Culicidae) in Iğdır Plain, Turkey”. *Kafkas Üniv Vet Fak Derg* 15 (1): 103–110.

Allan, Brian F., et al. 2009. “Ecological correlates of risk and incidence of West Nile virus in the United States”. *Oecologia* 158 (4): 699–708. ISSN: 00298549. doi:10.1007/s00442-008-1169-9.

Almeida Costa, E. A. P. de, et al. 2006. “Impact of small variations in temperature and humidity on the reproductive activity and survival of *Aedes aegypti* (Diptera , Culicidae)”. *Revista Brasileira de Entomologica* 54 (3): 488–493.

Almirón, W. R., and M. E. Brewer. 1996. “Winter biology of *Culex pipiens quinquefasciatus* Say , (Diptera : Culicidae) from Córdoba , Argentina”. *Memórias do Instituto Oswaldo Cruz* 91 (5): 649–654.

Alonso, David, Menno J Bouma, and Mercedes Pascual. 2010. “Epidemic malaria and warmer temperatures in recent decades in an East African highland.” *Proceedings. Biological sciences / The Royal Society* 278 (1712): 1661–1669. ISSN: 0962-8452. doi:10.1098/rspb.2010.2020.

Alten, B, et al. 2000. “Species composition and seasonal dynamics of mosquitoes in the Belek region of Turkey”. *Journal of Vector Ecology* 25 (2): 146–154.

Altizer, Sonia, et al. 2006. "Seasonality and the dynamics of infectious diseases." *Ecology letters* 9, no. 4 (): 467–84. ISSN: 1461-0248. doi:10.1111/j.1461-0248.2005.00879.x. http://www.ncbi.nlm.nih.gov/pubmed/16623732.

Alto, B. W., E. J. Muturi, and R. L. Lampman. 2012. "Effects of nutrition and density in *Culex pipiens*". *Medical and veterinary entomology* 26 (4): 396–406. ISSN: 1365-2915. doi:10.1111/j.1365-2915.2012.01010.x.

Alto, B. W., et al. 2008. "Larval competition alters susceptibility of adult *Aedes* mosquitoes to dengue infection." *Proceedings of the Royal Society B: Biological Sciences* 275 (): 463–471. ISSN: 0962-8452. doi:10.1098/rspb.2007.1497.

Alto, B. W., et al. 2014. "Survival of West Nile virus-challenged Southern house mosquitoes, *Culex pipiens quinquefasciatus*, in relation to environmental temperatures". *Journal of Vector Ecology* 39 (1): 123–133. ISSN: 19487134. doi:10.1111/j.1948-7134.2014.12078.x.

Alto, Barry W., and Steven a. Juliano. 2001. "Temperature effects on the dynamics of Aedes albopictus (Diptera: Culicidae) populations in the laboratory". *Journal of Medical Entomology* 38 (4): 548–556. ISSN: 0022-2585. doi:10.1603/0022-2585-38.4.548. http://www.bioone.org/doi/abs/10.1603/0022-2585-38.4.548.

Amarasekare, P., and R. M. Coutinho. 2013. "The intrinsic growth rate as a predictor of population viability under climate warming." *The Journal of animal ecology* 82 (): 1240–1253. ISSN: 1365-2656. doi:10.1111/1365-2656.12112.

Amarasekare, Priyanga, and Renato M Coutinho. 2014. "Effects of Temperature on Intraspecific Competition in Ectotherms". *The American naturalist* 184 (3): E50–E65. ISSN: 1537-5323. doi:10.1086/677386. http://www.ncbi.nlm.nih.gov/pubmed/25141149.

Amraoui, Fadila, et al. 2012. "*Culex pipiens*, an experimental efficient vector of West Nile and Rift Valley fever viruses in the Maghreb region". *PLoS ONE* 7 (5): 4–11. ISSN: 19326203. doi:10.1371/journal.pone.0036757.

Anderson, D. R., K. P. Burnham, and G. C. White. 1994. "AIC model selection in overdispersed capture-recapture data". *Ecology* 75:1780–1793.

Anderson, John F, and Andy J Main. 2006. "Importance of Vertical and Horizontal Transmission of West Nile Virus by *Culex pipiens* in the Northeastern United States". *The Journal of Infectious Diseases* 194:1577–1579.

Anderson, John F, et al. 2008. "Extrinsic Incubation Periods for Horizontal and Vertical Transmission of West Nile Virus by Culex pipiens pipiens (Diptera : Culicidae) Extrinsic Incubation Periods for Horizontal and Vertical Transmission of West Nile Virus by Culex pipiens pipiens (D". 45 (3): 445–451.

Anderson, John F, et al. 2004. "Prevalence of West Nile Virus in tree canopy-inhabiting *Culex pipiens* and associated mosquitoes". *The American Society of Tropical Medicine and Hygiene* 71 (1): 112–119.

Andreadis, S. S., O. C. Dimotsiou, and M. Savopoulou-Soultani. 2014. "Variation in adult longevity of *Culex pipiens f . pipiens*, vector of the West Nile Virus". *Parasitology Research* 113:4315–4319. doi:10.1007/s00436-014-4152-x.

Andreadis, Theodore G., John F. Anderson, and Charles R. Vossbrinck. 2001. "Mosquito surveillance for West Nile virus in Connecticut, 2000: Isolation from *Culex pipiens*, *Cx. restuans*, *Cx. salinarius*, and *Culiseta melanura*". *Emerging Infectious Diseases* 7 (4): 670–674. ISSN: 10806040. doi:10.3201/eid0704.010413.

Andreadis, Theodore G, Philip M Armstrong, and Waheed I Bajwa. 2010. "Studies on Hibernating Populations of *Culex pipiens* from a West Nile Virus Endemic Focus in New York City: Parity Rates and Isolation of West Nile Virus". *The American Mosquito Control Association* 26 (3): 257–264.

Angelini, R, et al. 2007. "Chikungunya in north-eastern Italy: a summing up of the outbreak". *Eurosurveillance* 12 (47).

Angelon, K. A., and J. W. Petranka. 2002. "Chemicals of predatory mosquitofish (*Gambusia affinis*) influence selection of oviposition site by culex mosquitoes". *Journal of Chemical Ecology* 28 (4): 797–806.

Armbruster, Peter A. 2016. "Photoperiodic Diapause and the Establishment of Aedes albopictus (Diptera: Culicidae) in North America". *Journal of Medical Entomology* 53, no. 5 (): 1013–1023. ISSN: 0022-2858. http://dx.doi.org/10.1093/jme/tjw037.

Asare, Ernest O, et al. 2016. "Mosquito breeding site water temperature observations and simulations towards improved vector-borne disease models for Africa". *Geospatial health* 11:67–77. doi:10.4081/gh.2016.391.

Awasthi, Amit kant, Cheng-Han Wu, and Jiang-Shiou Hwang. 2012. "Diving as an Anti-Predator Behavior in Mosquito Pupae". *Zoological Studies* 51 (8): 1225–1234.

Bailey, C. L., et al. 1982. "Winter survival of blood-fed and nonblood-fed *Culex pipiens L.*" *The American journal of tropical medicine and hygiene* 31 (5): 1054–61. ISSN: 0002-9637.

Bale, J S, and S A Hayward. 2010. "Insect overwintering in a changing climate". *J Exp Biol* 213 (6): 980–994. ISSN: 1477-9145. doi:10.1242/jeb.037911. http://www.ncbi.nlm.nih.gov/pubmed/20190123.

Balenghien, Thomas, et al. 2008. "Vector Competence of Some French *Culex* and *Aedes* Mosquitoes for West Nile Virus". *Vector-Borne and Zoonotic Diseases* 8, no. 5 (): 589–596. ISSN: 1530-3667. doi:10.1089/vbz.2007.0266. http://dx.doi.org/10.1089/vbz.2007.0266.

Balenghien, T., et al. 2006. "Horse-, bird-, and human-seeking behaviour and seasonal abundance of mosquitoes in a West Nile virus focus of Southern France". *Journal of Medical Entomology* 43 (5): 936–946.

Bancroft, T. L. 1906. "On the aetiology of dengue fever". *Australian Medical Gazette* 25:17–18.

Barker, C. M., B. F. Eldridge, and W. K. Reisen. 2010. "Seasonal abundance of *Culex tarsalis* and *Culex pipiens* complex mosquitoes (Diptera: Culicidae) in California". *Journal of medical entomology* 47 (5): 759–768.

Barker, Christopher M., et al. 2013. "Data-Driven Modeling to Assess Receptivity for Rift Valley Fever Virus". *PLoS Neglected Tropical Diseases* 7 (11): 1–10. ISSN: 19352727. doi:10.1371/journal.pntd.0002515.

Barton, Kamil. 2016. *Multi-Model Inference*.

Barzon, L., et al. 2013. "Large human outbreak of West Nile virus infection in north-eastern Italy in 2012." *Viruses* 5 (11): 2825–39. ISSN: 1999-4915. doi:10.3390/v5112825.

Barzon, L., et al. 2012. "New endemic West Nile virus lineage 1a in northern Italy, July 2012". *Eurosurveillance* 17 (31): 2011–2013. ISSN: 1025496X.

Becker, Norbert, and Herbert W Ludwig. 1983. "Mosquito Control in West Germany". *Bulletin of the Society of Vector Ecologists* 8 (2): 85–93.

Becker, N., et al. 2010. *Mosquitoes and Their Control*. 2nd. Springer.

Becker, N., et al. 2003. *Mosquitoes and their control*. 1st. New York: Kluwer Academic/-Plenum Publishers.

Beck-Johnson, L. M., et al. 2013. "The effect of temperature on anopheles mosquito population dynamics and the potential for malaria transmission." *PloS one* 8, no. 11 (): e79276. ISSN: 1932-6203. doi:10.1371/journal.pone.0079276.

Beier, J. C. 2002. "Vector Incrimination and Entomological Inoculation Rates". In *Malaria Methods and Protocols*, 72nd ed., ed. by Denise L. Doolan, 3–11. Humana Press Inc.

Beketov, M. A., and M. Liess. 2007. "Predation risk perception and food scarcity induce alterations of life-cycle traits of the mosquito *Culex pipiens*". *Ecological Entomology* 32 (4): 405–410. ISSN: 0307-6946. doi:10.1111/j.1365-2311.2007.00889.x.

Bellan, S. E. 2010. "The importance of age dependent mortality and the extrinsic incubation period in models of mosquito-borne disease transmission and control". *PLoS ONE* 5 (4). ISSN: 19326203. doi:10.1371/journal.pone.0010165.

Beniston, Martin, et al. 2007. "Future extreme events in European climate: An exploration of regional climate model projections". *Climatic Change* 81:71–95. ISSN: 01650009. doi:10.1007/s10584-006-9226-z.

Benton, Tim G, Stewart J Plaistow, and Tim N Coulson. 2006. "Complex population dynamics and complex causation: devils, details and demography". *Proceedings of the Royal Society B* 273 (1591): 1173–1181. ISSN: 0962-8452. doi:10.1098/rspb.2006.3495. http://www.pubmedcentral.nih.gov/articlerender.fcgi?artid=1560275&tool=pmcentrez&rendertype=abstract.

Bergsman, Louis D., James M. Hyman, and Carrie A. Manore. 2015. "A mathematical model for the spread of west nile virus in migratory and resident birds". *Mathematical Biosciences and Engineering* 13 (2): 401–424. ISSN: 1551-0018. doi:10.3934/mbe.2015009. http://www.aimsciences.org/journals/displayArticlesnew.jsp?paperID=12079.

Bernard, K. A., et al. 2001. "West Nile virus infection in birds and mosquitoes, New York State, 2000." *Emerging infectious diseases* 7 (4): 679–685. ISSN: 1080-6040. doi:10.3201/eid0704.010415.

Bessell, P. R., et al. 2014. "Quantifying the Risk of Introduction of West Nile Virus into Great Britain by Migrating Passerine Birds." *Transboundary and emerging diseases* (). ISSN: 1865-1682. doi:10.1111/tbed.12310. http://www.ncbi.nlm.nih.gov/pubmed/25516263.

Bessell, Paul R, et al. 2013. "Epidemic potential of an emerging vector borne disease in a marginal environment: Schmallenberg in Scotland." *Scientific reports* 3:1178. ISSN: 2045-2322. doi:10.1038/srep01178. http://www.pubmedcentral.nih.gov/articlerender.fcgi?artid=3560360&tool=pmcentrez&rendertype=abstract.

Bewick, Sharon. 2016. "Current and future challenges of predictive insect population modelling". *Functional Ecology* 30 (7): 1028–1029. ISSN: 13652435. doi:10.1111/1365-2435.12678.

Billard, L. 1977. "On Lotka–Volterra predator prey models". *Journal of Applied Probability* (Cambridge, UK) 14 (2): 375–381. doi:10.1017/S0021900200105054. https://www.cambridge.org/core/article/div-class-title-on-lotka-volterra-predator-prey-models-div/5A8C6297F188AE18DF1761418317BF0

Bisanzio, Donal, et al. 2011. "Spatio-temporal patterns of distribution of West Nile virus vectors in eastern Piedmont Region, Italy". *Parasites & vectors* 4 (230): 1–11.

Bogojević, M S, et al. 2009. "Seasonal dynamics of mosquitoes (Diptera: Culicidae) in Osijek (Croatia) for the period 1995-2004". *Biologia* 64 (4): 760–767. ISSN: 0006-3088. doi:10.2478/s11756-009-0138-z. http://www.scopus.com/inward/record.url?eid=2-s2.0-70349731612&partnerID=40&md5=0abbe481c0dd43

Bolling, B G, et al. 2007. "Entomological studies along the Colorado front range during a period of intense west nile virus activity". *Journal of the American Mosquito Control Association* 23 (1): 37–46.

Bolling, B. G., et al. 2009. "Seasonal patterns for entomological measures of risk for exposure to *Culex* vectors and west nile virus in relation to human disease cases in Northeastern Colorado". *Journal of Medical Entomology* 46 (6): 1519–1531.

Bomblies, Arne, Jean Bernard Duchemin, and Elfatih A B Eltahir. 2008. "Hydrology of malaria: Model development and application to a Sahelian village". *Water Resources Research* 44 (12): 1–26. ISSN: 00431397. doi:10.1029/2008WR006917.

Bowman, C., et al. 2005. "A mathematical model for assessing control strategies against West Nile virus". *Bulletin of Mathematical Biology* 67:1107–1133. ISSN: 00928240. doi:10.1016/j.bulm.2005.01.002.

Brady, Oliver J, et al. 2013. "Modelling adult *Aedes aegypti* and *Aedes albopictus* survival at different temperatures in laboratory and field settings". *Parasites & vectors* 6:351. ISSN: 1756-3305. doi:10.1186/1756-3305-6-351. http://www.pubmedcentral.nih.gov/articlerender.fcgi?artid=3867219&tool=pmcentrez&rendertype=abstract.

Brady, Oliver J., et al. 2016. "Vectorial capacity and vector control: Reconsidering sensitivity to parameters for malaria elimination". *Transactions of the Royal Society of Tropical Medicine and Hygiene* 110 (2): 107–117. ISSN: 18783503. doi:10.1093/trstmh/trv113.

Brown, J H, et al. 2004. "Toward a metabolic theory of ecology". *Ecology* 85 (7): 1771–1789. ISSN: 00129658. doi:Doi10.1890/03-9000.

Brownlie, J., et al. 2006. *Infectious Diseases: preparing for the future*. Tech. rep. London: Office of Science and Innovation.

Brun, Reto, et al. 2010. "Human African trypanosomiasis". *The Lancet* 375 (9709): 148–159. ISSN: 01406736. doi:10.1016/S0140-6736(09)60829-1. http://dx.doi.org/10.1016/S0140-6736(09)60829-1.

Bryant, Simon R., and Tim G. Shreeve. 2002. "The use of artificial neural networks in ecological analysis: estimating microhabitat temperature". *Ecological Entomology* 27:424–432.

BTO. 2017. *British trust for ornithology: BirdTrack data*. https://www.bto.org/volunteer-surveys/birdtrack/bird-recording/by-migration-season/spring-migration. VISITED ON 22/02/2017.

Burgdorfer, W. 1984. "Discovery of the Lyme disease spirochete and its relation to tick vectors". *Yale Journal of Biology and Medicine* 57 (4): 515–520. ISSN: 00440086.

Cailly, P., et al. 2012. "A climate-driven abundance model to assess mosquito control strategies". *Ecological Modelling* 227 (): 7–17. ISSN: 03043800. doi:10.1016/j.ecolmodel.2011.10.027.

Calistri, Paolo, et al. 2010. "Epidemiology of West Nile in Europe and in the Mediterranean Basin". *The Open Virology Journal* 4:29–37.

Calzolari, Mattia, et al. 2013. "Usutu Virus Persistence and West Nile Virus Inactivity in the Emilia-Romagna Region (Italy) in 2011". *PloS one* 8 (5). doi:10.1371/journal.pone.0063978.

Campbell, M S A. 1939. "Biological Indicators of Intensity of Stream Pollution". *Sewage Works Journal* 11 (1): 123–127.

Campbell-Lendrum, Diarmid, et al. 2015. "Climate change and vector-borne diseases: what are the implications for public health research and policy?" *Philosophical Transactions of the Royal Society B: Biological Sciences* 370, no. 1665 (). http://rstb.royalsocietypubl org/content/370/1665/20130552.abstract.

Carpenter, Simon, Anthony Wilson, and Philip S Mellor. 2009. "Culicoides and the emergence of bluetongue virus in northern Europe". *Trends in Microbiology* 17, no. 4 (): 172–178. ISSN: 0966-842X. doi:10.1016/j.tim.2009.01.001. http://dx.doi.org/10.1016/j.tim.2009.01.001.

Carrieri, M., et al. 2014. "Weather factors influencing the population dynamics of *Culex pipiens* (Diptera: Culicidae) in the Po Plain Valley, Italy (1997-2011)." *Environmental entomology* 43:482–90. ISSN: 1938-2936. doi:10.1603/EN13173.

Carrington, L B, et al. 2013. "Large diurnal temperature fluctuations negatively influence *Aedes aegypti* (Diptera: Culicidae) life-history traits". *Journal of Medical Entomology* 50 (1): 43–51. doi:10.1603/ME11242.

Caswell, Hal. 2001. *Matrix population models: Construction, analysis and interpretation*. 2nd. Sunderland, MA: Sinauer.

CDC. 2007. *Number of West Nile virus neuroinvasive disease cases by week of illness onset - United States 2007*. https://www.cdc.gov/MMWR/preview/mmwrhtml/mm5726a2.htm. VISITED ON 08/03/2017.

CDC, Arboviral Diseases Branch. 2016a. *ArboNET national arboviral surveillance system*. http://www.cdc.gov/westnile/resourcepages/survresources.html. VISITED ON 28/09/2016.

– . 2016b. *West Nile virus disease cases and deaths reported to CDC by year and clinical presentation 1999-2015*. http://www.cdc.gov/westnile/resources/pdfs/data/1-wnv-disease-cases-by-year_1999-2015_07072016.pdf. VISITED ON 27/09/2016.

Chapman, G. E., et al. 2016. "Potential vectors of equine arboviruses in the UK". *Veterinary Record*: vetrec–2016–103825. ISSN: 0042-4900. doi:10.1136/vr.103825. http://veterinaryrecord.bmj.com/lookup/doi/10.1136/vr.103825.

Charrel, R. N., et al. 2005. "Emergence of Toscana Virus in Europe". *Nature* 11 (11): 1–8.

Charron, Maud V P, et al. 2011. "Seasonal spread and control of Bluetongue in cattle". *Journal of Theoretical Biology* 291 (1): 1–9. ISSN: 00225193. doi:10.1016/j.jtbi.2011.08.041. http://dx.doi.org/10.1016/j.jtbi.2011.08.041.

Chase, J. M., and T. M. Knight. 2003. "Drought-induced mosquito outbreaks in wetlands". *Ecology Letters* 6, no. 11 (): 1017–1024. ISSN: 1461023X. doi:10.1046/j.1461-0248.2003.00533.x.

Chaskopoulou, Alexandra, et al. 2013. "Detection and early warning of West Nile Virus circulation in Central Macedonia, Greece, using sentinel chickens and mosquitoes." *Vector borne and zoonotic diseases* 13 (10): 723–32. ISSN: 1557-7759. doi:10.1089/vbz.2012.1176. http://www.ncbi.nlm.nih.gov/pubmed/23919609.

Chaves, Luis F., et al. 2012. "Nonlinear impacts of climatic variability on the density-dependent regulation of an insect vector of disease". *Global Change Biology* 18 (2): 457–468. ISSN: 13541013. doi:10.1111/j.1365-2486.2011.02522.x.

Ciota, A. T., and L. D. Kramer. 2013. "Vector-virus interactions and transmission dynamics of West Nile virus". *Viruses* 5:3021–3047. ISSN: 19994915. doi:10.3390/v5123021.

Ciota, A. T., et al. 2011. "Emergence of Culex pipiens from overwintering hibernacula." *Journal of the American Mosquito Control Association* 27 (1): 21–29. ISSN: 8756-971X. doi:10.2987/8756-971X-27.1.21.

Ciota, A. T., et al. 2014. "The effect of temperature on life history traits of *Culex* mosquitoes". *Journal of Medical Entomology* 51 (1): 55–62.

Ciota, A. T., et al. 2013. "The evolution of virulence of West Nile virus in a mosquito vector: implications for arbovirus adaptation and evolution." *BMC evolutionary biology* 13 (1): 71. ISSN: 1471-2148. doi:10.1186/1471-2148-13-71.

Ciota, Alexander T., et al. 2012. "Dispersal of *Culex* Mosquitoes (Diptera: Culicidae) From a Wastewater Treatment Facility". *Journal of Medical Entomology* 49 (1): 35–42. ISSN: 0022-2585. doi:10.1016/j.pestbp.2011.02.012.Investigations. arXiv: NIHMS150003. http://www.ncbi.nlm.nih.gov/pmc/articles/PMC3278816/%5Cnhttp://www.ncbi.nlm.nih.gov/pmc/articles/PMC3278816/pdf/nihms352542.pdf.

Cochrane, A. 1972. "Body weight and blood meal weight as factors affecting egg production of the tree-hole mosquito, *Aedes triseriatus* (Say)". In *Proceedings of the New Jersey Mosquito Extermination Association*, 65–78.

Coffey, Lark L, and William K Reisen. 2016. "West Nile Virus Fitness Costs in Different Mosquito Species". *Trends in Microbiology* 24, no. 6 (): 429–430. ISSN: 0966-842X. doi:http://dx.doi.org/10.1016/j.tim.2016.04.005. http://www.sciencedirect.com/science/article/pii/S0966842X16300191.

Colinet, H., et al. 2014. "Insects in fluctuating thermal environments." *Annual review of entomology* 60 (7): 1–18. ISSN: 1545-4487. doi:10.1146/annurev-ento-010814-021017.

Colless, D. H., and W. T. Chellapah. 1960. "Effects of body weight and size of blood-meal upon egg production in *Aedes aegypti* (linnaeus) (diptera, culicidae)". *Annals of Tropical Medicine and Parasitology* 54 (4): 475–482.

Colpitts, Tonya M., et al. 2012. "West Nile virus: Biology, transmission, and human infection". *Clinical Microbiology Reviews* 25 (4): 635–648. ISSN: 08938512. doi:10.1128/CMR.00045-12.

Connell, Joseph H. 1983. "On the Prevalence and Relative Importance of Interspecific Competition: Evidence from Field Experiments". *The American Naturalist* 122, no. 5 (): 661–696. ISSN: 0003-0147. doi:10.1086/284165. http://dx.doi.org/10.1086/284165.

Cornel, A J, P G Jupp, and N K Blackburn. 1993. "Environmental temperature on the vector competence of Culex univittatus (Diptera: Culicidae) for West Nile virus." *Journal of medical entomology* 30 (2): 449–56. ISSN: 0022-2585. doi:10.1093/jmedent/30.2.449. http://www.ncbi.nlm.nih.gov/pubmed/8459423.

Cornet, Stéphane, et al. 2013. "Both infected and uninfected mosquitoes are attracted toward malaria infected birds." *Malaria journal* 12:179. ISSN: 1475-2875. doi:10.1186/1475-2875-12-179. http://eutils.ncbi.nlm.nih.gov/entrez/eutils/elink.fcgi?dbfrom=pubmed&id=23731595&retmode=ref&cmd=prlinks%5Cnpapers2://publication/doi/10.1186/1475-2875-12-179.

Corwin, S P, D Sarafyan, and S Thompson. 1997. "DKLAG6: A code based on continuously imbedded sixth-order Runge-Kutta methods for the solution of state-dependent functional differential equations". *Applied Numerical Mathematics* 24 (2-3): 319–330. ISSN: 0168-9274. doi:10.1016/S0168-9274(97)00029-9.

Costanzo, Katie S, Kimberly Mormann, and Steven A Juliano. 2005. "Asymmetrical competition and patterns of abundance of *Aedes albopictus* and *Culex pipiens* (Diptera: Culicidae)." *Journal of medical entomology* 42 (4): 559–570. ISSN: 0022-2585. doi:10.1016/j.biotechadv.2011.08.021.Secreted. arXiv: NIHMS150003. http://www.pubmedcentral.nih.gov/articlerender.fcgi?artid=1995070&tool=pmcentrez&rendertype=abstract.

Couret, J., E. Dotson, and M. Q. Benedict. 2014. "Temperature, larval diet, and density effects on development rate and survival of *Aedes aegypti* (Diptera: Culicidae)." *PloS one* 9 (2): e87468. ISSN: 1932-6203. doi:10.1371/journal.pone.0087468.

Crick, Humphrey Q. P., David Wingfield Gibbons, and Robert D. Magrath. 1993. "Seasonal Changes in Clutch Size in British Birds". *Journal of Animal Ecology* 62 (2): 263–273.

Cruz-Pacheco, Gustavo, Lourdes Esteva, and Cristobal Vargas. 2009. "Seasonality and outbreaks in West Nile Virus infection". *Bulletin of Mathematical Biology* 71 (6): 1378–1393. ISSN: 00928240. doi:10.1007/s11538-009-9406-x.

Cruz-Pacheco, G., et al. 2005. "Modelling the dynamics of West Nile Virus." *Bulletin of mathematical biology* 67, no. 6 (): 1157–72. ISSN: 0092-8240. doi:10.1016/j.bulm.2004.11.008.

Dawson, Jennifer R., et al. 2007. "Crow deaths caused by West Nile virus during winter". *Emerging Infectious Diseases* 13 (12): 1912–1914. ISSN: 10806040. doi:10.3201/eid1312.070413.

Decker, Kimberlee D. 2012. "Dengue Fever: Re-Emergence of an Old Virus". *Journal for Nurse Practitioners* 8 (5): 389–393. ISSN: 15554155. doi:10.1016/j.nurpra.2011.09.004. http://dx.doi.org/10.1016/j.nurpra.2011.09.004.

Dehghan, Hossein, Javid Sadraei, and Seyed Hassan Moosa-kazemi. 2011. "The morphological variations of *Culex pipiens* (Diptera: Culicidae) in central Iran". *Asian Pacific Journal of Tropical Medicine* 4 (3): 215–219. ISSN: 1995-7645. doi:10.1016/S1995-7645(11)60072-2. http://dx.doi.org/10.1016/S1995-7645(11)60072-2.

Denlinger, David L, and Peter A Armbruster. 2014. "Mosquito Diapause". *Annual Review of Entomology* 59:73–93. ISSN: 1545-4487. doi:10.1146/annurev-ento-011613-162023.

Dobson, A P. 1987. "A Comparison of Seasonal and Annual Mortality for Both Sexes of Fifteen Species of Common British Birds". *Ornis Scandinavica* 18 (2): 122–128.

Dodson, Brittany L, Laura D Kramer, and Jason L Rasgon. 2012. "Effects of larval rearing temperature on immature development and West Nile virus vector competence of Culex tarsalis". *Parasites & Vectors* 5 (1): 199. ISSN: 1756-3305. doi:10.1186/1756-3305-5-199. Parasites%20&%20Vectors.

Dohm, David J, Michael R Sardelis, and Michael J Turell. 2002a. "Experimental Vertical Transmission of West Nile Virus by *Culex pipiens* (Diptera: Culicidae)". *Journal of medical entomology* 39 (4): 640–644.

Dohm, J, Monica L O Guinn, and Michael J Turell. 2002b. "Effect of Environmental Temperature on the Ability of Culex Pipiens To Transmit West Nile Virus". 39 (1): 221–225.

Duquesne, S, et al. 2011. "The potential of cladocerans as controphic competitors of the mosquito *Culex pipiens*". *J Med Entomol* 48 (3): 554–560. ISSN: 00222585. doi:10.1603/ME09282. http://www.ncbi.nlm.nih.gov/pubmed/21661316.

Durand, Benoit, et al. 2010. "A metapopulation model to simulate West Nile virus circulation in Western Africa, Southern Europe and the Mediterranean basin." *Veterinary research* 41 (3): 32. ISSN: 09284249. doi:10.1051/vetres/2010004.

Dusek, Robert J., et al. 2009. "Prevalence of West Nile virus in migratory birds during spring and fall migration". *American Journal of Tropical Medicine and Hygiene* 81 (6): 1151–1158. ISSN: 00029637. doi:10.4269/ajtmh.2009.09-0106.

ECDC. 2017. *ECDC VectorNet*. http://ecdc.europa.eu/en/healthtopics/vectors/VectorNet/Pages/VectorNet.aspx. VISITED ON 23/01/2017.

– . 2016a. *ECDC West Nile virus cases map*. http://ecdc.europa.eu/en/healthtopics/west_nile_fever/west-nile-fever-maps/pages/index.aspx. VISITED ON 06/01/2017.

– . 2016b. *ECDC West Nile Virus Historical Data*. http://ecdc.europa.eu/en/healthtopics/west_nile_fever/West-Nile-fever-maps/Pages/historical-data.aspx. VISITED ON 08/11/2016.

Eid, M. A. A., et al. 1992. "Effect of the duck-weed, *Lemna minor* vegetations on the mosquito, *Culex pipiens pipiens*". *International Journal of Tropical Insect Science* 13 (3): 357–361.

Eldridge, B. F. 1966. "Environmental control of ovarian development in mosquitoes of the *Culex pipiens* complex". *Science* 151.

Eldridge, Bruce F, and Charles L Bailey. 1979. "Experimental Hibernation Studies in *Culex Pipiens* (Diptera: Culicidae): Reactivation of Ovarian Development and Blood-Feeding in Prehibernating Females". *Journal of Medical Entomology* 15, **numbers** 5-6 (): 462–467. ISSN: 0022-2858. http://dx.doi.org/10.1093/jmedent/15.5-6.462.

Engler, Olivier, et al. 2013. "European surveillance for West Nile virus in mosquito populations". *International Journal of Environmental Research and Public Health* 10 (10): 4869–4895. ISSN: 16617827. doi:10.3390/ijerph10104869.

Erickson, R. A., et al. 2010a. "A dengue model with a dynamic *Aedes albopictus* vector population". *Ecological Modelling* 221 (24): 2899–2908. ISSN: 03043800. doi:10.1016/j.ecolmodel.2010.08.036.

Erickson, R. A., et al. 2010b. "A stage-structured, *Aedes albopictus* population model". *Ecological Modelling* 221, no. 9 (): 1273–1282. ISSN: 03043800. doi:10.1016/j.ecolmodel.2010.01.018.

Erickson, S. M., et al. 2006. "The potential of *Aedes triseriatus* (Diptera: Culicidae) as an enzootic vector of West Nile virus". *Journal of Medical Entomology* 45 (3): 966–970.

Ernst, Crystal M., and Christopher M. Buddle. 2015. "Drivers and patterns of ground-dwelling beetle biodiversity across northern Canada". *PLoS ONE* 10 (4): 1–16. ISSN: 19326203. doi:10.1371/journal.pone.0122163.

Evans, Matthew R., et al. 2013. "Do simple models lead to generality in ecology?" *Trends in Ecology and Evolution* 28 (10): 578–583. ISSN: 01695347. doi:10.1016/j.tree.2013.05.022. http://dx.doi.org/10.1016/j.tree.2013.05.022.

Ewing, D. A., et al. 2016a. "Modelling the effect of temperature on the seasonal population dynamics of temperate mosquitoes". *Journal of Theoretical Biology* 400:65–79. ISSN: 10958541. doi:10.1016/j.jtbi.2016.04.008. http://dx.doi.org/10.1016/j.jtbi.2016.04.008.

Ewing, David A., et al. 2016b. *Temperate-Mosquito-DDE v1.0*. doi:10.5281/zenodo.48525. http://zenodo.org/record/48525.

Ezenwa, V O, et al. 2006. "Avian diversity and West Nile virus: testing associations between biodiversity and infectious disease risk". *Proceedings of the Royal Society of London B* 273 (1582): 109–117. ISSN: 0962-8452. doi:10.1098/rspb.2005.3284.

Fan, Guihong, et al. 2010. "The impact of maturation delay of mosquitoes on the transmission of West Nile virus". *Mathematical Biosciences* 228 (2): 119–126. ISSN: 00255564. doi:10.1016/j.mbs.2010.08.010. http://dx.doi.org/10.1016/j.mbs.2010.08.010.

Farid, M. A. 1948. "Relationships between certain populations of *Culex pipiens linnaeus* and *Culex quinquefasciatus* say in the United States". *American Journal of Tropical Medicine and Hygiene* 49:83–100.

Fauci, Anthony S, and David M Morens. 2016. "Zika Virus in the Americas - Yet Another Arbovirus Threat". *New England Journal of Medicine* 374, no. 7 (): 601–604. ISSN: 0028-4793. doi:10.1056/NEJMp1600297. http://dx.doi.org/10.1056/NEJMp1600297.

Fillinger, Ulrike, et al. 2008. "A tool box for operational mosquito larval control: preliminary results and early lessons from the Urban Malaria Control Programme in Dar es Salaam, Tanzania." *Malaria journal* 7 (1): 20. ISSN: 1475-2875. doi:10.1186/1475-2875-7-20. http://www.malariajournal.com/content/7/1/20.

Fischer, S., D. Pereyra, and L. Fernández. 2012. "Predation ability and non-consumptive effects of *Notonecta sellata* (Heteroptera: Notonectidae) on immature stages of *Culex pipiens* (Diptera: Culicidae)". *Journal of Vector Ecology* 37 (1): 245–251.

Fischer, S., et al. 2013. "Effect of habitat complexity on the predation of *Buenoa fuscipennis* (Heteroptera: Notonectidae) on mosquito immature stages and alternative prey". *Journal of Vector Ecology* 38 (2): 215–223.

Focks, D A, et al. 1995. "A simulation model of the epidemiology of urban dengue fever: literature analysis, model development, preliminary validation, and samples of simulation results." *American Journal of Tropical Medicine and Hygiene* 53 (5): 489–506.

Focks, D A, et al. 1993a. "Dynamic life table model for *Aedes aegypti* (Diptera: Culicidae): analysis of the literature and model development". *Journal of medical entomology* 30 (6): 1003–1017.

– . 1993b. "Dynamic life table model for *Aedes aegypti* (Diptera: Culicidae): simulation results and validation." *Journal of medical entomology* 30 (6): 1018–1028. ISSN: 0022-2585. doi:10.1093/jmedent/30.6.1018.

Foerster, H von. 1959. "Some remarks on changing populations". *The Kinetics of Cellular Proliferation, Grune and Stratton*: 382–407.

Forsythe, W. C., et al. 1995. "A model comparison for daylength as a function of latitude and day of year". *Ecological Modelling* 80 (1): 87–95. ISSN: 03043800. doi:10.1016/0304-3800(94)00034-F.

Fros, Jelke J., et al. 2015. "Comparative Usutu and West Nile virus transmission potential by local *Culex pipiens* mosquitoes in north-western Europe". *One Health* 1:31–36. ISSN: 23527714. doi:10.1016/j.onehlt.2015.08.002. http://dx.doi.org/10.1016/j.onehlt.2015.08.002.

Futami, Kyoko, et al. 2008. "Diving Behavior in *Anopheles gambiae* (Diptera: Culicidae): Avoidance of a Predacious Wolf Spider (Araneae: Lycosidae) in Relation to Life Stage and Water Depth". *Journal of Medical Entomology* 45 (6): 1050–1056. ISSN: 00222585. doi:10.1603/0022-2585(2008)45[1050:DBIAGD]2.0.CO;2. http://www.scopus.com/inward/record.url?eid=2-s2.0-56749091183&partnerID=tZOtx3y1.

Garmendia, AE, et al. 2000. "Recovery and identification of West Nile virus from a hawk in winter". *Journal of Clinical Microbiology* 38:3110–3111.

Geery, P. R., and R. E. Holub. 1989. "Seasonal abundance and control of *Culex* spp. in catch basins in Illinois." *Journal of the American Mosquito Control Association* 5 (4): 537–540. ISSN: 8756-971X.

Gibbs, Samantha E J, et al. 2005. "Persistence of Antibodies to West Nile Virus in Naturally Infected Rock Pigeons (Columba livia)". *Clinical and Diagnostic Laboratory Immunology* 12 (5): 1–4. doi:10.1128/CDLI.12.5.665.

Gibbs, SEJ, et al. 2006. "West Nile Virus Antibodies in Avian Species of Georgia, USA: 2000–2004". *Vector borne and zoonotic diseases* 6 (1): 57–72.

Githeko, A. K., et al. 2000. "Climate change and vector-borne diseases: a regional analysis." *Bulletin of the World Health Organization* 78 (9): 1136–47. ISSN: 0042-9686.

Gjullin, C. M., and Richard F. Peters. 1952. "Recent studies of mosquito resistance to insecticides in California". *Mosquito News*: 1–7.

Goddard, L, et al. 2003. "Extrinsic incubation period of West Nile virus in four California Culex (Diptera: Culicidae) species". *Proceedings of the Mosquito Vector Control Association of California* 71:70–75.

Golding, N. 2013. "Mapping and understanding the distributions of potential vector mosquitoes in the UK : new methods and applications". PhD thesis, University of Oxford.

Golding, Nick, Miles A Nunn, and Bethan V Purse. 2015. "Identifying biotic interactions which drive the spatial distribution of a mosquito community". *Parasites & Vectors* 8 (1): 367. ISSN: 1756-3305. doi:10.1186/s13071-015-0915-1. http://www.parasitesandvectors.com/content/8/1/367.

Golding, N., et al. 2012. "West Nile virus vector *Culex modestus* established in southern England." *Parasites & vectors* 5 (1): 32. ISSN: 1756-3305. doi:10.1186/1756-3305-5-32.

Gordo, Oscar, Juan José Sanz, and Jorge M Lobo. 2010. "Determining the environmental factors underlying the spatial variability of insect appearance phenology for the honey bee, Apis mellifera, and the small white, Pieris rapae." *Journal of insect science (Online)* 10 (34): 34. ISSN: 1536-2442. doi:10.1673/031.010.3401.

Graczyk, Thaddeus K, Ronald Knight, and Robert H Gilman. 2001. "The role of non-biting flies in the epidemiology of human infectious diseases". *Microbes and Infection* 3:231–235.

Grandadam, M., et al. 2011. "Chikungunya virus, Southeastern France". *Emerging Infectious Diseases* 17 (5): 910–913. ISSN: 10806040. doi:10.3201/eid1705.101873.

Grassi, B, A Bignami, and G Bastianelli. 1899. "Ulteriore ricerche sul ciclo dei parassiti malarici umani sul corpo del zanzarone". *Atti Reale Accad Lincei* 8:21–28.

Grechka, Dmitry A., et al. 2016. "Universal, easy access to geotemporal information: FetchClimate". *Ecography* 39 (9): 904–911. ISSN: 16000587. doi:10.1111/ecog.02321.

Gu, W., et al. 2006. "Source reduction of mosquito larval habitats has unexpected consequences on malaria transmission." *Proceedings of the National Academy of Sciences of the United States of America* 103 (46): 17560–17563. ISSN: 0027-8424. doi:10.1073/pnas.0608452103.

Gubler, D J. 1998. "Resurgent vector-borne diseases as a global health problem." *Emerging infectious diseases* 4 (3): 442–50. ISSN: 1080-6040. doi:10.3201/eid0403.980326. http://www.ncbi.nlm.nih.gov/pubmed/9716967%5Cnhttp://www.pubmedcentral.nih.gov/articlerender.fcgi?artid=PMC2640300.

Gubler, D. J. 2002. "The Global Emergence / Resurgence of Arboviral Diseases As Public Health Problems". *Archives of Medical Research* 33:330–342. doi:S0188440902003788[pii]

Gündüz, Yaşar Kemal, Adnan AldemİR, and Bülent Alten. 2009. "Seasonal dynamics and nocturnal activities of mosquitoes (Diptera: Culicidae) in the Aras Valley, Turkey". *Turkish Journal of Zoology* 33:269–276. doi:10.3906/zoo-0808-11.

Gurney, W. S. C., R. M. Nisbet, and J. H. Lawton. 1983. "The systematic formulation of tractable single-species population models incorporating age structure". *Journal of Animal Ecology* 52 (2): 479–495.

Hahn, D. A., and D. L. Denlinger. 2007. "Meeting the energetic demands of insect diapause: nutrient storage and utilization". *Journal of insect physiology* 53, no. 8 (): 760–73. ISSN: 0022-1910. doi:10.1016/j.jinsphys.2007.03.018.

Hamer, Gabriel L., et al. 2014. "Dispersal of Adult *Culex* Mosquitoes in an Urban West Nile Virus Hotspot: A Mark-Capture Study Incorporating Stable Isotope Enrichment of Natural Larval Habitats". *PLoS Neglected Tropical Diseases* 8 (3): 6–12. ISSN: 19352735. doi:10.1371/journal.pntd.0002768.

Hamer, Gabriel L, et al. 2009. "Host Selection by *Culex pipiens* Mosquitoes and West Nile Virus Amplification". *The American Society of Tropical Medicine and Hygiene* 80 (2): 268–278.

Hart, John, et al. 2014. "West Nile virus neuroinvasive disease: neurological manifestations and prospective longitudinal outcomes." *BMC infectious diseases* 14:248. ISSN: 1471-2334. doi:10.1186/1471-2334-14-248. http://www.pubmedcentral.nih.gov/articlerender.fcgi?artid=4020876&tool=pmcentrez&rendertype=abstract.

Hartemink, N A, et al. 2007. "Importance of Bird-to-Bird Transmission for the Establishment of West Nile Virus". *Vector-Borne and Zoonotic Diseases* 7, no. 4 (): 575–584. ISSN: 1530-3667. doi:10.1089/vbz.2006.0613. http://dx.doi.org/10.1089/vbz.2006.0613.

Hartemink, Nienke, Daniela Cianci, and Paul Reiter. 2015. "R0 for vector-borne diseases: impact of the assumption for the duration of the extrinsic incubation period." *Vector borne and zoonotic diseases* 15 (3): 215–7. ISSN: 1557-7759. doi:10.1089/vbz.2014.1684. http://www.ncbi.nlm.nih.gov/pubmed/25793478%5Cnhttp://www.pubmedcentral.nih.gov/articlerender.fcgi?artid=PMC4369930.

Hartemink, N., et al. 2011. "Integrated mapping of establishment risk for emerging vector-borne infections: A case study of canine leishmaniasis in Southwest France". *PLoS ONE* 6 (8). ISSN: 19326203. doi:10.1371/journal.pone.0020817.

Hartley, D. M., et al. 2012. "Effects of temperature on emergence and seasonality of West Nile virus in California." *The American journal of tropical medicine and hygiene* 86, no. 5 (): 884–94. ISSN: 1476-1645. doi:10.4269/ajtmh.2012.11-0342.

Helbing, C. M., D. L. Moorhead, and L. Mitchell. 2015. "Population dynamics of *Culex restuans* and *Culex pipiens* (Diptera: Culicidae) related to climatic factors in Northwest Ohio". *Environmental Entomology* 44 (4): 1022–1028. ISSN: 0046225X. doi:10.1093/ee/nvv094.

Higgs, Stephen, Keith Snow, and Ernest A. Gould. 2004. "The potential for West Nile virus to establish outside of its narural range: A consideration of potential mosquito vectors in the United Kingdom". *Transactions of the Royal Society of Tropical Medicine and Hygiene* 98 (2): 82–87. ISSN: 00359203. doi:10.1016/S0035-9203(03)00004-X.

Higgs, S., et al. 2005. "Larval Competition Differentially Affects Arbovirus Infection in *Aedes* Mosquitoes". *Ecology* 86 (12): 3279–3288.

Hijmans, Robert J., et al. 2005. "Very high resolution interpolated climate surfaces for global land areas". *International Journal of Climatology* 25:1965–1978. ISSN: 08998418. doi:10.1002/joc.1276.

Hinton, M G, et al. 2015. "West Nile Virus Activity in a Winter Roost of American Crows (*Corvus brachyrhynchos*): Is Bird-to-Bird Transmission Important in Persistence and Amplification?" *Journal of medical entomology* 52 (4): 683–692. doi:10.1093/jme/tjv040.

Hoekman, D., et al. 2016. "Design for mosquito abundance, diversity, and phenology sampling within the National Ecological Observatory Network". *Ecosphere* 7 (5): 1–13. ISSN: 21508925. doi:10.1002/ecs2.1320.

Hutchinson, R A, P A West, and S W Lindsay. 2007. "Suitability of two carbon dioxide-baited traps for mosquito surveillance in the United Kingdom." *Bulletin of entomological research* 97:591–597. ISSN: 0007-4853. doi:10.1017/S0007485307005263.

Ibanez-Justicia, A., et al. 2015. "National mosquito (Diptera: Culicidae) survey in the Netherlands 2010-2013". *Journal of Medical Entomology* 52 (2): 185–198. ISSN: 00222585. doi:10.1093/jme/tju058.

Imhoff, Marc L., et al. 2010. "Remote sensing of the urban heat island effect across biomes in the continental USA". *Remote Sensing of Environment* 114 (3): 504–513. ISSN: 00344257. doi:10.1016/j.rse.2009.10.008. http://dx.doi.org/10.1016/j.rse.2009.10.008.

Ishii, T. 1963. "The effect of population density on the larval development of *Culex pipiens pallens*". *The Ecological Society of Japan* 13 (4): 128–132.

Jackson, Bryan T, and Sally L Paulson. 2006. "Seasonal abundance of *Culex restuans* and *Culex pipiens* in southwestern Virginia through ovitrapping". *The American Mosquito Control Association* 22 (2): 206–212.

Jang, Sophia R.-J. 2007. "On a discrete West Nile epidemic model". *Computational & Applied Mathematics* 26 (3): 397–414. ISSN: 0101-8205. doi:10.1590/S0101-82052007000300

http://www.scielo.br/scielo.php?script=sci_arttext&pid=S0101-82052007000300005&lng=en&nrm=iso&tlng=en.

Jansen, V. A. A., R. M. Nisbet, and W. S. C. Gurney. 1990. "Generation cycles in stage structured populations". *Bulletin of Mathematical Biology* 52 (3): 375–396.

Jensen, J. L. W. V. 1906. "Sur Les Fonctions Convexes Et Les Inegalites Entre Les Valeurs Moyennes". *Acta Mathematica* 30 (1): 175–193.

Jian, Yun, et al. 2014a. "The temporal spectrum of adult mosquito population fluctuations: Conceptual and modeling implications". *PLoS ONE* 9 (12): 1–21. ISSN: 19326203. doi:10.1371/journal.pone.0114301.

Jian, Y., et al. 2014b. "Environmental forcing and density-dependent controls of *Culex pipiens* abundance in a temperate climate (Northeastern Italy)". *Ecological Modelling* 272 (): 301–310. ISSN: 03043800. doi:10.1016/j.ecolmodel.2013.10.019.

Jobling, B. 1938. "On Two Subspecies of *Culex Pipiens L* (Diptera)". *Transactions of the Royal Entomological Society of London* 87:193–215.

Jones, KE Kate E, et al. 2008. "Global trends in emerging infectious diseases". *Nature* 451 (7181): 990–3. ISSN: 1476-4687. doi:10.1038/nature06536. arXiv: arXiv:1011.1669v3. http://www.ncbi.nlm.nih.gov/pubmed/18288193%5Cnhttp://www.nature.com/nature/journal/vaop/ncurrent/full/nature06536.html.

Jones, P., et al. 2009. *Projections of future daily climate for the UK from the Weather Generator*. Tech. rep.

Jourdain, E, et al. 2007. "Bird species potentially involved in introduction, amplification, and spread of West Nile virus in a Mediterranean wetland, the Camargue (Southern France)". *Vector borne and zoonotic diseases* 7 (1): 15–33. ISSN: 1530-3667. doi:10.1089/vbz.2006.0543.

Juliano, S. A. 2007. "Population Dynamics". *Journal of American Mosquito Control Association* 23 (2): 265–275. ISSN: 15378276. doi:10.1016/j.biotechadv.2011.08.021.Secreted. arXiv: NIHMS150003.

Jupp, P G. 1976. "The susceptibility of four South African species of *Culex* to West Nile and sindbis viruses by two different infecting methods". *Mosquito News* 36 (2): 166–173.

Jupp, P G, and B M McIntosh. 1970. "Quantitative Experiments on the Vector Capability of *Culex univittatus theobald* with West Nile and Sindbis Viruses 1". *Journal of Medical Entomology* 7, no. 3 (): 371–373. ISSN: 0022-2858. http://dx.doi.org/10.1093/jmedent/7.3.371.

Kalluri, Satya, et al. 2007. "Surveillance of arthropod vector-borne infectious diseases using remote sensing techniques: A review". *PLoS Pathogens* 3 (10): 1361–1371. ISSN: 15537366. doi:10.1371/journal.ppat.0030116.

Kelly, Jeffrey F., et al. 2016. "Novel measures of continental-scale avian migration phenology related to proximate environmental cues". *Ecosphere* 7 (8): 1–13. ISSN: 21508925. doi:10.1002/ecs2.1434.

Kelly-Hope, Louise A, and F Ellis McKenzie. 2009. "The multiplicity of malaria transmission: a review of entomological inoculation rate measurements and methods across sub-Saharan Africa." *Malaria journal* 8 (1): 19. ISSN: 1475-2875. doi:10.1186/1475-2875-8-19. http://www.malariajournal.com/content/8/1/19.

Kemenesi, G, et al. 2014. "West Nile virus surveillance in mosquitoes, April to October 2013, Vojvodina province , Serbia: implications for the 2014 season". *Euro surveillance* 19 (16): 20779.

Kermack, W. O., and A. G. McKendrick. 1927. "A Contribution to the Mathematical Theory of Epidemics". *Proceedings of the Royal Society of London A* 115:700–721. ISSN: 1364-5021. doi:10.1098/rspa.1983.0054.

Kettle, Helen, and David Nutter. 2015. "StagePop: Modelling stage-structured populations in R". *Methods in Ecology and Evolution* 6 (12): 1484–1490. ISSN: 2041210X. doi:10.1111/2041-210X.12445.

Kilpatrick, A. M., Shannon LaDeau, and Peter P. Marra. 2007. "Ecology of West Nile Virus Transmission and Its Impact on Birds in the Western Hemisphere". *The Auk* 124 (4): 1121–1136.

Kilpatrick, A. Marm, et al. 2006. "West Nile virus epidemics in North America are driven by shifts in mosquito feeding behavior". *PLoS Biology* 4 (4): 606–610. ISSN: 15457885. doi:10.1371/journal.pbio.0040082.

Kim, Heung Chul, et al. 2003. "Seasonal Prevalence of Mosquitoes Collected from Light Traps in Korea (1999-2000)". *Korean Journal of Entomology* 33 (1): 9–16. ISSN: 1738-2297. doi:10.1111/j.1748-5967.2003.tb00043.x. http://doi.wiley.com/10.1111/j.1748-5967.2003.tb00043.x.

Kim, Heung Chul, et al. 2009. "Seasonal prevalence of mosquitoes collected from light traps in the Republic of Korea, 2006". *Entomological Research* 39 (4): 248–256. ISSN: 17382297. doi:10.1111/j.1748-5967.2009.00229.x.

Kim, Heung Chul, et al. 2010. "Seasonal prevalence of mosquitoes collected from light traps in the Republic of Korea, 2007". *Entomological Research* 40:136–144. doi:10.1111/j.1748-5967.2010.00271.x.

Kim, Heung Chul, et al. 2007. "Seasonal prevalence of mosquitoes collected from light traps with notes on malaria in the Republic of Korea, 2004". *Entomological Research* 37 (3): 180–189. ISSN: 17382297. doi:10.1111/j.1748-5967.2007.00110.x.

Klomp, H. 1964. "Intraspecific Competition and the Regulation of Insect Numbers". *Annual Review of Entomology* 9:17–40.

Knies, Jennifer L, and Joel G Kingsolver. 2010. "Erroneous Arrhenius: modified arrhenius model best explains the temperature dependence of ectotherm fitness." *The American naturalist* 176 (2): 227–233. ISSN: 0003-0147. doi:10.1086/653662.

Komar, Nicholas, et al. 2003. "Experimental Infection of North American Birds with the New York 1999 Strain of West Nile Virus". *Emerging Infectious Disease journal* 9 (3): 311. ISSN: 1080-6059. doi:10.3201/eid0903.020628. http://wwwnc.cdc.gov/eid/article/9/3/02-0628.

Kulasekera, Varuni L., et al. 2001. "West Nile virus infection in mosquitoes, birds, horses, and humans, Staten Island, New York, 2000". *Emerging Infectious Diseases* 7 (4): 722–725. ISSN: 10806040. doi:10.3201/eid0704.010421.

Lalubin, F., et al. 2013. "Temporal changes in mosquito abundance (*Culex pipiens*), avian malaria prevalence and lineage composition." *Parasites & vectors* 6, no. 1 (): 307. ISSN: 1756-3305. doi:10.1186/1756-3305-6-307.

Lambrechts, Louis, et al. 2011. "Impact of daily temperature fluctuations on dengue virus transmission by *Aedes aegypti*". *Proceedings of the National Academy of Sciences of the United States of America* 108 (18): 1–6. ISSN: 0027-8424. doi:10.1073/pnas.1101377108. http://www.pubmedcentral.nih.gov/articlerender.fcgi?artid=3088608&tool=pmcentrez&rendertype=abstract.

Lampman, Richard, et al. 2006. "*Culex* Population Dynamics and West Nile Virus Transmission in East-Central Illinois". *The American Mosquito Control Association* 22 (3): 390–400.

Landesman, William J., et al. 2007. "Inter-annual associations between precipitation and human incidence of West Nile virus in the United States." *Vector borne and zoonotic diseases* 7 (3): 337–343.

Landscapes, Infectious. 2016. *Culex pipiens life cycle figure*. http://www.infectionlandsca
org/2012/05/lymphatic-filariasis.html. VISITED ON 10/11/2016.

Lardeux, F. J., et al. 2008. "A physiological time analysis of the duration of the gonotrophic cycle of *Anopheles* pseudopunctipennis and its implications for malaria transmission in Bolivia." *Malaria journal* 7 (): 141. ISSN: 1475-2875. doi:10.1186/1475-2875-7-141.

Lauritsen, Ryan G., and Jeffrey C. Rogers. 2012. "U.S. Diurnal temperature range variability and regional causal mechanisms, 1901-2002". *Journal of Climate* 25 (20): 7216–7231. ISSN: 08948755. doi:10.1175/JCLI-D-11-00429.1.

Lebl, K., K. Brugger, and F. Rubel. 2013. "Predicting *Culex pipiens/restuans* population dynamics by interval lagged weather data." *Parasites & vectors* 6, no. 1 (): 129. ISSN: 1756-3305. doi:10.1186/1756-3305-6-129.

Lee, J. H., and W. A. Rowley. 2000. "The abundance and seasonal distribution of *Culex* mosquitoes in Iowa during 1995-97." *Journal of the American Mosquito Control Association* 16 (4): 275–278. ISSN: 8756-971X.

Legros, M., A. L. Lloyd, and Y. Huang. 2009. "Density-dependent intraspecific competition in the larval stage of *Aedes aegypti* (Diptera : Culicidae): revisiting the current paradigm". *Journal of Medical Entomology* 46 (3): 409–419.

Leslie, P. H. 1945. "On the Use of Matrices in Certain Population Mathematics". *Biometrika* 33 (3): 183–212.

– . 1948. "Some further notes on the uses of matrices in population mathematics". *Biometrika* 35 (3/4): 213–245. doi:10.1093/biomet/35.3-4.213.

Linard, C., et al. 2009. "A multi-agent simulation to assess the risk of malaria re-emergence in southern France". *Ecological Modelling* 220, no. 2 (): 160–174. ISSN: 03043800. doi:10.1016/j.ecolmodel.2008.09.001.

Liu, Rongsong, et al. 2006. "Modeling spatial spread of west nile virus and impact of directional dispersal of birds". *Mathematical biosciences and engineering* 3 (1): 145–160. ISSN: 1551-0018. doi:10.3934/mbe.2006.3.145.

Liu, Shengqiang, Lansun Chen, and R Agarwal. 2002. "Recent progress on stage-structured population dynamics". *Mathematical and Computer Modelling* 36 (02): 1319–1360. ISSN: 08957177. doi:10.1016/S0895-7177(02)00279-0.

Loetti, V., N. Schweigmann, and N. Burroni. 2011. "Development rates, larval survivorship and wing length of *Culex pipiens* (Diptera: Culicidae) at constant temperatures". *Journal of Natural History* 45, **numbers** 35-36 (): 2203–2213. ISSN: 0022-2933. doi:10.1080/00222933.2011.590946.

Lončarić, Z., and B. K. Hackenberger. 2013. "Stage and age structured *Aedes vexans* and *Culex pipiens* (Diptera: Culicidae) climate-dependent matrix population model." *Theoretical population biology* 83 (): 82–94. ISSN: 1096-0325. doi:10.1016/j.tpb.2012.08.002.

Lord, C. C. 2007. "Modelling and biological control of mosquitoes". *Journal of the American Mosquito Control Association* 23 (2): 252–264.

– . 2004. "Seasonal population dynamics and behaviour of insects in models of vector-borne pathogens". *Physiological Entomology* 29 (3): 214–222. ISSN: 15378276. doi:10.1016/j.biotechadv.2011.08.021.Secreted. arXiv: NIHMS150003.

Lord, Cynthia C., and Jonathan F. Day. 2001. "Simulation Studies of St. Louis Encephalitis and West Nile Viruses: The Impact of Bird Mortality". *Vector borne and zoonotic diseases* 1 (4).

Loss, Scott R., et al. 2009. "Avian host community structure and prevalence of West Nile virus in Chicago, Illinois". *Oecologia* 159 (2): 415–424. ISSN: 00298549. doi:10.1007/s00442-008-1224-6.

Lotka, A J. 1925. *Elements of Physical Biology*. Williams / Wilkins.

Lounibos, L. P., R. L. Escher, and R. Lourenço-De-Oliveira. 2003. "Asymmetric Evolution of Photoperiodic Diapause in Temperate and Tropical Invasive Populations of Aedes albopictus (Diptera: Culicidae)". *Annals of the Entomological Society of America* 96 (4): 512–518. ISSN: 00138746. doi:10.1603/0013-8746(2003)096[0512:AEOPDI]2.0.CO;2. http://aesa.oxfordjournals.org/content/96/4/512.abstract.

Lunde, Torleif Markussen, et al. 2013. "A dynamic model of some malaria-transmitting anopheline mosquitoes of the Afrotropical region. I. Model description and sensitivity analysis." *Malaria journal* 12:28. ISSN: 1475-2875. doi:10.1186/1475-2875-12-28. http://www.malariajournal.com/content/12/1/28.

Luo, Y et al. 2011. "Ecological forecasting and data assimilation in a data-rech era". *Ecological Applications* 21(5) (July): 1429–1442. ISSN: 10510761. doi:10.1890/09-1275.1.

Lutambi, A. M., et al. 2013. "Mathematical modelling of mosquito dispersal in a heterogeneous environment". *Mathematical biosciences* 241 (2): 198–216.

Lyimo, E. O., W. Takken, and J. C. Koella. 1992. "Effect of rearing temperature and larval density on larval survival, age at pupation and adult size of *Anopheles gambiae*". *Entomologia Experimentalis et Applicata* 63 (3): 265–271.

MacDonald, G., C. B. Cuellar, and C. V. Foll. 1968. "The dynamics of malaria." *Bulletin of the World Health Organization* 38 (5): 743–755. ISSN: 00429686.

Maciel-de-Freitas, R., J. C. Koella, and R. Lourenço-de-Oliveira. 2011. "Lower survival rate, longevity and fecundity of Aedes aegypti (Diptera: Culicidae) females orally challenged with dengue virus serotype 2". *Transactions of the Royal Society of Tropical Medicine and Hygiene* 105 (8): 452–458. ISSN: 00359203. doi:10.1016/j.trstmh.2011.05.006.

Madder, D. J., G. A. Surgeoner, and B. V. Helson. 1983a. "Induction of diapause in *Culex pipiens* and *Culex restuans* (Diptera: Culicidae) in southern Ontario". *The Canadian Entomologist* 115 (8): 877–883.

– . 1983b. "Number of generations, egg production, and developmental time of *Culex pipiens* and *Culex restuans* (Diptera: Culicidae) in Southern Ontario". *Journal of medical entomology* 20 (3): 275–287.

Madder, D. J., et al. 1980. "The use of oviposition activity to monitor populations of *Culex pipiens* and *Culex restuans* (Diptera: Culicidae)". *The Canadian Entomologist* 112:1013–1017.

Magori, Krisztian, et al. 2009. "Skeeter Buster: A Stochastic , Spatially Explicit Modeling Tool for Studying *Aedes aegypti* Population Replacement and Population Suppression Strategies". *PLoS Neglected Tropical Diseases* 3 (9). doi:10.1371/journal.pntd.0000508.

Maidana, N. A., and H. M. Yang. 2009. "Spatial spreading of West Nile Virus described by traveling waves". *Journal of Theoretical Biology* 258:403–417.

Maier, W A, and M Seitz. 1987. "Pathology of Malaria-infected Mosquitoes". *Parasitology Today* 3 (7): 216–218. ISSN: 01694758. doi:10.1016/0169-4758(87)90063-9.

Marini, Giovanni, et al. 2017. "Exploring vector-borne infection ecology in multi-host communities : A case study of West Nile virus". *Journal of Theoretical Biology* 415 (January 2016): 58–69. ISSN: 0022-5193. doi:10.1016/j.jtbi.2016.12.009. http://dx.doi.org/10.1016/j.jtbi.2016.12.009.

Marini, Giovanni, et al. 2016. "The role of climatic and density dependent factors in shaping mosquito population dynamics:The case of culex pipiens in northwestern Italy". *PLoS ONE* 11 (4): 1–15. ISSN: 19326203. doi:10.1371/journal.pone.0154018.

Marti, G. A., et al. 2006. "Predation efficiency of indigenous larvivorous fish species on *Culex pipiens* L. larvae (Diptera: Culicidae) in drainage ditches in Argentina." *Journal of vector ecology* 31 (1): 102–6. ISSN: 1081-1710.

McKee, Eileen M, et al. 2015. "West Nile Virus antibody decay rate in free-ranging birds". *USDA National Wildlife Research Center - Staff Publications*.

McLean, R G, et al. 2001. "West Nile virus transmission and ecology in birds". *Ann N Y Acad Sci* 951:54–57. ISSN: 0077-8923. doi:10.1111/j.1749-6632.2001.tb02684.x. http://www.ncbi.nlm.nih.gov/pubmed/11797804.

McLennan-Smith, T. A., and G. N. Mercer. 2014. "Complex behaviour in a dengue model with a seasonally varying vector population." *Mathematical biosciences* 248 (): 22–30. ISSN: 1879-3134. doi:10.1016/j.mbs.2013.11.003.

Medlock, J. M., K. R. Snow, and S. Leach. 2005. "Potential transmission of West Nile virus in the British Isles: An ecological review of candidate mosquito bridge vectors". *Medical and Veterinary Entomology* 19 (1): 2–21. ISSN: 0269283X. doi:10.1111/j.0269-283X.2005.00547.x.

Medlock, J. M., and K.R. Snow. 2008. "Natural predators and parasites of British mosquitoes–a review". *European Mosquito Bulletin* 25 (April): 1–11. http://e-m-b.org/sites/e-m-b.org/files/EMB25_1.pdf.

Medlock, J. M., et al. 2014. "Potential vector for West Nile virus prevalent in Kent." *The Veterinary record*: 2014–2016. ISSN: 2042-7670. doi:10.1136/vr.g5679.

Medlock, Jolyon M., and Alexander G.C. Vaux. 2015. "Seasonal dynamics and habitat specificity of mosquitoes in an English wetland: implications for UK wetland management and

restoration". *Journal of Vector Ecology* 40 (1): 90–106. ISSN: 10811710. doi:10.1111/jvec.12137. http://doi.wiley.com/10.1111/jvec.12137.

Meillon, B. de, A. Sebastian, and Z. H. Khan. 1967. "Time of arrival of gravid *Culex pipiens fatigans* at an oviposition site, the oviposition cycle and the relationship between time of feeding and time of oviposition." *Bulletin of the World Health Organization* 36 (1): 39–46. ISSN: 00429686.

Menon, P. K., and P. K. Rajagopalan. 1981. "Seasonal changes in survival rates of immatures of Culex pipiens fatigans in different habitats in Pondicherry". *Indian Journal of Medical Research* 73:136–138.

MetOffice. 2009. *Met Office UK Climate Impacts Programme Temperature Projections*. http://ukclimateprojections.metoffice.gov.uk/21708?projections=23833.

– . 2010. *Met Office: UKCP09: Regional values of 1961-1990 baseline averages*. http://www.metoffice.gov.uk/climatechange/science/monitoring/ukcp09/download/longterm/regional_values.html. (Visited on 06/02/2015).

Micieli, María V, et al. 2013. "Vector competence of Argentine mosquitoes (Diptera: Culicidae) for West Nile virus (Flaviviridae: Flavivirus)". *Journal of medical entomology* 50 (4): 853–62. ISSN: 0022-2585. doi:10.1603/ME12226. http://www.pubmedcentral.nih.gov/articlerender.fcgi?artid=3932752&tool=pmcentrez&rendertype=abstract.

Microsoft. 2014. *FetchClimate2*. http://fetchclimate2.cloudapp.net. (Visited on 06/02/2015).

Mirski, T., M. Bartoszcze, and A. Bielawska-Drozd. 2012. "Impact of climate change on infectious diseases." *Polish Journal of Environmental Studies* 21 (3): 525–532. ISSN: 1668-3501. doi:10.1590/S0325-00752012000100009.

Mitchell, Carl J. 1983. "Differentiation of Host-Seeking Behavior from Blood-Feeding Behavior in Overwintering *Culex Pipiens* (Diptera: Culicidae) and Observations on Gonotrophic Dissociation". *Journal of Medical Entomology* 20, no. 2 (): 157–163. ISSN: 0022-2858. http://dx.doi.org/10.1093/jmedent/20.2.157.

Mitchell, Carl J, and Hans Briegel. 1989. "Inability of diapausing *Culex pipiens* (Diptera: Culicidae) to use blood for producing lipid reserves for overwinter survival". *Journal of medical entomology* 26 (4): 318–326.

Mogi, M, and T Okazawa. 1990. "Factors influencing development and survival of *Culex pipiens pallens* larvae (Diptera: Culicidae) in polluted urban creeks". *Researches on Population Ecology* 32:135–149.

Monaco, F, et al. 2011. "2009 West Nile disease epidemic in Italy: First evidence of overwintering in Western Europe?" *Research in Veterinary Science* 91 (2): 321–326. ISSN:

0034-5288. doi:10.1016/j.rvsc.2011.01.008. http://dx.doi.org/10.1016/j.rvsc.2011.01.008.

Montarsi, Fabrizio, et al. 2015. "Seasonal and daily activity patterns of mosquito (Diptera: Culicidae) vectors of pathogens in Northeastern Italy". *Journal of Medical Entomology* 52 (1): 56–62. ISSN: 00222585. doi:10.1093/jme/tju002.

Montosi, E., et al. 2012. "An ecohydrological model of malaria outbreaks". *Hydrology and Earth System Sciences* 16, no. 8 (): 2759–2769. ISSN: 1607-7938. doi:10.5194/hess-16-2759-2012. http://www.hydrol-earth-syst-sci.net/16/2759/2012/.

Morin, C. W., and A. C. Comrie. 2013. "Regional and seasonal response of a West Nile virus vector to climate change." *Proceedings of the National Academy of Sciences of the United States of America* 110, no. 39 (): 15620–5. ISSN: 1091-6490. doi:10.1073/pnas.1307135110.

Mulatti, P., et al. 2014. "Determinants of the population growth of the West Nile virus mosquito vector *Culex pipiens* in a repeatedly affected area in Italy." *Parasites & vectors* 7 (): 26. ISSN: 1756-3305. doi:10.1186/1756-3305-7-26.

Murdoch, W. W., C. J. Briggs, and R. M. Nisbet. 2003. *Consumer-Resource Dynamics*. Ed. by S. A. Levin and H. S. Horn. Princeton University Press.

Muriu, S. M., et al. 2013. "Larval density dependence in *Anopheles gambiae s.s.*, the major African vector of malaria." *The Journal of animal ecology* 82, no. 1 (): 166–74. ISSN: 1365-2656. doi:10.1111/1365-2656.12002.

Murphy, James, et al. 2010. *UK Climate Projections science report: Climate change projections*. Tech. rep. doi:10.1787/9789264086876-5-en.

Najera, Jose A., Matiana Gonzalez-Silva, and Pedro L. Alonso. 2011. "Some lessons for the future from the global malaria eradication programme (1955-1969)". *PLoS Medicine* 8 (1). ISSN: 15491277. doi:10.1371/journal.pmed.1000412.

Nasci, Roger S., et al. 2001. "West Nile virus in overwintering *Culex* mosquitoes, New York City, 2000". *Emerging Infectious Diseases* 7 (4): 742–744. ISSN: 10806040. doi:10.3201/eid0704.010426.

Nelder, J A, and R W M Wedderburn. 1972. "Generalized Linear Models". *Journal of the Royal Statistical Society. Series A (General)* 135 (3): 370–384. ISSN: <null>. doi:10.2307/2344614. http://www.jstor.org/stable/2344614%5Cnhttp://www.jstor.org/page/info/about/policies/terms.jsp%5Cnhttp://www.jstor.org.

Nelms, Brittany M, et al. 2013. "Overwintering Biology of *Culex* (Diptera: Culicidae) Mosquitoes in the Sacramento Valley of California". *Journal of medical entomology* 50 (4): 773–790.

Nemeth, Nicole M, Paul T Oesterle, and Richard A Bowen. 2009. "Humoral Immunity to West Nile Virus Is Long-Lasting and Protective in the House Sparrow (Passer domesticus)". *American Journal of Tropical Medicine and Hygiene* 80 (5): 864–869. ISSN: 15378276. doi:10.1126/scisignal.2001449.Engineering. arXiv: NIHMS150003.

Newton, Ian. 2007. *The Migration Ecology of Birds*. 1st. Oxford: Academic Press. ISBN: 978-0-12-517367-4. doi:http://dx.doi.org/10.1016/B978-012517367-4.50000-0. http://www.sciencedirect.com/science/article/pii/B9780125173674500000.

Nicholson, AJ. 1954. "An outline of the dynamics of animal populations". *Australian Journal of Zoology* 2:9–65.

Nisbet, R. M., and W. S. C. Gurney. 1983. "The systematic formulation of population models for insects with dynamically varying instar duration". *Theoretical Population Biology* 23:114–135.

Nowicki, Piotr, et al. 2009. "Relative importance of density-dependent regulation and environmental stochasticity for butterfly population dynamics". *Oecologia* 161 (2): 227–239. ISSN: 00298549. doi:10.1007/s00442-009-1373-2.

Olejnícek, J., and I. Gelbic. 2000. "Differences in response to temperature and density between two strains of the mosquito, *Culex pipiens molestus* Forskal." *Journal of vector ecology* 25 (2): 136–45. ISSN: 1081-1710.

Onyeka, J. O. A. 1983. "Studies on the natural predators of *Culex pipiens* L. and *C. torrentium* Martini (Diptera: Culicidae) in England". *Bulletin of Entomological Research* 73 (02): 185–194. ISSN: 0007-4853. doi:10.1017/S0007485300008798.

Onyeka, J. O. A., and P. F. L. Boreham. 1987. "Population studies, physiological state and mortality factors of overwintering adult populations of females of *Culex pipiens* L. (Diptera: Culicidae)". *Bulletin of entomological research* 77:99–111.

Orshan, L, et al. 2008. "Mosquito Vectors of West Nile Fever in Israel". *Journal of medical entomology* 45 (5): 939–947.

Osborn, Timothy J, and Mike Hulme. 2002. "Evidence for Trends in Heavy Rainfall Events over the UK". *Philosophical Transactions: Mathematical, Physical and Engineering Sciences* 360 (1796): 1313–1325. ISSN: 1364503X. http://www.jstor.org/stable/3066443.

Paaijmans, Krijn P, and Bert G Heusinkveld. 2008. "A simplified model to predict diurnal water temperature dynamics in a shallow tropical water pool". *International Journal of Biometeorology* 52:797–803. doi:10.1007/s00484-008-0173-4.

Paaijmans, Krijn P, et al. 2010. "Relevant microclimate for determining the development rate of malaria mosquitoes and possible implications of climate change". *Malaria journal* 9:196. ISSN: 1475-2875. doi:10.1186/1475-2875-9-196.

Pawelek, Kasia A, et al. 2014. "Modeling Dynamics of *Culex pipiens* Complex Populations and Assessing Abatement Strategies for West Nile Virus". *Plos one* 9 (9). doi:10.1371/journal.pone.0108452.

Paz, S., and I. Albersheim. 2008. "Influence of warming tendency on *Culex pipiens* population abundance and on the probability of West Nile fever outbreaks (Israeli Case Study: 2001-2005)." *EcoHealth* 5, no. 1 (): 40–8. ISSN: 1612-9210. doi:10.1007/s10393-007-0150-0.

Paz, S., et al. 2013. "Permissive summer temperatures of the 2010 European West Nile fever upsurge." *PloS one* 8 (2): e56398. ISSN: 1932-6203. doi:10.1371/journal.pone.0056398.

Peel, A J, et al. 2014. "The effect of seasonal birth pulses on pathogen persistence in wild mammal populations". *Proceedings of the Royal Society B: Biological Sciences* 281.

Pérez-Ramírez, Elisa, Francisco Llorente, and Miguel Ángel Jiménez-Clavero. 2014. "Experimental infections of wild birds with West Nile virus". *Viruses* 6 (2): 752–781. ISSN: 19994915. doi:10.3390/v6020752.

Pervanidou, D., et al. 2014. "West Nile virus outbreak in humans, Greece, 2012: third consecutive year of local transmission." *Euro surveillance* 19 (13): 1–11. ISSN: 1560-7917.

Peters, T. M., and P. Barbosa. 1977. "Influence of population density on size, fecundity, and developmental rate of insects in culture". *Annual Review of Entomology* 22:431–450.

Petersen, L. R., et al. 2013. "Estimated cumulative incidence of West Nile virus infection in US adults, 1999-2010." *Epidemiology and infection* 141 (3): 591–5. ISSN: 1469-4409. doi:10.1017/S0950268812001070.

Petersen, Lyle R, and John T Roehrig. 2001. "West Nile Virus: A reemerging global pathogen". *Rev Biomed* 12:208–216. ISSN: 1080-6040. doi:10.3201/eid0704.010401. http://www.medigraphic.com/pdfs/revbio/bio-2001/bio013h.pdf.

PHE. 2016. *Mosquito Surveillance*. https://www.gov.uk/government/publications/mosquito-surveillance. VISITED ON 28/09/2016.

Ponçon, Nicolas, et al. 2007a. "Effects of local anthropogenic changes on potential malaria vector *Anopheles hyrcanus* and West Nile virus vector *Culex modestus*, Camargue, France". *Emerging Infectious Diseases* 13 (12): 1810–1815. ISSN: 10806040. doi:10.3201/eid1312.070730.

Ponçon, N., et al. 2007b. "Population dynamics of pest mosquitoes and potential malaria and West Nile virus vectors in relation to climatic factors and human activities in the Camargue, France". *Medical and Veterinary Entomology* 21 (4): 350–357. ISSN: 0269283X. doi:10.1111/j.1365-2915.2007.00701.x.

Preud'homme, Eric B, and Heinz G Stefan. 1992. *Relationship Between Water Temperatures and Air Temperatures for Central U.S. Streams*. Tech. rep. 333. Duluth: U.S. Environmental Protection Agency.

Purse, Bethan V., and Nick Golding. 2015. "Tracking the distribution and impacts of diseases with biological records and distribution modelling". *Biological Journal of the Linnean Society* 115 (3): 664–677. ISSN: 10958312. doi:10.1111/bij.12567.

Quiroz-martinez, H., and A. Rodriguez-Castro. 2007. "Aquatic insects as predators of mosquito larvae". *The American Mosquito Control Association* 23 (2): 110–117.

R Core Team. 2013. *R: A Language and Environment for Statistical Computing*. Vienna, Austria.

Rajagopalan, P. K., M. Yasuno, and P. K. Menon. 1976. "Density effect on survival of immature stages of Culex pipiens fatigans in breeding sites in Delhi villages". *Indian Journal of Medical Research* 64 (5): 688–708.

Reed, Walter, James Carroll, and Jesse W Lazear. 1900. "The etiology of Yellow Fever - a preliminary note". *Philadelphia Medical Journal* 121 (2): 37–53. ISSN: 0002-9629. http://content.wkhealth.com/linkback/openurl?sid=WKPTLP:landingpage%7B&%7Dan=00000441-190102000-00019%5Cnhttp://content.wkhealth.com/linkback/openurl?sid=WKPTLP:landingpage&an=00000441-190102000-00019.

Reiner, R. C., et al. 2013. "A systematic review of mathematical models of mosquito-borne pathogen transmission: 1970-2010". *Journal of the Royal Society, Interface* 10.

Reisen, W K, Y Fang, and V M Martinez. 2005. "Avian host and mosquito (Diptera: Culicidae) vector competence determine the efficiency of West Nile and St. Louis encephalitis virus transmission." *Journal of medical entomology* 42 (3): 367–375. ISSN: 0022-2585. doi:10.1603/0022-2585(2005)042[0367:AHAMDC]2.0.CO;2.

Reisen, W. K., Y. Fang, and V. M. Martinez. 2006a. "Effects of temperature on the transmission of west nile virus by *Culex tarsalis* (Diptera: Culicidae)." *Journal of medical entomology* 43, no. 2 (): 309–17. ISSN: 0022-2585.

Reisen, William K. 2013. "Ecology of West Nile Virus in North America". *Viruses* 5:2079–2105. doi:10.3390/v5092079.

Reisen, William K, et al. 2006b. "Overwintering of West Nile Virus in Southern California". *J. Med. Entomol* 43 (2): 344–355. ISSN: 0022-2585. doi:10.1603/0022-2585(2006)043[0344:OOWNVI]2.0.CO;2.

Reiskind, M. H., and L. P. Lounibos. 2009. "Effects of intraspecific larval competition on adult longevity in the mosquitoes Aedes aegypti and Aedes albopictus". *Medical and Veterinary Entomology* 23 (1): 62–68. ISSN: 0269283X. doi:10.1111/j.1365-2915.2008.00782.x. arXiv: NIHMS150003.

Reiskind, M. H., and M. L. Wilson. 2004. "*Culex restuans* (Diptera: Culicidae) oviposition behavior determined by larval habitat quality and quantity in Southeastern Michigan". *Journal of Medical Entomology* 41 (2): 179–186. ISSN: 00222585. doi:10.1603/0022-2585-41.2.179.

Resh, Vincent H, and Ring T Cardé, eds. 2009. *Encyclopedia of Insects*. 2nd.

Richards, S. L., S. L. Anderson, and S. A. Yost. 2012. "Effects of blood meal source on the reproduction of *Culex pipiens quinquefasciatus* (Diptera : Culicidae)". *Society for Vector Ecology* 37 (1): 1–7.

Rinehart, J. P., R. M. Robich, and D. L. Denlinger. 2006. "Enhanced cold and desiccation tolerance in diapausing adults of *Culex pipiens*, and a role for Hsp70 in response to cold shock but not as a component of the diapause program". *Entomological Society of America* 43 (4): 713–722.

Robertson, Suzanne L., and Kevin A. Caillouet. 2016. "A host stage-structured model of enzootic West Nile virus transmission to explore the effect of avian stage-dependent exposure to vectors". *Journal of Theoretical Biology* 399:33–42. ISSN: 10958541. doi:10.1016/j.jtbi.2016.03.031. http://dx.doi.org/10.1016/j.jtbi.2016.03.031.

Robich, Rebecca M, and David L Denlinger. 2005. "Diapause in the mosquito *Culex pipiens* evokes a metabolic switch from blood feeding to sugar gluttony." *Proceedings of the National Academy of Sciences of the United States of America* 102 (44): 15912–15917. ISSN: 0027-8424. doi:10.1073/pnas.0507958102.

Rogers, D. J., and S. E. Randolph. 2006. "Climate change and vector-borne diseases." *Advances in parasitology* 62, no. 05 (): 345–81. ISSN: 0065-308X. doi:10.1016/S0065-308X(05)62010-6.

Rosà, Roberto, et al. 2014. "Early warning of West Nile virus mosquito vector: climate and land use models successfully explain phenology and abundance of *Culex pipiens* mosquitoes in north-western Italy." *Parasites & vectors* 7:269. ISSN: 1756-3305. doi:10.1186/1756-3305-7-269. http://www.pubmedcentral.nih.gov/articlerender.fcgi?artid=4061321&tool=pmcentrez&rendertype=abstract.

Ross, Ronald. 1910. *The prevention of malaria*. 1st. New York.

– . 1898. "The Role of the Mosquito in the Evolution of the Malarial Parasite". *The Lancet*: 488–489.

RSPB. 2017. *RSPB house sparrow breeding information*. https://www.rspb.org.uk/birds-and-wildlife/bird-and-wildlife-guides/bird-a-z/h/housesparrow/nesting.aspx. VISITED ON 21/02/2017.

Rubel, F., et al. 2008. "Explaining Usutu virus dynamics in Austria: model development and calibration." *Preventive veterinary medicine* 85, **numbers** 3-4 (): 166–86. ISSN: 0167-5877. doi:10.1016/j.prevetmed.2008.01.006.

Rueda, L. M., et al. 1990. "Temperature-dependent development and survival rates of *Culex quinquefasciatus* and *Aedes aegypti* (Diptera: Culicidae)." *Journal of medical entomology* 27, no. 5 (): 892–8. ISSN: 0022-2585.

Rund, Samuel S. C., and M.E. Martinez. 2017. "Creating a National Vector Surveillance System: Integrated mosquito trap data and digital epidemiology". *bioRxiv*: 1–27. doi:https://doi.org/10.1101/096875. http://biorxiv.org/content/early/2016/12/27/096875.article-metrics.

Rund, Samuel S C, et al. 2016. "Daily rhythms in mosquitoes and their consequences for malaria transmission". *Insects* 7 (2): 1–20. ISSN: 20754450. doi:10.3390/insects7020014.

Ruybal, Jordan E, Laura D Kramer, and A Marm Kilpatrick. 2016. "Geographic variation in the response of *Culex pipiens* life history traits to temperature." *Parasites & vectors* 9 (1): 116. ISSN: 1756-3305. doi:10.1186/s13071-016-1402-z. http://parasitesandvectors.biomedcentral.com/articles/10.1186/s13071-016-1402-z.

Rydzanicz, K, and E Lonc. 2003. "Species composition and seasonal dynamics of mosquito larvae in the Wrocław, Poland area." *Journal of vector ecology* 28 (2): 255–266. ISSN: 1081-1710.

Sabatino, Daria Di, et al. 2014. "Epidemiology of West Nile Disease in Europe and in the Mediterranean Basin from 2009 to 2013". *BioMed Research International*.

Sæther, Bernt-Erik, et al. 2016. "Demographic routes to variability and regulation in bird populations". *Nature communications* 7 (1432): 1–8. ISSN: 2041-1723. doi:10.1038/ncomms12001. http://dx.doi.org/10.1038/ncomms12001.

Sambri, V., et al. 2013. "West Nile virus in Europe: emergence, epidemiology, diagnosis, treatment, and prevention." *Clinical microbiology and infection : the official publication of the European Society of Clinical Microbiology and Infectious Diseases* 19:699–704. ISSN: 1469-0691. doi:10.1111/1469-0691.12211.

Sanburg, L. L., and J. R. Larsen. 1973. "Effect of photoperiod and temperature on ovarian development in *Culex pipiens pipiens*". *Journal of insect physiology* 19, no. 6 (): 1173–90. ISSN: 0022-1910.

Sardelis, Michael R., et al. 2001. "Vector competence of selected North American *Culex* and *Coquillettidia* mosquitoes for West Nile virus". *Emerging Infectious Diseases* 7 (6): 1018–1022. ISSN: 10806040. doi:10.3201/eid0706.010617.

Savage, Harry M, et al. 2006. "Oviposition Activity Patterns and West Nile Virus Infection Rates for Members of the *Culex pipiens* Complex at Different Habitat Types within the

Hybrid Zone , Shelby County, TN, 2002 (Diptera: Culicidae)". *Journal of medical entomology* 43 (6): 1227–1238.

Schaeffer, B., B. Mondet, and S. Touzeau. 2008. "Using a climate-dependent model to predict mosquito abundance: application to *Aedes (Stegomyia) africanus* and *Aedes (Diceromyia) furcifer* (Diptera: Culicidae)." *Infection, genetics and evolution* 8, no. 4 (): 422–32. ISSN: 1567-1348. doi:10.1016/j.meegid.2007.07.002.

Schaffner, Francis, and Alexander Mathis. 2013. *Spatio-temporal diversity of the mosquito fauna (Diptera: Culicidae) in Switzerland*. Tech. rep. August. doi:10.5167/uzh-110446.

Schaffner, Francis, Veerle Versteirt, and Jolyon Medlock. 2014. *Guidelines for the surveillance of native mosquitoes in Europe*. Tech. rep. Stockholm: ECDC.

Scheitlin, Kelsey N., and P. Grady Dixon. 2010. "Diurnal temperature range variability due to land cover and airmass types in the Southeast". *Journal of Applied Meteorology and Climatology* 49 (5): 879–888. ISSN: 15588424. doi:10.1175/2009JAMC2322.1.

Schoener, Thomas W. 1983. "Field Experiments on Interspecific Competition". *The American Naturalist* 122, no. 2 (): 240–285. ISSN: 0003-0147. doi:10.1086/284133. http://dx.doi.org/10.1086/284133.

Searle, Kate R., et al. 2014. "Environmental Drivers of Culicoides Phenology: How Important Is Species-Specific Variation When Determining Disease Policy?" *PLoS ONE* 9 (11): e111876. ISSN: 1932-6203. doi:10.1371/journal.pone.0111876. http://dx.plos.org/10.1371/journal.pone.0111876.

Searle, K.R., et al. 2013. "Identifying environmental drivers of insect phenology across space and time: Culicoides in Scotland as a case study". *Bulletin of Entomological Research* 103 (02): 155–170. ISSN: 0007-4853. doi:10.1017/S0007485312000466. http://www.journals.cambridge.org/abstract_S0007485312000466.

Semenza, J. C., and B. Menne. 2009. "Climate change and infectious diseases in Europe." *The Lancet infectious diseases* 9, no. 6 (): 365–75. ISSN: 1474-4457. doi:10.1016/S1473-3099(09)70104-5.

Semenza, Jan C, et al. 2016. "Climate change projections of West Nile virus infections in Europe: implications for blood safety practices." *Environmental health : a global access science source* 15 Suppl 1 (1): 28. ISSN: 1476-069X. doi:10.1186/s12940-016-0105-4. http://ehjournal.biomedcentral.com/articles/10.1186/s12940-016-0105-4.

Service, M. W. 1969. "Observations on the ecology of some British mosquitoes". *Bulletin of entomological research* 59:161–194.

Shaalan, E. A., and D. V. Canyon. 2009. "Aquatic insect predators and mosquito control". *Tropical Biomedicine* 26 (3): 223–261.

Shaman, Jeffrey, Jonathan F. Day, and Nicholas Komar. 2010. "Hydrologic conditions describe west nile virus risk in Colorado". *International Journal of Environmental Research and Public Health* 7:494–508. ISSN: 16604601. doi:10.3390/ijerph7020494.

Shaman, Jeffrey, Jonathan F Day, and Marc Stieglitz. 2005. "Drought-induced amplification and epidemic transmission of West Nile virus in southern Florida." *Journal of medical entomology* 42 (2): 134–141. ISSN: 0022-2585. doi:10.1603/0022-2585(2005)042[0134:DAAETO]2.0.CO;2.

Shaman, J., et al. 2006. "A hydrologically driven model of swamp water mosquito population dynamics". *Ecological Modelling* 194, no. 4 (): 395–404. ISSN: 03043800. doi:10.1016/j.ecolmodel.2005.10.037.

Sharpe, F R, and A J Lotka. 1911. "A problem in age-distribution". *Philosophical Magazine Series 6* 21, no. 124 (): 435–438. ISSN: 1941-5982. doi:10.1080/14786440408637050. http://dx.doi.org/10.1080/14786440408637050.

Silva, Ivoneide M, et al. 2005. "Laboratory evaluation of mosquito traps baited with a synthetic human odor blend to capture Aedes aegypti." *Journal of the American Mosquito Control Association* 21 (2): 229–233. ISSN: 8756-971X. doi:10.2987/8756-971X(2005)21[229:LEOMTB]2.0.CO;2.

Sim, Cheolho, and David L. Denlinger. 2013. "Insulin signaling and the regulation of insect diapause". *Frontiers in Physiology* 4 JUL (July): 1–10. ISSN: 1664042X. doi:10.3389/fphys.2013.00189.

Sinclair, A. R. E., and R. P. Pech. 1996. "Density dependence, stochasticity, compensation and predator regulation". *Oikos* 75 (2): 164–173.

Smith, D. L., et al. 2014. "Recasting the theory of mosquito-borne pathogen transmission dynamics and control." *Transactions of the Royal Society of Tropical Medicine and Hygiene* 108, no. 4 (): 185–97. ISSN: 1878-3503. doi:10.1093/trstmh/tru026.

Smith, D. L., et al. 2012. "Ross, Macdonald, and a theory for the dynamics and control of mosquito-transmitted pathogens." *PLoS pathogens* 8, no. 4 (): e1002588. ISSN: 1553-7374. doi:10.1371/journal.ppat.1002588.

Smith, David L., Jonathan Dushoff, and F. Ellis McKenzie. 2004. "The risk of a mosquito-borne infection in a heterogeneous environment". *PLoS Biology* 2 (11). ISSN: 15449173. doi:10.1371/journal.pbio.0020368.

Smith, David L, and F Ellis McKenzie. 2004. "Statics and dynamics of malaria infection in *Anopheles* mosquitoes." *Malaria journal* 3:13. ISSN: 1475-2875. doi:10.1186/1475-2875-3-13.

Smith, David L., et al. 2013. "Mosquito Population Regulation and Larval Source Management in Heterogeneous Environments". *PLoS ONE* 8 (8). ISSN: 19326203. doi:10.1371/journal.pone.0071247.

Smithburn, K. C., et al. 1940. "A Neurotropic Virus Isolated from the Blood of a Native of Uganda". *The American journal of tropical medicine and hygiene* 20:471–492.

Soti, V., et al. 2012. "Combining hydrology and mosquito population models to identify the drivers of Rift Valley fever emergence in semi-arid regions of West Africa." *PLoS neglected tropical diseases* 6, no. 8 (): e1795. ISSN: 1935-2735. doi:10.1371/journal.pntd.0001795.

Spielman, A. 2001. "Structure and seasonality of nearctic *Culex pipiens* populations." *Annals of the New York Academy of Sciences* 951:220–34. ISSN: 0077-8923.

Spielman, A., and J. Wong. 1973. "Environmental control of ovarian diapause in *Culex pipiens*". *Annals of the Entomological Society of America* 66 (4): 905–907. ISSN: 0013-8746.

Stainforth, David A, Sandra C Chapman, and Nicholas W Watkins. 2013. "Mapping climate change in European temperature distributions". *Environmental Research Letters* 8 (3): 034031. ISSN: 1748-9326. doi:10.1088/1748-9326/8/3/034031. http://iopscience.iop.org/1748-9326/8/3/034031/article/.

Succo, Tiphanie, et al. 2016. "Autochthonous dengue outbreak in Nimes, South of France, July to September 2015". *Eurosurveillance* 21 (21): 1–7. ISSN: 15607917. doi:10.2807/1560-7917.ES.2016.21.21.30240. http://www.eurosurveillance.org/images/dynamic/EE/V21N21/art22485.pdf.

Sulaiman, S., and M. W. Service. 1983. "Studies on hibernating populations of the mosquito *Culex pipiens* L. in southern and northern England". *Journal of Natural History* 17 (6): 849–857. ISSN: 0022-2933. doi:10.1080/00222938300770661.

Tabachnick, W J. 2010. "Challenges in predicting climate and environmental effects on vector-borne disease episystems in a changing world." *The Journal of experimental biology* 213 (6): 946–954. ISSN: 0022-0949. doi:10.1242/jeb.037564.

Tamburini, Giovanni, et al. 2013. "Effects of climate and density-dependent factors on population dynamics of the pine processionary moth in the Southern Alps". *Climatic Change* 121 (4): 701–712. ISSN: 01650009. doi:10.1007/s10584-013-0966-2.

Tate, P., and M. Vincent. 1933. "The biology of autogenous and anautogenous races of *Culex pipiens linnaeus* (Diptera: Culicidae)". *Parasitol* 28:115–145.

Tatem, A J, D J Rogers, and S I Hay. 2006. "Global Transport Networks and Infectious Disease Spread". In *Global Mapping of Infectious Diseases: Methods, Examples and Emerging Applications*, ed. by Alastair Graham Simon I. Hay and David J Rogers B T - Advances in Parasitology, vol. Volume 62, 293–343. Academic Press. ISBN: 0065-308X. doi:http://doi.org/10.1016/S0065-308X(05)62009-X. http://www.sciencedirect.com/science/article/pii/S0065308X0562009X.

Tauber, MJ, CA Tauber, and S Masaki. 1986. *Seasonal adaptations of insects*. New York: Oxford University Press.

Thomas, D. M., and B. Urena. 2001. "A model describing the evolution of West Nile-like encephalitis in New York City". *Mathematical and Computer Modelling* 34 (7-8): 771–781. ISSN: 08957177. doi:10.1016/S0895-7177(01)00098-X.

Thompson, S., and L. Shampine. 2004. "A Friendly Fortran DDE Solver". In *The Third International Conference on the Numerical Solution of Volterra and Delay Equations*, 1–23.

Tiawsirisup, Sonthaya, et al. 2004. "Susceptibility of *Ochlerotatus trivittatus* (Coq.), *Aedes albopictus* (Skuse), and *Culex pipiens* (L.) to West Nile Virus Infection". *Vector-Borne and Zoonotic Diseases* 4, no. 3 (): 190–197. ISSN: 1530-3667. doi:10.1089/vbz.2004.4.190. http://dx.doi.org/10.1089/vbz.2004.4.190.

Toma, Luciano, et al. 2008. "First report on entomological field activities for the surveillance of West Nile disease in Italy." *Veterinaria italiana* 44 (3): 483–97, 499–512. ISSN: 1828-1427. http://www.ncbi.nlm.nih.gov/pubmed/20405446.

Townroe, S., and A. Callaghan. 2014. "British container breeding mosquitoes: the impact of urbanisation and climate change on community composition and phenology." *PloS one* 9 (4): e95325. ISSN: 1932-6203. doi:10.1371/journal.pone.0095325.

Townroe, S, and A Callaghan. 2015. "Morphological and fecundity traits of Culex mosquitoes caught in gravid traps in urban and rural Berkshire, UK". *Bulletin of Entomological Research* 105 (5): 615–620. ISSN: 0007-4853. doi:10.1017/S000748531500053x.

Tran, Annelise, et al. 2008. "Using remote sensing to map larval and adult populations of *Anopheles hyrcanus* (Diptera: Culicidae) a potential malaria vector in Southern France". *International Journal of Health Geographics* 7 (1): 9. ISSN: 1476-072X. doi:10.1186/1476-072X-7-9. http://ij-healthgeographics.biomedcentral.com/articles/10.1186/1476-072X-7-9.

Tran, A., et al. 2013. "A rainfall- and temperature-driven abundance model for *Aedes albopictus* populations." *International journal of environmental research and public health* 10 (5): 1698–719. ISSN: 1660-4601. doi:10.3390/ijerph10051698.

Tukey, John W. 1949. "Comparing Individual Means in the Analysis of Variance". *Biometrics* 5 (2): 99–114.

Turell, M J, M O'Guinn, and J Oliver. 2000. "Potential for New York mosquitoes to transmit West Nile virus". *Am J Trop Med Hyg* 62 (3): 413–414. ISSN: 0002-9637. http://www.ncbi.nlm.nih.gov/pubmed/11037788.

Turell, Michael J., et al. 2005. "An Update on the Potential of North American Mosquitoes (Diptera: Culicidae) to Transmit West Nile Virus". *Journal of Medical Entomology* 42 (1): 57–62. ISSN: 0022-2585. doi:10.1093/jmedent/42.1.57. http://jme.oxfordjournals.org/content/42/1/57.abstract.

Turell, Michael J, et al. 2002. "Potential vectors of west nile virus in North America". In *Japanese Encephalitis and West Nile Viruses*, 241–252.

Turell, Michael J, et al. 2001. "Vector Competence of North American Mosquitoes (Diptera: Culicidae) for West Nile Virus". *Journal of medical entomology* 38 (2): 130–134.

UEA, Climatic Research Unit. 2015. *Temperature data (HadCRUT4)*. http://www.cru.uea.ac.uk/cru/data/temperature/. (Visited on 06/02/2015).

UKCIP. 2010. *Met Office UK Climate Impacts Programme Temperature Projections*. http://ukclimateprojections.metoffice.gov.uk/21708?projections=23833. (Visited on 06/02/2015).

Valdez, L. D., et al. 2017. "Effects of rainfall on Culex mosquito population dynamics". *Journal of Theoretical Biology* 421:28–38. ISSN: 10958541. doi:10.1016/j.jtbi.2017.03.024. arXiv: 1703.08915. http://arxiv.org/abs/1703.08915.

Vaux, Alexander G C, et al. 2015. "Enhanced West Nile virus surveillance in the North Kent marshes, UK." *Parasites & vectors* 8 (1): 91. ISSN: 1756-3305. doi:10.1186/s13071-015-0705-9. http://www.parasitesandvectors.com/content/8/1/91.

Ventim, Rita, et al. 2012. "Avian malaria infections in western European mosquitoes". *Parasitology Research* 111:637–645. doi:10.1007/s00436-012-2880-3.

Vezzani, D., and A. P. Albicocco. 2009. "The effect of shade on the container index and pupal productivity of the mosquitoes *Aedes aegypti* and *Culex pipiens* breeding in artificial containers". *Medical and Veterinary Entomology* 23 (1): 78–84. ISSN: 0269283X. doi:10.1111/j.1365-2915.2008.00783.x.

Vinogradova, E. B. 2000. *Culex pipiens pipiens mosquitoes: taxonomy, distribution, ecology, physiology, genetics, applied importance and control*. 2nd ed. PENSOFT.

Volterra, V. 1926. "Variazioni e fluttuazioni del numero d'individui in specie animali conviventi". *Mem. Acad. Lincei Roma* 2:31–113.

Votýpka, Jan, Veronika Seblová, and Jana Rádrová. 2008. "Spread of the West Nile virus vector *Culex modestus* and the potential malaria vector *Anopheles hyrcanus* in central Europe." *Journal of vector ecology : journal of the Society for Vector Ecology* 33 (2): 269–277. ISSN: 1081-1710. doi:10.3376/1081-1710-33.2.269.

Walker, Ian R. 2001. "Midges: Chironomidae and Related Diptera". In *Tracking Environmental Change Using Lake Sediments*, ed. by John P Smol, H John B Birks, and William M Last, 43–66. Dordrecht: Springer Netherlands. ISBN: 978-0-306-47671-6. doi:10.1007/0-306-47671-1_3. http://dx.doi.org/10.1007/0-306-47671-1_3.

Wang, J., N. H. Ogden, and H. Zhu. 2011. "The impact of weather conditions on *Culex pipiens* and *Culex restuans* (Diptera: Culicidae) abundance: a case study in Peel region".

Journal of Medical Entomology 48, no. 2 (): 468–475. ISSN: 00222585. doi:10.1603/ME10117.

Wang, Xia, Sanyi Tang, and Robert A. Cheke. 2016. "A stage structured mosquito model incorporating effects of precipitation and daily temperature fluctuations". *Journal of Theoretical Biology* 411 (July): 27–36. ISSN: 00225193. doi:10.1016/j.jtbi.2016.09.015.

Washino, Robert K. 1977. "The Physiological Ecology of Gonotrophic Dissociation and Related Phenomena in Mosquitoes". *Journal of Medical Entomology* 13, **numbers** 4-5 (): 381–388. ISSN: 0022-2858. http://dx.doi.org/10.1093/jmedent/13.4-5.381.

Wearing, H. J., et al. 2004. "The dynamical consequences of developmental variability and demographic stochasticity for host-parasitoid interactions." *The American naturalist* 164 (4): 543–558.

Wearing, Helen J., Pejman Rohani, and Matt J. Keeling. 2005. "Appropriate models for the management of infectious diseases". *PLoS Medicine* 2 (7): 0621–0627. ISSN: 15491277. doi:10.1371/journal.pmed.0020174.

Weissenböck, H., et al. 2002. "Emergence of Usutu virus, an African mosquito-borne flavivirus of the Japanese encephalitis virus group, central Europe". *Emerging Infectious Diseases* 8 (7): 652–656. ISSN: 10806040. doi:10.3201/eid0807.020094.

White, M. T., et al. 2011. "Modelling the impact of vector control interventions on *Anopheles gambiae* population dynamics." *Parasites & vectors* 4 (1): 153. ISSN: 1756-3305. doi:10.1186/1756-3305-4-153.

White, S. M., P. Rohani, and S. M. Sait. 2010. "Modelling pulsed releases for sterile insect techniques: fitness costs of sterile and transgenic males and the effects on mosquito dynamics". *Journal of Applied Ecology* 47 (6): 1329–1339. ISSN: 00218901. doi:10.1111/j.1365-2664.2010.01880.x.

Wilder-Smith, Annelies, et al. 2017. "Epidemic arboviral diseases: priorities for research and public health". *The Lancet Infectious Diseases* 17, no. 3 (): e101–e106. ISSN: 1473-3099. doi:10.1016/S1473-3099(16)30518-7. http://dx.doi.org/10.1016/S1473-3099(16)30518-7.

Wilton, D. P., and G. C. Smith. 1985. "Ovarian diapause in three geographic strains of *Culex pipiens* (Diptera: Culicidae)". *Journal of medical entomology* 22 (5): 524–528.

Wimberly, Michael C, et al. 2014. "Regional Variation of Climatic Influences on West Nile Virus Outbreaks in the United States". *The American journal of tropical medicine and hygiene* 91 (4): 677–684. ISSN: 1476-1645. doi:10.4269/ajtmh.14-0239. http://www.ncbi.nlm.nih.gov/pubmed/25092814.

Wonham, Marjorie J, Tomás De-Camino-Beck, and Mark a Lewis. 2004. "An epidemiological model for West Nile virus: invasion analysis and control applications." *Proceedings. Biological sciences / The Royal Society* 271, no. 1538 (): 501–7. ISSN: 0962-8452. doi:10.1098/rspb.2003.2608. http://www.pubmedcentral.nih.gov/articlerender.fcgi?artid=1691622&tool=pmcentrez&rendertype=abstract.

Wonham, Marjorie J., et al. 2006. "Transmission assumptions generate conflicting predictions in host-vector disease models: A case study in West Nile virus". *Ecology Letters* 9 (6): 706–725. ISSN: 1461023X. doi:10.1111/j.1461-0248.2006.00912.x.

Wooldridge, J. M. 1999. "Quasi-Likelihood Methods for Count Data". Chap. 8 in *Handbook of Applied Econometrics Volume II: Microeconomics*, ed. by M. H. Pesaran and Peter Schmidt, 352–406.

Yee, Donald A., Banugopan Kesavaraju, and Steven A Juliano. 2004. "Larval feeding behaviour of three co-occurring species of container mosquitoes". *Journal of Vector Ecology* 29 (2): 315–322.

Yusoff, N., H. Budin, and S. Ismail. 2012. "Simulation of population dynamics of *Aedes aegypti* using climate dependent model". *International Journal of Mathematical, Computational, Physical and Quantum Engineering* 6 (2): 1–6.

Zell, Roland. 2004. "Global climate change and the emergence/re-emergence of infectious diseases". *International Journal of Medical Microbiology Supplements* 293:16–26. ISSN: 14331128. doi:10.1016/S1433-1128(04)80005-6.

Zeller, H. G., and I. Schuffenecker. 2004. "West Nile virus: An overview of its spread in Europe and the Mediterranean basin in contrast to its spread in the Americas". *European Journal of Clinical Microbiology and Infectious Diseases* 23 (3): 147–156. ISSN: 09349723. doi:10.1007/s10096-003-1085-1.

Zeuss, Dirk, Stefan Brunzel, and Roland Brandl. 2017. "Environmental drivers of voltinism and body size in insect assemblages across Europe". *Global Ecology and Biogeography* 26:154–165. ISSN: 14668238. doi:10.1111/geb.12525.